SAKARYA UNIVERSITY
INSTITUTE OF SCIENCE AND TECHNOLOGY

RESERVOIR EVALUATION BY WELL-LOGGING OF AL-RAJA FIELD, ALIF MEMBER, MARIB-SHABWAH (SAB'ATAYN) BASIN, REPUBLIC OF YEMEN

M.Sc. THESIS

Mustafa AL-ARIKI

Department : GEOPHYSICAL ENGINEERING

Supervisor : Prof. Dr. Levent GÜLEN

Co-Advisor : Dr. Nabeel AL-AZAZI

September 2021

SAKARYA UNIVERSITY
INSTITUTE OF SCIENCE AND TECHNOLOGY

RESERVOIR EVALUATION BY WELL-LOGGING OF AL-RAJA FIELD, ALIF MEMBER, MARIB-SHABWAH (SAB'ATAYN) BASIN, REPUBLIC OF YEMEN

M.Sc. THESIS

Mustafa AL-ARIKI

Department	**:**	**GEOPHYSICAL ENGINEERING**
Supervisor	**:**	**Prof. Dr. Levent GÜLEN**
Co-Advisor	**:**	**Dr. Nabeel AL-AZAZI**

This thesis has been accepted unanimously by the examination committee on 20. 09.2021

Prof. Dr. Levent GÜLEN	**Prof. Dr. Bülent ORUÇ**	**Prof. Dr. Murat UTKUCU**
Head of Jury	**Jury Member**	**Jury Member**

DECLARATION

I hereby declare that all data used in this thesis have been obtained within the framework of academic rules, no falsification has been made in the data, all visual and written information and results are presented in accordance with academic and ethical rules, references are made in accordance with scientific norms in case the works of others are used, and that to the best of my knowledge the data of this thesis have not been used in any thesis of this university or any other university.

Mustafa AL-ARIKI

20.09.2021

ACKNOWLEDGEMENT

First of all, all praise is due to Allah with whose favors all good can be accomplished and all praises and thanks be to Allah, who has guided us to this, and never could we have found guidance, were it not that Allah had guided us!

I would like to express my deepest sense of gratitude to my supervisor and adviser the former head of Geophysical Engineering, Sakarya University Prof. Dr. Levent GÜLEN, who offered his continuous advice, invaluable guidance, and elating encouragement throughout the course of this thesis. He always gave me the right advice and pointed me in the right direction. I want to thank him again for his sincerity and father care. I am also thankful to my Co-Advisor the Head of Oil and Natural Gas Engineering Department, Aden University, Yemen, Dr. Nabeel AL-AZAZI for his assistance, recommendations and critical suggestions while making this work.

I offer my sincere appreciation for all the academic staff of the Geophysical Engineering Department of Sakarya University, especially Assist. Prof. Dr. Ayhan KESKINSEZER, Assist. Prof. Dr. Günay BEYHAN, Assist. Prof. Dr. Şefik RAMAZANOĞLU, and Prof. Dr. Murat UTKUCU for teaching and guiding me while studying and for their support, special helpfulness, and encouragement for me as a foreign student.

I cannot express enough thanks to my caring, loving, and supportive family starting with my father -may Allah bless him-, my great mother and my siblings. Their prayers as well as encouragement when the times got rough will not be forgotten.

Finally, I'd like to thank my committee members for attending my defense and thank you for accepting to be a reader.

TABLE OF CONTENTS

LIST OF SYMBOLS & ABBREVIATIONS

API	:	American Petroleum Institute
Av. PHIE %	:	Average of effective porosity
Av. S_{hyd}	:	Average of hydrocarbon saturation
Av. S_w %	:	Average of water saturation
BS	:	Bit Size
BVW	:	Bulk Volume Water
CAL	:	Calliper log
D	:	Depth
DW	:	Dostour Al-Wihdah Field
FD	:	Formation depth
FT	:	Formation temperature
ft	:	Foot
G	:	Gross thickness
GG	:	Geothermal Gradient
GR	:	Gamma Ray Log
GWC	:	Gas water contact
ILD	:	Deep Induction Log
ILM	:	Medium Induction Log
m	:	Meter
N	:	Net thickness
NPHI	:	Neutron Porosity Log
NPHIC	:	Corrected Neutron Porosity Log
PEF	:	Photoelectric Factor
PEFC	:	Corrected Photoelectric Factor
PHIE	:	Effective porosity
PHIT	:	The total porosity (%)

PHtemp	:	Bottom Hole Temperature
RHOZ	:	Bulk Density
RJ	:	Al-Raja Field
SFLU	:	Spherically Focused Log
S_{hyd}	:	Hydrocarbon Saturation
Stemp	:	Surface temperature
S_w	:	Water saturation
TD	:	Total depth
V_{sh}	:	Shale volume
YTS	:	Yemen Trap Series
YVS	:	Yemen Volcanic Series
Φ	:	Porosity

LIST OF FIGURES

LIST OF TABLES

SUMMARY

Keywords: Well Logging, Petrophysics, Hydrocarbon Potential, Republic of Yemen, Marib-Shabwah Basin, Sab'atayn Formation, Alif Member, Arabian Plate, Al-Raja.

This study aims to evaluate the hydrocarbon reservoir in Al-Raja Field, which is formed within the Alif Member of the Upper Jurassic age Sab'atayn Formation in the Marib-Shabwah Basin, Republic of Yemen. This study is mainly based on well logging data of seven boreholes. We processed, analyzed, and interpreted the well log data to determine important petrophysics parameters of each well individually, identified the lithology of the reservoir and in consequence evaluated the Alif Member. Schlumberger Interactive Petrophysics (IP) software has been used for this task. Besides, the results obtained from this study have been processed by the means of Surfer program to generate maps of the distribution of hydrocarbon and other petrophysics parameters within the field.

This study indicates that the hydrocarbon present in the reservoir is gas, and the reservoir is mainly dominated by sandstone, but minor amounts of shale are also present. In addition, Alif Member have been divided vertically into three zones ordered from the top downwards: Alif Formation Top, Alif Sandstone A zone, and Alif Sandstone B zone, but the productive zones are Alif Sandstone A, and Alif Sandstone B zones.

Several distribution maps of gross thickness, net pay thickness, shale volume, effective porosity, water saturation, and hydrocarbon saturation were generated using Surfer 17 software. These distribution maps of the Alif Member obtained from the seven wells indicate that the study area is a promising field for continued hydrocarbon exploration due to its petrophysical parameters and it has a good hydrocarbon potential. In fact, the shale content has low values that range between 15.3% and 22.7% and it decreases north-westwards, with high effective porosity values ranging from 12.9% to 19.7% and they increase also in the same direction. The net thickness varies between 100.5 ft and 340.5 ft going higher from the north towards the southern, and the north-eastern areas of the study field. Furthermore, the water saturations range from 11.1% to 23.5% and the values decrease towards the north-west. Finally, the hydrocarbon saturations have high values that range from 76.5% to 88.9% and they increase towards the north-west of the study area.

KUYU LOGLARIYLA REZERVUAR DEĞERLENDİRMESİ: AL-RAJA SAHASI, ALİF ÜYESİ, MARİB-SHABWAH (SAB'ATAYN) BASENİ, YEMEN CUMHURİYETİ

ÖZET

Anahtar Kelimeler: Kuyu Logu, Petrofizik, Hidrokarbon Potansiyeli, Yemen Cumhuriyeti, Marib-Shabwah Havzası, Sab'atayn Formasyonu, Alif Üyesi, Al-Raja.

Bu çalışma, Yemen Cumhuriyetinin Marib-Shabwah Havzasında Üst Jura yaşlı Sab'atayn Formasyonunun Alif Üyesi bünyesinde oluşan Al-Raja Sahası'ndaki hidrokarbon rezervuarını değerlendirmeyi amaçlamaktadır. Bu çalışma temel olarak, yedi sondaj kuyusunun kuyu log verilerine dayanmaktadır. Her bir kuyunun önemli petrofizik parametrelerini ayrı ayrı hesaplamak, rezervuarın litolojisini belirlemek ve sonuç olarak Alif Üyesini değerlendirmek için kuyu log verileri işlenmiş, analiz edilmiş ve yorumlanmıştır. Bunun için Schlumberger (IP) yazılımı kullanılmıştır. Ayrıca elde edilen sonuçlar, hidrokarbon ve sahadaki diğer petrofizik parametrelerinin dağılımının yatay haritalarını çizdirmek için Surfer programından yararlanılmıştır.

Bu çalışma, rezervuarda bulunan hidrokarbonun gaz olduğunu belirlemiş ve rezervuarda kumtaşının hâkim olduğunu, ancak küçük miktarlarda şeylin de bulunduğunu göstermiştir. Bunun yanı sıra, Alif Üyesi üç zona ayrılmıştır. Bunlar: Üst Alif Formasyonu, Alif Kumtaşı A ve Alif Kumtaşı B zonlarıdır.

Surfer 17 aracılığıyla oluşturulmuş yedi kuyuda bulunan Alif Üyesi 'nin dağılım haritaları, çalışma sahasının iyi bir hidrokarbon potansiyelinin olduğunu ve petrofiziksel parametreleri nedeniyle daha fazla hidrokarbon keşfi için iyi bir gelecek vaadeden saha olduğunu göstermektedir. Aslına; şeyl içeriği %15,3 ile %22,7 arasında değişen düşük değerlere sahiptir ve kuzey-batıya doğru gittikçe azalmaktadır. Üstelik, bu saha %12,9 ile %19,7 arasında değişen ve aynı yönde artan yüksek etkin gözeneklilik değerlerine de sahiptir. Suya doygunluk oranları ise %11,1 ile %23,5 arasında değişmekte olup kuzeybatıya doğru daha düşük değerler gözlenmektedir. Son olarak, hidrokarbon doygunluklarının %76,5 ile %88,9 arasında değişen yüksek değerlere sahip olmasının yanısıra çalışma sahasının kuzey-batısına doğru arttığı saptanmıştır.

CHAPTER 1. PLATE TECTONIC & GEOLOGICAL SETTING

1.1. Arabian Plate Tectonic Setting

The Arabian Plate extends over most of the regions known as the Arab Middle East, which covers the Arabian Peninsula together with some northern Arab countries (Wagner, 2011). It is one of the youngest and smallest lithospheric plates of the Earth (see Figure 1.1.). The Arabian Plate was formed 25 million years ago by the rifting of the NE Africa Plate to form the Red Sea and the Gulf of Aden (Stern and Johnson, 2010). It extends from the Red Sea in the west to the Zagros in the east, which is the convergence zone between the Arabian and Eurasian Plates (Hessami, Nilforoushan and Talbot, 2006; Tavakoli-Shirazi *et al.*, 2013), and from the Gulf of Aden in the south to the Taurus Mountains in the north (Vita-Finzi, 2001).

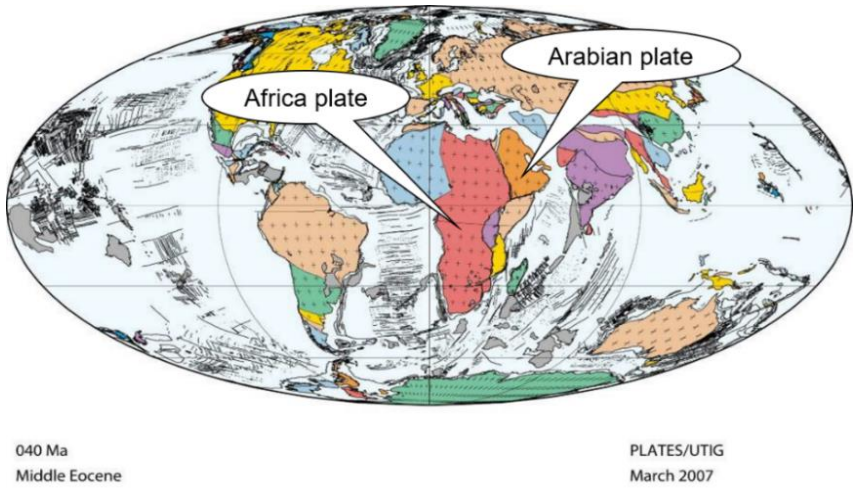

Figure 1.1. Position of Arabian and Africa plates 40 million years ago (Lawver et al., 2007)

At present, the Arabian Plate is home to the countries illustrated in Figure 1.5. which are as follows: Yemen, Kuwait, Bahrain, Qatar, the United Arab Emirates, Oman, Saudi Arabia, Syria, Jordan, and Iraq (Geert *et al.*, 2001).

The present Arabian Plate's boundaries include all kinds of tectonic regimes, as seen in Figure 1.2. They include collision in the Bitlis and Zagros sutures zones, rifting and sea-floor spreading in the Gulf of Aden and the Red Sea, subduction along the Makran zone, and transform movement along the Dead Sea and Owen-Sheba fault zones (Geert *et al.*, 2001).

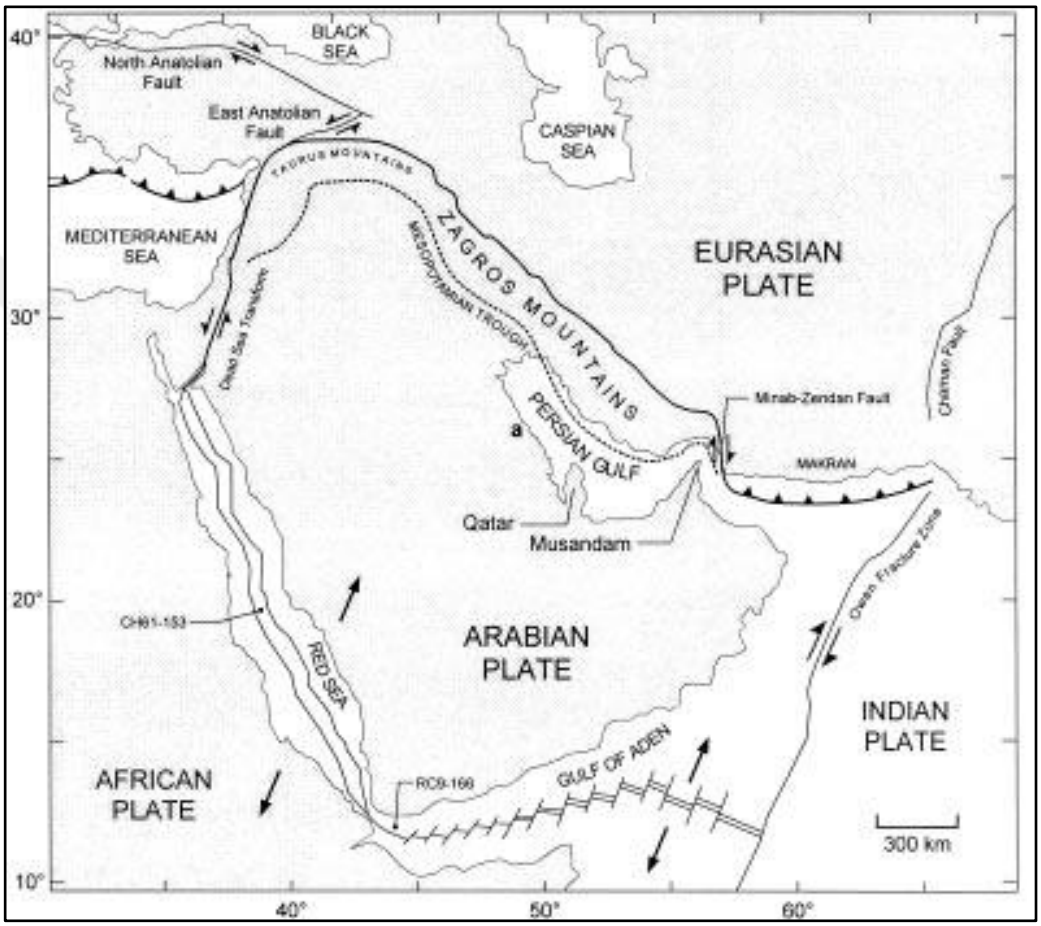

Figure 1.2. Location map showing the tectonic setting of the Arabian plate (Vita-Finzi, 2001)

Recent studies (especially in the last 30 years) have achieved important advances concerning the driving forces behind plate tectonics (McQuarrie *et al.*, 2003). The new constraints indicate that the convergence of Arabia-Eurasia has been rather constant at 2 to 3 cm/yr since 56 million years ago, but since about 25 million years ago, the motion of Africa-Eurasia has slowed down to become less than 1 cm/yr. Thus, as a result of these events, the Arabian Plate moved away from Africa about 25 million years ago, which led to the rifting of Africa and Arabia, and this resulted in opening

the Red Sea as well as the Gulf of Aden as shows Figure 1.3. (Johnson, 1998; McQuarrie *et al.*, 2003).

By the progression of the Red Sea's expansion, the northward subducting Neotethys Ocean has been closed in the northeast about 10 million years ago and the Arabian Plate ultimately collided with Eurasia (Figure 1.4.). This collision zone is defined by the Bitlis-Zagros Fold and Thrust Belt (McQuarrie *et al.*, 2003; Hessami, Nilforoushan and Talbot, 2006; Stern and Johnson, 2010).

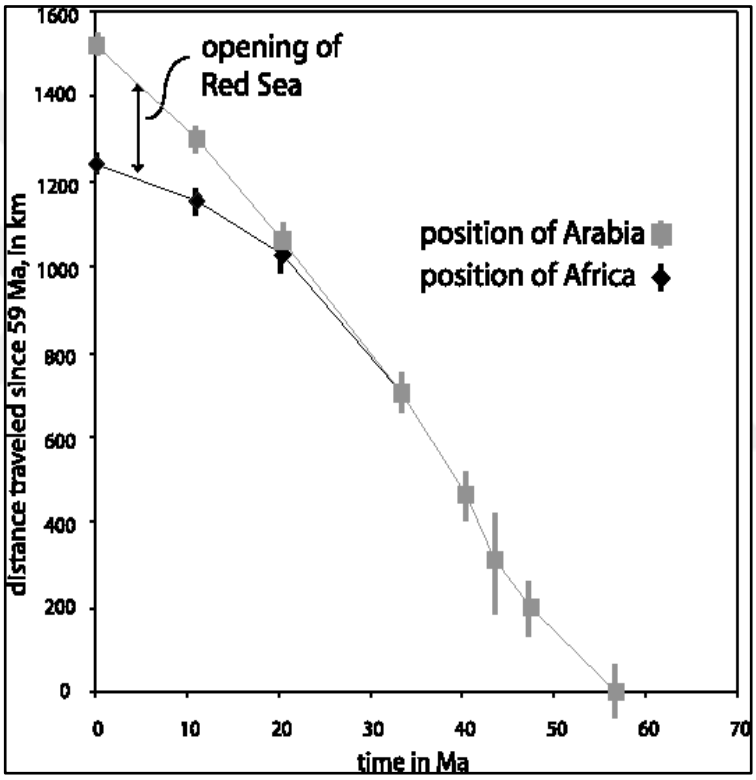

Figure 1.3. Graph describing the opening of the Red Sea (McQuarrie *et al.*, 2003)

The Arabian Plate has developed according to these main stages (Wagner, 2011):

- The plate's basement rocks were formed as part of the Nubian-Arabian craton during the Precambrian era.
- During the Paleozoic era to the Permian, the sector including the present Arabian Plate was a marginal shelf on the Gondwana supercontinent.

- In the early Mesozoic era was the development of the plate boundaries on the northwest, north, northeast, and southeast margins in parallel with the opening of the Indian Ocean and the Neo-Tethys.
- During the middle until the late Tertiary, the collision of the Eurasian Plate with the Arabian Plate resulted in the compression and the modification of the northeastern and the northern margins of the plate. Meanwhile, the rifts in tectonics opening the Red Sea, the Gulf of Aden, and the Dead Sea Graben created the south and southwest margins and a new northwest margin.

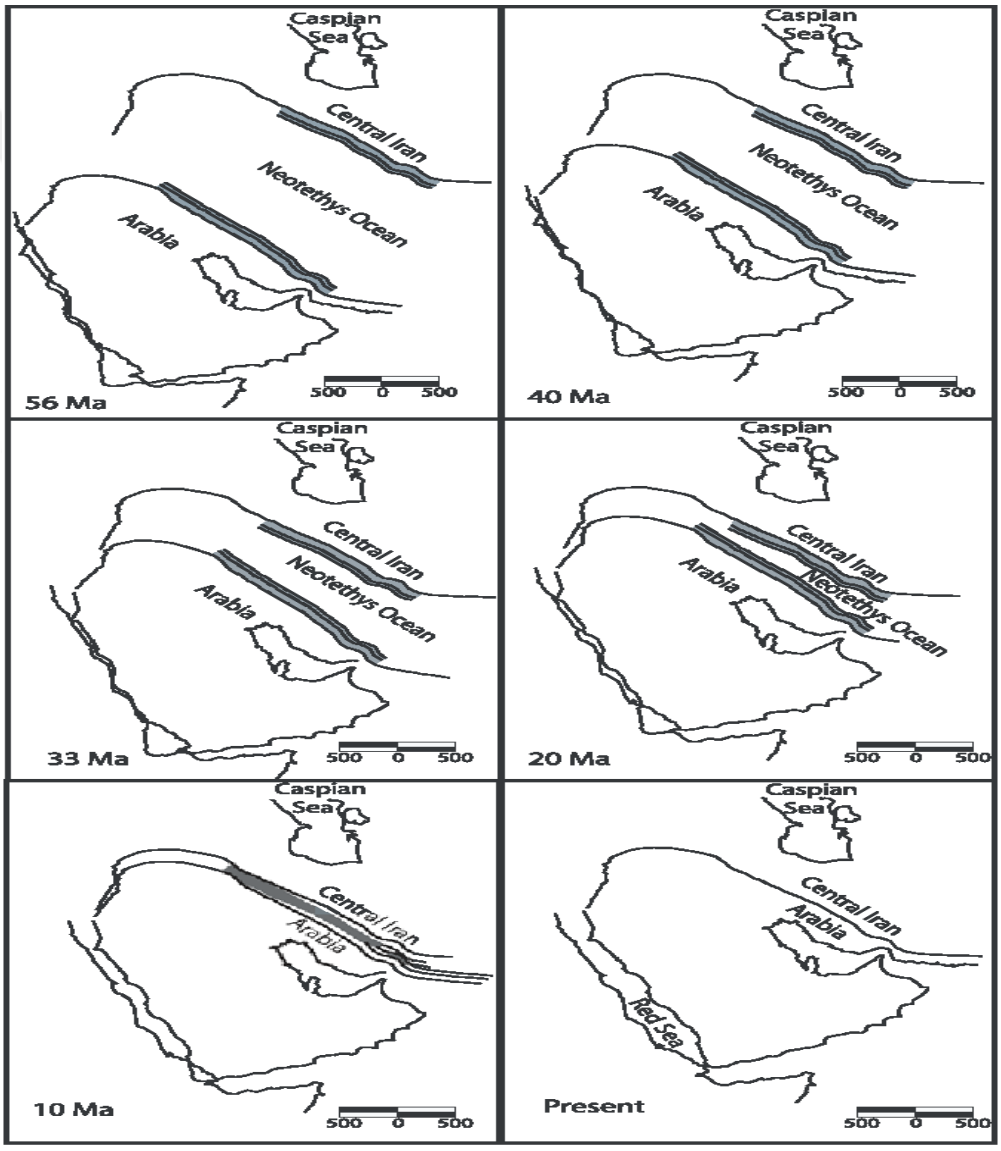

Figure 1.4. Maps showing the relationship between the collision of Arabia and Eurasia and the opening of the Red Sea. The gray-shaded represents the size of the shortened crust in Eurasia (80 km) and on the Arabian plate (70 km). Narrower (inside) bands represent passive margins (50 km) on both the north and south side of the Neotethyan ocean basin (McQuarrie *et al.*, 2003)

The Arabian Plate is made up of two major geological units: the Arabian Shield and the Arabian Shelf (Wagner, 2011).

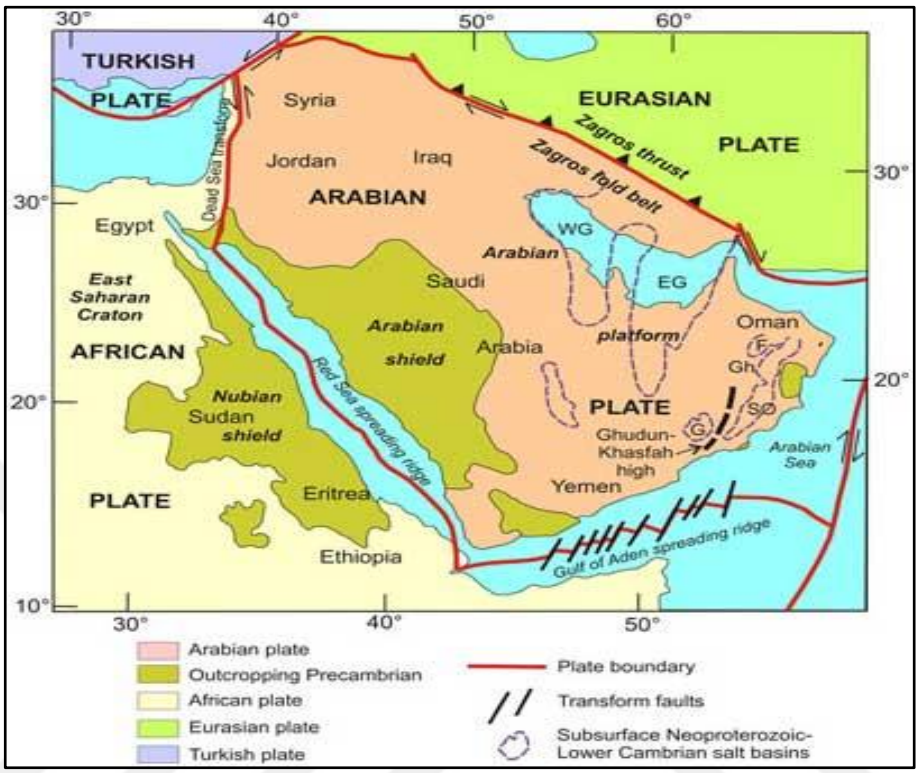

Figure 1.5. Outcropping Precambrian rocks in the Arabian plate (Gad and Kusky, 2007)

1.1.1. Arabian shield

The Arabian shield occupies the west and southwestern parts of the Arabian Plate extending over about 770,000 km^2 from Yemen across western Saudi Arabia into Jordan (Wagner, 2011) as seen in Figure 1.5.

The Precambrian parts of both the northeast of Africa and the Arabian Shield were connected till the early Tertiary forming the Nubo-Arabian Shield. The Arabian Shield has a Precambrian basement sequence of a thickness of about 9-15 km. It is generally composed of volcanic, igneous, and metamorphic rocks and has been penetrated extensively by granitic plutons. The "basement gneiss" represents the oldest rocks exposed on the Arabian shield and it exists mainly in intrusive or diapiric structures (Wagner, 2011).

The Precambrian rocks outcrop in the western third of Saudi Arabia and some parts in Yemen and Jordan, which are referred to as the Arabian Shield. Precambrian rocks also outcrop locally in some parts in Oman (see Figure 1.5.) (Johnson, 1998). By the end of the Precambrian era, most of the Arabian Plate constituted an eroded peneplain, and since then, the shield has been, to some extent, a stable landmass (Wagner, 2011).

1.1.2. Arabian shelf

The Arabian Shelf is located in the northern and eastern parts of the Arabian Plate (Figure 1.6.), which extends from the boundaries of the Arabian Shield to the margins of the Arabian Plate in the north, east, and northwest. The Arabian shelf was inundated during several periods of marine transgression from the Palaeozoic era until the early Cenozoic by epicontinental seas (Wagner, 2011).

1.2. Geological Setting of Yemen

1.2.1. General location of Yemen

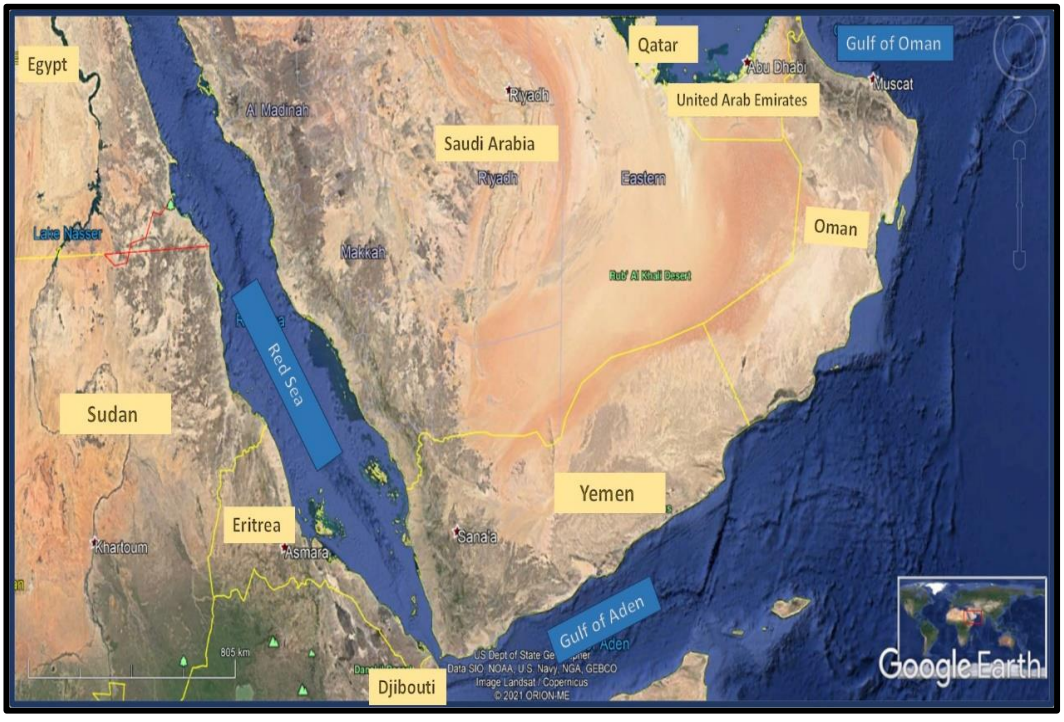

Figure 1.6. Location and boundaries of Yemen in the Arabian Plate (*Google Earth 7.3.3*, 2020)

Yemen is situated between latitudes 12˚ and 19˚ N, and between longitudes 42˚ and 53˚ E in the southwestern part of the Arabian Peninsula, as shown in Figure 1.6. and Figure 1.10. (As-Saruri, Sorkhabi and Baraba, 2010). It covers an area of approximately 536,870 km^2 (Beydoun *et al.*, 1998). Yemen shares land boundaries with Saudi Arabia (1458 km) to the north and Oman (288 km) to the east, as seen in Figure 1.5. Yemen also has maritime boundaries to the west by the Red Sea and the south by the Gulf of Aden and the Arabian Sea, which is part of the Indian Ocean (As-Saruri and Sorkhabi, 2014).

1.2.2. General stratigraphy of Yemen

Yemen's geology consists mainly of the Cenozoic volcanic, the sedimentary cover, and the basement rocks (Al-Azazi, 2010), as shown in the geologic map in Figure 1.8. and the geologic column in Figure 1.9.

1.2.2.1. Basement rocks

Yemen's geology is generally related to the geology of the Arabian Plate (Peninsula). The geology of the Precambrian basement rocks of Yemen belongs to the geology of the Arabian Shield, a part of the Arabian Nubian Shield (Figure 1.5. and Figure 1.6.). In other words, geologically, the overall structure of west Yemen represents the domination of the Precambrian Arabian Shield, while a thick and extensive Phanerozoic sub-horizontal sediments cover dominates the east. The southeast of the Arabian–Nubian Shield is represented by the Precambrian basement igneous and metamorphic rocks of the country (Van der Gun and Ahmed, 1995; Beydoun *et al.*, 1998; As-Saruri, Sorkhabi and Baraba, 2010; Veeningen *et al.*, 2015; PEPA, no date a). Figure 1.8. shows the terranes represented by the Precambrian rocks in Yemen:

- Asir terrane: extends from Saudi Arabia to Yemen and contains an arc-type volcanic and a basement gneiss (Albaroot *et al.*, 2016). This terrane's isotopic data is unavailable for the Yemeni side, but its age was assigned as 840-740 Ma in Saudi Arabia's side (Whitehouse *et al.*, 2001).

- Abas terrane: dominated by gneiss and metasedimentary rocks and metavolcanics in gneiss (Albaroot *et al.*, 2016).
- Al-Bayda terrane: formed in arc environment, and it is predominantly consisting of schist and meta-volcanics (Albaroot *et al.*, 2016).
- Al-Mahfid terrane: consists mainly of granite and gneiss (Albaroot et al., 2016).
- Mukalla terrane: largely consisting of granites (Albaroot *et al.*, 2016).

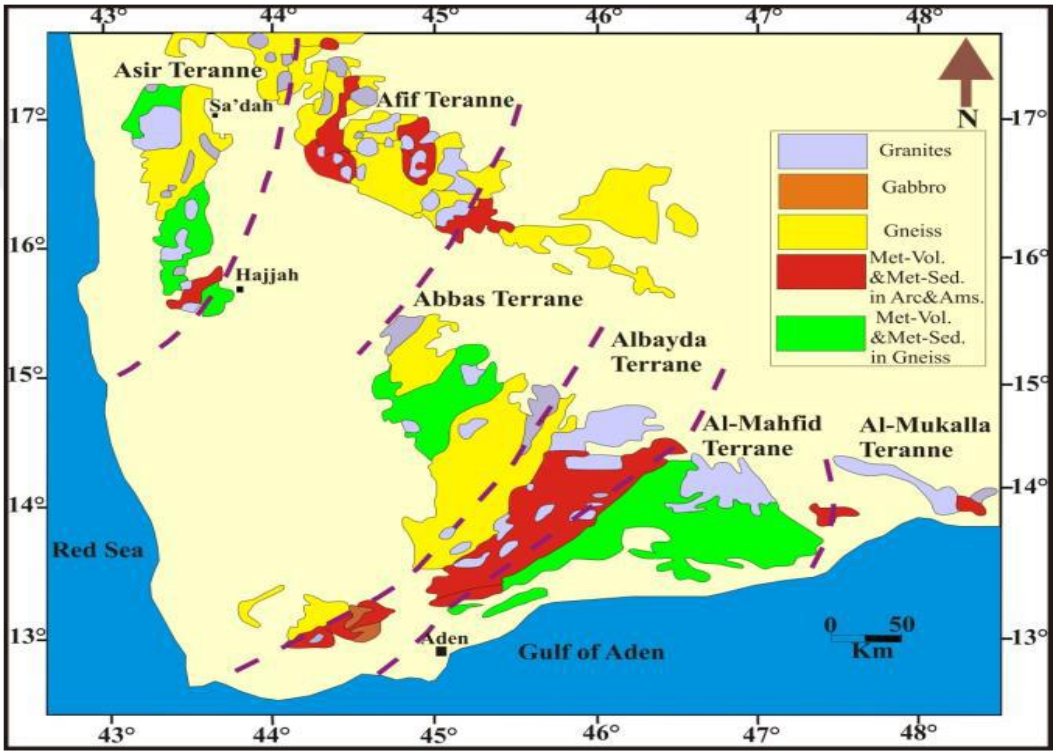

Figure 1.7. Distribution of the basement rocks in Yemen (Albaroot *et al.*, 2016)

1.2.2.2. Sedimentary cover

The sedimentary rocks extend over large areas in Yemen, and most of these rocks belong to the Mesozoic and Cenozoic geological periods except the Wajid formation (sandstone) and the Akbara Formation (shale), which are confined to the north-western region of Yemen (Sa'ada region). These rocks were formed in the Paleozoic age. As seen in Figure 1.7., Amran, Tawilah, Hadramout, Tihama, and other groups are examples of the sedimentary groups in Yemen (Beydoun *et al.*, 1998).

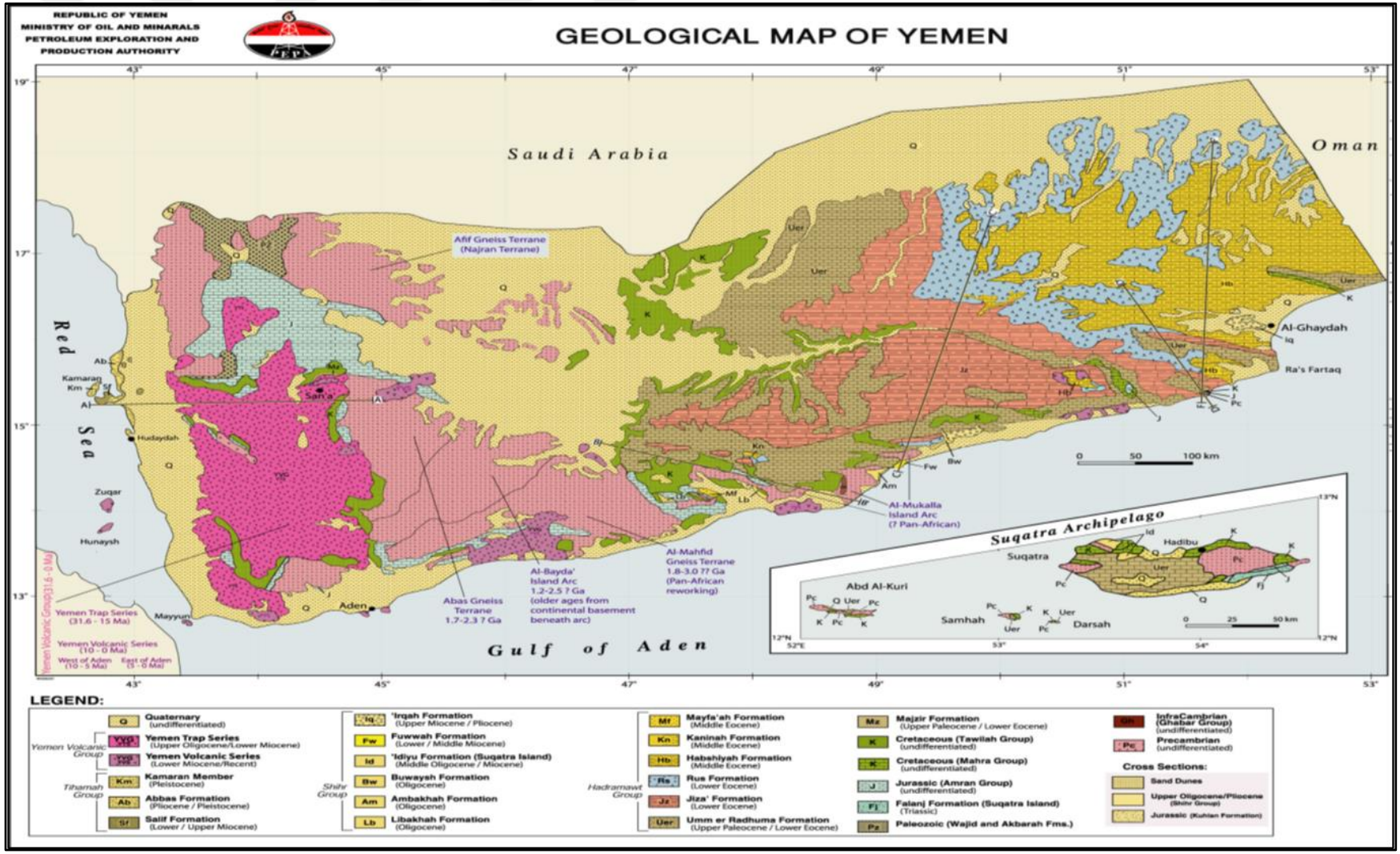

Figure 1.8. Geological map of Yemen (As-Saruri, 2004)

1.2.2.3. Yemen volcanic group

The Yemen Volcanic Group includes all the Cenozoic volcanic rocks, which are related to the opening of the Red Sea and the Gulf of Aden and are divided according to their geological age into:

- Yemen Trap Series (YTS): These series occupy the Yemen volcanic group's lowest part and represent the extended volcanic activities at varying periods since the Oligocene to the early Miocene, which resulted in the formation of thick series of volcanic rocks. The thickness of the YTS reaches its maximum value in the western parts (2500 m of different volcanic rocks), and it goes lower eastward to become some tens of meters. The YTS extends over an area of almost 45,000 km^2 of Yemen containing basalt, andesite, trachyte, rhyolite, and volcanic glass. This type of series exists in some areas such as Sana'a, Sumara, Taiz (YGSMR, no date; Albaroot *et al.*, 2016).

- Yemen Volcanic Series (YVS): represent volcanic activities that occurred during various periods since the lower Miocene and dominated in the Quaternary. They are thinner than YTS with a thickness of a few hundreds of meters and cover separated areas in Yemen. YVS are divided according to the volcanic rocks' age into older and younger volcanic rocks. The older volcanic rocks (10-5 Ma) intruded western Aden, and the younger ones (5-0 Ma) exist in East Aden. Northwest of Sana'a, Amran, Marib, and Bir Ali are examples of where the Yemen Volcanic Series are found (PEPA, no date a; YGSMR, no date).

The geologic map of Yemen (Figure 1.8.) shows a variety of structures between the western and eastern parts of the country. As seen in that figure, west Yemen is mostly highlands formed of Cenozoic volcanic caps and a Pre-Cambrian basement, whereas the east is predominated by lowlands and a sedimentary cover (As-Saruri and Sorkhabi, 2014).

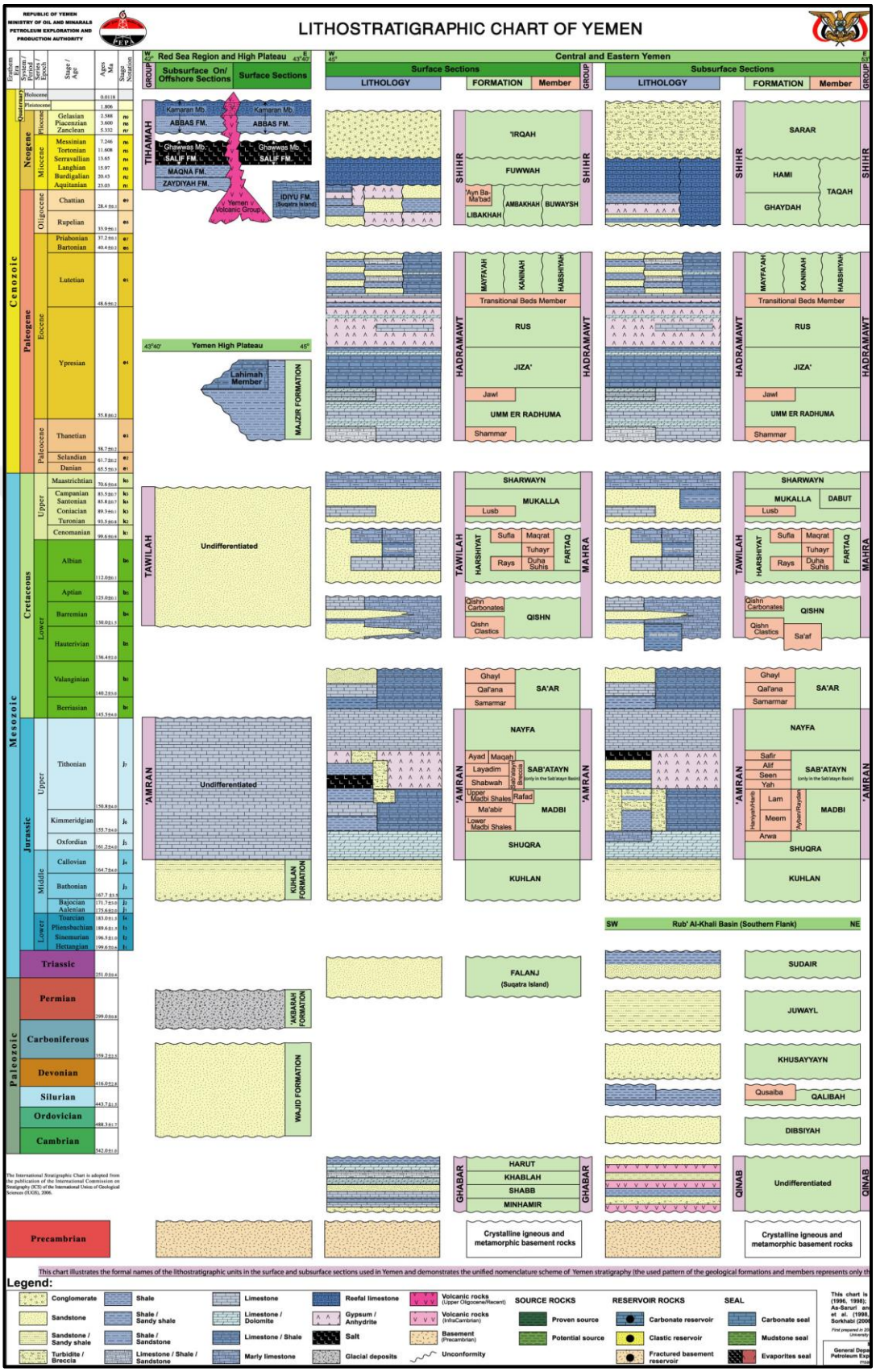

Figure 1.9. Lithostratigraphy chart of Yemen (As-Saruri, 2003 ⁄2004)

1.2.3. Sedimentary basins of Yemen

Figure 1.10. shows the Yemen's main Phanerozoic basins. The majority of the shown basins are divided into sub-basins and are separated by high structures as a result of rift systems: the Late Jurassic and the Red Sea rifting (Al-Azazi, 2010; As-Saruri, Sorkhabi and Baraba, 2010; As-Saruri and Sorkhabi, 2014). The Yemen sedimentary basins are grouped according to the geological age (see Figure 1.10.) to Cenozoic basins, Mesozoic basins, and Paleozoic basins (Al-Azazi, 2010; As-Saruri, Sorkhabi and Baraba, 2010; As-Saruri and Sorkhabi, 2014).

1.2.3.1. Paleozoic basins in Yemen

- Rub'al Khali (the Empty Quarter) Basin: This basin extends over a large area in Saudi Arabia, having its southern flank shared with Oman and Yemen (Figure 1.10.). This southern flank is longer than 650 km along with the Hadramawt Arch, and its wideness is between 70 km and 100 km. The thickness of its sedimentary column increases from 2 km to 4 km as we move from the arch of Hadramout to the border of Yemen and Saudi Arabia. The southern flank of the Rub' Al-Khali Basin is considered the oldest basin in Yemen (Beydoun *et al.*, 1998; As-Saruri, Sorkhabi and Baraba, 2010). The part of the Rub’ Al-Khali Basin that exists in Yemen is thought to contain productive source rocks by analogy with the central part of Saudi Arabia, but there is no comprehensive and detailed exploratory study of the basin yet (As-Saruri, Sorkhabi and Baraba, 2010)**.**

- Sana'a Basin: It is situated in the northwestern part of Yemen, specifically in the northwest of the capital Sana'a (Figure 1.10.). The Paleozoic sediments in this basin are overlined by a thick sedimentary succession from the Jurassic age of the Mesozoic era (Al-Azazi, 2010).

- Socotra Basin: It exists in the southwest and the south of Socotra, the

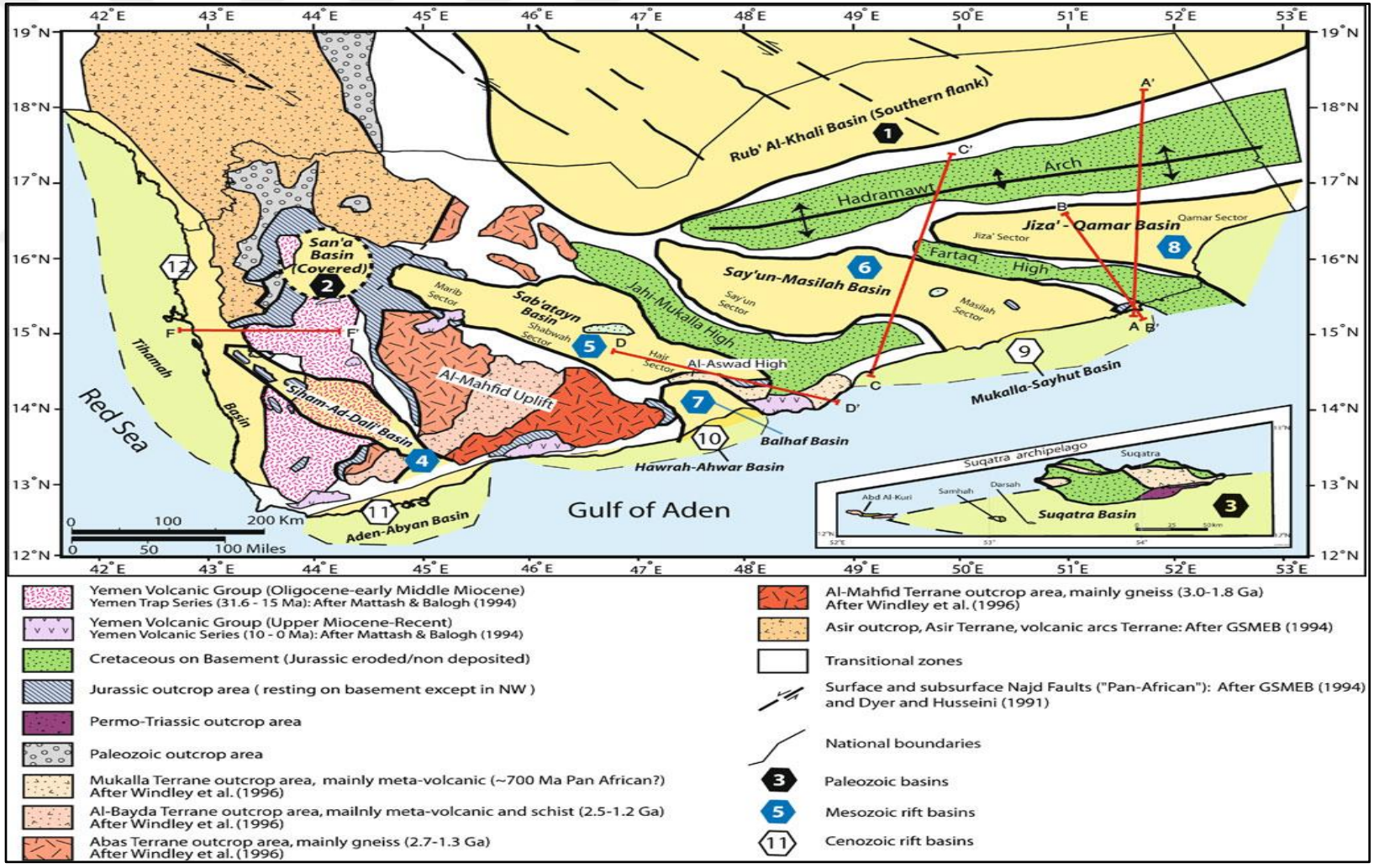

Figure 1.10. Map showing the outcrop geology, sedimentary basins and main structural highs of Yemen (As-Saruri, Sorkhabi and Baraba, 2010)

archipelago. It was considered as a part of the Mesozoic rifting till the realization of the new marine drillings, and the comparison of the Socotra Basin with some of the East African Karoo Basins showed that they have similar Karoo-type sedimentations and therefore proved that the development of this basin was the product of the Late Karoo rifting (Al-Azazi, 2010; As-Saruri, Sorkhabi and Baraba, 2010).

1.2.3.2. Mesozoic basins in Yemen

Tectonic stresses are related to the Gondwana's disintegration, the rifting between west India and Afro-Arabian Plate along the old Najd fracture, and the opening of Indian Ocean in the early Mesozoic era. All these events affected the Arabian plate including Yemen along the Najd Fault System existing in the western part of the Arabian Peninsula specifically during the Jurassic Period which ends by a series of rift basins across Yemen (Beydoun *et al.*, 1998; Al-Azazi, 2010; As-Saruri, Sorkhabi and Baraba, 2010). Researches indicate that there is no association of these basins with any volcanic activity related to the rifting (As-Saruri and Sorkhabi, 2014). As a result, five basins formed successively from the west to the ESE, having almost the same direction as the Najd Fault System (NW-SE) but with the angles of the rift orientation gradually becoming smaller as shown in Figure 1.10. Siham-Ad Dali' Basin is the basin formed to the west with the direction NNW–SSE. It is followed to the east by the Balhaf Basin and the Sab’atayn Basin, which are sub-parallel to each other and oriented to the NW–SE.

In the center, there is the Say’un-Masilah Basin having a direction WNW–ESE. Finally, Jiza’–Qamar is the easternmost basin. It is almost oriented in E–W (see Figure 1.10.) (Bosence, 1997; Beydoun *et al.*, 1998; Al-Azazi, 2010; As-Saruri, Sorkhabi and Baraba, 2010; As-Saruri and Sorkhabi, 2014). The sedimentary sequence of the Mesozoic basins of Yemen has a thickness of about 4–6 km in the east versus 1.8–3 km in the West (As-Saruri, Sorkhabi and Baraba, 2010).

As mentioned before, the Mesozoic basins' locations were affected by the basement grain of the Najd fault system. Besides, the structure of different sectors of these basins was also influenced by the activity of the same fault system at different times. In fact, the localized, sporadic, and brief pulses of the activity and the erosion of the Najd Fault resulted in the incidental subsidence of the Mesozoic basins and the lift of structural differentiation into horsts between the basins, half-grabens, and sub-basins (As-Saruri, Sorkhabi and Baraba, 2010). The Mesozoic basins of Yemen are, indeed, grabens (see Figure 1.11.) rather than wholly developed basins (As-Saruri and Sorkhabi, 2014).

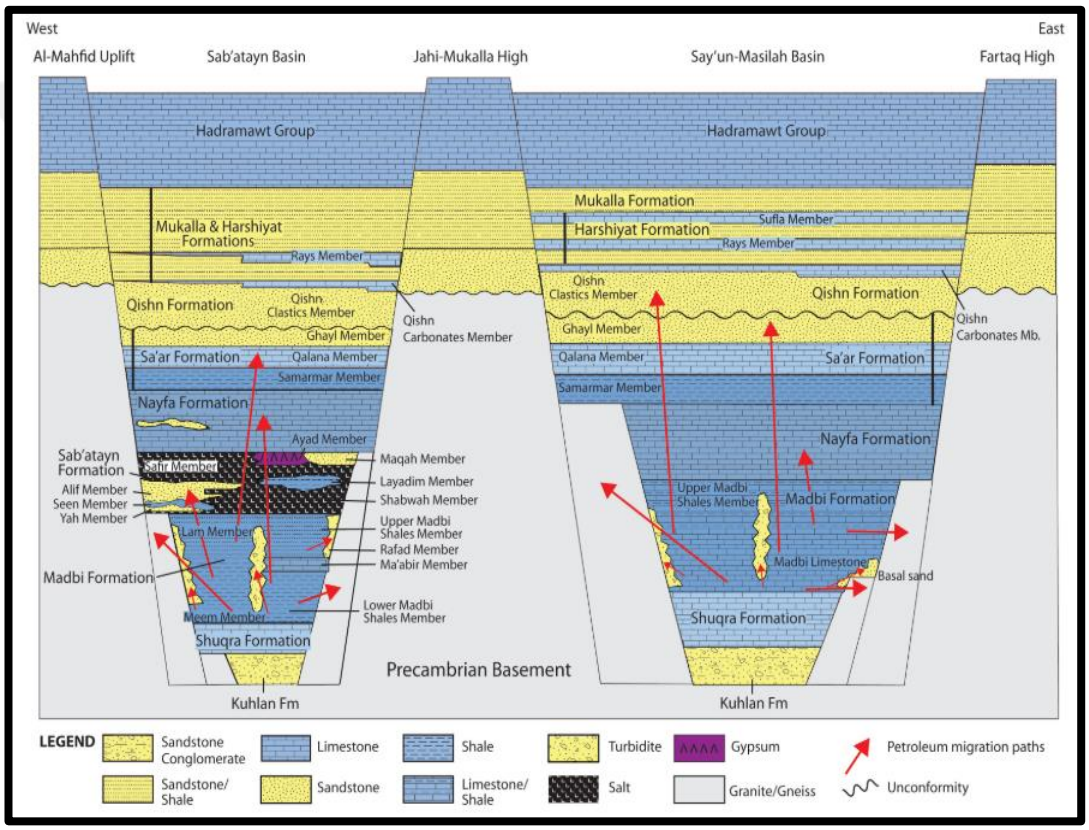

Figure 1.11. A simplified cross-section showing examples of the grabens and horsts through the Mesozoic basins and hydrocarbon migration paths (As-Saruri and Sorkhabi, 2014)

The intra-basin sedimentation and the way of the generation, the movement, and the accumulation of hydrocarbons in the basins mentioned earlier were influenced by the intra-basin highs and lows caused by the episodic tectonic extension. These events made the Say'un–Masilah Basin and the Sab'atayn (Marib-Shabwah) Basin the only hydrocarbon producers in Yemen up to now (As-Saruri, Sorkhabi and Baraba, 2010).

The sediments thickness and distribution of the Mesozoic basins were also controlled by the large structures of the paleo-highs shown in Figure 1.10. and Figure 1.11. which contain:

- The Fartaq High between the Jiza'–Qamar Basin and the Say'un–Masilah Basin.
- The Jahi–Mukalla highs that separate the Say'un– Masilah Basin from the Sab'atayn.
- The Jabal Al-Aswad highs separating the Hajr sector located in the southern Sab'atayn Basin from the Balhaf Basin.
- The uplift of the Mahfid basement (ANS Precambrian terranes) between the Sab'atayn Basin and the Siham–Ad-Dali Basin (As-Saruri, Sorkhabi and Baraba, 2010).

The Hadramout Arch is a large lineament that separates the Paleozoic Rub' Al-Khali Basin in the northern side from the Jiza'–Qamar Basin and the Say'un–Masilah Basin situated in the southern side (see Figure 1.10.). It appears that the Hadramout Arch was a structural barrier, which had continued to exist from the early Paleozoic era and had periodic activities since then (As-Saruri, Sorkhabi and Baraba, 2010).

1.2.3.3. Cenozoic basins in Yemen

The Cenozoic basins (also called Tertiary basins) are importantly associated with the Neogene subsidence, which is related to the opening as well as the expansion of the Red Sea and the Gulf of Aden; and these are the result of the separation and the continuous movement of divergence of the Arabian Plate and Africa. The four basins that have appeared in the Cenozoic era are the Tihama, the Aden–Abyan, the Hawrah-Ahwar, and the Mukalla–Sayhut Basins. As seen in Figure 1.12., these basins are, for the most part, situated offshore along the Red Sea and the Arab Sea through the Gulf of Aden. The Mukalla–Sayhut, Hawrah–Ahwar and Aden–Abyan extend parallel to the trending of the Gulf of Aden (ENE -W) while the Tihamah Basin has as a direction

NNW-SSE being parallel to the Red Sea (Al-Azazi, 2010; As-Saruri and Sorkhabi, 2014).

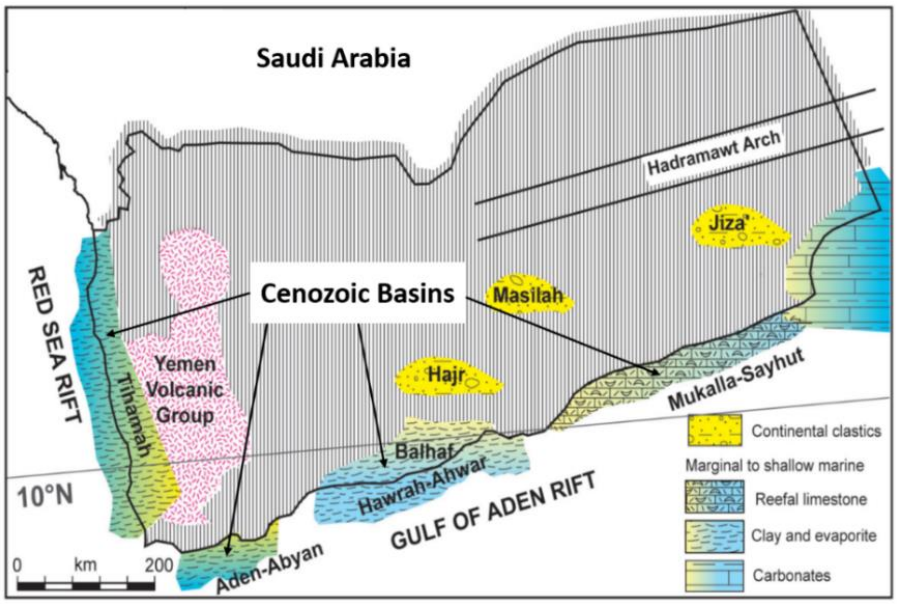

Figure 1.12. Map showing the Cenozoic basins in Yemen (As-Saruri and Sorkhabi, 2014)

1.3. Study Area: Al-Raja Field, Marib-Shabwah (Sab'atayn) Basin

All the oil and gas produced in the Republic of Yemen was produced from 13 blocks out of 105 blocks until the outbreak of the current war in 2015. All these blocks were producing from two main basins: the Say'un–Masilah Basin and the Marib-Shabwah Basin (PEPA, no date c). The Marib-Shabwah (Sab'atayn) Basin is divided into two sub-basins: the Shabwah sub-basin to the southeast, and the Marib-Aljawf sub-basin to the northwest of the basin (Alaug *et al.*, 2011), to which the Block-18 belongs. This block contains the study area Al-Raja Field (PEPA, no date b).

The Block-18 is a producing block located in the Marib Al-Jawf sub-basin (or sector) of the Marib Shabwah (also called Sab'atayn) Basin in central Yemen extending from Shabwah to Al-Jawf provinces through Marib province. The Block-18 is about 100 km away from the Yemeni capital, Sana'a (Woodmakenize, 2019), with an area of about 8,479 km^2 (PEPA, no date b).

The first production well in Yemen was drilled in the Alif Field in this block in 1986. The major reservoir rocks of the Block-18 are Alif and Seen sand members in the Sab'atayn Formation. The Block-18 is generally one of the largest blocks that produce oil and gas in Yemen and includes 14 oil and gas fields, as shown in Figure 1.13.a. and b. The total wells drilled in this block were 692 until the end of 2011. This block is operated by Safer Company (SEPOC) (PEPA, no date b).

The Al-Raja (RJ) Field is the study area of this work. It is a gas condensate field situated on the southeastern boundary of the block-18 between (618000 - 638000 m E) and (1716000 -1730000 m N) in the UTM system. Figures 1.13.a., b and c show the RJ Field as one of the largest fields of the Block-18 with an area of 15284.814 acres (61,855 km^2). The reservoir of the Al-Raja Field is bounded on the South, West, and North by major faults and on the southeast by GWC. The structure of the reservoir extends to the east across the Block-18 crossing the boundary into the adjacent block, Jannah Block (see Figure 1.13.b.) (SEPOC, 2012).

The RJ Field was discovered by drilling the first well (RJ-01) in 1989. At first, it was thought that the part of the field which is located in its north is a separate field having the name Dostour Al-Wihdah (DW) until a test was realized on the RJ-04 and DAW-01 and the fact that they are producing from the same reservoir (Alif sand reservoirs) was found out.

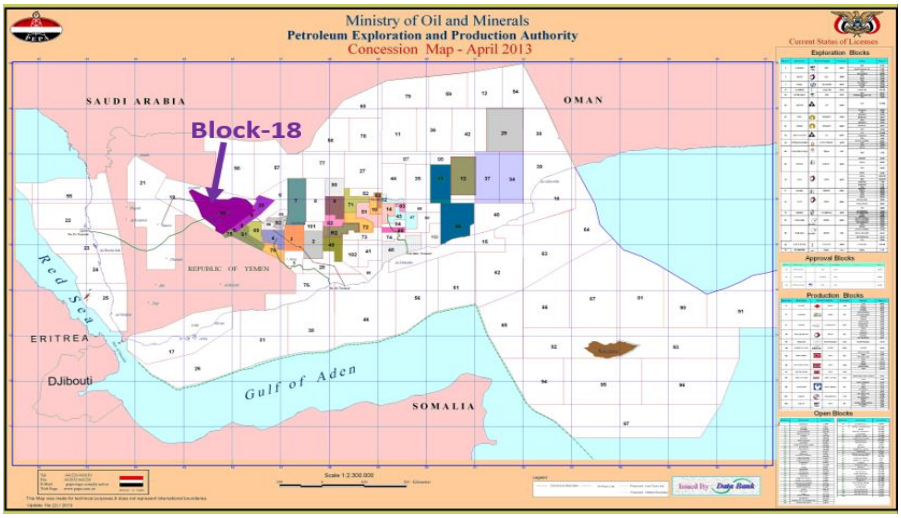

(a)

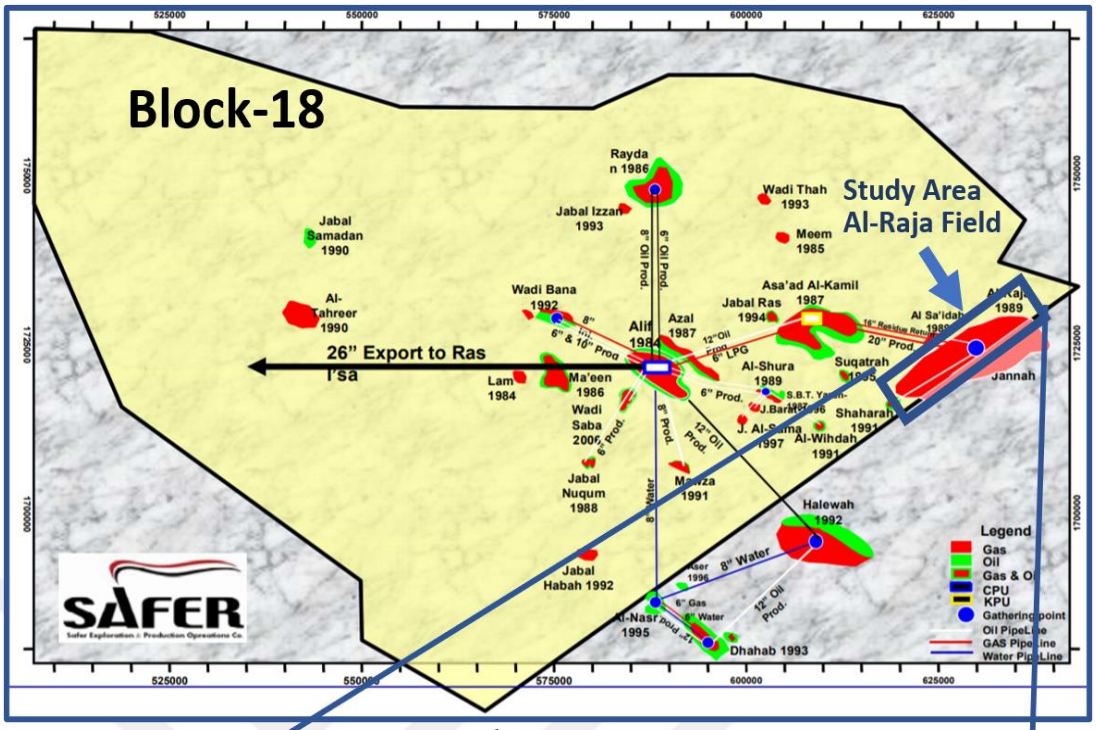

(b)

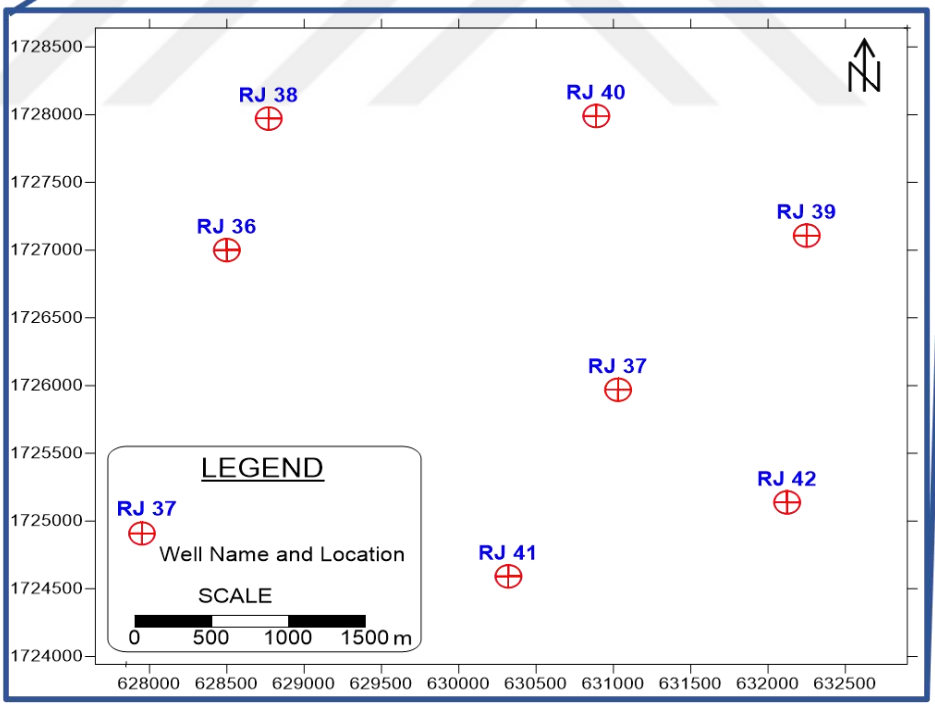

(c)

Figure 1.13. Map showing (a) the distribution of blocks in Yemen (Ministry of Oil and Minerals, 2010) (b) the location of the Al-Raja Field and other Oil-Gas fields in the Block-18 (Gunawan and Al-abbasi, 2011) (c) the location of the study wells within the Al-Raja Field obtained by Surfer 17

Actually, in spite of the connection of the Alif sand reservoirs, they are different in terms of quality and this is what makes them divided into two main units: Alif A and Alif B. Petrophysically, the quality of Alif A is better than Alif B (Gunawan and Al-abbasi, 2011; SEPOC, 2012).

1.4. Evolution of Marib – Shabwah Basin

The tectonic development of Yemen has taken place in two significant tectonic periods. The first major tectonic activities occurred in the period between the Late Jurassic to the Early Cretaceous, and the second period events occurred in the Cenozoic period. The Sayun–Masila and the Marib-Shabwah Basins were developed as a result of the first tectonic activities. They generally include thousands of meters of Jurassic deposits, while the opening of the Red Sea and the Gulf of Aden, the formation of new sedimentary basins in Yemen and the reactivation of the basins formed in the Mesozoic period were the result of the second tectonic events in the Cenozoic (Redfern and Jones, 1995; McQuarrie *et al.*, 2003; Csato, 2005; As-Saruri and Sorkhabi, 2014).

As noted in previous sections, the hydrocarbons are mainly produced from two rift basins in Yemen: The Marib-Shabwah (Sab'atayn) Basin in west Yemen and the Sayun–Masila Basin in east Yemen. These major basins are indeed grabens separated by a structural high known as the Jahi- Mukalla High and it was shown in Figure 1.10. In some references, these basins are referred to as sub-basins or grabens (Al-Azazi, 2010; As-Saruri, Sorkhabi and Baraba, 2010).

Geologically, the Sab'atayn (Marib-Shabwah) Basin belongs to the Late Jurassic age, however its roots belong to major events that occurred from 955 Ma to 615 Ma years ago and to the Najed fault systems that developed in the western part of the Arabian Peninsula during the period from 620 to 540 Ma (Stern, 1985; Al-Azazi, 2010).

Beydoun *et al.*, (1998) divided the Marib-Shabwah Basin rifting into three sectors Marib or Marib-Aljawf sector, Shabwah sector, and Hajar sector in a row from the

northwest to the southeast, as shown in Figure 1.10. The northwest-southeast-trending Marib Shabwah Basin is considered a Mesozoic rift basin, as mentioned before. The evolution of the Marib-Shabwah Basin occurred through three important tectonostratigraphic stages during the Jurassic period, which are sorted from the oldest as following (Brannan *et al.*, 1999; Hakimi and Abdullah, 2015):

1.4.1. Pre-rifting phase (Permian-Oxfordian)

In this stage, the Mesozoic pre-rift sequence contains a basement composed predominantly of metamorphosed complexes belonging to the Archean to Cambrian periods. It also includes other formations such as the Kuhlan Sandstone (non-marine and shallow-marine clastic rocks) deposited in the Lower-Middle Jurassic and the Shuqra Limestone (shallow-marine carbonates). The Kuhlan Formation is overlain by marine transgression that grades into shallow marine Carbonates of the Shuqra Limestone Formation (As-Saruri, Sorkhabi and Baraba, 2010; Sachsenhofer *et al.*, 2012; Hakimi and Abdullah, 2015).

1.4.2. Syn-rifting phase (Kimmeridgian – Tithonian to Early Berriasian)

This rift started in the Kimmeridgian, and its activity lasted until the Early Berriasian. The interbedded fault blocks and horsts (late Jurassic - lower Cretaceous) are the main characteristics of the sequence of this stage, in which the Madbi and Sab'atayn Formations developed. First of all, the Meem Member deposited containing source rocks and reservoir rocks (sandy turbidites), and over it deposited the basin's one of the most prolific oil source rocks: the Lam Member. These lower Meem and upper Lam Members developed during the Kimmeridgian age, and they together form the formation called Madbi. The deposition of late syn-rift of the Sab'atayn sequence occurred throughout the Tithonian period.

The Sab'atayn Formation is composed of a thick sequence of sandstones, evaporites, and shale (Figure 1.14.). It consists of four members sorted upward to the Yah, Seen, Alif, and Safer Members (Figure 1.11. and Figure 1.14.). The most productive

reservoir rocks in the Marib-Shabwah Basin is the Alif Member covering more than 90 % of recoverable hydrocarbon (oil and gas). However, Safir Member, which is mainly dominated by halite also contains sandstones with intra-evaporate and minor

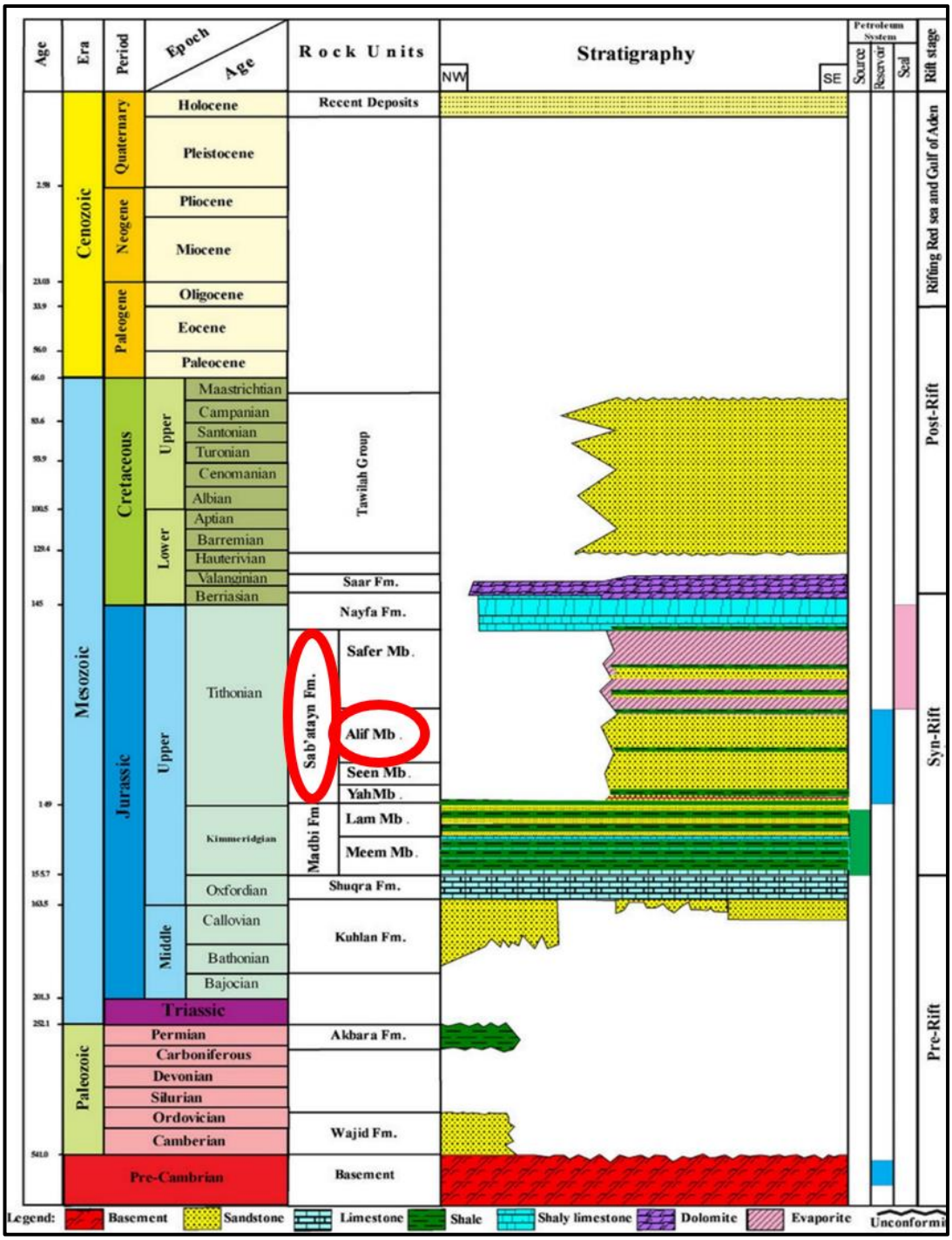

Figure 1.14. Stratigraphic nomenclature showing the evolution stages of Marib Shabwah (Sab'atayn) Basin, Yemen (Al-hasani *et al.*, 2018)

mudstones (see Figure 1.15.). It is considered an excellent seal rock for the reservoirs of the Alif Member. It also includes minor local hydrocarbon reservoirs, which contain evaporite deposits internally (Figure 1.14.). During the late Jurassic age, the oceans' extent became limited in the Marib-Shabwah Basin, and a massive quantity of halite continued to deposit through the Safer Member of the Sab'atayn Group. Actually, the thickness of the Sab'atayn sequence is controlled to a great extent by salt tectonics. From the last period of the Upper Jurassic to the Earliest period of the Cretaceous, the subsidence rate of the rift system had become lower associated with the beginning of the deposition of the Nayfa Formation through shallow-marine shelf by carbonate accumulation (Sachsenhofer *et al.*, 2012; Hakimi and Abdullah, 2015). More detailed geologic information about these formations is given in 1.4.

1.4.3. Post-rifting stage (early Cretaceous – upper Cretaceous)

The post-rift section unconformably overlies the syn-rift section (Hakimi and Abdullah, 2015). At the beginning of the post-rift period, the basin was isolated from the ocean from the southeast. That is why the deposition rate of carbonate decreased, and the Sab'atayn Formation underwent a massive salt deposition, as noted in the previous section. The salt deposition did not last long till the marine carbonate was back to deposit to develop the Nayfa Formation in the Late Tithonian-Berrisian in the lowest Early Cretaceous (Brannan *et al.*, 1999). The Saar Formation developed conformably over the Nayfa and it was followed by the Qishn, which overlies the Nayfa unconformably and underlies the Tawilah group. These formations make the post-rift sediments (Figure 1.14.) (Hakimi and Abdullah, 2015; Albaroot *et al.*, 2016). The development of the Saar sediments occurred during the transgression from the Late Berriasian to the Early Valanginian in the Early Cretaceous by the deposition of mainly carbonate rocks (limestones and dolomites), sandstone and shale (Beydoun *et al.*, 1998). "Qishn clastics were deposited in a series of discrete, elongate salt withdrawal basins" (Brannan *et al.*, 1999, p9). Tawilah, the Upper Cretaceous group, underwent a partial erosion after the uplift resulting in the opening of the Red Sea. In the Marib sector that belongs to the Marib-Shabwah Basin, the thickness of this erosion is estimated to be 1000 m (Hakimi and Abdullah, 2015). In the Early Tertiary, the

basin again underwent submergence that resulted in the deposition of carbonates and evaporites to develop the vast Hadramout Group, which lost considerable parts in the Marib-Shabwah Basin during the Late Tertiary due to the erosion and the uplift (Brannan *et al.*, 1999).

1.5. Lithostratigraphy of Marib-Shabwah Basin

Several publications and reports have discussed multiple sides of the basins' lithostratigraphy, including the Marib-Shabwah Basin since 1964, and it is worthy to note that the last 30 years have brought more research projects and writings related to this subject. In this study, we will summarize the lithostratigraphy of the Marib-Shabwah (Sab'atayn) Basin by citing some of these reports and papers. The stratigraphy column of the Marib-Shabwah Basin contains sequences from the middle Jurassic to Cretaceous periods lying over the basement rocks, as seen in Figure 1.15. It is worth noting that a 2.5 km thick Mesozoic sequence dominates the column (Alaug *et al.*, 2011). These rock units have been represented in the wells of the study area; they are described and discussed below from the bottom to top.

1.5.1 Basement rocks

The basement rocks are mostly represented by the Precambrian rocks to Lower Cambrian; more precisely, highly metamorphosed rocks that belong to the Archean to Lower Proterozoic and slightly metamorphosed rocks related to the Late Proterozoic till the Earlier Cambrian (Al-Azazi, 2016).

1.5.2. Wajid sandstone formation

The Wajid Sandstone Formation was first named in 1948 by Gierhart and Owens in an unpublished ARAMCO report (Beydoun et al., 1998). Some recent studies indicate its age as the early Paleozoic (Cambrian and Ordovician) (Albaroot *et al.*, 2016). Consequently, it is considered the earliest sedimentary formation in Yemen (Beydoun *et al.*, 1998). The Wajid Formation disconformably overlies the Precambrian basement

rocks (the south of Arabian Shield) (Albaroot *et al.*, 2016). In other words, the southeast border of the Arabian shield in Yemen is covered by the Wajid Formation (see Figure 1.15.) (Brown, Schmidt and Huffman Jr, 1989) and the Wajid Formation is overlain by the Akbarah (shale) Formation of the Lower Permian or unconformably by the Kuhlan Sandstone Formation of the Jurassic (Beydoun *et al.*, 1998).

The Wajid Formation name was given in Saudi Arabia about 110 km north-northeast far from the Najran zone at the Jabal Al-Wajid (long. 44° 07' lat. 170 30'). It extends into north Yemen covering a vast area in the northern part of the Sa'dah governorate and the eastern and northern parts of the Jawf governorate. It is about 150 m (492 ft) and 950 m (3116 ft) thick on average, respectively, in Yemen and Saudi Arabia. The Wajid sandstone has been run across in some drilled wells in the Marib-Al Jawf sub-basin of the major Marib-Shabwah Basin as well as other wells in the southern flank of the Yemeni Rub' Al-Khali Basin (Beydoun *et al.*, 1998). The composition of the Wajid succession is dominated by sandstone (see Figure 1.15.) with minor quantities of shale within it (Redfern and Jones, 1995; Beydoun *et al.*, 1998). Its depositional environment in the Yemeni side is probably a fluvial environment being the result of rivers flowing from the southeast (Beydoun *et al.*, 1998). This environment is also thought to be a glacial environment (Redfern and Jones, 1995).

1.5.3. Akbarah shale formation

It was first named as "Akbara shales" by Roland (1979), and Kruck and Thiele (1983) used the same name to describe the Yemen's glacial deposits of the Late Paleozoic. Later in 1996, it was officially named "Akbarah Formation" by the Yemen Stratigraphic Commission. The Akbarah Formation is dominated by shales and contains sandstones, mudstones, and siltstones, too. The age of the Akbara Formation is dated as the late Carboniferous-Permian (SPT, 1994; Beydoun *et al.*, 1998; Albaroot *et al.*, 2016).

This formation spreads in the Sa'dah area (Block-21) in the northwest of Yemen (SPT, 1994; Beydoun *et al.*, 1998) with a maximum thickness of 130 m but its existence in

the Sab'atayn Basin is restricted to the northwestern part of its Marib-Aljawf sector with a 90-135 m thickness (Beydoun *et al.*, 1998; Alaug *et al.*, 2011). The Akbara Formation is in correlation with some similar formations discovered in Ethiopia and south Saudi Arabia, which were the result of the glaciation of Gondwana in the Late Carboniferous-Early Permian (Beydoun *et al.*, 1998).

The Wajid sandstone and the younger Akbarah Formations are considered the oldest sediments in the north and the northwest of the Sab'atayn Basin, and they are only selected as subsurface occurrences (Alaug *et al.*, 2011).

1.5.4. Kuhlan sandstone formation

The Kuhlan Formation was first mentioned by Lamer as "Kuhlan Series" in 1930, corrected to "Kuhlan Formation" by Beydoun in 1964, and formalized as "Kuhlan Formation" in 1997 by the Yemen Stratigraphic Commission (Beydoun *et al.*, 1998).

The Kuhlan Formation outcrops in the Kuhlan village (this is where the name Kuhlan Formation comes from), which is about 70 km far from Sana'a from the northwest, and it is about 200 m thick on average in that region (Albaroot *et al.*, 2016). It also propagates in different parts of Yemen. It is recorded in the Sab'atayn Basin only in the subsurface section. The Kuhlan Formation is conformably overlain by carbonates of the Amran group, and it generally overlies the basement rocks unconformably (As seen in Figure 1.14.). It is mainly composed of sandstone with minor conglomerate and shale and a little limestone (Beydoun *et al.*, 1998).

The official reports did not determine the certain age of the Kuhlan Formation since it does not contain reliable fossils that allow it, but they indicated that it is commonly considered as the latest Triassic - Middle Jurassic, but not older (Beydoun *et al.*, 1998; Albaroot *et al.*, 2016). The lowest deposits of the Kuhlan Formation represent a fluviatile environment, followed by nearshore and finally shallow marine depositional environments. Actually, these depositions were influenced by the early phase of Jurassic transgression (Beydoun *et al.*, 1998).

1.5.5. Amran group

It is a considerably thick sequence that was first described by Lamare in 1930 as "Amran Series"; then, Beydoun amended this name in 1964 to become "Amran group" in order to describe all the Upper Jurassic formations (Taheri *et al.*, 1992; Beydoun *et al.*, 1998). The name is, actually, derived from Amran city, in which the sequence appears clearly (Beydoun *et al.*, 1998).

The Amran group overlies the Kuhlan Sandstone Formation gradationally and conformably while two different formations rest on it locally. These are the Sa`ar Formation covering it conformably where it appears and the lower Cretaceous Qishn Formation that overlies it unconformably (Beydoun *et al.*, 1998) (see Figure 1.15.).

The group spreads widely in the Marib-Shabwah Basin, being an important research zone to many researchers because of its high hydrocarbon potentiality (Nabawy and Al-Azazi, 2015). It is divided into Shuqra, Madbi, Sab'atayn, and Nayfa Formations, sorted according to their age from the oldest, as shown in Figure 1.14. (Beydoun *et al.*, 1998; Nabawy and Al-Azazi, 2015). More information about these formations will be given in the next section.

1.5.5.1. Shuqra formation

The type section of this formation was selected at Jabal Urays, 15 km N17°E far from Shuqra City (this last city is situated on the Coast of Aden Gulf), in 1950 when Wetzel and Morton measured in an unpublished report a 98 m thick limestone formation (Albaroot *et al.*, 2016). The Shuqra Formation is possibly aged Callovian to Kimmeridgian, according to SPT (1994), while Beydoun *et al.*, (1998) indicated that its age probably ranges from the Bathonian to Oxfordian as shown in the Figure 1.15., but it may extend to the Early Kimmeridgian and Al-hasani et al. (2018) claims that it is aged Oxfordian as shown in Figure 1.14.

In the Marib-Shabwah Basin, the Shuqra Formation was found to be unconformably underlain by the Kuhlan Formation (lower contact), and it is generally conformably overlain by the Madbi Formation (upper contact) (Beydoun *et al.*, 1998; Nabawy and Al-Azazi, 2015). The development of the Shuqra Formation resulted from the deposition of shallow marine carbonates (platform carbonates) in a shallow marine environment. These platform carbonates are composed mainly of limestone, locally shale/silty with some dolomite and wackstones (SPT, 1994; Beydoun *et al.*, 1998; Al-Azazi, 2016; Albaroot *et al.*, 2016). The upper part of the Shuqra Formation located in the Marib sector of the Marib-Shabwah Basin is called Arwa Member (Beydoun *et al.*, 1998).

1.5.5.2. Madbi formation

This formation was first named in 1964 by Beydoun and then it was formalized by Greenwood and Beydoun in 1968 as "Madbi Formation" (Beydoun *et al.*, 1998).

Since numerous wells were drilled by the YHOC for hydrocarbon exploration in the Marib-Shabwah Basin, precisely in its Marib-Al Jawf sector (this sector includes the study area), a clear and detailed idea about the age, the depositional environment and the components of the Madbi Formation was obtained. Its stratotype was selected at Jabal Madbi (lat. 14° 17' long. 48° 05') in Shabwah governorate in the Middle of Yemen having a thickness of about 787 ft (240 m) (Beydoun *et al.*, 1998; Alaug *et al.*, 2014; Albaroot *et al.*, 2016). The Madbi Formation at the type section (Jabal Madbi in Shabwah) represents a variety of colour degrees due to the different mixtures of its components. Principally, it is a sequence of generally rubbly marls of different degrees of grey, which is interbedded with shale/mudstone in extensive parts, with limestone in some other parts and with siltstones in a few parts. This formation also contains some bands of sandstone (SPT, 1994; Beydoun *et al.*, 1998; Tari *et al.*, 2016).

The Madbi Formation is conformably underlain by the Shuqra Formation and locally unconformably overlain by the Nayfa Formation, the Tawilah Group and the Sab'atayn Formation (SPT, 1994; Beydoun *et al.*, 1998; Albaroot *et al.*, 2016).

The age of this formation is possibly dated from the early Kimmeridgian in the Jurassic to the Middle Tithonian of the same Jurassic period. Actually, the Madbi deposition is a result of the Late Jurassic rifting in the Marib-Shabwah Basin. It is the first formation deposited during the rift in a pelagic environment, with periods of anoxia and periodic margin through the rift basins (Beydoun *et al.*, 1998; Albaroot *et al.*, 2016).

The Madbi Formation in the Marib-Al Jawf sector consists of two main members by age ascending order the Meem Member and the Lam Member, as seen in Figure 1.14. Other members also belong to the Madbi Formation and spread along the southern and northern margins of the Marib-Shabwah Basin, such as Raydan, Ayban, Haniyah, and Harib (Beydoun *et al.*, 1998).

Generally, this formation is rich in organic content, and it is considered the source rock for all the hydrocarbons discovered until now in the Marib-Shabwah Basin and the Say'un-Masila Basin (Beydoun *et al.*, 1998).

1.5.5.2.1. Ayban member

In 1992, it was named "Ayban Formation" by the Yemen Hunt Oil Company, this name being later amended by the Yemen Stratigraphic Commission to "Ayban Member" of the Marib- Shabwah Basin in 1997 (Beydoun *et al.*, 1998).

The Ayban Member exists only in the Marib-Shabwah Basin, precisely in the subsurface of the north of the Marib-AlJawf sector. In fact, its type section was selected by the YHOC from the northeastern part of this sector, precisely the exploration well called Jabal Ayban-1 (lat .15° 52' long. 45° 59'). It is located in depths between 2560 ft (780 m) and 8987 ft (2739 m) with a thickness of 6427 ft (1959 m) on average, partially overlying the lower part of the the Meem Member, which is also equivalent to the Ayban Member laterally, and disconformably underlying the Sab'atayn Formation (Beydoun *et al.*, 1998).

Its main component is sandstone, which varies from white to gray and from granular into medium-grained to soft, with conglomerates, argillaceous limestones, and rare dolomites. It is aged as Kimmeridgian until the early Tithonian (Upper Jurassic) (Beydoun *et al.*, 1998).

The Ayban Member is confined to the northern margin of the Marib-Al Jawf sector as noted, equivalent to each of the Harib and Haniyah Members, the Meem Member and in some parts the Rafad Member, existing respectively in the northwest, the centre and the southeast of the sector (Taheri *et al.*, 1992; Beydoun *et al.*, 1998).

1.5.5.2.2. Meem member (lower Madbi shale member)

It used to be known as "Meem Formation" after the Yemen Hunt Oil Company gave it this name in 1992. It was later corrected by the Yemen Stratigraphic Commission to "Meem Member of the Madbi Formation" in 1997. The YHOC selected its stratotype in the Marib-Shabwah Basin, in the northwestern Marib sector, precisely in the Lam-1 borehole (lat. 15° 33' long. 45° 40'), extending from 8261 ft (2518 m) depth to 10206 ft (3110 m) depth and being 1945 ft (593 m) thick (Beydoun *et al.*, 1998).

The age of the Meem Member is dated as Kimmeridgian to lower Tithonian. The Meem Member is recorded only in the subsurface, extending southeastwards from the Marib-Al Jawf sector to the north of the Shabwah sector, having a thickness that varies from a maximum value of 4710 ft (1435 m) to a minimum value of 197 ft (60 m). It is generally underlain by the Shuqra Formation, and it is overlain by the Lam Member (Beydoun *et al.*, 1998).

The Meem Member consists of a diversity of components containing mostly deep-water shales/calcareous mudstone, deep-water carbonates in the form of limestones (principally in the lower section), and dolomite, and sandstone (SPT, 1994; Beydoun *et al.*, 1998). The Meem Member contains high-quality shale source rocks and clastic turbidites forming reservoir rocks in the west of the Sab'atayn Basin (Ahlbrandt, 2002; Hakimi and Abdullah, 2015).

1.5.5.2.3. Lam member (upper Madbi member)

It was known as "Lam Formation" since 1992 when the YHOC gave it this name until the Yemen Stratigraphic Commission amended it in 1977 as "Lam Member of the Sab'atayn Basin." The section type of this member was selected by the YHOC from the Marib-Aljawf sector belonging to the Marib-Shabwah Basin from the Alif-1 borehole exactly located in lat. 15° 33' long. 45° 48' (Its thickness is about 3205 ft (977 m) in this well) and from other wells in other fields (Beydoun *et al.*, 1998).

The Lam Member probably developed during the lower (early) Tithonian (Beydoun *et al.*, 1998). It is generally overlain by the Sab'atayn formation (SPT, 1994), and conformably underlain by the Meem Member (Beydoun *et al.*, 1998).

The lithology of this member is similar to the lower Meem Member as it represents a continuation of this last member. It deposited in a deep-water pelagic environment during the syn-rift stage and contains more shale (SPT, 1994; Beydoun *et al.*, 1998; Hakimi and Abdullah, 2015) (see Figure 1.14. and Figure 1.15.). Although the Lam Member is less sandy than the Meem Member (Figure 1.14.), it is still considered one of the hydrocarbon-richest source rocks in the area (Beydoun *et al.*, 1998; Hakimi and Abdullah, 2015).

This member is only recorded in the subsurface section in the Marib-Aljawf sector, and it extends to the Shabwah and Hajar sectors of the Marib-Shabwah Basin (Beydoun *et al.*, 1998).

1.5.5.3. Sab'atayn formation

Discovered in 1950, and named first as "Sab'atayn Series" by Wetzel and Morton in an unpublished report of Iraq Petroleum Company (I.P.C) (Beydoun *et al.*, 1998), but it is known as the Amla'ah Group (Taheri *et al.*, 1992; SPT, 1994) by some companies: Its name was corrected and formalized to "Sab'atayn Formation" by Beydoun in 1964 (Beydoun *et al.*, 1998).

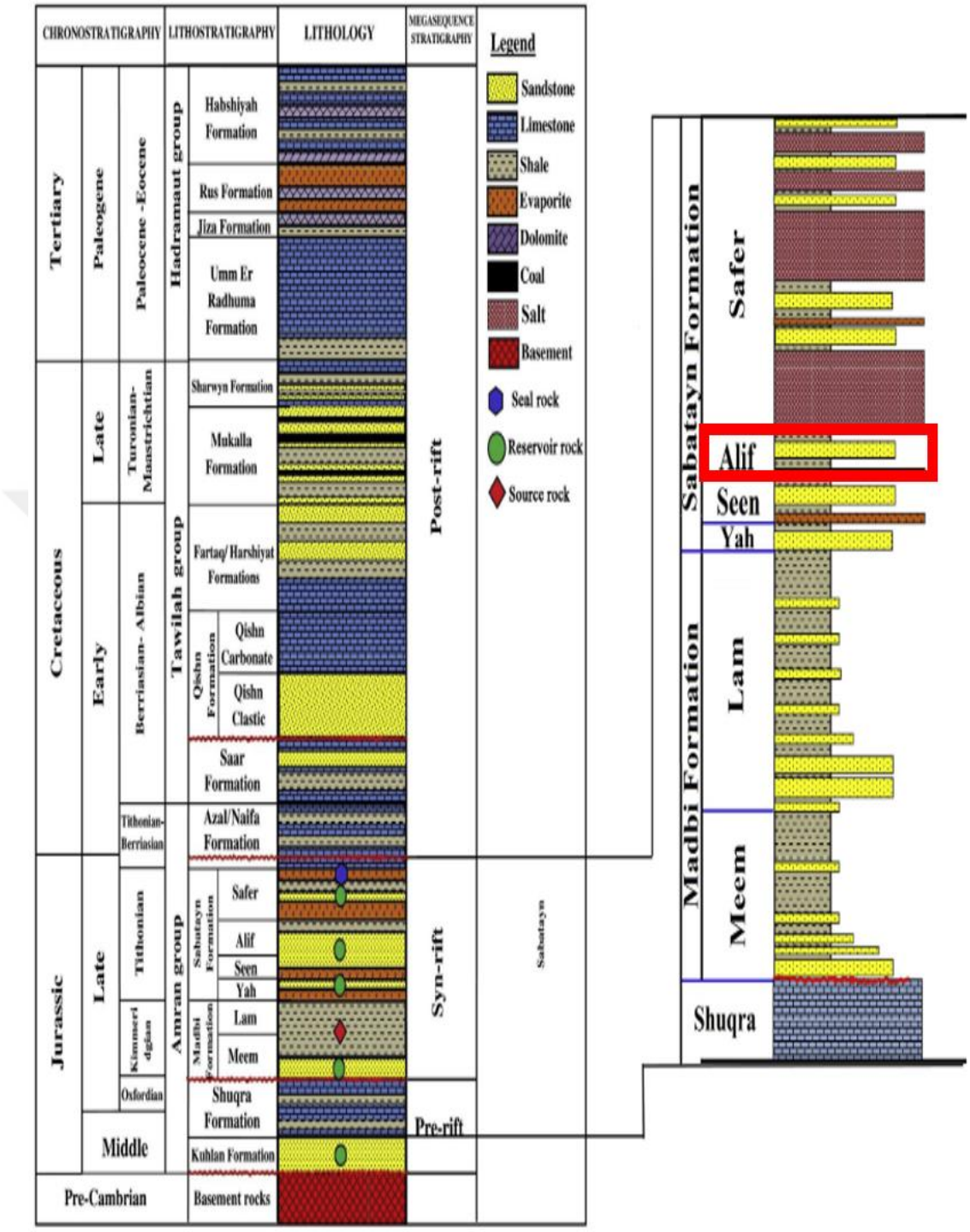

Figure 1.15. Stratigraphic column of Marib–Shabwah Basin focusing on the Late Jurassic period (Hakimi, AlMatary and Salad Hersi, 2018)

This Formation contains sandstones with evaporates, interbedded with some clay (Figure 1.14., Figure 1.15.) (SPT, 1994; Beydoun *et al.*, 1998; Alaug *et al.*, 2014).

The Sab'atayn Formation appears on the surface in Hadramawt and Shabwah governorates with different thicknesses in several salt domes considered surface members of the Sab'atayn Formation. It corresponds to 300 m of the Ayad dome, 101 m of the Layadim dome, 178 m of the Milh Maqah dome, 70 m of the Milh Khirwa dome, 150-200 m of the Safir dome, 198 m of the Mintaq dome, 130 m of the Jubah dome, 15 m of the Sial Al-Milh dome (Beydoun *et al.*, 1998).

However, it exists as a subsurface unit only in the Marib-Shabwah (Sab'atayn) Basin, encountered in many boreholes in its Marib-Aljawf sector (Beydoun *et al.*, 1998) with an average thickness of about 1788 ft (545 m) (Albaroot *et al.*, 2016) and a maximum thickness that reaches 2771 ft (845 m) (Nabawy and Al-Azazi, 2015).

The age of the Sab'atayn Formation is dated as Upper Jurassic (Tithonian period) (SPT, 1994). In the Sab'atayn (Marib-Shabwah) Basin, the Sab'atayn Formation overlies the Madbi Formation and underlies diachronously the Nayfa Formation (Beydoun *et al.*, 1998). The subsurface Sab'atayn Formation is subdivided into the Yah, Seen, Alif, and Safir/Safer Members (Figure 1.15.) from the lowest upwards (Beydoun *et al.*, 1998).

1.5.5.3.1. Yah member

This member was described by the Yemen Hunt Oil Company (YHOC) as "Yah Formation" in 1992. Later in 1997, this name was amended by the Yemen Stratigraphic Commission to "Yah Member" (Beydoun *et al.*, 1998).

The type section of the Yah Member was selected in the Marib-Shabwah Basin, more precisely in its Marib-Aljawf sector, exactly in the Yah-l borehole (lat. 15° 36' long. 45° 28') from the depth 5604 m (1708 ft) to the depth 5925 ft (1805 m), having an average thickness of about 321 ft (97 m). It is unconformably underlain, there, by the Madbi Formation (the Lam Member) and conformably overlain by the Seen Member. In this sector of this basin, the Sab'atayn Formation has the Yah Member, whose age is dated as Early Tithonian, as a basal unit (Beydoun *et al.*, 1998).

The Yah Member consists principally of sandstones with local evaporates (halite), thin interbedded shales/mudstones, and minor limestone deposited in a shallow marine environment and a deeper marine environment from respectively the west and the east (SPT, 1994; Beydoun *et al.*, 1998).

1.5.5.3.2. Seen member

This member was described by the Yemen Hunt Oil Company (YHOC) as "Seen Formation" in 1992, and then in 1997, it was officially given the name "Seen Member" by the Yemen Stratigraphic Commission (Beydoun *et al.*, 1998).

The YHOC had selected its type section from the well Ma'een-l existing in the north western sector of the Marib-Shabwah Basin (Marib-Al Jawf Sector). This well's exact location is lat. 15°34' long. 45° 43", and the thickness of this member measured there was 523 ft (159 m) from the depth 4585 ft (1397 m) to the depth 5108 ft (1557 m) (Beydoun *et al.*, 1998).

The Seen Member consists of sandstones, and mudstones/shales with interbedded evaporites and minor dolomite, especially in the lower part. The upper part of this member is dominated by sandstones (see Figure 1.14.) (Beydoun *et al.*, 1998). The age of the Seen Member dated as the Lower/Middle Tithonian (SPT, 1994; Beydoun *et al.*, 1998). It overlies the Yah Member conformably and underlies the Alif Member (Beydoun *et al.*, 1998).

1.5.5.3.3. Alif member

In 1992, the Yemen Hunt Oil Company (YHOC) first described this member by the "Alif Formation" name, and the Yemen Stratigraphic Commission amended it in 1997 into "Alif Member" (Beydoun *et al.*, 1998).

The YHOC selected its stratotype from the Alif-l borehole (lat. 15° 33', long. 45° 48') situated in the north western Marib-Aljawf sector included in the Marib-Shabwah

(Sab'atayn) Basin (Beydoun 1998,); measured its thickness as 378 ft (115 m) between 5200 ft (1585 m) and 5578 ft (1700 m) of depth (Beydoun *et al.*, 1998).

The Alif Member represents lowstand events being predominantly composed of sandstones, thin mudstone with interbedded evaporates, local anhydrite lenses, and minor dolomitic limestones (SPT, 1994; Beydoun *et al.*, 1998; Alaug *et al.*, 2014); these components being deposited in a shallow-marine depositional environment (Beydoun *et al.*, 1998).

The age of the Alif Member is dated as Middle to Late Tithonian in Upper Jurassic. It is generally conformably underlain by the Seen Member, and it underlies the Safir Member of the Sab'atayn Formation unconformably (Beydoun *et al.*, 1998). The Alif Member is extensively encountered in the east of the Marib-Al Jawf sector, extending southwards to the west of the Shabwah sector, but generally, no presence of the Alif Member is recorded in the westernmost part of the Sab'atayn (Marib-Shabwah) Basin (Beydoun *et al.*, 1998).

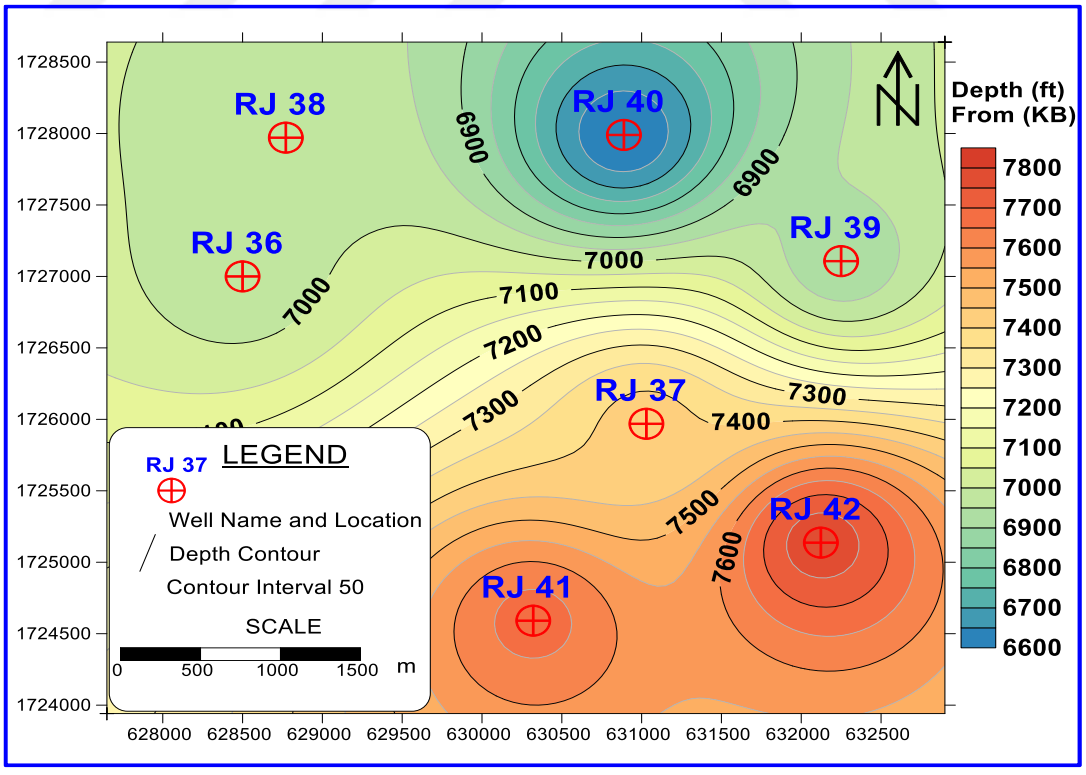

(a)

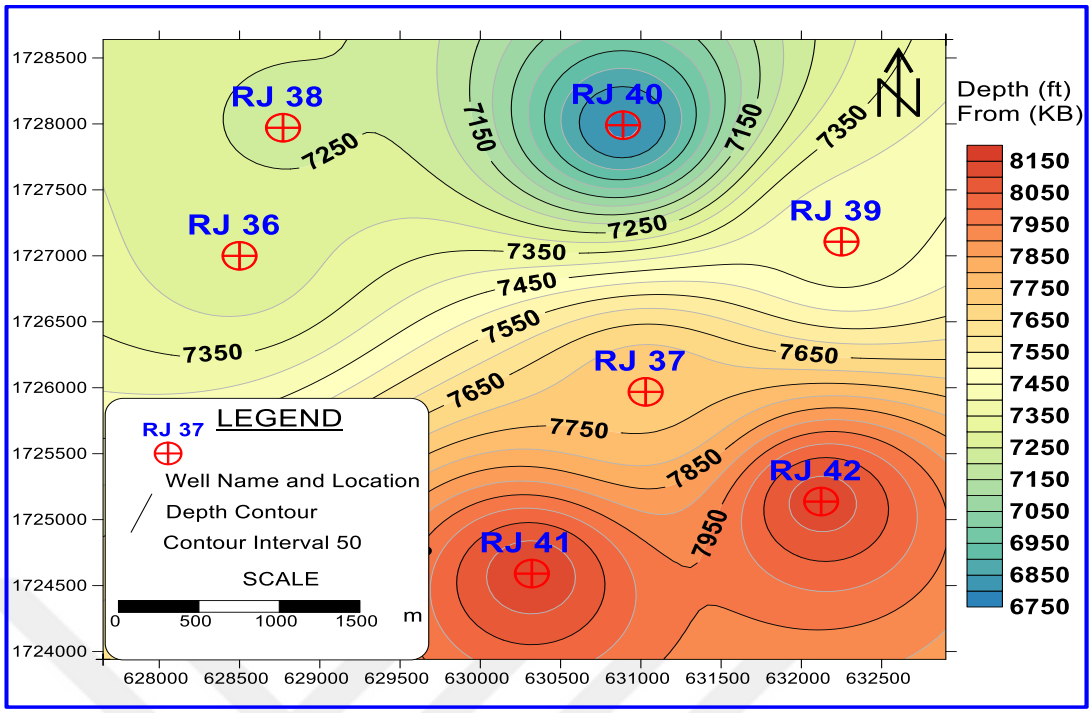

(b)

Figure 1.16. Maps of the (a) top and (b) bottom structural contour of the Alif Member in the study area through the study wells by Surfer 17

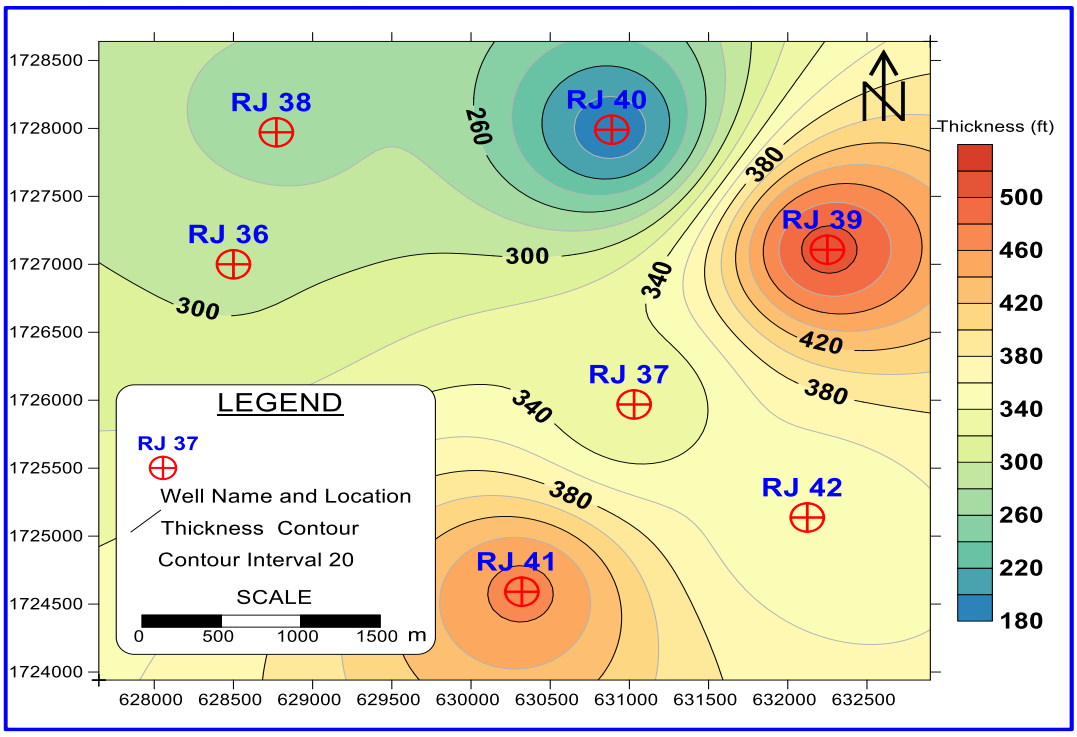

Figure 1.17. Map of the gross thickness structural contour of the Alif Member in the study area through the study wells by Surfer 17

The Alif Member covers more than 90 % of the recoverable hydrocarbon of the Marib-Shabwah Basin (Hakimi and Abdullah, 2015; Nabawy and Al-Azazi, 2015). Consequently, it is considered the main hydrocarbon prolific reservoir formation of its Marib-Aljawf sector (SPT, 1994; Beydoun *et al.*, 1998; Alaug *et al.*, 2014; Hakimi and Abdullah, 2015; Nabawy and Al-Azazi, 2015).

The isopach map of Figure 1.17. displays the Alif Member gross thickness in the study area and it shows the variation between wells from a minimum thickness of 189 ft detected at the well RJ-40 and a maximum value of 508 ft at the RJ-39. According to this map, it appears that the gross thickness decreases northwards and increases towards the south, east and south-east of the study area.

1.5.5.3.4. Safir member

In 1992, this member was described by the Yemen Hunt Oil Company (YHOC) and given the name "Safir Formation" and in 1997. Its name was amended by the Yemen Stratigraphic Commission to" Safir Member" (Beydoun *et al.*, 1998).

The section type of this member was described from the Ma'een well-I (lat. 15° 34' long. 45° 43') as a 1438 ft (438 m)-thick member existing between the depths 2892 ft (881 m) and 4330 ft (1319 m); that well being located in the Sab'atayn (Marib-Shabwah) Basin in its Marib-Aljawf Sector (Beydoun *et al.*, 1998).

The age of the Safir Member is dated as Late Tithonian (Beydoun 1998, p177-178). It corresponds to the uppermost part of the Sab'atayn group overlain conformably by the Nayfa Formation in the Marib-Shabwah Basin (SPT, 1994) and it is considered a perfect seal rock for the reservoirs of Alif Member sitting under it (Beydoun *et al.*, 1998; Hakimi and Abdullah, 2015; Nabawy and Al-Azazi, 2015).

The lithology of the Safir Member is dominated by evaporates (massive halite and local anhydrite) separated by thinner bands of shale and sandstone. It also contains minor limestone and dolomites (SPT, 1994; Beydoun *et al.*, 1998; Nabawy and Al-

Azazi, 2015). Sometimes, it represents local productive hydrocarbon reservoirs (Beydoun *et al.*, 1998; Hakimi and Abdullah, 2015; Nabawy and Al-Azazi, 2015).

1.5.5.4. Nayfa formation

The Nayfa Formation was discovered and called "Neifa Limestone" by Pike and Wofford in an unpublished report of I.P.C. (Irak Petroleum Company) in 1939 and then in 1946. Its name was amended in "The Stratigraphy and Structure of the Eastern Aden Protectorate" of Beydoun to "Nayfa Formation" (Beydoun *et al.*, 1998).

It was recorded in many exposed late Jurassic areas in Shabwah and Hadramout governorates. As for in the subsurface, the Nayfa Formation was encountered in all the basins developed as a result of the Late Jurassic rift systems: the Say'un-Masila Basin, the Jiza'-Qamar Basin and the Marib-Shabwah (Sab'atayn) Basin. It is worth to note that the YHOC reports refer to the Nayfa Formation of the Marib Sector as "Azal Formation" as an unofficial name (Beydoun *et al.*, 1998).

The Nayfa Formation is principally a limestone sequence, with restricted dolomite, mudstone and minor sandstone beds (SPT, 1994; Beydoun *et al.*, 1998; Alaug *et al.*, 2014; Albaroot *et al.*, 2016), mainly deposited in pelagic (open marine) environments (Beydoun *et al.*, 1998). Its thickness in the Marib-Shabwah Basin is about 1312 ft (400 m) (Alaug *et al.*, 2014). The Nayfa Formation is aged Late Tithonian-Berrisian (Beydoun *et al.*, 1998), and it generally underlies the Sa'ar Formation conformably (SPT, 1994).

1.5.5.5. Sa'ar formation

This formation was described in 1992 from the Al-Qam-1 borehole (lat. 15° 45' long. 48° 13') located in the westernmost part of the Say'un sector, which belongs to the Say'un-Masilah Basin by the Total Oil Company of Yemen. It was referred to as "Sarr Formation" in their final report, then, and this name was amended later by the Yemen Stratigraphic Commission to Sa'ar Formation (Beydoun *et al.*, 1998).

This formation rests on the Nayfa deposits conformably (Hakimi and Abdullah, 2015; Albaroot *et al.*, 2016) and under the Qishn Formation unconformably (Beydoun *et al.*, 1998; Hakimi and Abdullah, 2015). It corresponds to a shallow marine carbonate sequence with minor open sea clastic sediments (SPT, 1994). It constitutes of limestones mostly, and minor mudstones and sandstones (SPT, 1994; Albaroot *et al.*, 2016), as shows Figure 1.14. The age of the Sa'ar Formation is dated as Late Berriasiam to Early Valanginian in the Early cretaceous (Beydoun *et al.*, 1998), and Oil companies divided the Sa'ar Formation into upper Sa'ar clastic and lower Saar carbonate (Albaroot *et al.*, 2016).

1.6. Hydrocarbon Exploration History of Marib- Shabwah Basin

It is worth noting that in general there are no sufficient wide studies made on Yemen. There is especially lack in the studies made on the subsurface. Most of the geological studies focus on the exposed part of the geological column of Yemen. Also, the sandstone part of the Sab'atayn Formation, which is considered one of the most important reservoir rocks in the Marib-Shabwah Basin has not been studied sufficiently. It was only studied by some Petroleum companies. Recently, more interest was paid to the Sab'atayn Basin by a few authors. Some of the most important studies are summarized as the following.

In 1968, Wetzel and Morton have suggested the name of "Sab'atayn Series" which was emended by Beydoun in 1964 to "Sab'atayn Formation". In 1984, the first oil production well in Yemen was drilled by the Yemen Hunt Oil Company, which proved the economic importance of this formation (Al-Areeq, 2004).

Taheri *et al.*, (1992) described all the Upper Jurassic formations referring to the Sab'atayn Formation as Amla'ah Formation. This study is a combination of the efforts of the Yemen Ministry of Oil, Schlumberger Middle East company and Yemen Hunt Oil Company; in which they evaluated and reviewed the deposition of the Aljawf-Marib sector belonging to the major Marib-Shabwah Basin and studied the tectonic events in order to understand the hydrocarbon system of Yemen. In the same year, the

Yemen Hunt Oil Company (YHOC) first described the Alif Member as "Alif Formation" (Beydoun *et al.*, 1998).

In 1994, the Simon Petroleum Company (SPT) made Micropaleontological and palynological studies and mentioned in an unpublished report that the Alif Member refers to the late Tithonian age (SPT, 1994).

In 1995, the Ministry of Oil and Mineral Resources appointed the project of the Yemen Stratigraphic Commission to create the overall international lexicon of stratigraphy of which was the fruit of 3 years of hard work, being released in 1998. It is a lexicon that unifies, formalizes, and describes the stratigraphic column of the sedimentary cover of the Republic of Yemen, discusses all the formations present in it, and identifies their characteristics. It is the official resource in Yemen. It includes a detailed study of the lithostratigraphy of the Marib-Shabwah Basin. This lexicon divided the Amran group into four formations: Sab'atayn, Shuqra, Nayfa, and Madbi Formations, and most of these formations are divided into their members (Beydoun *et al.*, 1998). (More details are in section 1.5).

According to (Beydoun *et al.*, 1998), the Amran group contains in its middle section the Sab'atayn Formation (sequence) containing the Alif Formation that was amended into "Alif Member" by the Yemen Stratigraphic Commission. This member is the target member of this study as well as the issue of great interest of a lot of companies and researchers (Beydoun et al., 1998). (Beydoun et al., 1998) also validated the division of the Sab'atayn Formation into Alif, Seen, Safir, and Yah Members.

Brannan *et al.*, (1999) discussed the tectonic and geological evolution of the Sab'atayn Basin, Yemen, during the Upper Jurassic Rifting. It divided this rifting into three stages: Pre-rift, syn-rift, and post-rift in a row and explained the conditions and the formations that developed during every stage. The three stages were discussed in detail in the section 1.4.

The (Ahlbrandt, 2002) report published by the U.S. Geological Survey in 2002, considers Yemen a promising country due to its hydrocarbon potential. This report put the light on the geologic evolution and the petroleum system in the Marib-Shabwah Basin considered an important sedimentary basin. It studied the development of the rift basin and its stages (pre-rift, syn-rift, and post-rift), as well as the total hydrocarbon system in Yemen, focusing on the Jurassic sequence: the Madbi/Amran Formations of the Sab'atayn (Marib-Shabwah) Basin; this sequence containing the main source rocks and reservoir rocks of the basin.

Alaug *et al.*, (2011) studied the major Madbi source rocks (the Lam and Meem Members) through the Marib-Aljawf sector (Block-18) applying the Rock-Eval pyrolysis method to determine the thermal maturity and the hydrocarbon generative potential of the source rocks. They used 183 cutting and core samples from seven wells and the isopach map of the main reservoir unit in the sector (Alif Member). The study on the samples showed that the value of Total Organic Carbon (TOC) of the Meem and Lam Members is sufficient. Moreover, the Petroleum Index (PI) of these same members has good value. Besides, the majority of the studied cuttings of the Lam and Meem members of Madbi Formation are in the Metagenesis stage (mature stage) according to the maximum temperature (T_{max}), whose average value is 436.34° F (224.63° C). The isopach map shows that the Alif Reservoir Member gets thicker eastwards and westwards.

Sachsenhofer *et al.*, (2012) discussed the environment of deposition of the Upper Jurassic section of the Sab'atayn (Marib-Shabwah) Basin, focusing on the Madbi source rock. They analysed 60 cutting samples from the basin and proved that the Lam Member source rock of the Madbi Formation has a very good Total Organic Carbon (TOC) content. This makes it considered an excellent hydrocarbon (oil and gas) source rock.

Nabawy and Al-Azazi, (2015) studied the Seen and Alif Members in the Alif Field situated in the Marib-Aljwaf sector of the Marib-Shabwah Basin to define their potential reservoir zones. They used as a basis the core analysis data and petrophysical

characteristics analysis. This study deduced that the Alif Member has high and excellent hydrocarbon potentiality.

(Al-Azazi, 2016) carried out a comprehensive evaluation of the Alif and Seen Members (Upper Jurassic age) by studying the important petrophysical properties of the economically important members. This study was made on twelve wells in the Wadi Bana Field in the Marib-Shabwah Basin by applying several techniques such as core analysis and well loggings. This study produced several maps and results, but the most important result is showing that the Alif Member is containing a promising reservoir with shale volume content ranging between 3,8 % and 11.5 %, effective porosity of values between 15.9 % and 21 %, water saturation values that range from 2.8 % to 27.3 %, and hydrocarbon saturation of 72.7 % to 97.2 %. The study indicates that the reservoir of the Alif Member of the study area is dominated by sandstone with amounts of shale and has a significant net thickness of 30 to 171 ft.

(Albaroot, M., Ahmad A.H.M., Nabil Al-Areeq, 2017) examined some of the petrophysical characteristics in the Alif Member in the Marib- Shabwah Basin. This work aims to evaluate the Alif Member by analysing and interpreting the well log data through 4 wells in the Halewah Field, such as Gamma-ray, Neutron, density, resistivity logs. As a result of this work, important petrophysical characteristics including the average ranges of shale volume, fluid (water and hydrocarbon) saturations, and porosity were determined as 18 to 25 %, 12 to 31 %, 13 to 34 % and 13 to 34 % respectively. This study confirms that the Alif member of the study area contains an economic reservoir, and it recommends more exploration works on the Sab'atayn members, especially the Alif Member.

1.7. Hydrocarbon Production History of Yemen

Yemen is not one of the biggest oil and gas producer countries and is not a member of OPEC (the Organization of the Petroleum Exporting Countries), but according to the estimations, it is a promising country. Yemen oil and gas production depends mostly on foreign oil companies that the government has production-sharing agreements with

them (SEPOC, no date). Shell, BP, British Gas, Axon, and Chevron are examples of these oil and gas international companies (Al-Azazi, 2010).

Yemen started the exploration of the two types of gas (associated gas and free gas) all together with oil exploration (Ministry of Oil and Minerals, no date c) in the summer of 1984, when the Hunt Oil Company discovered the Alif Field (oil and gas field), Block-18, the first commercial oil discovery in Yemen. The average oil production of the Alif well was 8000 BOPD (Barrel Per Day). The discovery of oil and gas in the Block 18, Marib, was then followed by successive oil exploration activities in the other fields. More than 14 oil and gas fields were discovered; the block's surface plants were built, and a pipeline was constructed to the Red Sea (PEPA, no date d).

The production and exportation of the first oil shipment were done from the Block-18 in September 1986, under the Yemen government's guidance. Meanwhile, other oil and gas explorations kept going in other blocks (PEPA, no date d). In 1987, Techno-Export, a former Russian Company, announced the discovery of oil in three fields present in the Block-4 in Shabwah province: East Ayad, West Ayad, and Amel Fields (PEPA, no date d). In 1989, the Total Company drilled the Mintaq-1 well as well as other wells in the Block-49 in the northeast of the Aswad Ridge. Total also discovered condensate gas in the Shuqra Formation. This was the first discovery of hydrocarbon in the Balhaf Block situated in East Shabwah (Al-Azazi, 2010).

In 1991, the Canadian Occidental Petroleum company, which is called Canadian Nexen Petroleum now, made significant discoveries of oil in the Block-14 (Masila Block) located in the Sounah Field. The surface plants of the Masila Block were built, and its oil pipeline was constructed to Al-Dhabah area in Hadhramout province, on the Arab Sea (PEPA, no date d). In the same year, the Chevron company started to operate the Block-3 located in Shabwah area (Al-Azazi, 2010).

During the period between 1991 to 1995, the Chevron company drilled a number of wells such as Al-Hamah-1, Bilad Al-Samsd-1, Al-Harrah-1, Al-Harsh-1, and North Al-Harsh-1. When all the exploration requirements finished, Chevron Co. left the

Block-3, and Agip became the operator of the block (Al-Azazi, 2010). Again in 1991, Total company drilled the first well in the Block-5 called Jannah-1 well and penetrated condensate gas formations (Al-Azazi, 2010). Then, the Halewah-1 and Halewah-2 wells of this same block were drilled and tested by Total company, too, in 1994 (Al-Azazi, 2010). In September 1996, oil was also found in the Jannah block-5 of the Halewah Field by a consortium of companies operating there.

The Marib block-18's former operator the Hunt Yemen Company built the plants and carried the produced oil by the pipeline that delivered it to the port situated on the Red Sea (PEPA, no date d). Because the amount of the discovered gas was significant, the government signed the contract to implement the major project to liquefy and export natural gas in 1997 (Ministry of Oil and Minerals, no date a). Some oil discoveries were made by Total E&P Yemen in 1998 in different fields: Wadi Taribah, Atouf, and Kharir Fields that lie in East Shabwah, block-10. Production was related to the block-14 (Al-Masila block) (PEPA, no date d).

A Norwegian company called DNO announced that it discovered oil in the Hwarim block-32 on December 18, 1999 (the company was the operator of this block at that time) and started oil production and exportation through Al-Masila in November 2001 (PEPA, no date d). Dove Energy, a British company, announced the discovery of commercial oil in the Saar Block-53 on December 20, 2001. Production and exportation through the Al-Masila pipeline started in 2002 (PEPA, no date d). In October 2003, the American company Vintage, as the operator of the Damis block S1, discovered oil in this block, starting the production and exportation activities through the Jannah pipeline in March 2005 (PEPA, no date d).

In 2005, the government decided to launch the Liquefied Natural Gas project (LNG), the first natural gas liquefaction in Yemen, and signed agreements to sell the Yemeni Liquefied Petroleum Gas to some international companies such as Total Company (Ministry of Oil and Minerals, no date a).

The Canadian company Nexen Petroleum Yemen Ltd. was the operator of the Al-Hajr block-51. On December 17, 2003, it announced the discovery of oil, and on November 9, 2005, it started producing oil and exporting it through the Al-Masila pipeline (PEPA, no date d). DNO, the Norwegian Company started producing oil from the Block-43 in July 2005, too, as an operator of this block (PEPA, no date d). The Malik block-9's operator Calvally (a Canadian company) announced in October 2005, the commercial discovery of oil and started the production on December 29, 2005 (PEPA, no date d).

OMV, the Czech company and the Al-Uqlah block S2's operator discovered commercial oil in this block in January 2006 and started the production and exportation activities in December of the same year (PEPA, no date d). DNO, the Norwegian company was operating south Hood Block-47, too, and announced the discovery of Oil in March 2011 (Ministry of Oil and Minerals, no date a; PEPA, no date d).

1.7.1. Oil & gas reserve of Yemen

Table 1.1. Gas reserve of the producing blocks discovered until 2008 (Ministry of Oil and Minerals, no date c)

Block	**Proven Gas reserve (in Trillion ft^3)**
Marib -18	14.790
Jannah-5	1.282
Dames-S1	0.606
East Al Hajar -51	0.053
Al-Uqlah-S2	0.548
South Hawarem-43	0.028
East Shabwah-10	0.449
Hawarem-32	0.014
Malek-9	0.229
East Sa'ar-53	0.003
Al-Masilah-14	0.213
Total	**18.215**

Until the end of 2008, the total proven gas reserve of the republic of Yemen reached 18.215 trillion ft^3. According to an evaluation study realized by the Ministry of Oil and Minerals on the gas reserve of all of the fields in the producing blocks, these results were obtained:

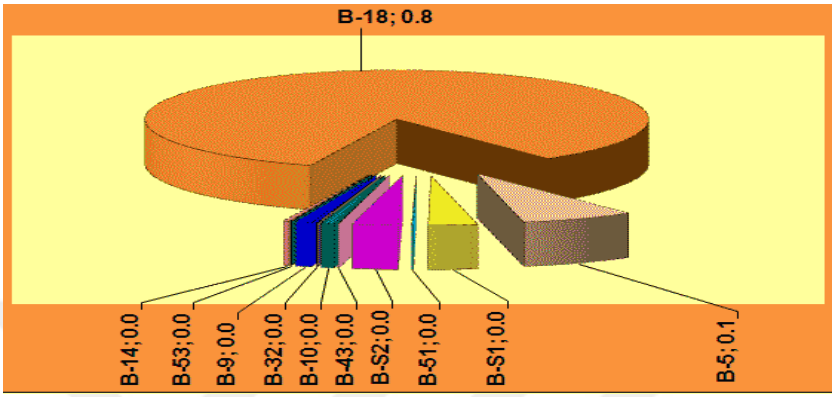

Figure 1.18. Percentage of proven gas in all production blocks – December 2010 (PEPA, no date d)

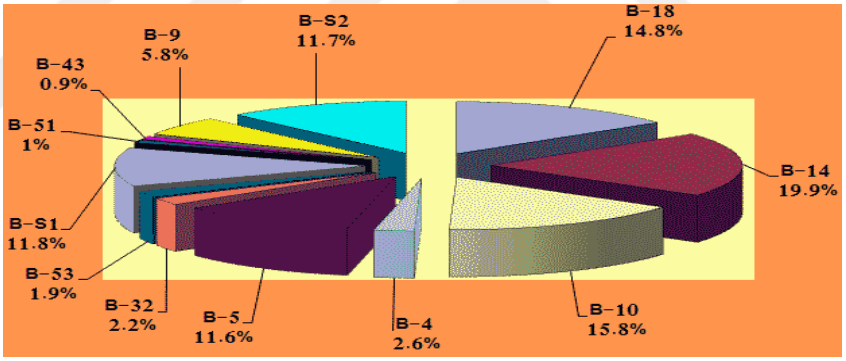

Figure 1.19. Percentage of proven oil reserve in all producing blocks – December 2010 (PEPA, no date d)

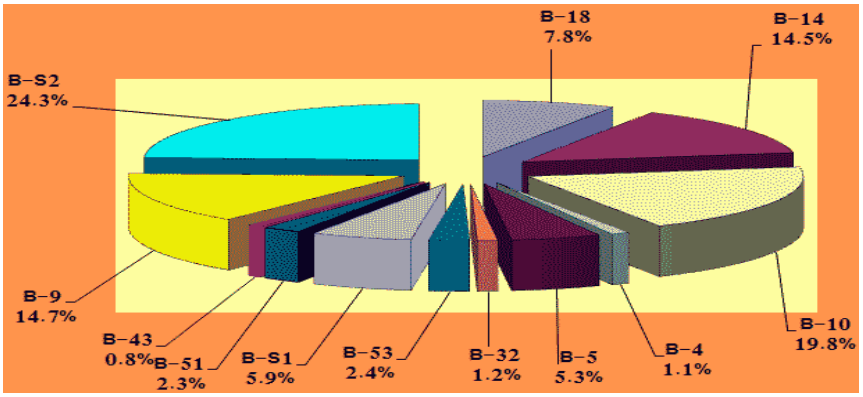

Figure 1.20. Percentage of oil reserve (Proven + possible + probable) in all producing blocks – December 2010 (PEPA, no date d)

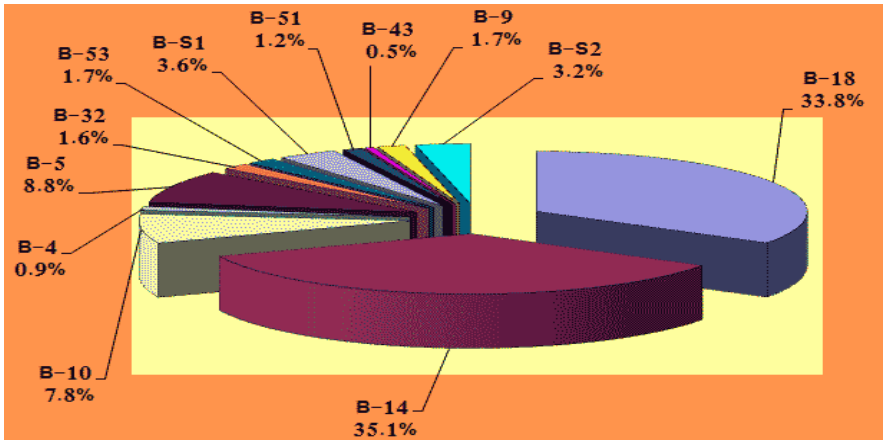

Figure 1.21. Percentage of ultimate proven oil recovery in all producing blocks–December 2010 (PEPA, no date d)

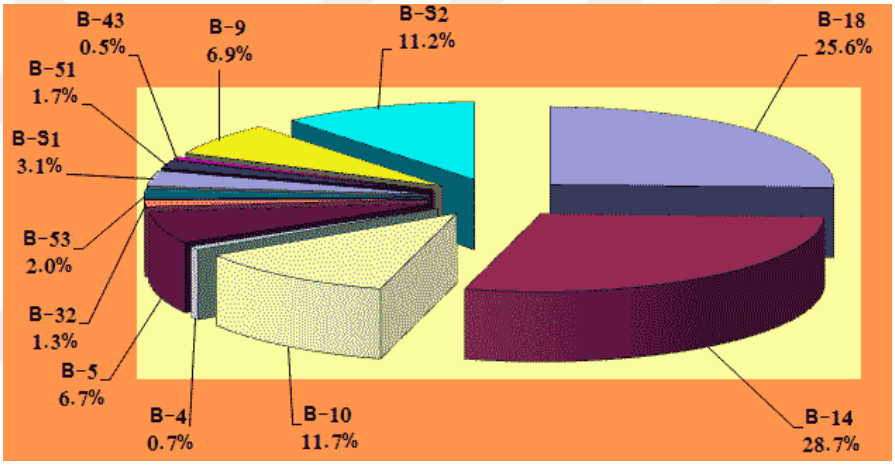

Figure 1.22. Percentage of ultimate oil recovery (including proven, possible and probable) in all producing blocks–December 2010 (PEPA, no date d)

1.7.2. Exploration & production history of the study area

In 1989, the RJ-01 well was drilled, and this was the first discovery of the Al–Raja Field. Al-Raja Field is, as noted in the previous sections, a gas condensate field that is situated in the Block-18 on its boundary with the Block-5. In February 1991, another field was discovered: Dostour Al-Wihdah by drilling the DAW-01 well. The Al-Raja Field was delineated, its boundary limits were determined by drilling several wells through it, and it was announced as a commercial discovery by May 1991. At that moment, the two fields (Al-Raja and Dostour Al-Wihdah) were still thought to be separate fields, but according to the pressure data in the initial long-term production

period that lasted nine months from March to November 1993 (before the field is fully developed) and was the first gas production, it was confirmed that the wells were connected and that the fields are, indeed, one large field that was given the name Al-Raja. Production during this period was from the RJ-04 and DAW-01 wells. Its rate was 80 MMscf/d, in the beginning, as a part of the wells' tests mentioned in section 1.3. (Gunawan and Al-abbasi, 2011).

In January 1994, the number of the producing wells increased to 9 producers, and the injector wells became 9. The production increased then to 13,000 Bopd (Barrel of Oil Per Day) with a rate of 332 MMscfd (Million standard cubic feet per day) of gas production (Gunawan and Al-abbasi, 2011). In 2000, the production rates increased to over 24,000 bopd and more than 700 MMscfd as a result of increasing the number of drilled wells (Gunawan and Al-abbasi, 2011). From 2003 and on, the production was from 13 production wells; the average gas production rate was increased to over 800 MMscfd (containing the Jannah-4 well located in the Jannah Field near the Al-Raja Field) (SEPOC, 2012). Throughout the years 2008 and 2010, some additional producers were drilled in the north of the Al-Raja Field, but the results obtained were not as good as expected (SEPOC, 2012). This field has a gathering point for all the production wells to transfer the produced gas to the initial processing units then to the main export line to the port of Balhaf in south Yemen. (Yemen LNG Company, no date).

Figure 1.23. Oil and gas fields and pipelines in Yemen (Ministry of Oil and Minerals, no date a)

Because of the war taking place in Yemen, the oil and gas production was negatively affected and decreased progressively till it definitively stopped by 2015 (Ministry of Oil and Minerals, no date b).

1.8. Aim of Present Work

This study aims principally to evaluate the hydrocarbon reservoir formed in the Upper Jurassic age in the Marib-Shabwah Basin through the Al-Raja Field in the block-18 by well logging analysis and interpretation. The petrophysical characteristics of the Alif Member will be studied vertically by the means of IP (Interactive Petrophysics TM) through the seven boreholes mentioned in this study, while the area will be studied horizontally by Surfer Software. The vertical study of the study area will produce an estimation of the important petrophysical parameters of the Alif Member such as porosity, shale volume, the existing fluid saturations (hydrocarbon and water), etc. Besides, the reservoir flag and net pay will be determined. The main lithology of the reservoir will be identified in parallel, too. Then, the obtained results will be represented horizontally in distribution maps by Surfer Software. The evaluation of the hydrocarbon potential will be based on the results obtained from the IP and Surfer software outputs.

CHAPTER 2. INPUT AND CORRECTION OF THE STUDY WELLS RAW DATA

2.1. Well Logging Principles

Well logging is used to calculate the physical and chemical properties of the rocks, especially the sedimentary rocks in the oil and gas fields. Measurements are taken by special tools running inside the borehole and the recorded data is transferred into its surface well logging unit by insulated cables. The data is represented in the form of logs according to the depths as the tools are running continuously from the bottom to the surface. Various measurements are made for different purposes: The hydrocarbon exploration operations or the calculations of the existing reserve of oil and gas in the reservoir. Other particular measurements are taken to investigate and interpret the production problems or study the cementing situation of the cased hole, or other important intents (Avedissian, 1988).

Well logging is one of the most common techniques used in open and cased holes to detect the hydrocarbon reservoirs as the fundamental function of well log analysis in the reservoir evaluation. This technique has a useful and effective role to determine the hydrocarbon reservoir characteristics such as porosity and permeability, fluid saturations, and shale volume. In addition, well logging has significance in determining the type of lithology, the thickness and depth of the reservoir, the hydrocarbon reserve, the gas-oil contact (GOW), the oil-water contact (OWC), and the productive zones …etc (Pirson, 1963; Avedissian, 1988; Zhao *et al.*, 2016).

In this study, we will evaluate the Alif Member which belongs to the Sab'atayn Formation aged the Upper Jurassic through different log tools that have been used to obtain the data from the selected seven wells (Al-Raja -36, 37, 38, 39, 40, 41, 42) drilled in the Al-Raja Field in the block-18 located in the Marib-Shabwah Basin

(Figure 1.15.). The main purpose of the evaluation is to estimate the hydrocarbon zones in the study area.

Technologically, we can say that one of the best units of petroleum engineering is the well-logging analysis that can be treated by computer software. Well log data can be transferred into a continuous numerical sequence as well as curves. More, computer programs have in their backgrounds all the equations, formulas, and correction environments used to process the data and evaluate the formation. The obtained output can then be operated, printed, and saved in different formats (Schlumberger, 2008).

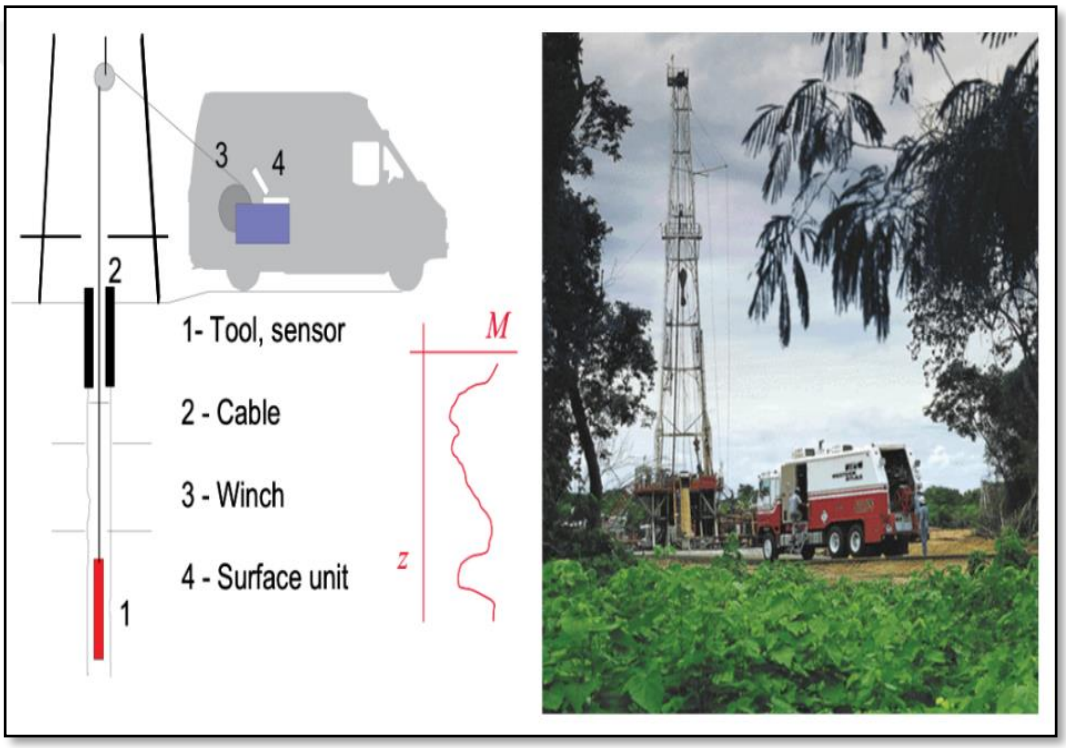

Figure 2.1. Well Logging system's components (Jurgen, 2015)

Gamma-ray log, bite-size, caliper log, photoelectric factor log, porosity tool which provides two logs: density log and neutron log, resistivity logs of the three zones: the flushed, transfer, and uninvaded zones, and depth log (Table 2.1.) are the primary logging data of the wells to be studied. These logs will be used in the comprehensive analytical evaluation of the hydrocarbon reservoirs in the study area by the means of the Interactive Petrophysics ^{TM} (IP) software, version (3.5).

2.2. About IP Interactive Petrophysics Software

Interactive Petrophysics TM (IP) is a software application used to evaluate the reservoir characteristics passing through correction and interpretation processes (Figure 2.2.) of the logs' raw data in order to estimate the hydrocarbon amounts to be produced. IP software (version 3.5) was developed in Scotland by Senergy Ltd. in December 2008 but marketed and sold only by Schlumberger. Schlumberger company is providing all the technical support for IP software by its unit: Schlumberger Information Solutions (SIS) (Schlumberger, 2008).

IP software is quick, many-sided, and to some extent easy to use in the analysis and interpretation of the log data. This program is optimal for experienced Petrophysicists to get accurate and reliable results. Using the program facilities (Figure 2.2.) effectively allows us to calculate and determine the reservoir parameters within the confines of the selected zones which mainly include clay volume, saturation of fluids (water, oil, and gas), porosity, lithology, formation evaluation (reservoir flag and pay flag), and other parameters (Schlumberger, 2008). In addition, (GOC) and (OWC) can be defined respectively from the relation between the density log and the neutron log of the borehole, and from the resistivity logs (Avedissian, 1988; Darling, 2005). Another advantage of IP is that it minimizes the manual operations (Schlumberger, 2008). In fact, IP Petrophysics software is one of the best choices for hydrocarbon reservoir interpretation and evaluation. The Interactive Petrophysics MT IP program provides reliable and accurate output results based on the analysis of the well-logging data as well as minimizing the user errors and providing all the necessary tools to cover all stages.

2.3. Technique of Formation Evaluation

Basically, this technique is achieved analytically by applying several equations and formulae. These procedures of formation evaluation will be clarified detailly as follows:

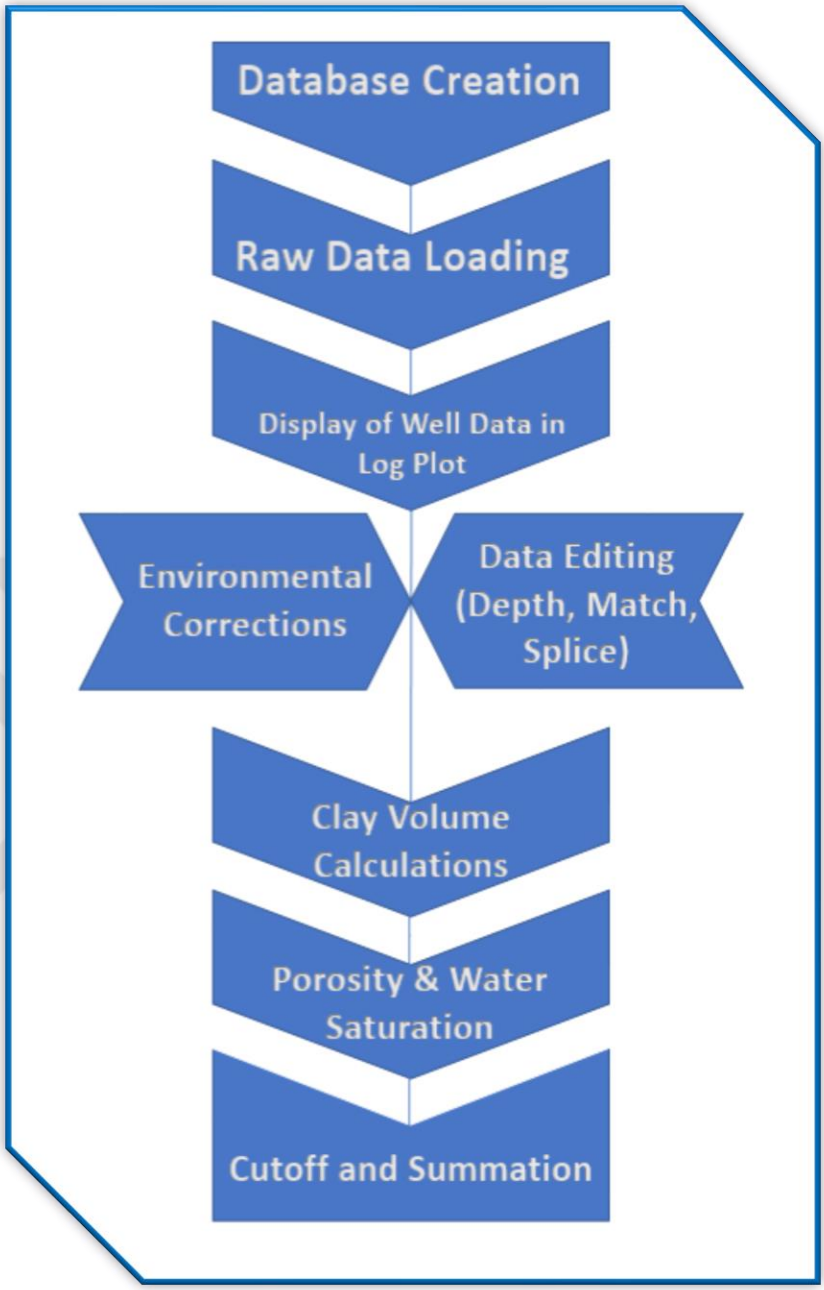

Figure 2.2. Summation flow diagram in IP (Interactive Petrophysics)

2.3.1. Raw data loading

The digital raw data is loaded into the IP software as a first step of the work. This data was initially obtained from the electrical log of the seven wells to be studied. This available digital data was collected and organized in LAS format (Figure 2.3.). It can be inputted in different formats to the program such as ASCII, LAS, and DLIS

(Schlumberger, 2008). In this study, the available log data are prepared in LAS format file (Figure 2.3.). Table 2.1. shows the available raw data of the studied wells. In this step, the digital logs data of each well is transferred to curves by loading the data to the IP program as seen in Figures 2.4., 2.5., 2.6., 2.7., 2.8., 2.9., 2.10. The data also contains some drilling and geological reports of the operating company which include some supporting data such as the penetrated formation types, mud type, mud weight, temperatures, etc.

DEPT	TNPH	TENS	RHOZ	PEFZ	HDRA	HCAL	GR	BS	AE90	AE60	AE30	AE20
7366.5	0.2548	1840.0000	-999.2500	-999.2500	-999.2500	8.4127	143.0618	8.5000	3.9979	3.9527	5.9480	8.7727
7366.0	0.2548	1840.0000	-999.2500	-999.2500	-999.2500	8.4127	143.0618	8.5000	3.9989	3.9534	5.9475	8.7700
7365.5	0.2548	1816.0000	-999.2500	-999.2500	-999.2500	8.4127	143.0618	8.5000	4.0003	3.9542	5.9473	8.7673
7365.0	0.2548	1819.0000	-999.2500	-999.2500	-999.2500	8.4127	143.0618	8.5000	4.0016	3.9550	5.9469	8.7644
7364.5	0.2548	1825.0000	-999.2500	-999.2500	-999.2500	8.4127	143.0618	8.5000	4.0029	3.9558	5.9465	8.7613
7364.0	0.2548	1815.0000	-999.2500	-999.2500	-999.2500	8.4127	143.0618	8.5000	4.0042	3.9565	5.9461	8.7585
7363.5	0.2548	1793.0000	-999.2500	-999.2500	-999.2500	8.4127	143.0618	8.5000	4.0053	3.9571	5.9454	8.7551
7363.0	0.2548	1768.0000	-999.2500	-999.2500	-999.2500	8.4127	143.0618	8.5000	4.0064	3.9577	5.9453	8.7532
7362.5	0.2548	1838.0000	-999.2500	-999.2500	-999.2500	8.4127	143.0618	8.5000	4.0077	3.9585	5.9451	8.7498
7362.0	0.2548	1829.0000	-999.2500	-999.2500	-999.2500	8.4127	143.0618	8.5000	4.0104	3.9606	5.9459	8.7477
7361.5	0.2548	1928.0000	-5668.0085	-5678.0701	-5667.4715	8.4127	143.0618	8.5000	4.0154	3.9650	5.9481	8.7450
7361.0	0.2548	2023.0000	2.5730	4.6114	1.8516	8.4127	143.0618	8.5000	4.0231	3.9720	5.9518	8.7425
7360.5	0.2548	2125.0000	2.5550	4.3223	0.9244	8.4127	143.0618	8.5000	4.0325	3.9806	5.9557	8.7420
7360.0	0.2548	2185.0000	2.5432	4.0372	0.0037	8.4127	143.0618	8.5000	4.0411	3.9884	5.9580	8.7394
7359.5	0.2548	2296.0000	2.5422	4.0420	0.0033	8.4127	143.0618	8.5000	4.0457	3.9924	5.9567	8.7341
7359.0	0.2548	2372.0000	2.5418	4.0453	0.0033	8.4127	143.0618	8.5000	4.0412	3.9875	5.9466	8.7388
7358.5	0.2548	2444.0000	2.5415	4.0477	0.0033	8.4127	143.0618	8.5000	4.0257	3.9720	5.9225	8.6812
7358.0	0.2548	2492.0000	2.5413	4.0494	0.0032	8.4127	143.0618	8.5000	4.0160	3.9622	5.9305	8.7235
7357.5	0.2548	2574.0000	2.5411	4.0506	0.0032	8.4127	143.0618	8.5000	4.0342	3.9798	5.9505	8.7365
7357.0	0.2548	2506.0000	2.5410	4.0514	0.0032	8.4127	143.0618	8.5000	4.0239	3.9699	5.9368	8.5763
7356.5	0.2548	2523.0000	2.5410	4.0519	0.0032	8.4127	143.0618	8.5000	4.0617	4.0074	5.9194	8.5786
7356.0	0.2548	2499.0000	2.5409	4.0522	0.0032	8.4127	143.0618	8.5000	4.1243	4.0692	6.0300	8.4820
7355.5	0.2548	2525.0000	2.5409	4.0524	0.0032	8.4127	143.0618	8.5000	4.1391	4.0875	5.9436	8.0565
7355.0	0.2548	2514.0000	2.5409	4.0526	0.0032	8.4127	143.0618	8.5000	4.0743	4.0294	5.7921	7.7130
7354.5	0.2548	2586.0000	2.5408	4.0527	0.0032	8.4127	143.0618	8.5000	3.8576	3.8237	5.5686	7.5311
7354.0	0.2548	2545.0000	2.5408	4.0528	0.0032	8.4127	143.0618	8.5000	3.5212	3.5003	5.4218	7.3395
7353.5	0.2548	2506.0000	2.5408	4.0529	0.0032	8.4127	143.0618	8.5000	3.2159	3.2054	5.0300	7.2569
7353.0	0.2548	2528.0000	2.5407	4.0539	0.0031	8.4127	143.0618	8.5000	2.8465	2.8443	4.9074	7.4304
7352.5	0.2548	2551.0000	2.5403	4.0562	0.0027	8.4127	143.0618	8.5000	2.7911	2.7946	5.2118	9.0655
7352.0	0.2548	2529.0000	2.5394	3.9788	0.0015	8.4127	143.0618	8.5000	3.0040	3.0140	6.6926	15.2764
7351.5	0.2548	2521.0000	2.5409	3.8498	0.0003	8.4127	143.0618	8.5000	3.7573	3.7822	8.8535	26.4593
7351.0	0.2548	2517.0000	2.5432	3.7396	-0.0015	8.4127	143.0618	8.5000	4.4483	4.4963	11.4495	44.4301
7350.5	0.2548	2527.0000	2.5510	3.7128	-0.0027	8.3964	143.0618	8.5000	7.0094	7.1559	14.8220	62.4063

Figure 2.3. Example of LAS files corresponding for Al-Raja -36 well (SEPOC, 2008)

The raw data can be corrected by various correction environments that the IP program provides according to the Service Companies such as Schlumberger corrections, Halliburton corrections, and Baker Atlas, etc. Note that we applied Schlumberger corrections in this study. Lithological identification, porosity, fluid saturations (gas, oil, and water), and clay volume will be obtained by making a series of calculations and relations, and with the help of particular histograms (Schlumberger, 2008).

Table 2.1. shows the presence of various logs obtained from the different logging tools having run in the study wells. These logs are expressed in different units tabulated in Table 2.2.

Table 2.1. The raw data of the seven wells in the study area

Well Name	Depths of Alif Member (ft)	K.B from Sea Level (ft)	Available Logs data
RJ- 36	6970.5- 7268.5	3007	GR- CAL- BS- ILM- ILD- MSFL- TNPH- RHOZ- HDRA – PEF- D
RJ- 37	7417- 7738	3003	GR- CAL- BS- ILM- ILD- MSFL- TNPH- RHOZ- HDRA – PEF- HTEM- D
RJ- 38	6967- 7236.5	3023	GR- CAL- BS- ILM- ILD- MSFL- TNPH- RHOZ- HDRA – PEF- HTEM- D
RJ- 39	6912- 7420	3003	GR- CAL- BS- ILM- ILD- MSFL- TNPH- RHOZ- HDRA – PEF- HTEM- D
RJ- 40	6602- 6791	2996	GR- CAL- BS- ILM- ILD- MSFL- TNPH- RHOZ- HDRA – PEF- HTEM- D
RJ- 41	7670- 8136	2998	GR- CAL- BS- ILM- ILD- MSFL- TNPH- RHOZ- HDRA – PEF- HTEM- D
RJ- 42	7782- 8126	2994	GR- CAL- BS- ILM- RT- MSFL- TNPH- RHOZ– PEF- D

Table 2.2. Units of the well logs data of the study

Abbreviation	Full Form	Unit
D	Depth	ft
CAL	Calliper log	in
B. S	Bit Size	in
GR	Gamma Ray Log	API
ILD	Deep Induction Log	Ω.m
ILM	Medium Induction Log	Ω.m
SFLU	Spherically Focused Log	Ω.m
HTEM	Temperature	°F
NPHI	Neutron Porosity Log	**%**
RHOZ	Bulk Density	gm/cc
HDRA	Bulk Density Correction	gm/cc
PEF	Photoelectric Factor	B/E

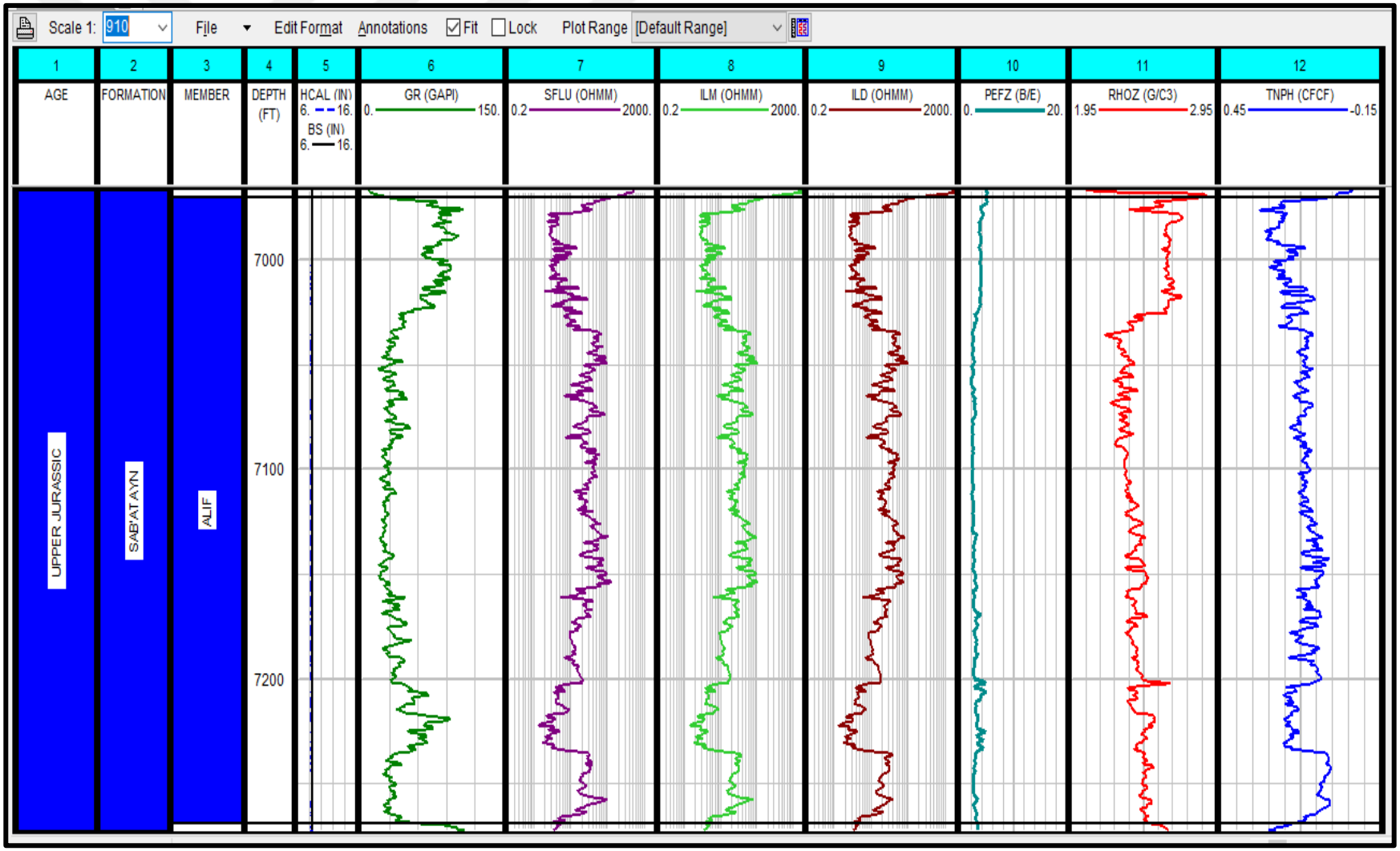

Figure 2.4. Digital raw data logs of Alif Member (6970.5 – 7268.5 ft) of Al-Raja -36 well converted to curves by IP (Interactive Petrophysics) software

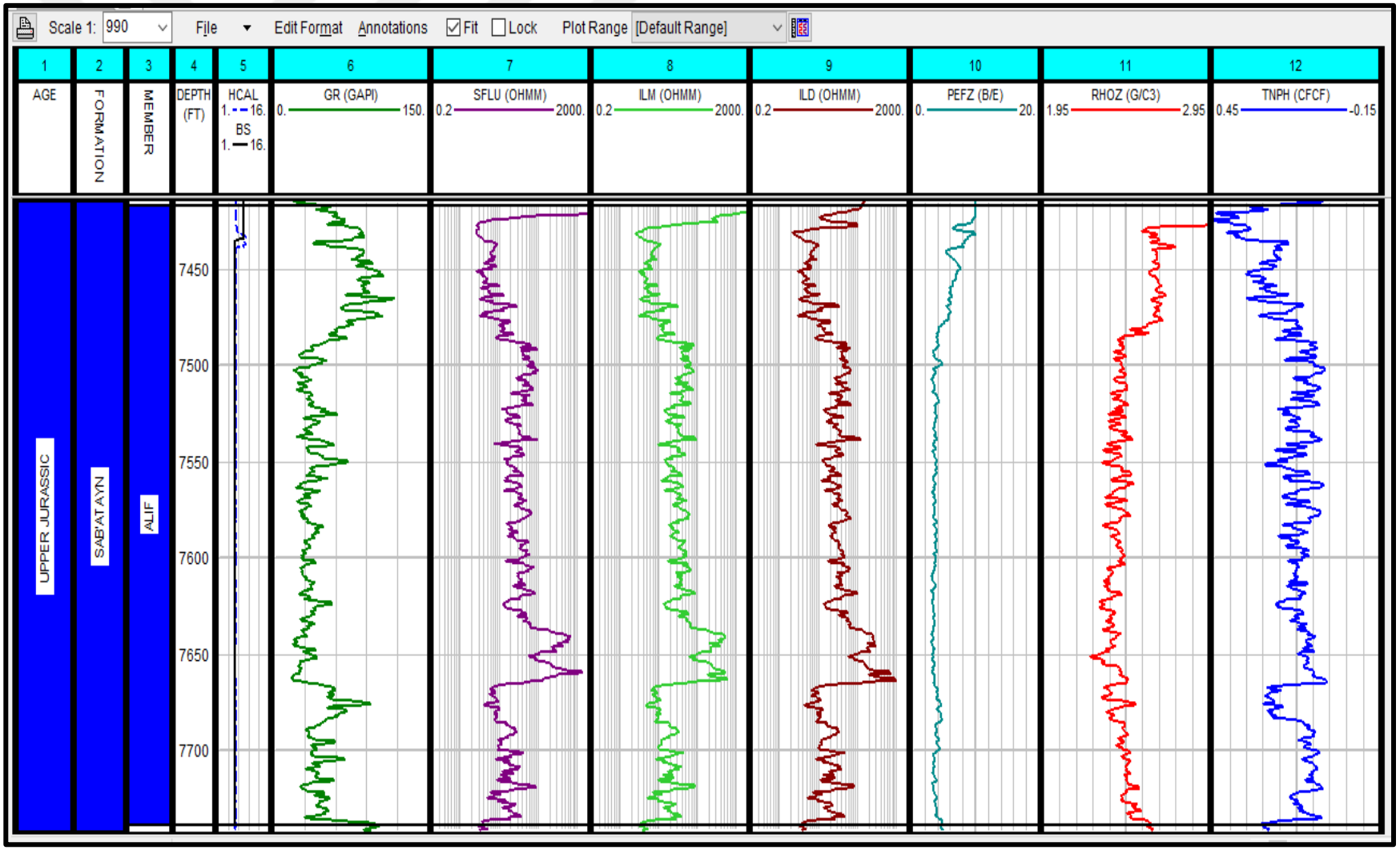

Figure 2.5. Digital raw data logs of Alif Member (7417 - 7738 ft) of Al-Raja-37 well converted to curves by IP (Interactive Petrophysics) software

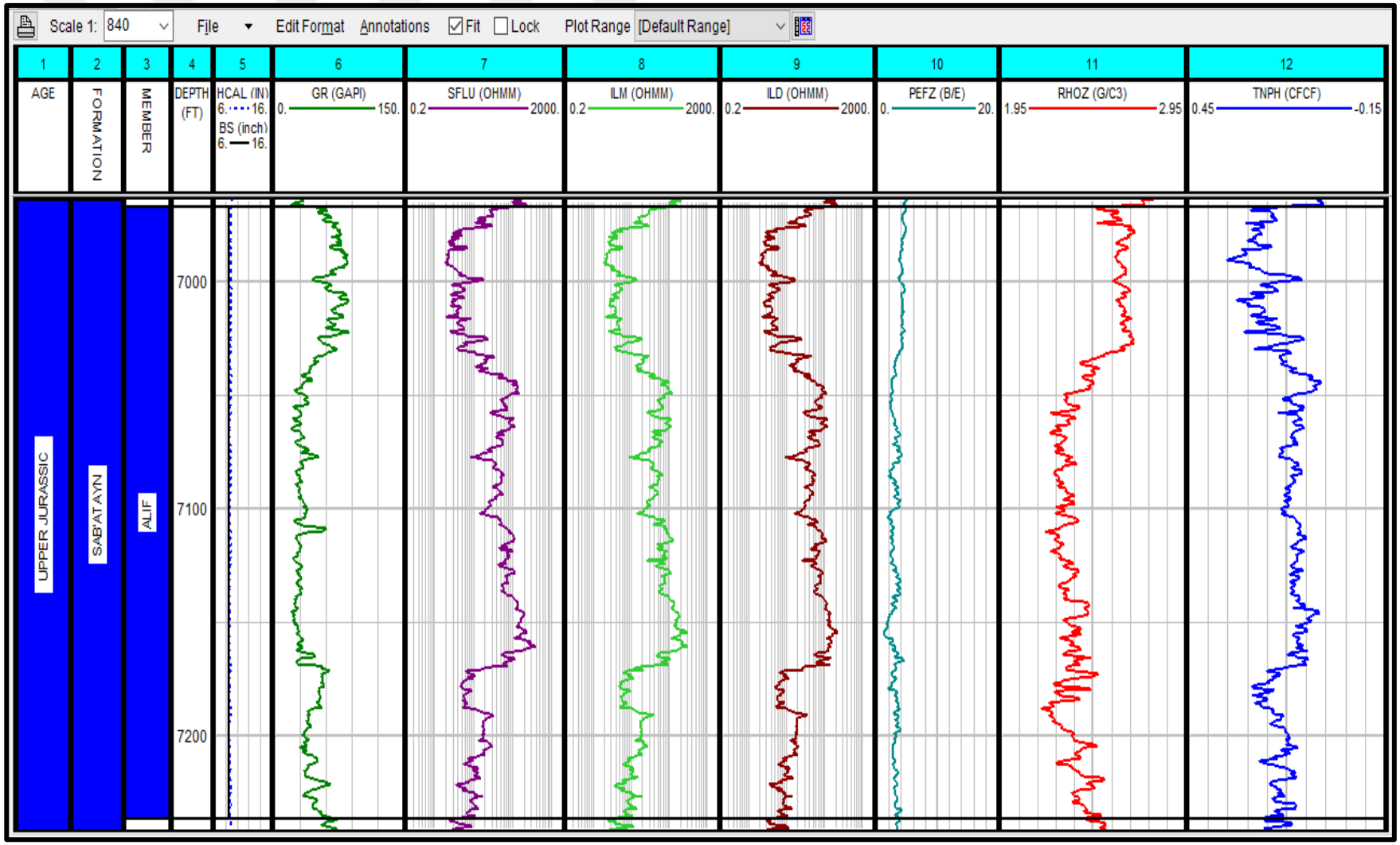

Figure 2.6. Digital raw data logs of Alif Member (6967 - 7236.5 ft) of Al-Raja-38 well converted to curves by IP (Interactive Petrophysics) software

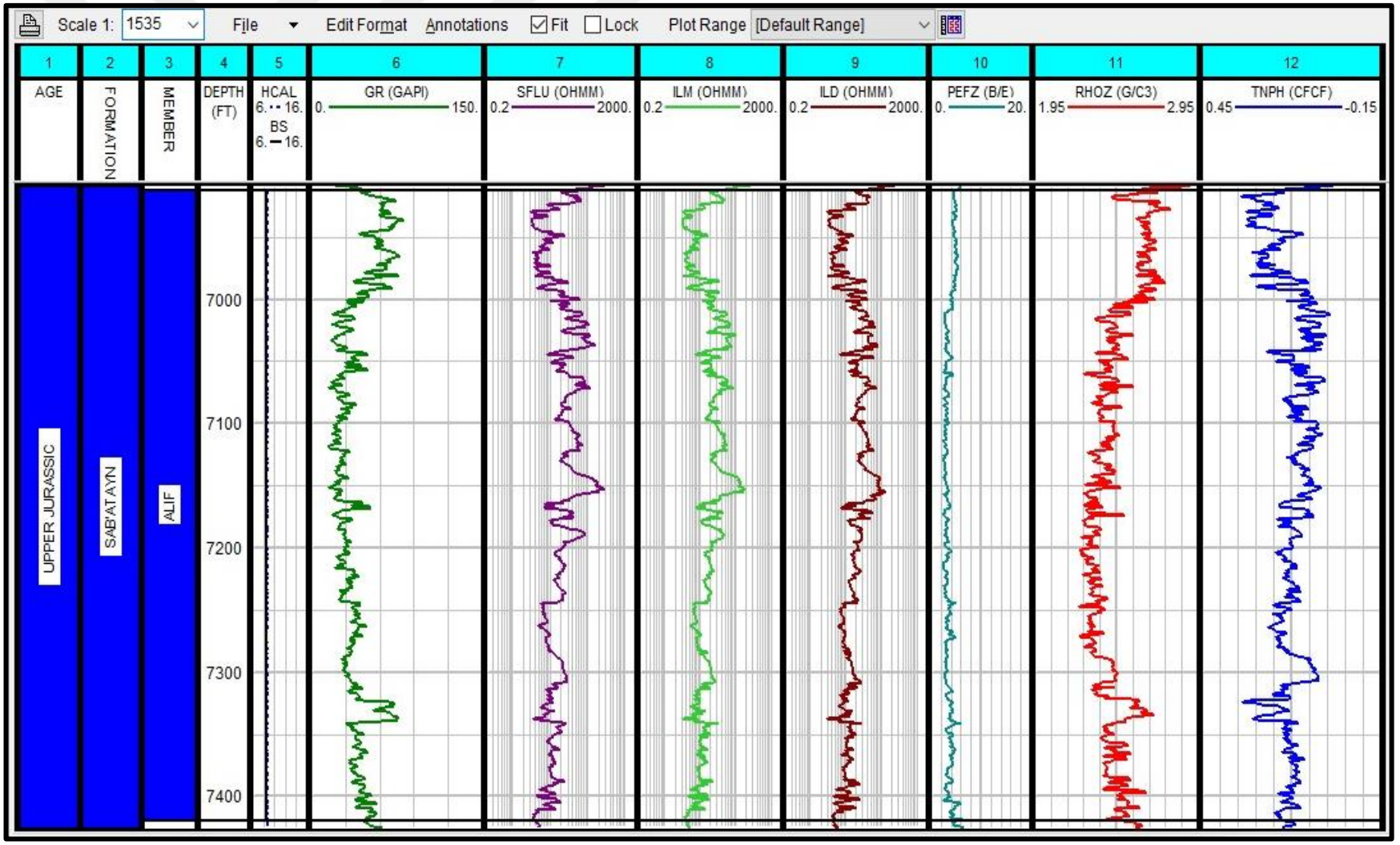

Figure 2.7. Digital raw data logs of Alif Member (6912 - 7420 ft) of Al-Raja-39 well converted to curves by IP (Interactive Petrophysics) software

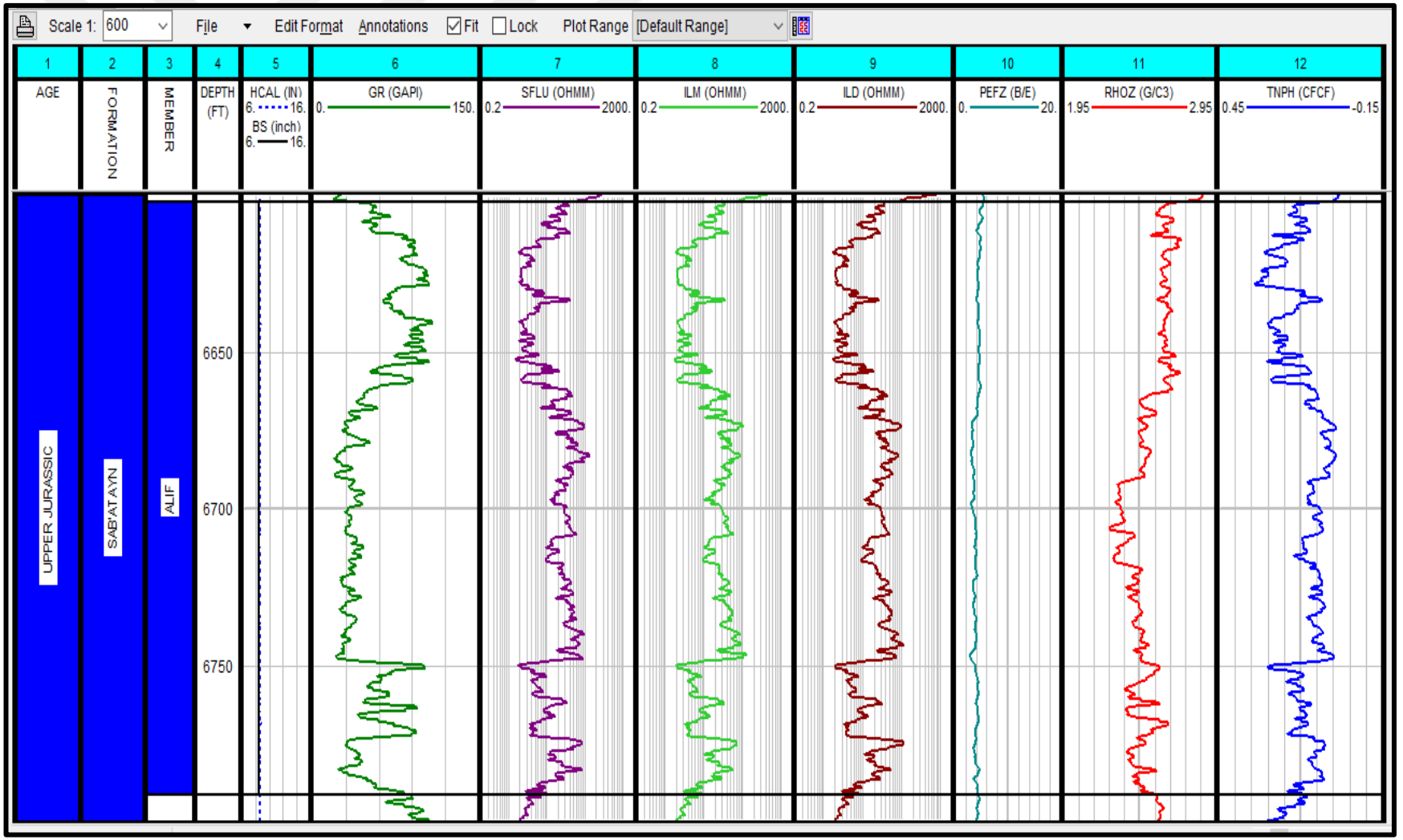

Figure 2.8. Digital raw data logs of Alif Member (6602 - 6791 ft) of Al-Raja-40 well converted to curves by IP (Interactive Petrophysics) software

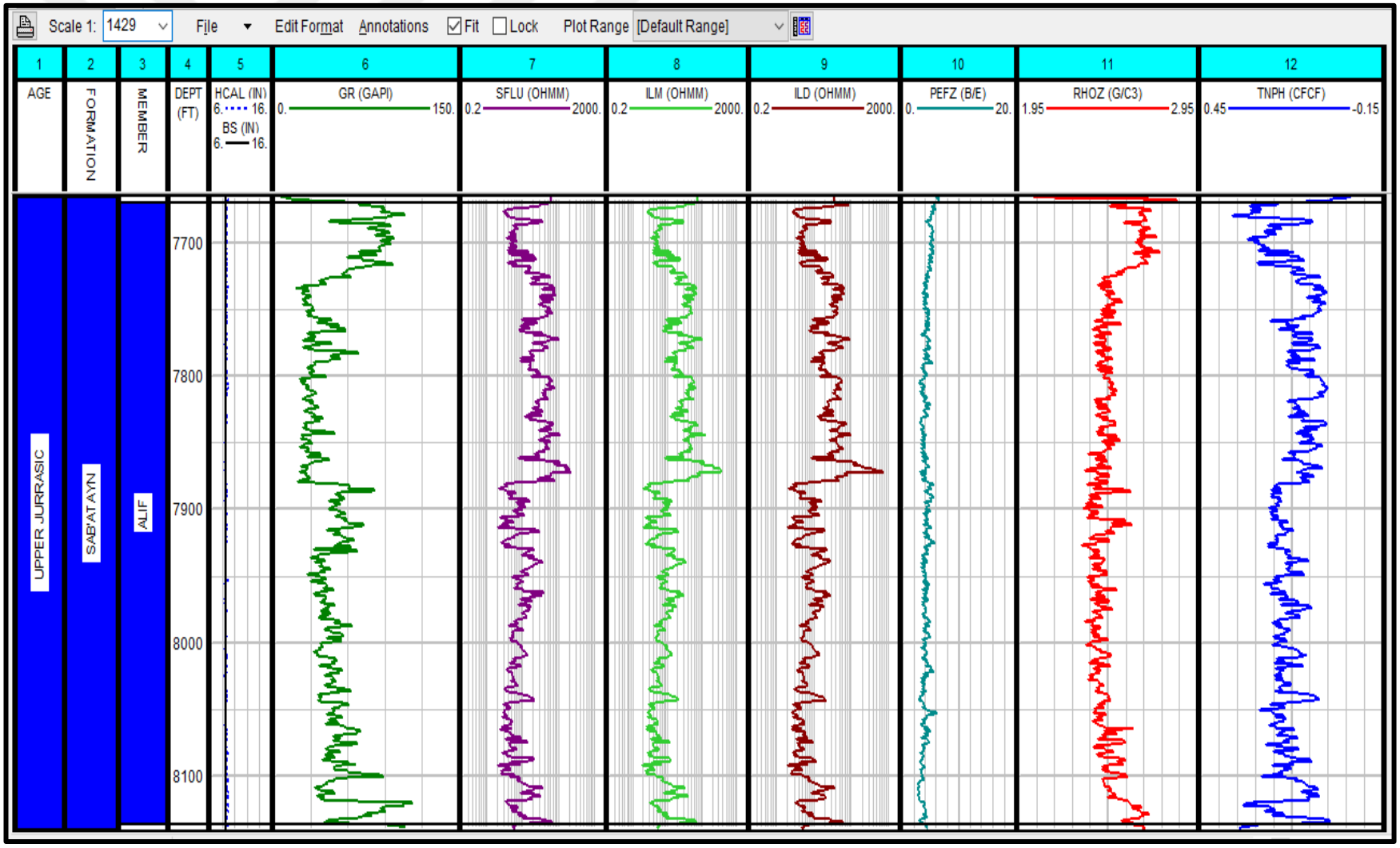

Figure 2.9. Digital raw data logs of Alif Member (7670 - 8136 ft) of Al-Raja-41 well converted to curves by IP (Interactive Petrophysics) software

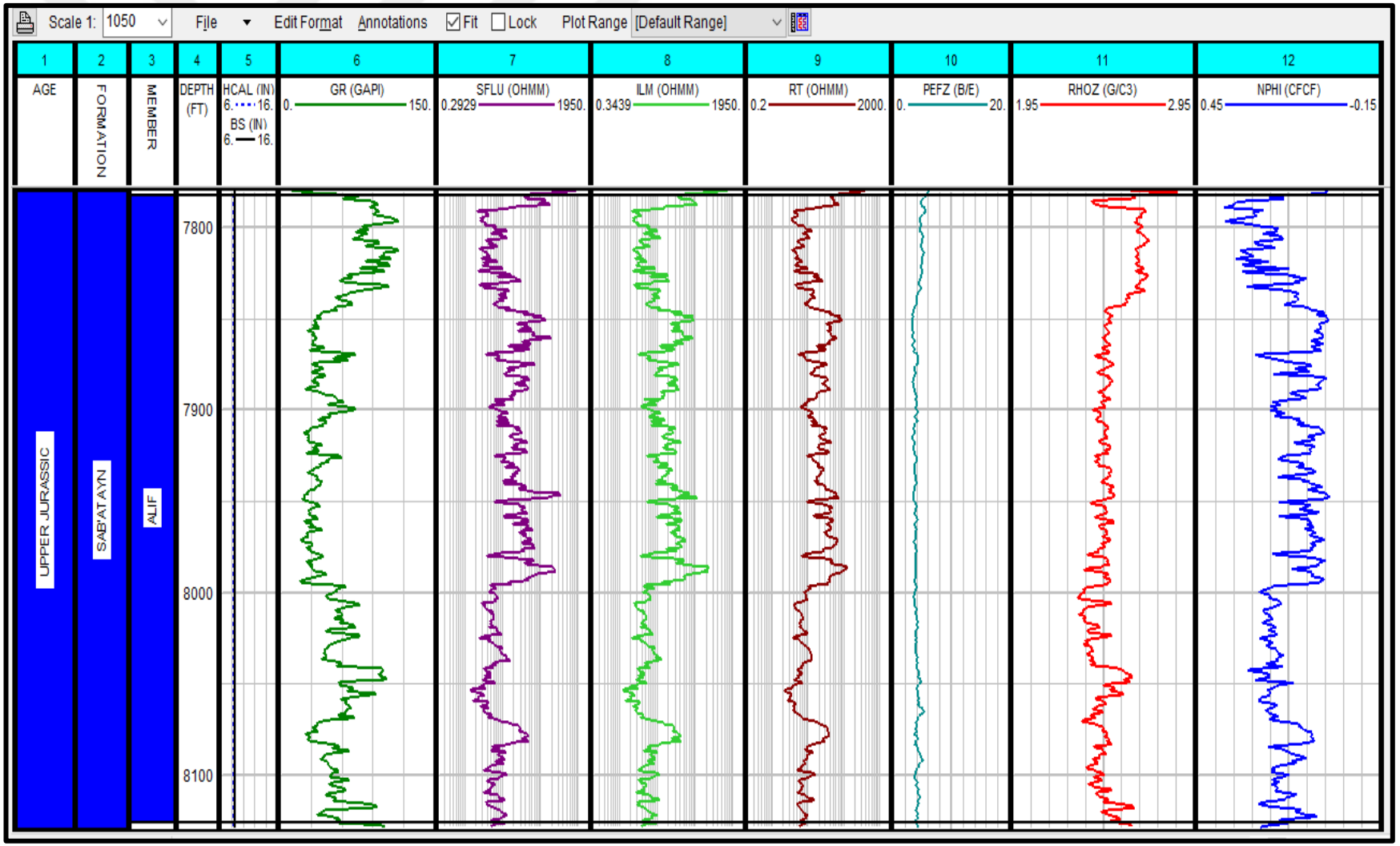

Figure 2.10. Digital raw data logs of Alif Member (7782 - 8126 ft) of Al-Raja-42 well converted to curves by IP (Interactive Petrophysics) software

2.3.2. Corrections and calculations

Several corrections have been applied by IP on the well log measurements. IP program offers the user the functionality of the conversion of several petrophysical parameters like temperature gradients. R_w can be converted from the spontaneous potential log, too. This operation is realized thanks to the correction and calculation modules, which also allow the calculation of the parameters and the log environmental corrections (Schlumberger, 2008).

2.3.2.1. Determination of geothermal gradient & formation temperature

The geothermal gradient can provide a continuous curve of temperature which is important for converting water resistivity to formation temperature since the variation of water resistivity is related to the depth. This module is expressed in the IP software in degree Fahrenheit (°F) or Celsius (°C) per 100 meters (m) or per 100 feet (ft) according to the unit of the borehole depth (Schlumberger, 2008).

The curve of formation temperature should be loaded to the IP software if it is available. Otherwise, it can be obtained by the geothermal gradient, which can be inputted directly as a fixed value from the well data. If it is not present, it is enough to enter the temperature values of some particular points to the program which will create the gradient and then calculate the temperature curve.

The temperature gradient can also be calculated based on the following equation (Asquith and Gibson, 1982) and used to create this curve (Schlumberger, 2008):

$$GG = \frac{(BHtemp - Stemp)}{TD} \tag{2.1}$$

$BHtemp$ = Bottom hole temperature expressed in °F or °C
$Stemp$ = Surface temperature expressed in °F or °C
TD= Total depth expressed in ft or m,
GG= Geothermal gradient.

Note that the geothermal gradient can be expressed in degree per 100 depth unit or degree per depth unit (Asquith and Gibson, 1982).

Formation temperature can be determined from the Formation Temperature Chart (Figure 2.11.) (Schlumberger, 1997) or from Asquith formula (2.2) depending on the temperature values of the surface and the bottom hole as well as the total depth of the borehole and the formation depth; in other words, in terms of the temperature gradient, surface temperature, and formation depth as following (Asquith and Gibson, 1982):

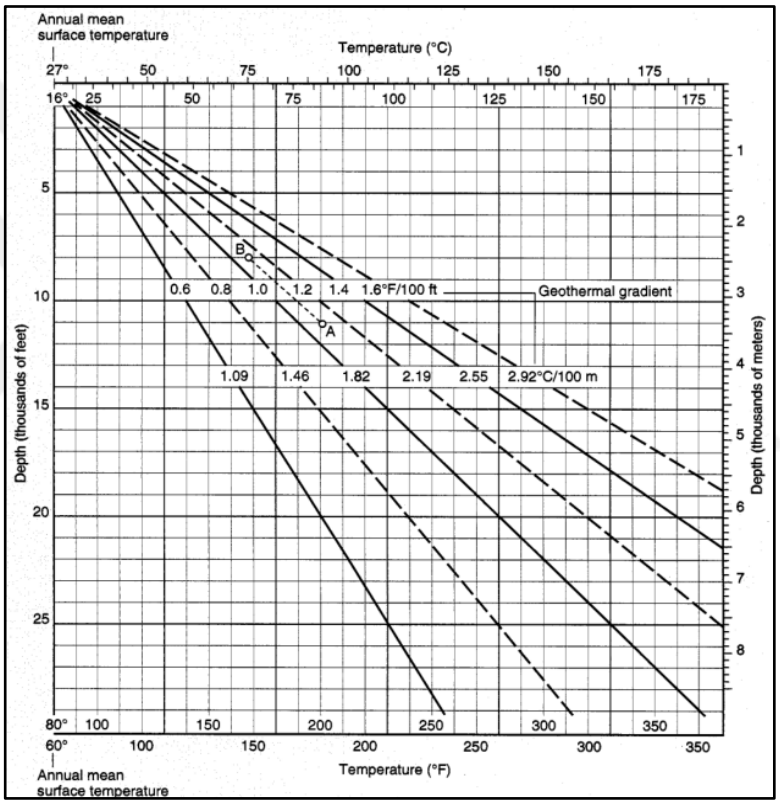

Figure 2.11. Formation temperature calculation chart (Schlumberger, 1997, 2009)

$$FT = Stemp + \left[\frac{BHtemp - Stemp}{TD}\right].FD \qquad (2.2)$$

Where:

FT= Formation temperature measured in (°F) or (°C)

FD= Formation depth measured in (m) or (ft).

Note: In the equations (2.1) and (2.2) and Figure 2.11., it is supposed that the relationship between the variables of temperature and depth is a linear relationship, in case there are no effects of anomalies on the temperature values (Asquith and Gibson, 1982; Avedissian, 1988).

In this study, bottom hole temperature as maximum and surface temperature as minimum temperature values were entered to IP software that enabled to calculate the temperature of the formation directly. Feet is the unit used for depth values throughout this study.

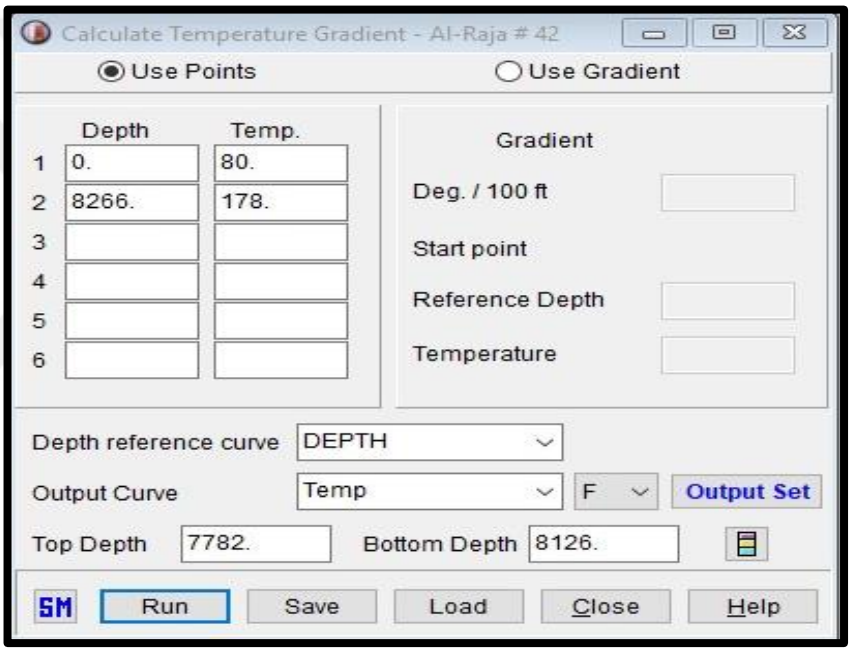

Figure 2.12. IP Software tab for calculating the temperature gradient for Al-Raja #42 well

2.3.2.2. Water resistivity (R_w)

Generally, in well-logging analysis, water resistivity (R_w) can be determined by various methods such as conductivity dip-cell, Archie equation in the water-saturated formations, SP log, etc. These methods give a continuous water resistivity curve which helps with the estimation of the resistivity values of the formation water throughout the selected section. The calculated resistivity of formation water will be corrected and then converted to the formation temperature which can take two different forms: a

fixed value or a continuous curve (Schlumberger, 2008). Determining the resistivity of the formation water is useful in well logging studies as it enters in the basic equations for calculating water saturation in the reservoirs (Schlumberger, 1989b, 2008).

The water resistivity value is given from the operating company in the Al-Raja as 0.04 Ω.m at 75° F (SEPOC, 2010).

2.3.2.3. Functions of basic log analysis module

This unit branches into five tabs, the main three of them are as follows: Porosity, R_w /S_w (Apparent water resistivity/Water saturation) and matrix. It enables converting several log parameters and making some simple calculations according to the analysis goals (Schlumberger, 2008).

2.3.2.4. Environmental corrections

Some companies called Logging Service Companies such as Halliburton, Baker Atlas, and Schlumberger offer some functions and methods for the determination of the different corrections like formation pressure, temperature, content of shale (shaliness), mud weight, mud cake effects, and borehole's effects. The environmental corrections of Schlumberger company have been applied to the data of this study (Table 2.1.). In the IP software, Schlumberger corrections process is usually applied on different logging tools such as (Schlumberger, 2008):

- Corrections of Neutron, Density, and sonic logs for formation fluids, borehole fluids, size of the borehole, and thickness of mud cake.
- Mud weight (MW), resistivity, and salinity.
- Gamma-ray corrections for mud weight, borehole diameter, and standoff tool.
- The effects of pressure and temperature.
- Corrections of resistivity tools for mud cake (R_{mc}), mud resistivity (R_m), and mud temperature (T_m).

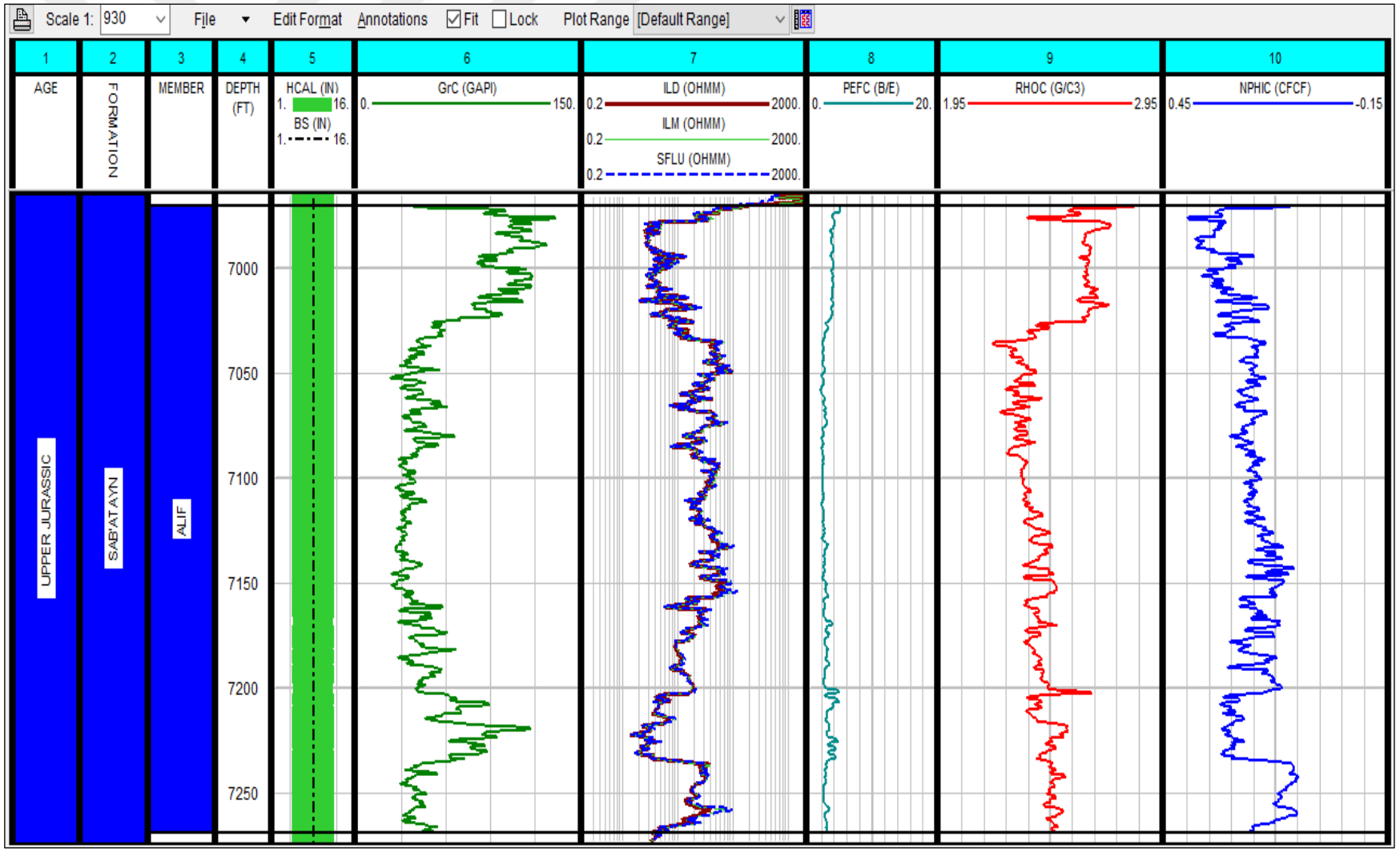

Figure 2.13. Corrected data logs of Alif Member (6970.5 – 7268.5 ft) of Al-Raja #36 well obtained by IP (Interactive Petrophysics) software

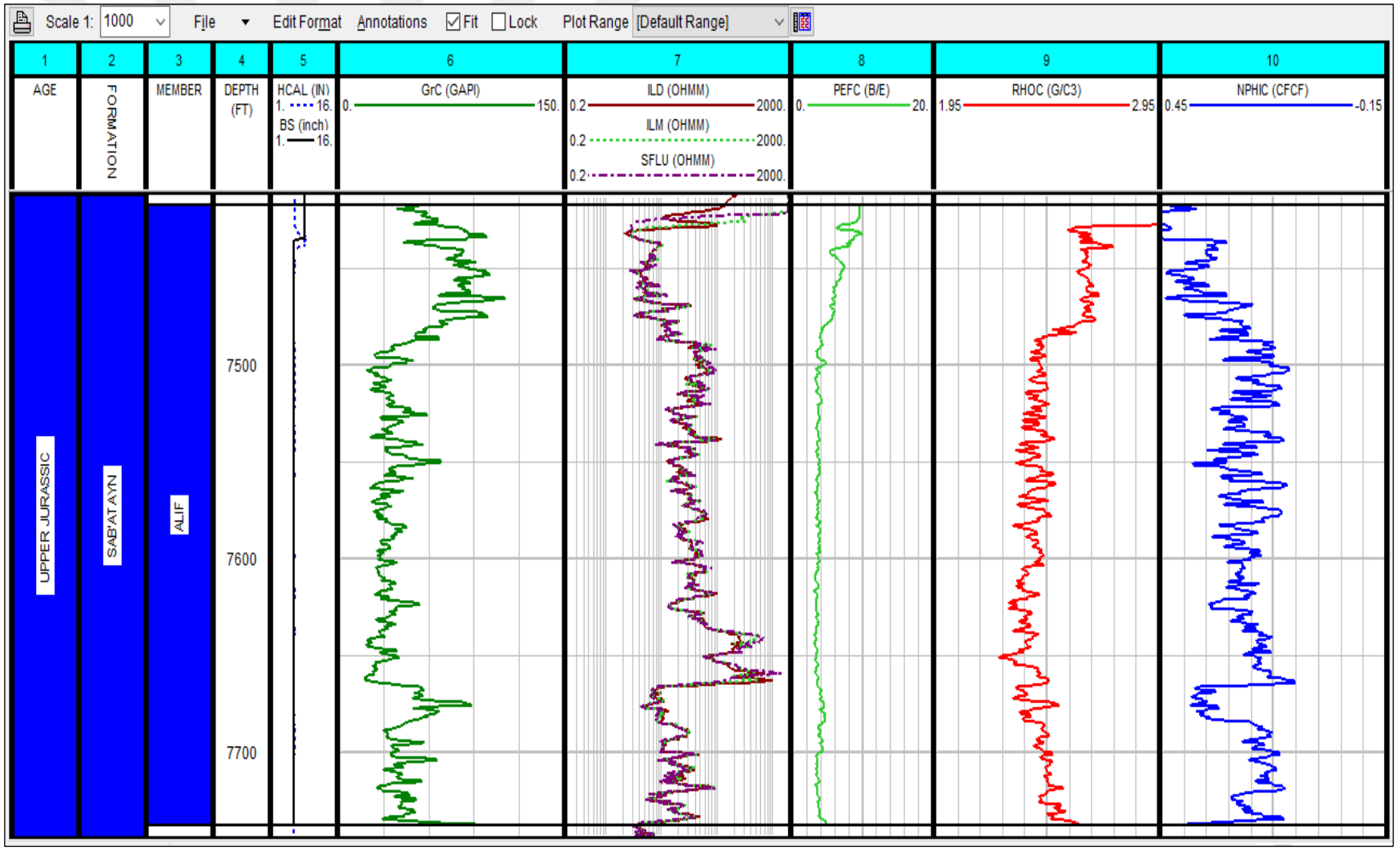

Figure 2.14. Corrected data logs of Alif Member (7417 – 7738 ft) of Al-Raja #37 well obtained by IP (Interactive Petrophysics) software

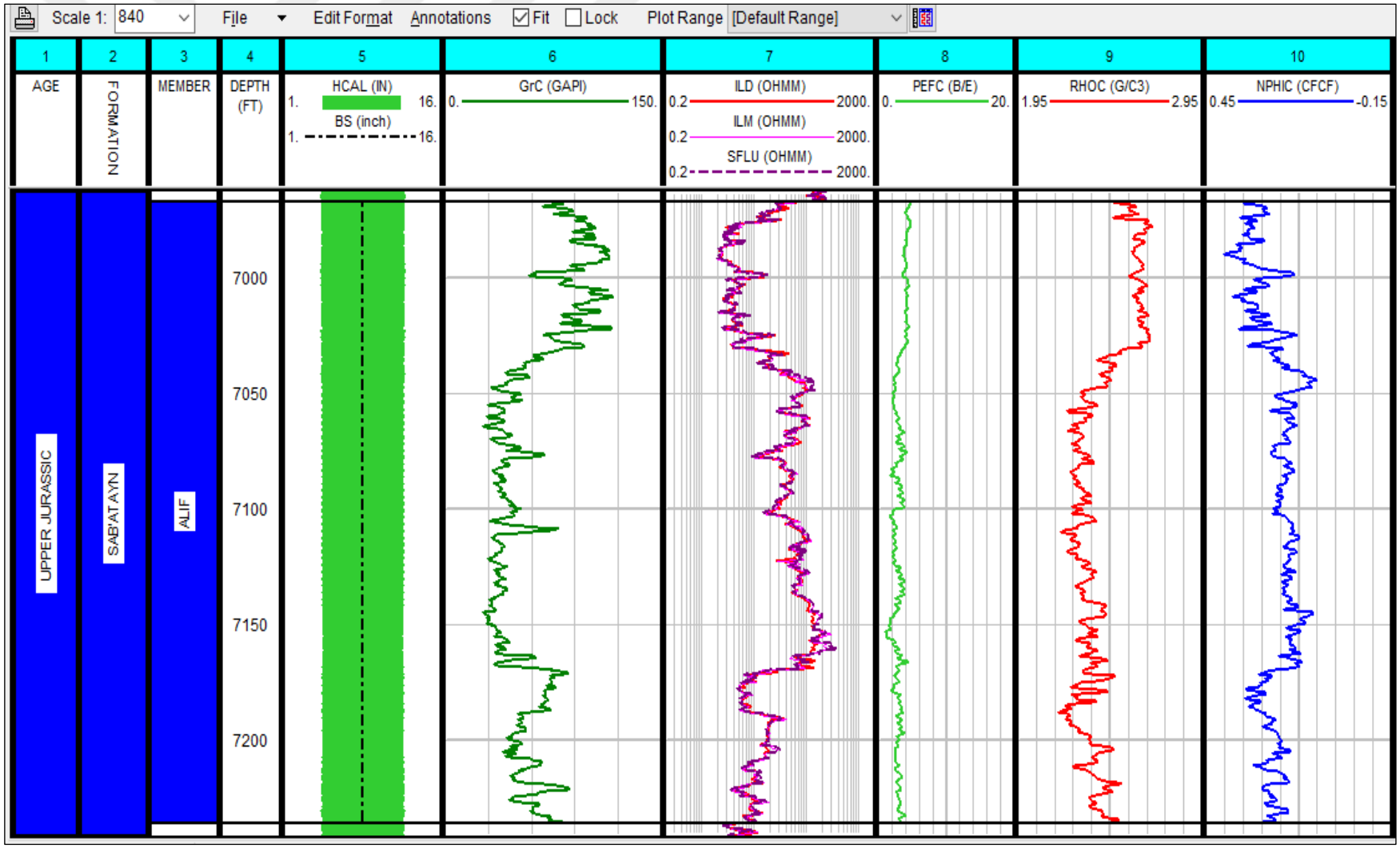

Figure 2.15. Corrected data logs of Alif Member (6967 – 7236.5 ft) of Al-Raja #38 well obtained by IP (Interactive Petrophysics) software

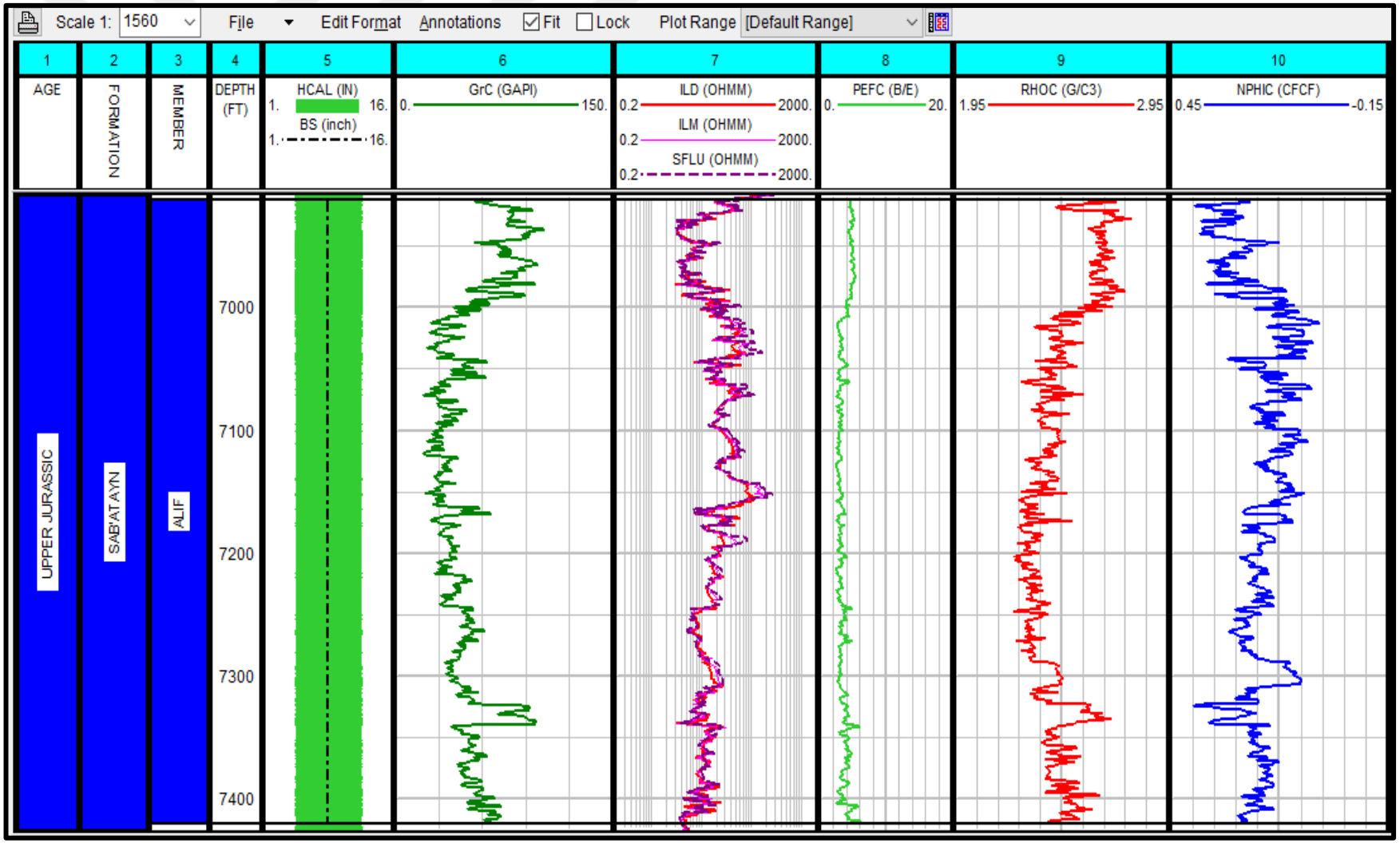

Figure 2.16. Corrected data logs of Alif Member (6912 – 7420 ft) of Al-Raja #39 well obtained by IP (Interactive Petrophysics) software

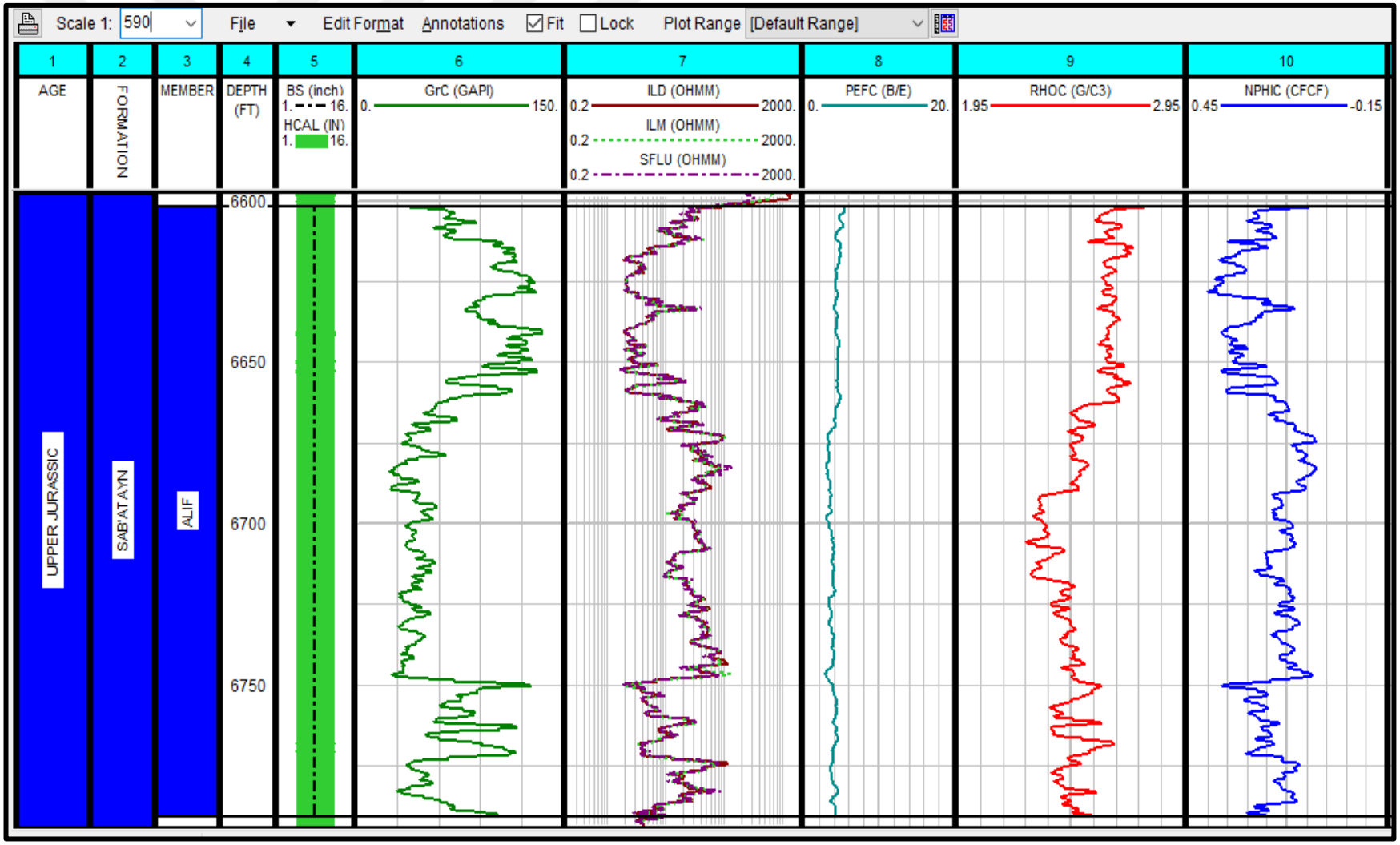

Figure 2.17. Corrected data logs of Alif Member (6602 – 6791 ft) of Al-Raja #40 well obtained by IP (Interactive Petrophysics) software

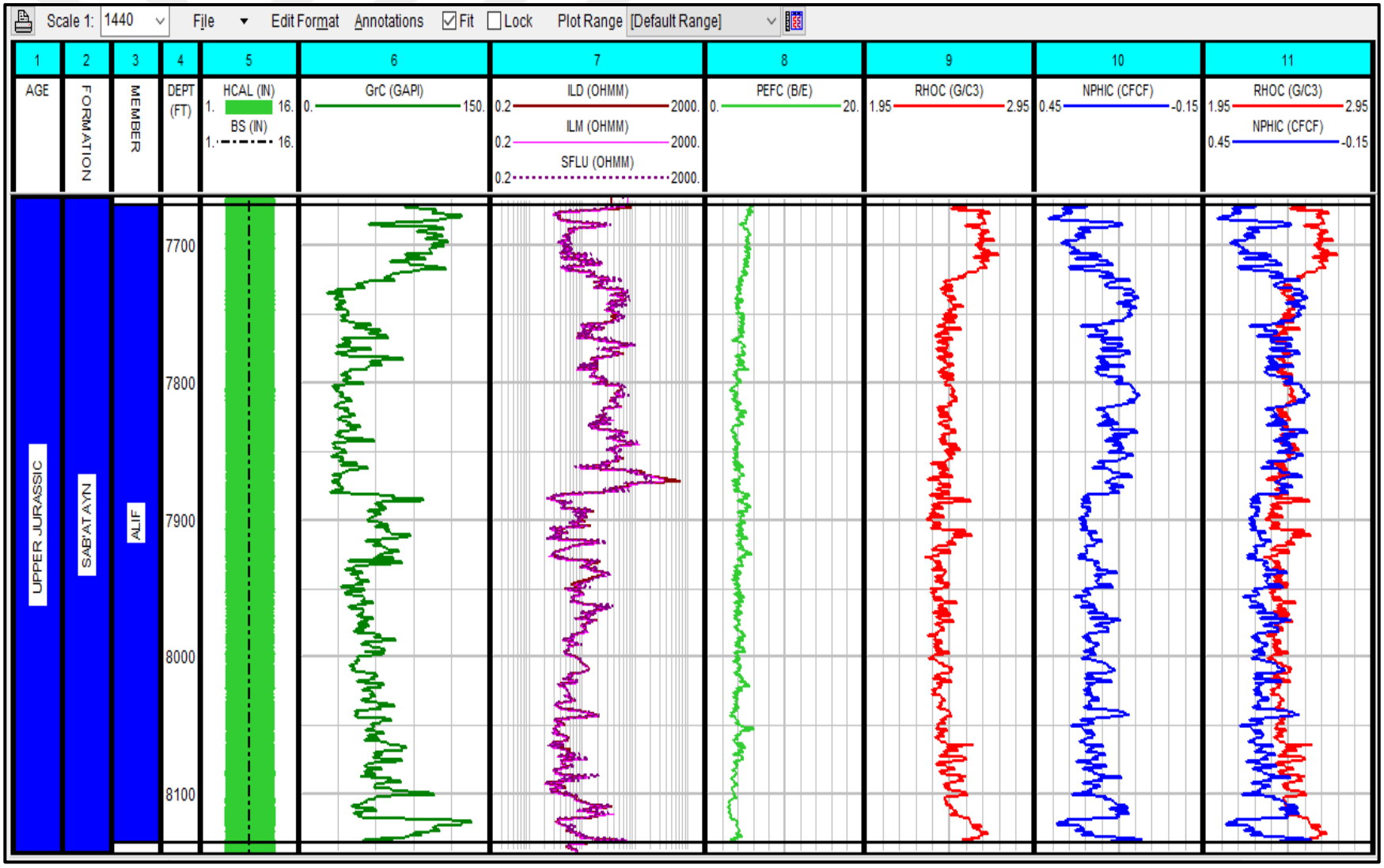

Figure 2.18. Corrected data logs of Alif Member (7670 – 8136 ft) of Al-Raja #41 well obtained by IP (Interactive Petrophysics) software

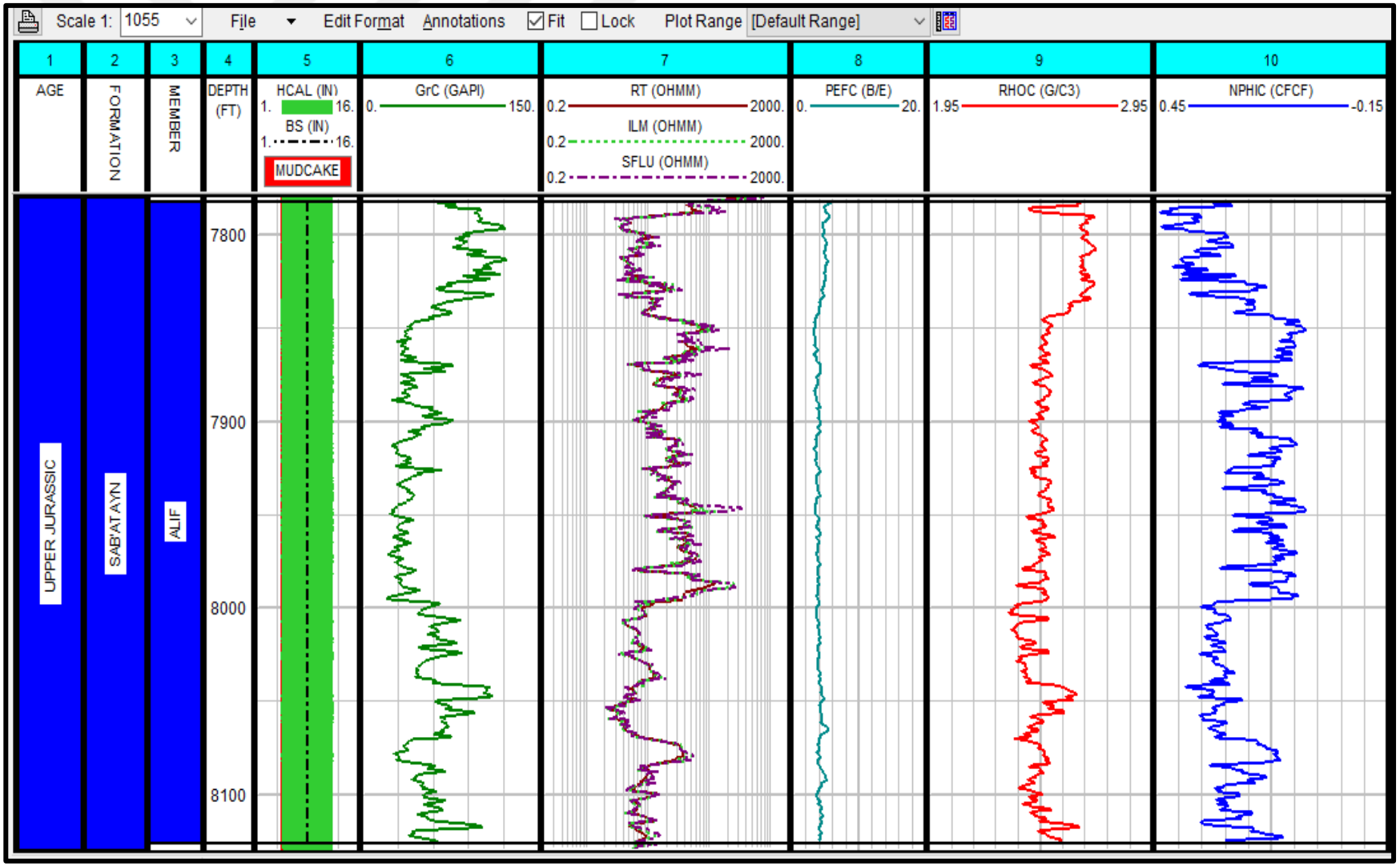

Figure 2.19. Corrected data logs of Alif Member (7782 – 8126 ft) of Al-Raja #42 well obtained by IP (Interactive Petrophysics) software

CHAPTER 3. INTERPRETATION AND CALCULATIONS

3.1. Interpretation Stage

This stage has been reached after the required correction, calculation, and conversion operations that were applied to the raw data. During the interpretation stage, the clay volume (V_{sh}), porosity (Φ), water saturation, and cut off, and summation will be respectively determined (Schlumberger, 2008).

3.2. Clay Volume

The interpretation of the clay volume enables the determination of the clay volume in the zones of interest which is considered one of the most important parameters in the evaluation process. The determination of the formation petrophysical parameters such as porosity, fluids saturation, lithology types are based fundamentally on the shale volume estimation. If the calculation of the existent shale volume is neglected, that could affect the readings of most of the logs (Kamel and Mabrouk, 2003). The Shale, which generally expresses clay materials, affects not only the well-logging readings but also the production properties of the reservoir (Avedissian, 1988). The shale is present in sand formations in one of these forms: dispersed, structural, and laminated (Al-Azazi, 2016).

Clay volume curves can be obtained from clay indicators. The window of clay volume analysis in IP software presents the input indicators of clay and the curves of the output related to them. Basically, single, and double clay indicators are the standard types of clay volume indicators. Gamma-ray (Gr), neutron (NPHI), deep resistivity (ILD) curves are examples of single clay indicators, whereas density with neutron curves, sonic with density curves are examples of double clay indicators (Kamel and Mabrouk,

2003; Schlumberger, 2008). The more indicators used, the more reliable estimation of shale content is obtained. The obtained value of shale ought to be corrected in order to get the final reliable value (Kamel and Mabrouk, 2003).

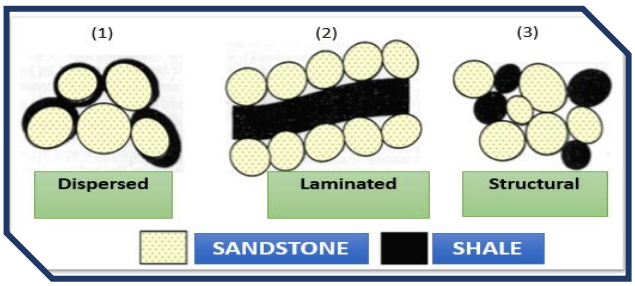

Figure 3.1. Distribution models of clay minerals in reservoir rocks (Avedissian, 1988)

3.2.1. Single-log indicators

Single clay indicators, as mentioned in the previous section, is one of two methods to calculate the shale volume in the reservoir evaluation process. According to this technique, the Gamma-ray (Gr), neutron (NPHI), deep resistivity (ILD) curves can be used individually to estimate the shale volume in the reservoir (Kamel and Mabrouk, 2003).

3.2.1.1. Gamma-ray log (GR)

GR tool is considered one of the best indicators used for detecting, differentiating the shale zones from the non-shale zones, and determine the volume of shale (Ramadan *et al.*, 2019). Gamma-ray is a sensitive tool to natural radioactive element emissions through the formations such as potassium (K), Uranium (U), and Thorium (Th). GR has a continuous log vs. depth. It has a standard unit called API (American Petroleum Institute) (Bassiouni, 1994). The reason why the gamma-ray tool is considered one of the best well logging tools to detect and determine the shale content in the reservoir is that in the sedimentary rocks, the shale formations commonly contain significant amounts of clay minerals which in turn give high gamma-ray readings in the log. In contrast, the clean formations (either not containing shale or containing a very low amount of the shale) usually give low responses of GR (Schlumberger, 1989b, 1989a;

Bassiouni, 1994). The index of Gamma-ray is determined as follows (Schlumberger, 1972 as cited in Al-Azazi, 2016):

$$GR_I \leq \frac{GR_{log} - GR_{cln}}{GR_{cl} - GR_{cln}} = X \quad (3.1)$$

GR_I= The index of shale
GR_{cln}= The minimum value of the gamma-ray in front of the clean formation (API)
GR_{cl}= The maximum value of the gamma-ray facing the shale formation (API)
GR_{log}= The reading of the gamma-ray in the zone of interest (API).

Thereafter, the Gamma-ray index helps with determining the shale volume according to these equations (Asquith and Gibson, 1982):

For the Palaeozoic and Mesozoic periods (earlier rocks), consolidated:

$$V_{sh} = 0.33 \times 2^{2 \times GRI} - 1.0 \quad (\%) \quad (3.2)$$

For the Tertiary period (later rocks) unconsolidated:

$$V_{sh} = 0.083 \times 2^{3.7 \times GRI} - 1.0 \quad (\%) \quad (3.3)$$

The shale volume V_{CL} is firstly calculated in this study through the clay indicator of Gamma-ray by the means of IP software according to the methodology as follows (Schlumberger, 2008):

- Linear:

$$V_{CLGR} = \frac{GR - GR_{cln}}{GR_{cl} - GR_{cln}} \quad (\%) \quad (3.4)$$

- Non-linear (curved) function:

$$X = V_{CLGR} = \frac{GR - GR_{cln}}{GR_{cl} - GR_{cln}} \quad (\%) \quad (3.5)$$

X equals V_{CLGR} as above (Schlumberger, 2008):

$$V_{CLGR}\ (\%) = \begin{cases} 0.0006078 \times (100.X)^{1.58527}, & X < 0.55 \quad (3.6) \\ 2.1212 \times X - 0.81667, & 0.55 < X < 0.73 \quad (3.7) \\ X, & 0.73 < X < 1.0 \quad (3.8) \end{cases}$$

- Clavier equation:

$$V_{CLGR} = 1.7 - \sqrt{3.38 - (X + 0.7)^2} \quad (\%) \quad (3.9)$$

- Stieber equation:

$$V_{CLGR} = \frac{0.5 \times X}{1.5 - X} \quad (\%) \quad (3.10)$$

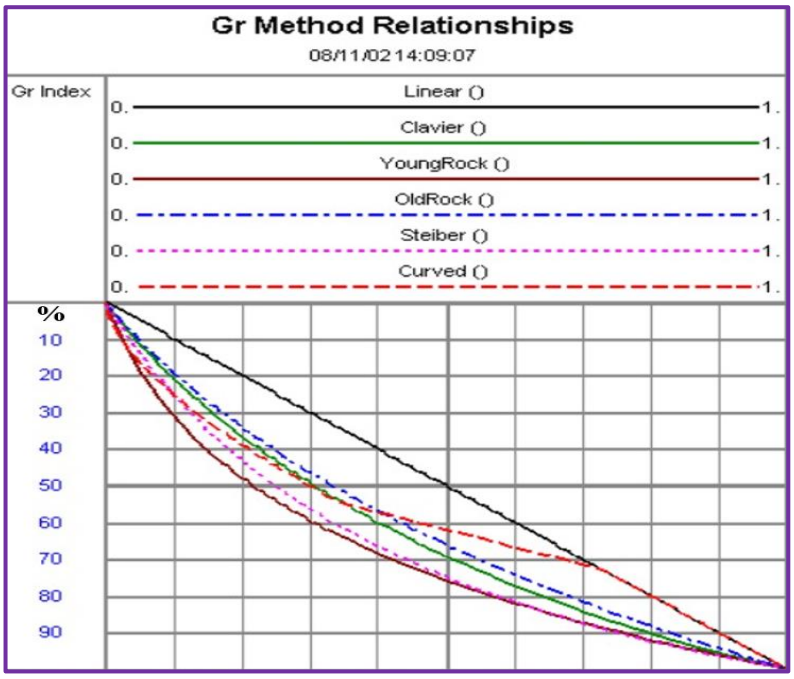

Figure 3.2. Gamma-ray methods relationships (Schlumberger, 2008)

- Larionov equation: for older rocks (Asquith and Gibson, 1982):

$$V_{CLGR} = 0.333 \times (2^{2\times X} - 1.0) \quad (\%) \quad (3.11)$$

- Larionov equation: for younger rocks (Asquith and Gibson, 1982):

$$V_{CLGR} = 0.083 \times (2^{3.7\times X} - 1.0) \quad (\%) \quad (3.12)$$

3.2.1.2. Neutron log

The neutron log is used to identify the lithology characteristics and to detect and calculate shale volume in the reservoir rocks. The response of the neutron log is principally a function of the quantity of Hydrogen existing in the formation. The gas reservoir can be detected through this log by comparison to other porosity logs or porosity measured in the lab (Avedissian, 1988; Schlumberger, 1989b). The shale content can be calculated by neutron log based on the following formula (Schlumberger, 1972 as cited in Al-Azazi, 2016):

$$V_{sh} \leq \frac{N_{log} - N_{cln}}{N_{cl} - N_{cln}} = X \quad (\%) \quad (3.13)$$

The shale volume V_{CL} is calculated in this study through the neutron log indicator by the means of IP software as follows (Schlumberger, 2008):

$$V_{CLNT} = \sqrt{\frac{N_{log}}{N_{cl}} X \frac{(N_{log} - N_{cln})}{(N_{cl} - N_{cln})}} \quad (\%) \quad (3.14)$$

Where

V_{CLNT}= Shale volume obtained from this method

N_{cln}= The reading of the neutron log in front of the clean zone

N_{cl}= The reading of the neutron log facing the shale zone

N_{log}= The reading of neutron log in front of the zone of interest.

3.2.1.3. Resistivity log indicator

Shale content can be detected and calculated through the indicator of resistivity log. When the resistivity log gives low values, that is an indicator of the existence of shale content. The existence of shale causes the diminution of the resistivity values. As a result, the hydrocarbon content can be differentiated from the water content by taking advantage of the contrast of resistivity values (Al-Azazi, 2016). The shale volume is calculated in this study through the clay single indicator of resistivity log (CL-Res) by the means of IP software as follows (Schlumberger, 2008):

$$X = \frac{R_{cl}}{R_t} \times \left(\frac{R_{cln} - R_t}{R_{cln} - R_{cl}} \right) \quad (\%) \tag{3.15}$$

$$V_{CLRT}\ (\%) = \begin{cases} 0.5 \times (2 \times X)^{0.67 \times (X+1)} & , \quad R_t > 2 \times R_{CL} \quad (3.16) \\ X & , \quad the\ other\ cases \quad (3.17) \end{cases}$$

R_t= The reading of the resistivity log in front of the zone of interest (Ω.m).
R_{cln}= The reading of the neutron log in front of the clean zone (Ω.m).
R_{cl}= The reading of the neutron log facing the shale zone (Ω.m).
V_{CLRT} = The shale volume determined by the resistivity log through IP software (%).

3.2.1.4. SP log (Spontaneous Potential)

One of the purposes of the spontaneous potential log is to differentiate between the impermeable shale formations which are non-reservoir rocks and the permeable sand formations which are reservoir rocks. SP has a relatively constant curve applicable to the shale baseline in front of the shale formations. In contrast, the SP curve changes to the negative side from the baseline in front of the permeable formation (non- shale rocks) (Avedissian, 1988). Thus, the volume of shale can be detected and calculated by SP log based on the following equation (Schlumberger, 2008):

$$V_{CLSP} = \frac{SP_{log} - SP_{cln}}{SP_{cl} - SP_{cln}} \quad (\%) \quad (3.18)$$

V_{CLSP} = Shale volume obtained from SP log.

SP_{cln}= The reading of the neutron log in front of the clean zone.

SP_{cl}= The reading of the SP log facing the shale section.

SP_{log}= The reading of SP log in front of the zone of interest.

In this work, we did not use the SP log because it was not available. Instead of that, we compensated by using other logs to get as reliable results as possible.

3.2.2. Double shale content indicators

It simply means the combination of the readings of two tools together in order to obtain the correct reservoir's shale volume ratio. The combination can be considered for the following pairs of logs: density and neutron curves, neutron and sonic curves, or density and sonic curves (Kamel and Mabrouk, 2003).

3.2.2.1. Density–Neutron indicator (N-D indicator)

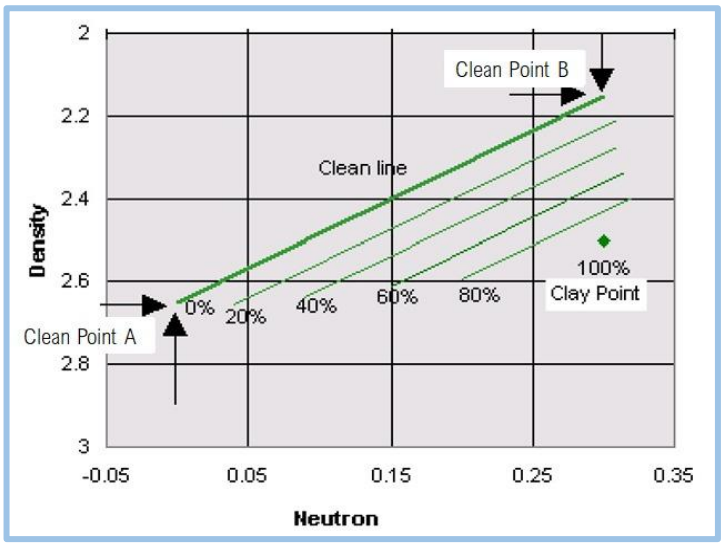

Figure 3.3. N- D cross plot shale indicator (Schlumberger, 2008)

Figure 3.3. shows the principle of calculating the shale volume in N-D indicator based on the clay point and the clean line (Schlumberger, 2008). The volume of shale of this study is determined based on the log readings of both density-neutron through IP software according to this formula (Schlumberger, 2008):

$$V_{CLDN} = \frac{(D_{clnB}-D_{clnA})\,(N_{log}-N_{clnA})-(D_{log}-D_{clnA})(N_{clnB}-N_{clnA})}{(D_{clnB}-D_{clnA})(N_{cl}-N_{clnA})-(D_{cl}-D_{clnA})(N_{clnB}-N_{clnA})} \quad (\%) \quad (3.19)$$

D_{log}= The reading of density log in front of the zone of interest.

N_{log}= The reading of neutron log in front of the zone of interest.

N_{cl} = The reading of the neutron log facing the shale section.

D_{cl}= The reading of the density log facing the shale section.

V_{CLDN}= The shale volume percentage determined by D-N curves indicators by IP software.

D_{clnA}, D_{clnB}, N_{clnA} and N_{clnB}= The values of neutron and density for both end parts of the clean line.

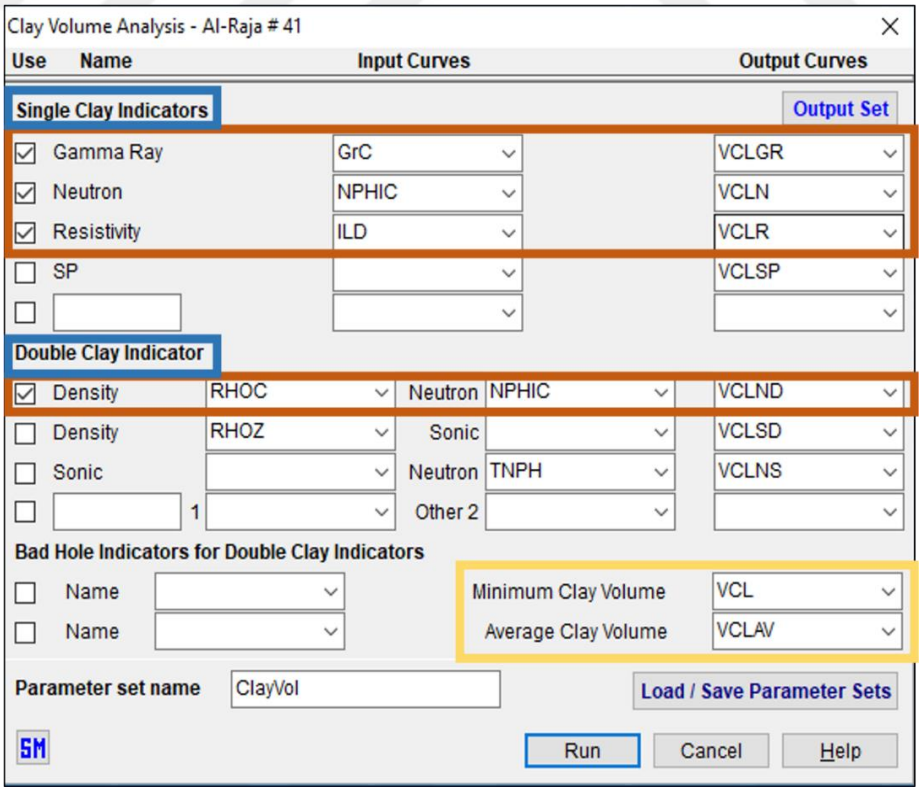

Figure 3.4. Methods used for calculating clay volume in this study – IP software

By applying the Schlumberger IP software, the shale volume (V_{cl}) in this study will be equal to the minimum value obtained from the following clay indicators (Kamel and Mabrouk, 2003): gamma-ray, neutron, density, and density – neutron as seen in Figures 3.5., 3.6., 3.7., 3.8., 3.9., 3.10. and 3.11.

3.3. Porosity and Water Saturation

These two parameters are quite important for the evaluation operation. This interpretation module of "Porosity and Water Saturation" is applied interactively to calculate water saturation (S_w), bulk water volume, hydrocarbon total saturation (S_{hyd})**,** matrix density (RHOMA), flushed zone water saturation (S_{xo}), hydrocarbon density (RHOHY), and total and effective porosity (PHI) (Schlumberger, 2008).

3.3.1. Porosity logs and calculations

Porosity is one of the most important petrophysical properties in the reservoir evaluation that enters effectively in the calculations of the fluid saturations (Schlumberger, 2008; Epuh and Joshua, 2020) as we will see later in this chapter. It is the ratio of the volume of rock pores filled by fluids to the total rock volume and can be calculated either by cores or well-logging (Avedissian, 1988):

$$\Phi = 100 \times \frac{Pr_{Vol}}{Bk_{Vol}} \quad (\%) \quad (3.20)$$

Where:

Φ= The percentage of porosity in the formation (%).

Pr_{Vol}= The pores volume (cm^3).

Bk_{Vol}= The bulk volume (cm^3).

This is called the bulk or absolute porosity whereas the interconnected pores are defined by effective porosity (Avedissian, 1988; Ramadan *et al.*, 2019).

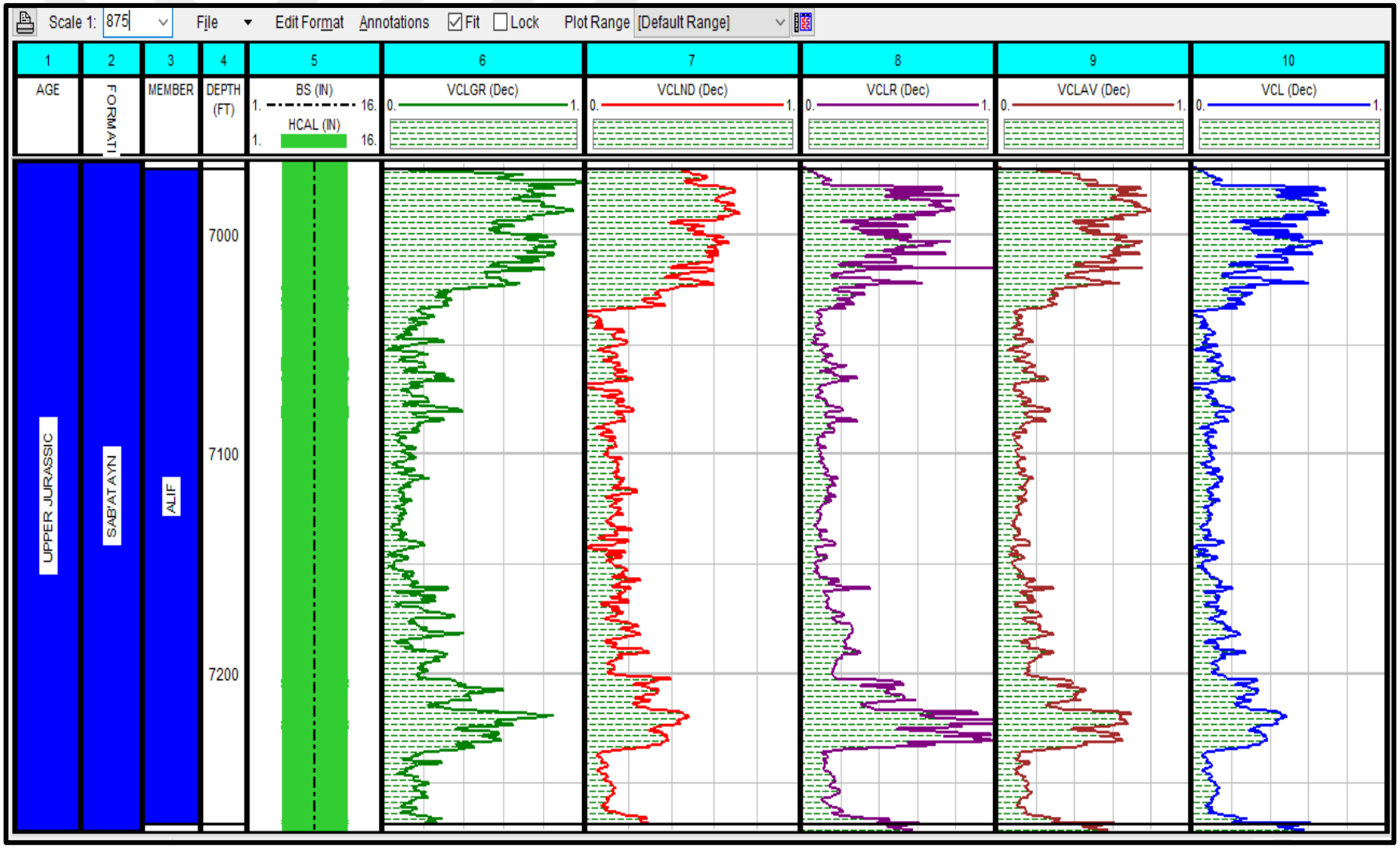

Figure 3.5. Clay volume of Alif Member (6970.5 – 7268.5 ft) determined through Al-Raja-36 well by IP (Interactive Petrophysics) software

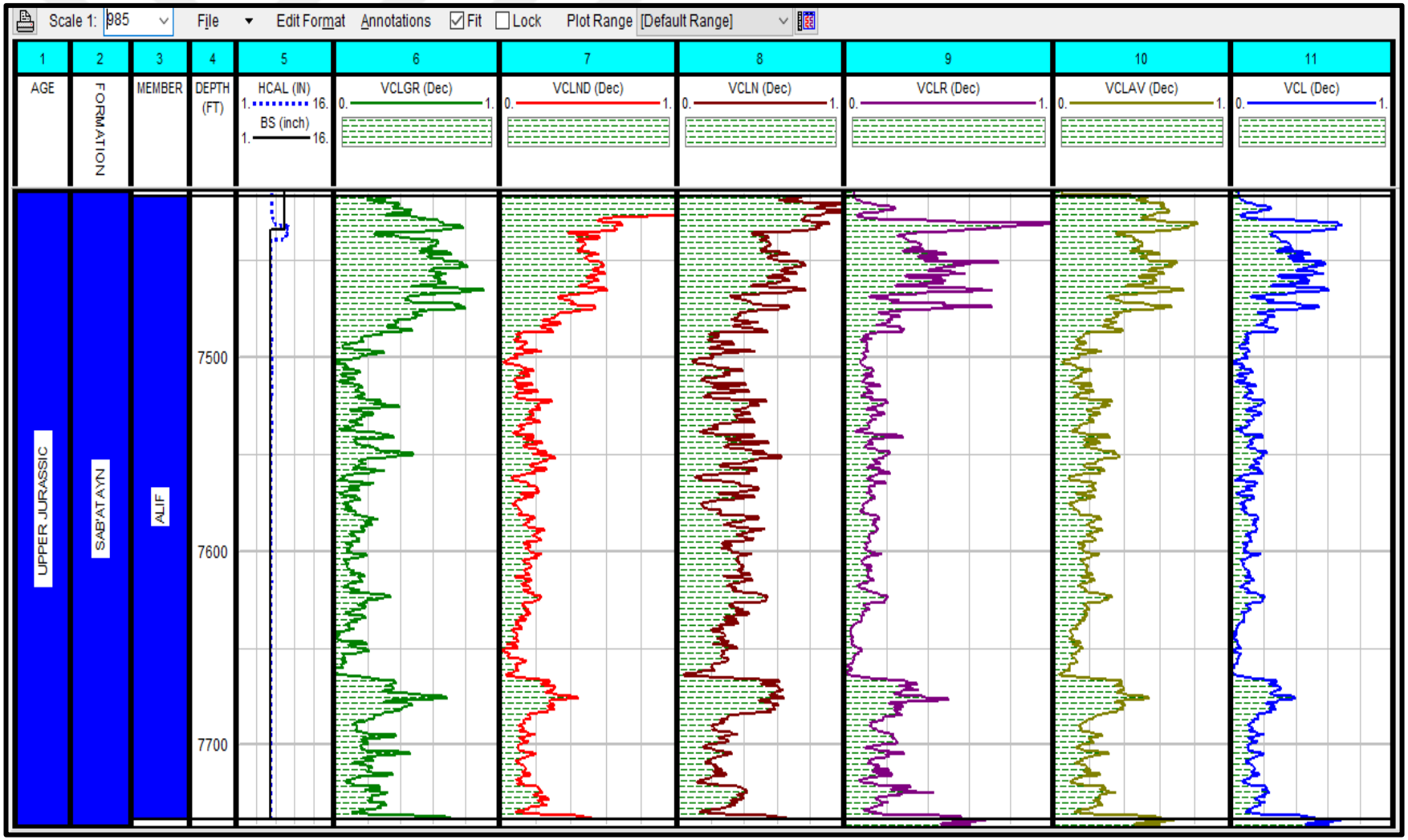

Figure 3.6. Clay volume of Alif Member (7417 - 7738 ft) determined through Al-Raja-37 well by Schlumberger IP (Interactive Petrophysics) software

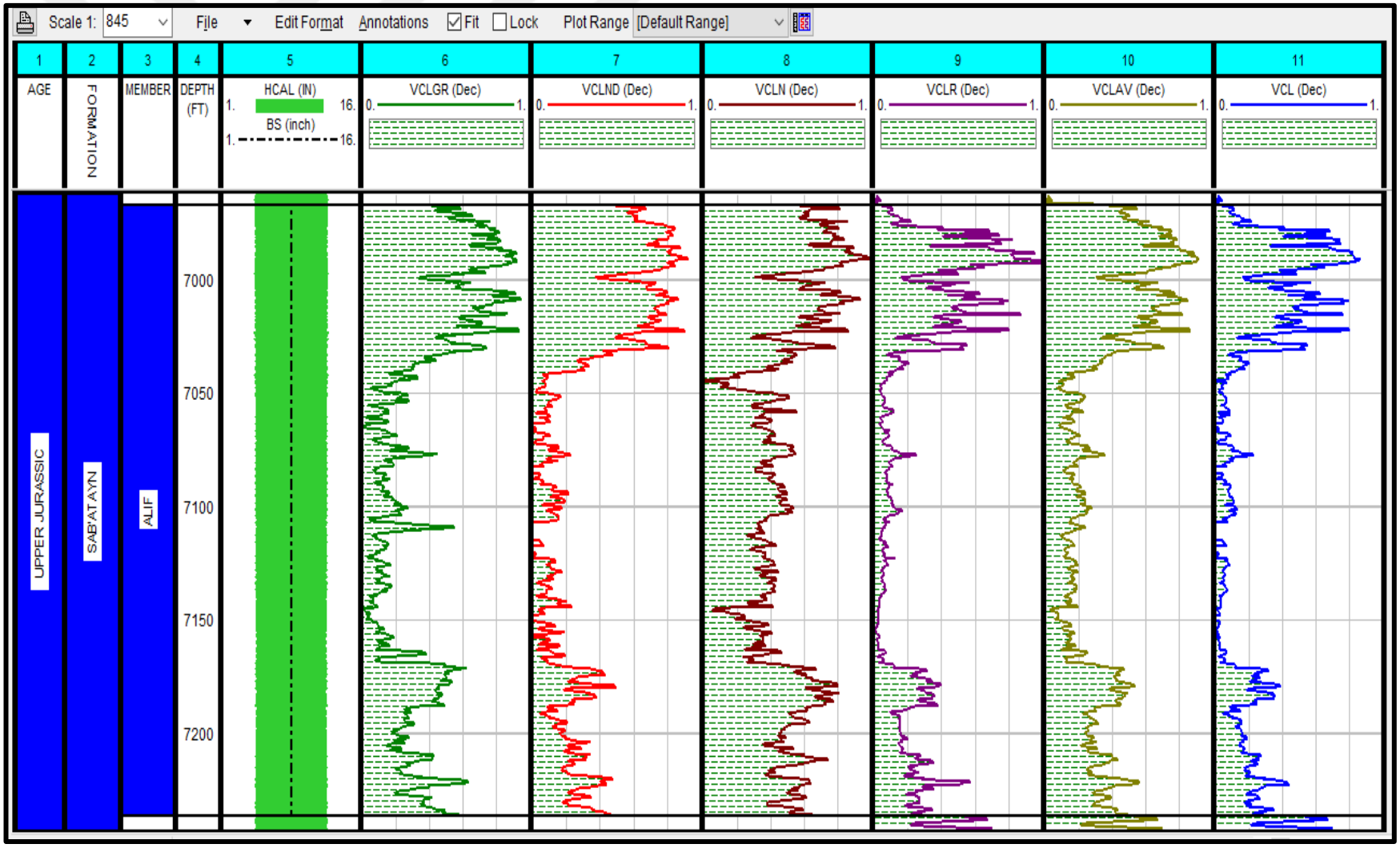

Figure 3.7. Clay volume of Alif Member (6967 - 7236.5 ft) determined through Al-Raja-38 well by Schlumberger IP (Interactive Petrophysics) software

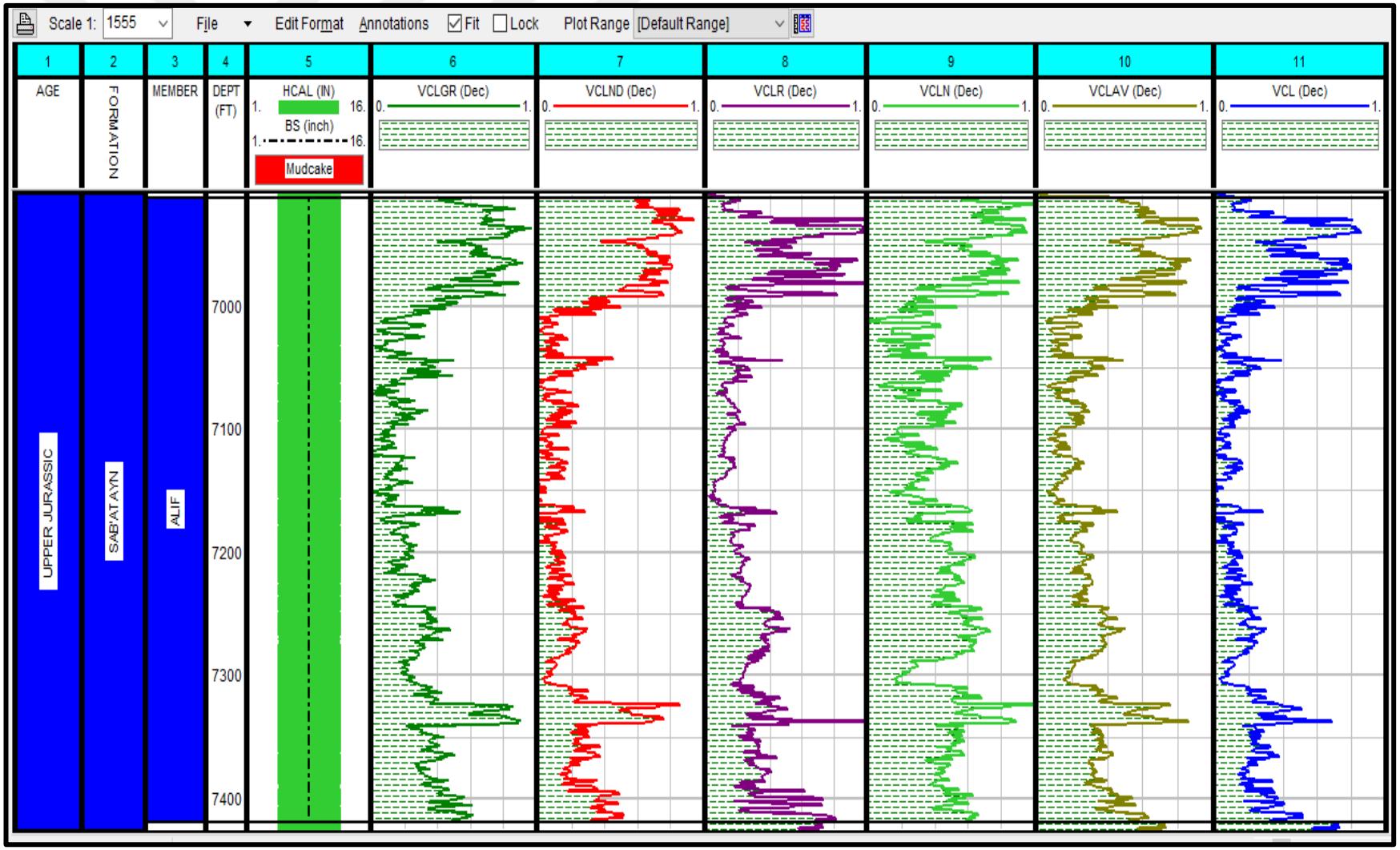

Figure 3.8. Clay volume of Alif Member (6912 - 7420 ft) determined through Al-Raja-39 well by Schlumberger IP (Interactive Petrophysics) software

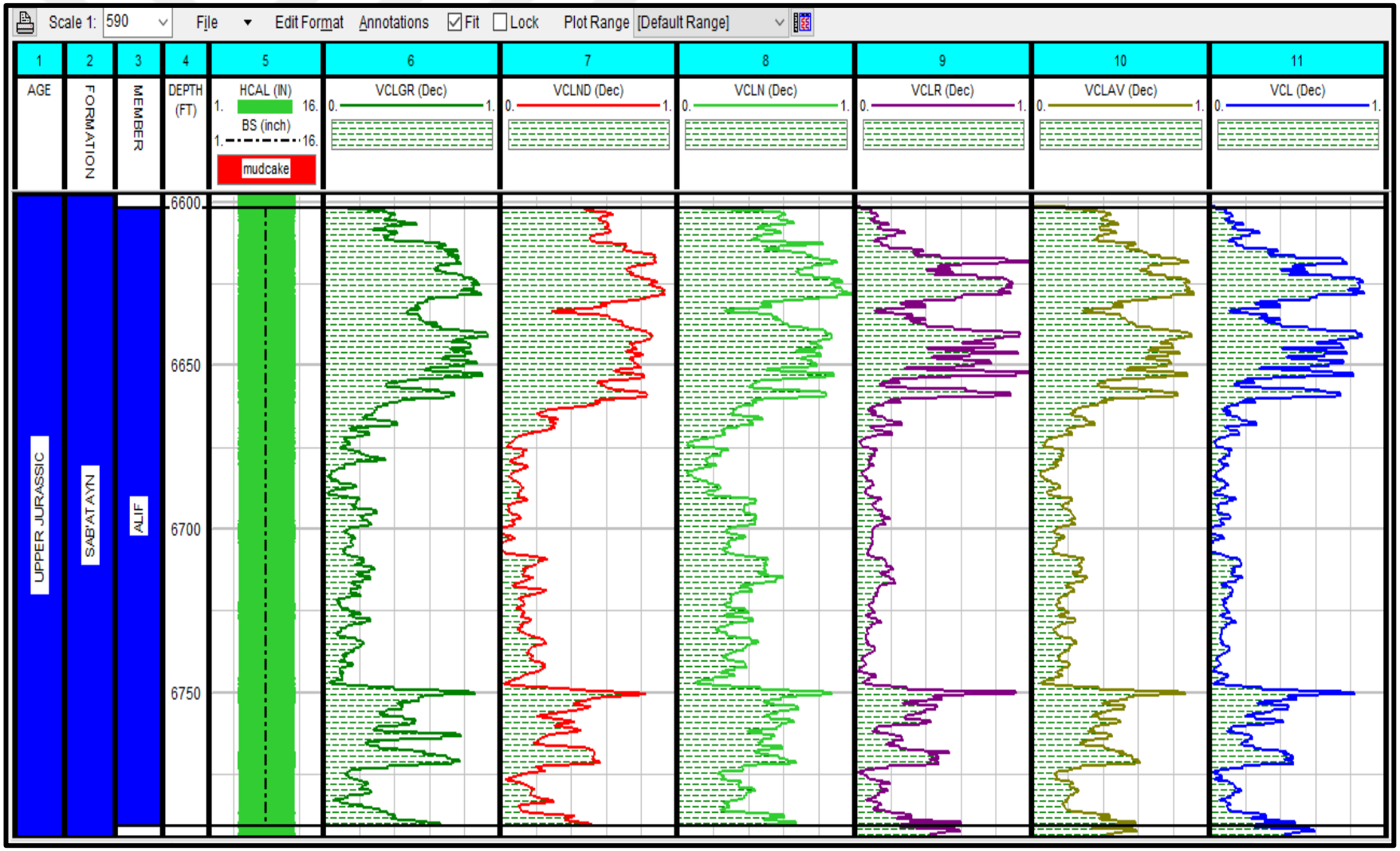

Figure 3.9. Clay volume of Alif Member (6602 - 6791 ft) determined through Al-Raja-40 well by Schlumberger IP (Interactive Petrophysics) software

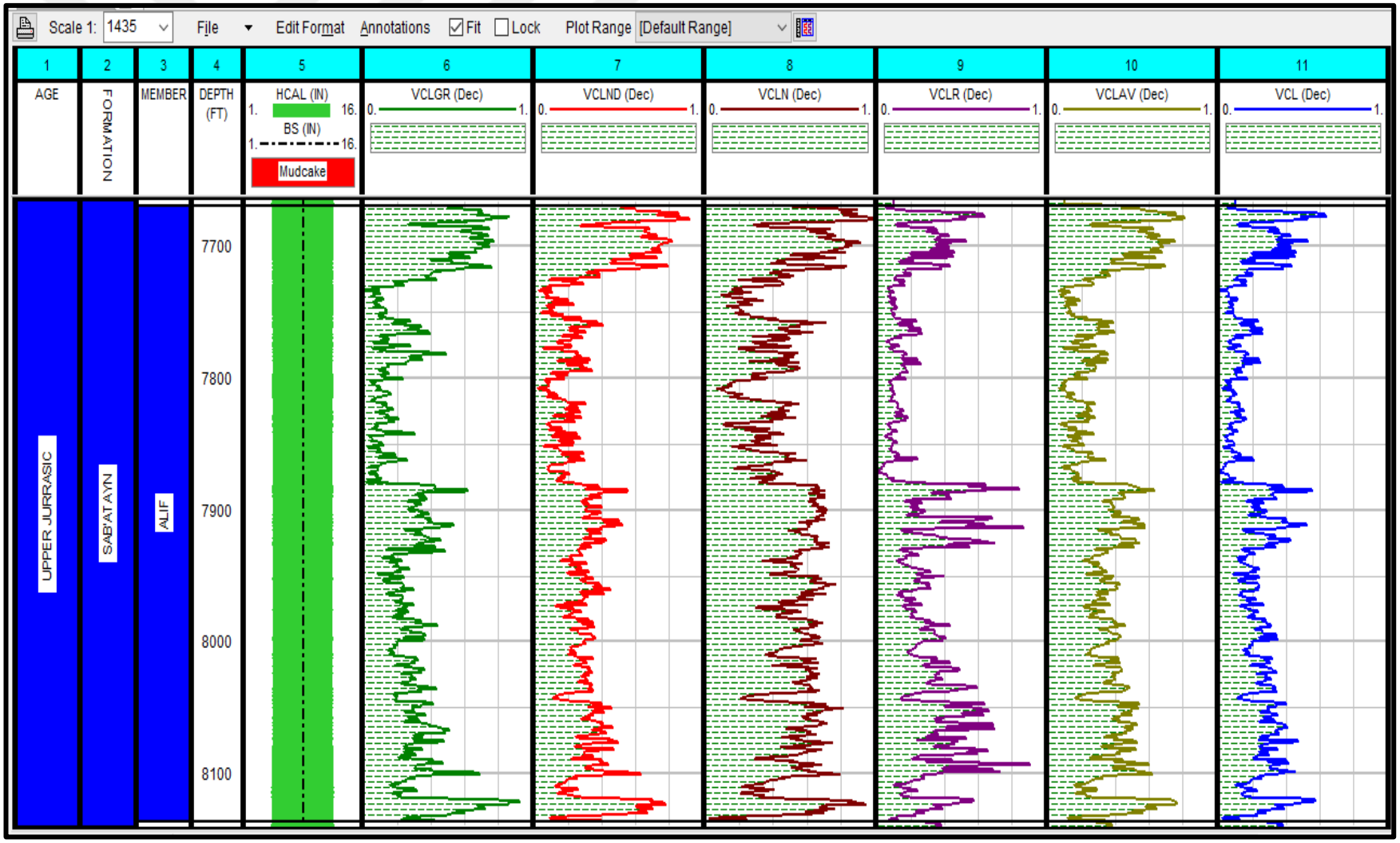

Figure 3.10. Clay volume of Alif Member (7670 - 8136 ft) determined through Al-Raja-41 well by Schlumberger IP (Interactive Petrophysics) software

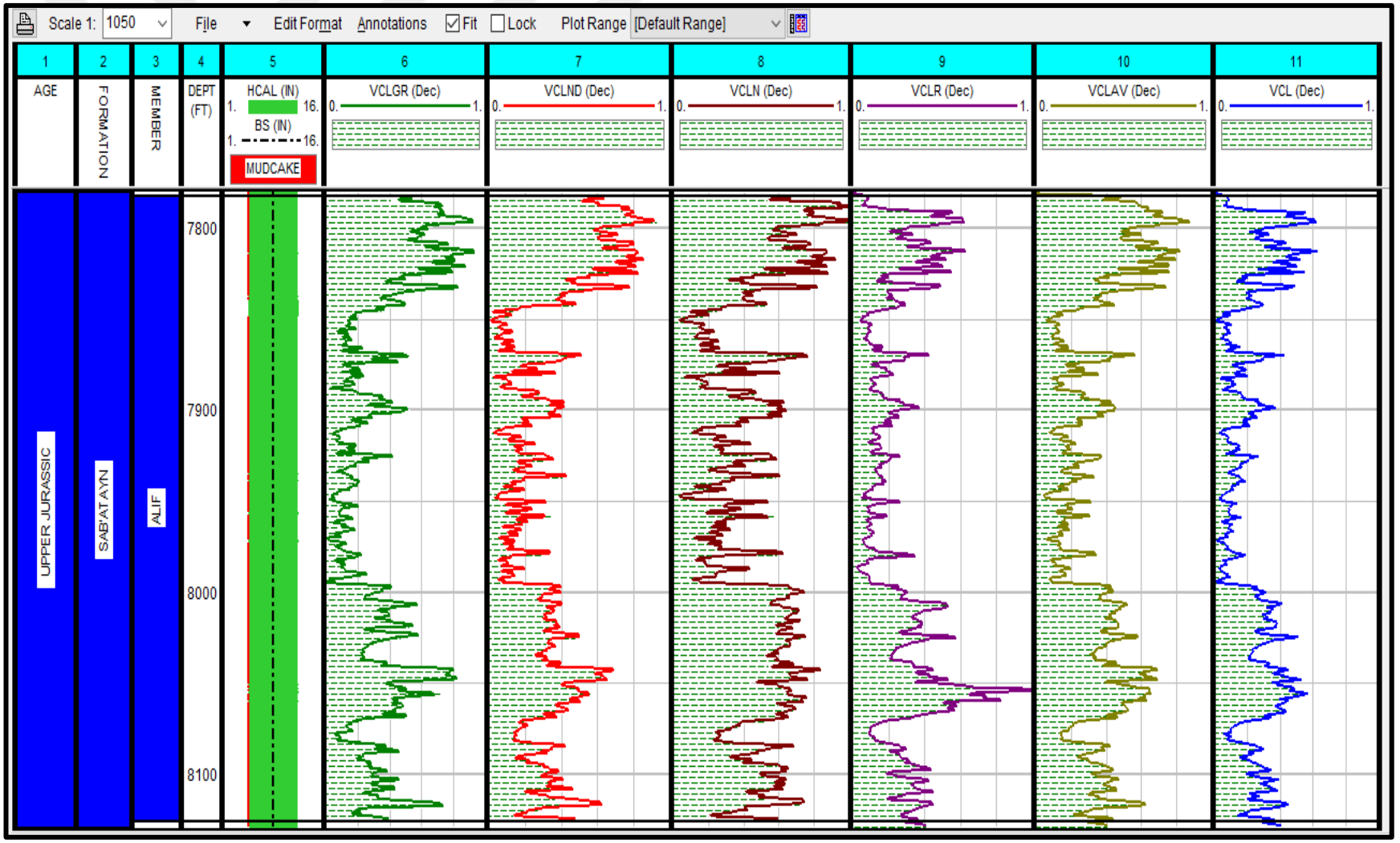

Figure 3.11. Clay volume of Alif Member (7782 - 8126 ft) determined through Al-Raja-42 well by Schlumberger IP (Interactive Petrophysics) software

The porosity of the sedimentary rocks commonly ranges between 0 to 40%. Porosity values are influenced by the lithology and the nature of fluids and the percentage of shale existing in the formation (Avedissian, 1988; Schlumberger, 1989a). The porosity can be calculated either by cores or well-logging. The porosity of the reservoir can be obtained through the common three types of logs called porosity logs: density log, neutron logs, and sonic log (Avedissian, 1988).

3.3.1.1. Density log

It is a porosity tool used to measure the formation electron density which has to do with the bulk density. The collisions of the gamma rays emitted by the radioactive source in the formation with the electrons of this formation result in a partial loss in the gamma-ray energy (Compton Scattering). The gamma-ray reflected and scattered is inversely proportional to the density of the formation and used to determine it. That means that the low formation density returns more intense gamma-ray radiation to the detector, and vice-versa. Then, the formation porosity is determined using the formation density. The value derived from the density log represents the bulk density and its unit of measurement (g/cc). The density log basically measures the bulk density from which the porosity of the formation can be obtained. The density log is influenced by several factors such as mud filtrate since the tool measures in shallow depth. The density log may also be affected by the presence of gas since the gas density is lower than the density of the rocks, which causes the porosity values to be high (Asquith and Gibson, 1982; Avedissian, 1988). If the gas density is not given. it is suggested to consider its value as 0.7 g/cc to make the required calculations. Oil does not influence greatly the porosity values, however (Asquith and Gibson, 1982; Glover, 2000). The porosity values are also influenced by high shale contents. The porosity is determined based on the density log either by Schlumberger charts (Figure 3.13.) or by the following formula (Asquith and Gibson, 1982):

$$\Phi_{\mathrm{Den}} = \frac{\rho_{\mathrm{mtx}} - \rho_{\mathrm{b}}}{\rho_{\mathrm{mtx}} - \rho_{\mathrm{fl}}} \quad (\%) \qquad (3.21)$$

ρ_{mtx} = Matrix density (g/ cc).

ρ_b= Bulk density of the formation (log reading) (g/ cc).

ρ_{fl}= Density of the fluid (0.7 for gas, 1.0 for fresh mud, 0.8 for oil, 1.1 for salty mud) (g/ cc).

Φ_{Den}= Density derived porosity (%).

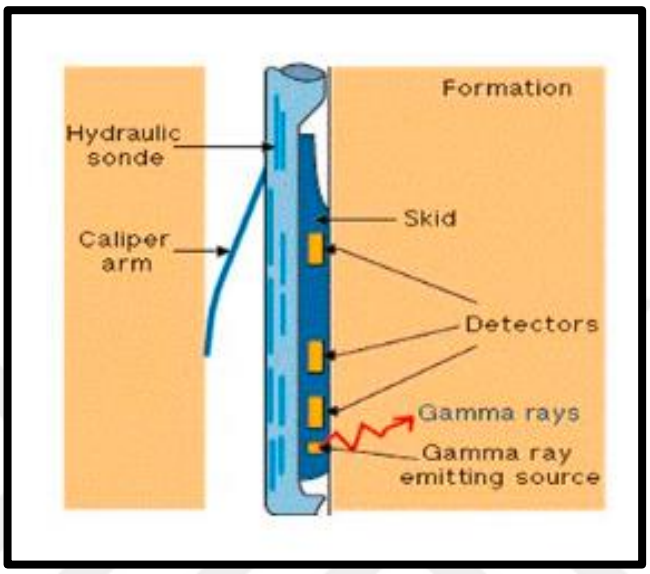

Figure 3.12. density logging technique (Schlumberger, 1989b)

The porosity values also are influenced by high shale contents. So, the correction of the porosity is required due to the effect of the shale volume. The porosity percentage, in this case, can be calculated in shale zones according to the following equations (Dewan, 1983):

$$\Phi_{DenC} = \Phi_{Den} - V_{cl} \times \Phi_{cl} \quad (\%) \quad (3.22)$$

$$\Phi_{DenC} = \frac{\rho_{mtx} - \rho_b}{\rho_{mtx} - \rho_{fl}} - V_{cl} \times \frac{\rho_{mtx} - \rho_{cl}}{\rho_{mtx} - \rho_{fl}} \quad (\%) \quad (3.23)$$

Where:

ρ_{mtx} = Matrix density (g/ cc).

ρ_b= Bulk density of the formation (log reading) (g/ cc).

ρ_{fl}= Density of the fluid (gm/cc).

ρ_{cl} = The reading of density log facing the shale zone (gm/cc).

V_{cl}= The shale volume (%).

Φ_{cl} = The porosity percentage which calculated based on the density log in the shale formation.

Φ_{Den}= Density derived porosity (%).

Φ_{DenC}= The corrected porosity derived by density log (%).

Table 3.1. Matrix density of the common reservoir rocks (Glover, 2000)

Rock Type	Standard Matrix Density (g/cc)
Sandstone	2.65
Limestone	2.71
Dolomite	2.87
Shale	2.97

In this study, Schlumberger IP software have been used to determine the porosity by the means of the density log based on the following equations (Schlumberger, 2008):

$$\Phi_{\mathrm{Den}} = \frac{[\rho_{\mathrm{mtx}} - \rho_{\mathrm{b}} - V_{\mathrm{cl}} \times (\rho_{\mathrm{ma}} - \rho_{\mathrm{cl}})]}{\rho_{\mathrm{mtx}} - \rho_{\mathrm{fl}} - S_{\mathrm{xo}} - \rho_{\mathrm{ApHyd}} \times (1 - S_{\mathrm{xo}})]} \quad (3.24)$$

$$\rho_{\mathrm{ApHyd}} = 2\rho_{\mathrm{Hyd.den}} \times \frac{(10 - 2.5\rho_{\mathrm{Hyd.den}})}{16 - 2.5\rho_{\mathrm{Hyd.den}}} \quad (3.25)$$

$$\rho_{fl} = 1.0 + 7 \times \text{salinity} \times 10^{-7} - (FT - 80)^2 \times 10^{-6} \quad (3.26)$$

Φ_{Den} = The porosity derived from density log by IP software (%).

ρ_{ApHyd}= The apparent density of the hydrocarbon (gm/cc).

S_{xo}= Water saturation of invaded zone (%).

$\rho_{\mathrm{Hyd.den}}$= The density of the hydrocarbon (gm/cc).

FT= Formation temperature (°F).

ρ_{fl}= Density of the fluid (gm/cc).

ρ_{cl}= Density of wet clay (gm/cc).

V_{cl}= Volume of wet clay (%).

ρ_{b}= Bulk density of the formation (log reading) (g/ cc).

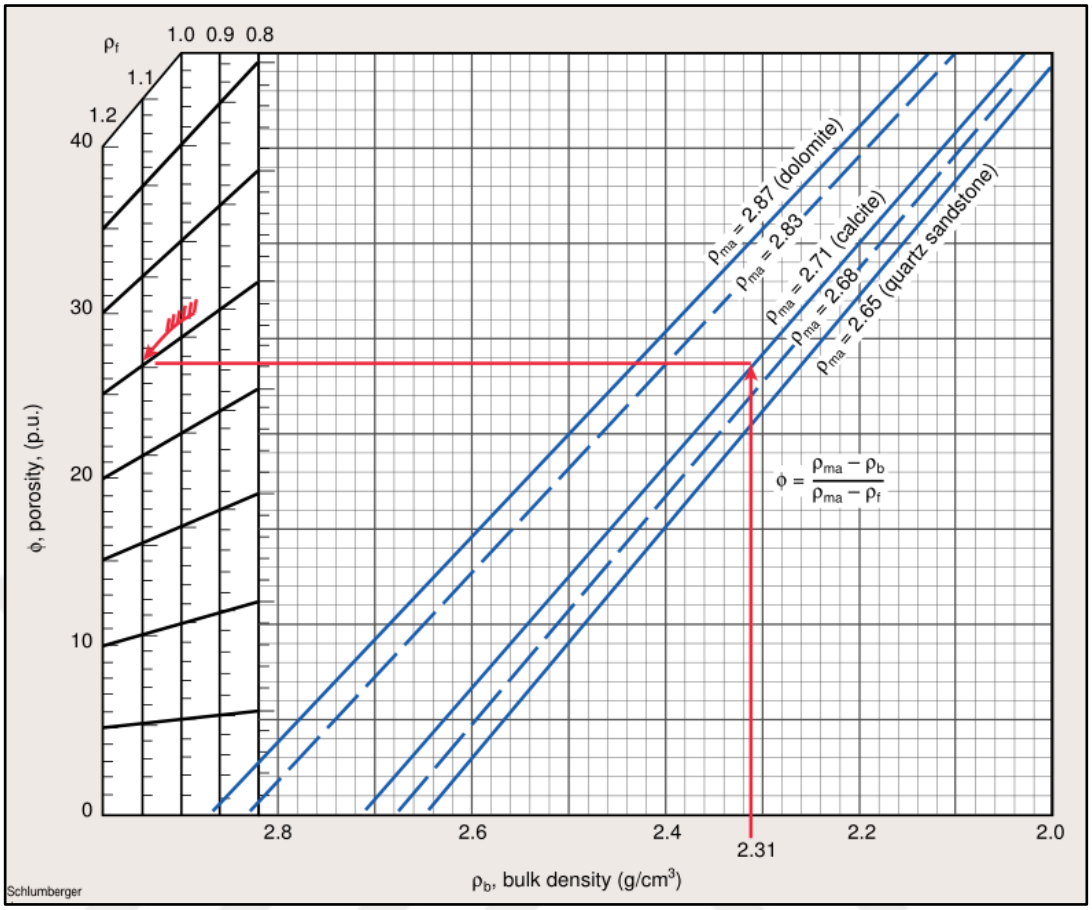

Figure 3.13. Chart of formation porosity determination from density log according to Schlumberger (Schlumberger, 1997)

3.3.1.2. Neutron log

Neutron log is a porosity log that detects the presence of hydrogen ions in the formations through the emission of ions from a radioactive source and measures their concentration. The Neutron log is used to measure the porosity of the formation directly. In fact, Hydrogen exists in the formation in all types of fluids: water, oil, and gas. The porosity values in this log are low in the gas-containing formations unlike the oil and water containing formations since gas contains lower concentrations of hydrogen (Glover, 2000).

The Compensated Neutron Log (CNL) was applied on the study wells by Schlumberger company to increase the investigation depth and to reduce the borehole effects on the log readings. CNL tool can be used in both open and cased wells, but

the results are more accurate in the open wells (Asquith and Gibson, 1982; Glover, 2000).

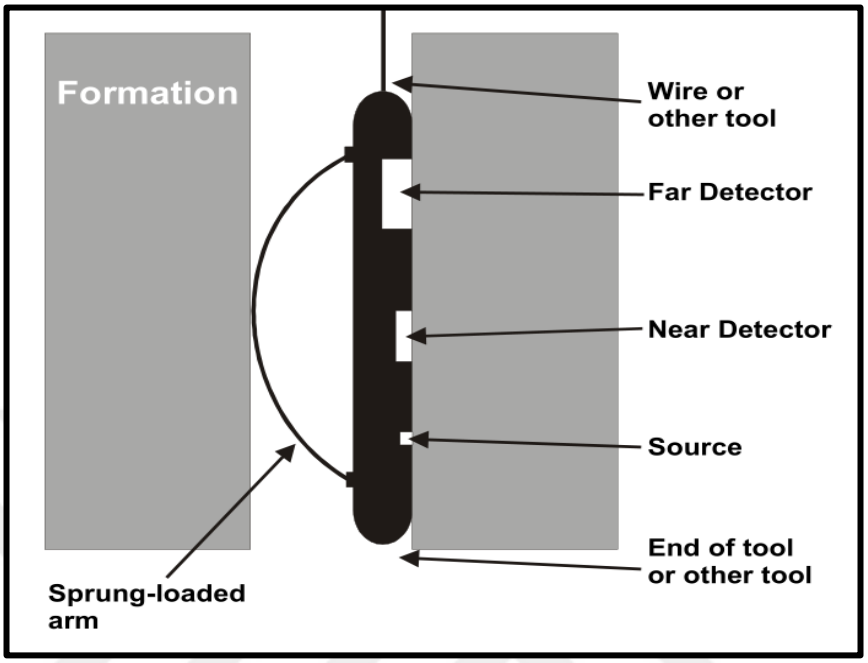

Figure 3.14. The CNL tool which is used in the study wells by Schlumberger (Glover, 2000)

This tool is already calibrated to display the porosity percentage directly. The limestone rock was chosen to be the calibrating unit in the CNL tool. This makes the correction of the porosity values of rocks other than limestone according to the Schlumberger correction chart (Figure 3.15.) necessary.

As mentioned before, when the pores of the clean formation are filled with liquid (oil or water), the neutron tool estimates the porosity percentage directly as follows (Al-Azazi, 2016):

$$\mathrm{Phi}_{\boldsymbol{neu}} = \mathrm{Phi}_{\log} \quad (\%) \quad (3.27)$$

Where:

$\mathrm{Phi}_{\mathrm{neu}}$ = Porosity measured through neutron log (%)

$\mathrm{Phi}_{\log}$= Neutron log reading (%)

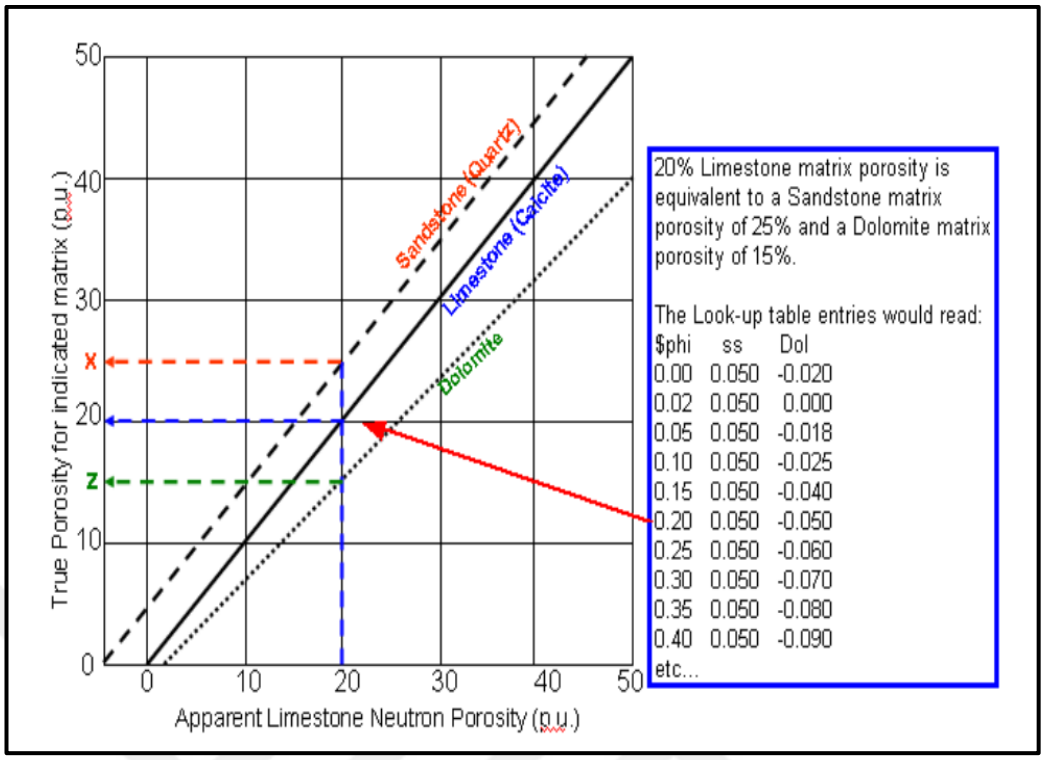

Figure 3.15. The correction chart of apparent porosity applied by Schlumberger company for the common lithologies of the hydrocarbon reservoirs (Schlumberger, 1997)

In shaly zones, the neutron readings should be corrected in order to get rid of the shale effects according to the following equation (Ramadan *et al.*, 2019):

$$\mathrm{Phi_{neuC}} = \mathrm{Phi_{log}} - \mathrm{V_{sh}} \times \mathrm{Phi_{neuSh}} \quad (\%) \qquad (3.28)$$

Where:

$\mathrm{Phi_{neuC}}$= The corrected porosity (%).

$\mathrm{V_{sh}}$= Shale volume in the formation (%).

$\mathrm{Phi_{neuSh}}$= The shale porosity (%).

In this study, Schlumberger IP software has been used to determine the porosity by the means of the neutron porosity model based on the following equations (Schlumberger, 2008):

$$\emptyset = \frac{(\emptyset_{neu} - V_{sh} \times Neu_{sh} + Neu_{ma} + Exfact + Neu_{sal})}{(Sxo + (1 - Sxo) \times Neu_{HyApHIn})} \qquad (3.29)$$

$$Exfact = (\frac{\rho_{ma}}{2.65})^2 \times \left(2 \times Sxo \times \emptyset_x{}^2 + 0.04 \times \emptyset_x\right) \times (1 - Swx) \quad (3.30)$$

$$\emptyset_x = Phi + V_{sh} \times Neu_{sh} \quad (3.31)$$

$$Swx = \frac{(\emptyset \times (Sxo + (1 - Sxo) \times Neu_{HyApHIn}) + V_{sh} \times Neu_{sh})}{\emptyset_x} \quad (3.32)$$

Where:

$\emptyset_{neu}$ = Input neutron log

$V_{sh} =$ The value of wet shale volume

$Neu_{sh} =$ The value of neutron wet shale

Neu_{sal}= The correction of the salinity of the neutron formation.

$Exfact =$ The factor of neutron excavation

$Neu_{HyApHIn} =$ The index of apparent hydrogen of the neutron hydrocarbon.

$Sxo =$ The water saturation of invaded zone.

3.3.1.3. Combination N-D log

It is a combination porosity log that is in fact the combination of density and neutron curves. This log is used at the same time in the calculation of the porosity of the formation, the identification of the gas-bearing zones and the lithology determination. In practice, the true porosity through the N-D log can be calculated by the following equations (Asquith and Gibson, 1982):

For the gas-bearing zones:

$$Phi_{N-D} = \sqrt{\frac{Phi_{Neu}^2 - Phi_{Den}^2}{2}} \quad (3.33)$$

For the water or oil-bearing zones:

$$Phi_{N-D} = \frac{Phi_{Neu} + Phi_{Den}}{2} \quad (3.34)$$

Where:

Phi_{N-D}= The true porosity calculated through a combination of neutron and density logs (%).

Phi_{Den}= The density porosity (%).

Phi_{Neu}= The Neutron porosity (%).

3.3.1.4 Effective porosity (PHIE)

This type of porosity is determined basically according to how much the pores of the rocks are interconnected, which forms channels. These channels make the fluids movement through the lithologic contents easier. Contrary to the shale rocks, the effective porosity of sandstone is good (Schlumberger, 1989b). The effective porosity is calculated through the following equation (Ramadan *et al.*, 2019):

$$PHIE = PHIT \times (1 - V_{sh}) \quad (3.35)$$

Where:

$PHIE$= The effective porosity (%).

$PHIT$= The total porosity (%).

V_{sh}= shale Volume (%).

The types of porosity curves (total and effective) have been realized based on the previous tools for all study wells by Schlumberger IP software (Schlumberger, 2008) as seen in Figures from 3.17. to 3.23., and from 3.24. to 3.30.

3.4. Fluids Saturation

The main purpose of this section is the discrimination and determination of the fluids existing in the formation whether it is oil, water, or gas. The values of fluids saturation

depend basically on the previously mentioned petrophysical parameters (Schlumberger, 2008; Al-Azazi, 2016).

3.4.1. Water saturation

Water saturation is one of the most essential parameters to determine due to its role in the calculation of the saturation of hydrocarbon existing in a reservoir. We estimate water saturation for the flushed (S_{xo}) as well as the uninvaded (S_w) zones. Actually, water saturation is defined as the rate of the volume of pores containing water to the total volume of the formation in percent (Schlumberger, 2008).

The equations of the calculation of water saturation for both S_w and S_{xo} were deduced after several studies and Schlumberger IP software works according to these equations which are as follows (Schlumberger, 2008):

- Archie Equation:

$$\frac{1}{Resis_{tr}} = \frac{(Phi)^m (S_W)^n}{a\ (Resis_W)} \tag{3.36}$$

- Archie PHIT Equation: It is similar to the Archie equation, but Phi is replaced by $PHIT$ (Schlumberger, 2008).

$$\frac{1}{Resis_{tr}} = \frac{(PHIT)^m (S_w)^n}{a\ (Resis_W)} \tag{3.37}$$

- Simandoux Equation:

$$\frac{1}{Resis_{tr}} = \frac{(Phi)^m (S_W)^n}{a\ (Resis_W)} + \frac{(V_{sh})(S_W)}{Resis_{sh}} \tag{3.38}$$

- Modified Simandoux Equation:

$$\frac{1}{Resis_{tr}} = \frac{(Phi)^m (S_W)^n}{a\,(Resis_W)(1 - V_{sh})} + \frac{(V_{sh})(S_W)}{Resis_{sh}} \quad (3.39)$$

- Indonesian Equation:

$$\frac{1}{\sqrt{\mathrm{Resis_t}}} = \left(\sqrt{\frac{(\mathrm{Phi})^{\mathrm{m}}}{\mathrm{a(Resis_W)}}} + \frac{(\mathrm{V_{sh}})^{\left(1-\frac{\mathrm{V_{sh}}}{2}\right)}}{\sqrt{\mathrm{Resis_{sh}}}} \right) (\mathrm{S_W})^{\left(\frac{\mathrm{n}}{2}\right)} \quad (3.40)$$

Phi= The porosity of the formation (%).

$PHIT$= The total porosity of the formation (%).

$Resis_W$= The resistivity of the formation water (Ω.m).

S_W= The uninvaded zone water saturation (%).

$Resis_{tr}$= The uninvaded zone true resistivity (Ω.m).

$Resis_{sh}$= The shale zone resistivity (Ω.m).

V_{sh}= The shale volume (%).

a= The tortuosity factor, its value varies according to the formation components. If it is non-consolidated sand a=0.62, while it is 0.81 if the formation is consolidated sand, and 1 in carbonate which is the case in this study.

n = The saturation exponent whose value is between 1.8 and 2.5, commonly taken as 2 which is the case it is in this study.

m= The cementation factor. Its value varies according to the formation type (for consolidated sands and carbonates m=2 like in this study, but m=2.15 for non-consolidated sands.

It should be noted that in this study the Indonesian equation was applied by IP software as the main equation for the calculation of water saturation.

3.4.1.1. Bulk volume water (BVW)

The Bulk Volume Water represents the water amount existing in the rock. BVW curve is obtained from the product of multiplying the effective porosity with water saturation. It is expressed in the following formula (Schlumberger, 2008):

$$BVW = S_W \times PHIE \quad (3.41)$$

Where:

PHIE= The effective porosity of the formation (%).

S_W = The uninvaded zone water saturation (%).

3.4.1.2. Bulk volume water in invaded zone (BVW_{Sxo})

The bulk volume water in the invaded zone can be calculated based on the following formula (Schlumberger, 2008; Al-Azazi, 2016):

$$BVW_{Sxo} = Sxo \times PHIE \quad (3.42)$$

Where:

BVW_{Sxo}= The bulk volume water in the invaded zone (%).

$PHIE$ = The effective porosity of the formation (%).

Sxo = The water saturation of invaded zone (%)

3.4.2. Hydrocarbon saturation (S_{hyd})

The hydrocarbon total saturation in both flushed and uninvaded zones was calculated by the means of Schlumberger IP software according to the formula below (Ramadan *et al.*, 2019):

$$S_{hyd} = 1 - S_W \quad (3.43)$$

Where:

S_{hyd}= Hydrocarbon saturation in the formation (%).

S_W= Water saturation in the formation (%).

There are two types of hydrocarbon saturation: the residual and movable hydrocarbon saturation. Both can be derived by the use of water saturation in both the flushed zone

(S_{xo}) and the one of the uninvaded zone (S_W), as show the following equations (Ramadan *et al.*, 2019):

$$S_{Rzd} = 1 - S_{xo} \quad (3.44)$$

$$S_{Mov.Hyd} = S_{hyd} - S_{Rzd.Hyd} \quad (3.45)$$

Then, we find the BVH (Bulk Volume Hydrocarbon) as follows (Ramadan *et al.*, 2019):

$$BVH = PHIE \times S_{Mov.Hyd} \quad (3.46)$$

S_{hyd} = Hydrocarbon saturation in the formation (%).
$S_{Mov.Hyd}$ = Movable hydrocarbon (%).
$S_{Rzd.Hyd}$= Residual hydrocarbon (%).
PHIE= Effective porosity in the formation (%).
BVH= Bulk volume hydrocarbon (%).
S_{xo}= Water saturation of invaded zone (%).

The interactive IP program was used to determine and display the values of water and hydrocarbons saturation and water saturation for all the study wells of this study as seen in the Figures 3.17., 3.18., 3.19., 3.20., 3.21., 3.22., 3.23. and 3.24., 3.25., 3.26., 3.27., 3.28., 3.29., 3.30.

3.5. Cut-Off and Summation

The module of 'Cut-off and Summation' presented by IP software enables the definition of the criteria as well as the zones of cut-off and the determination of pay flag and reservoir flag as seen in the study wells in Figures 3.17., 3.18., 3.19., 3.20., 3.21., 3.22., 3.23. and 3.24., 3.25., 3.26., 3.27., 3.28., 3.29., 3.30. Through the petrophysical interpretations this module allows, it is also possible to calculate the average values for every zone separately of water saturation, clay volume, and

porosity. The results can be printed or saved in different formats (Schlumberger, 2008).

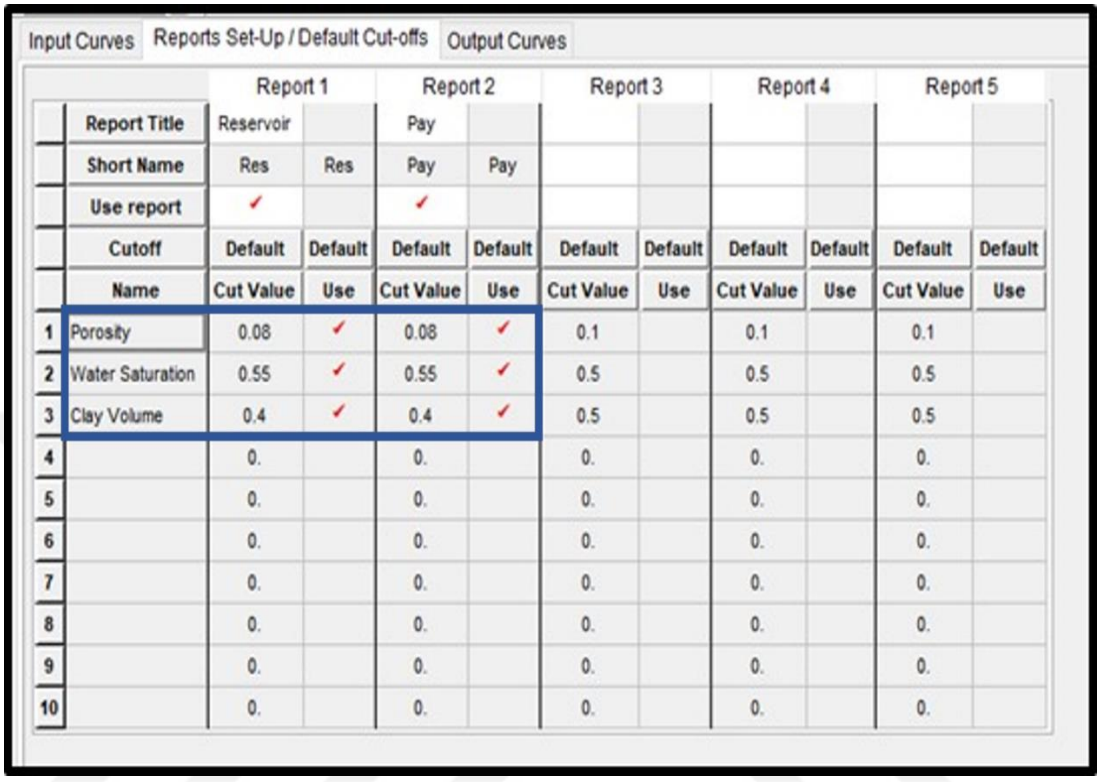

		Report 1		Report 2		Report 3		Report 4		Report 5	
	Report Title	Reservoir		Pay							
	Short Name	Res	Res	Pay	Pay						
	Use report	✓		✓							
	Cutoff	Default	Default	Default	Default	Default	Default	Default	Default	Default	Default
	Name	Cut Value	Use	Cut Value	Use	Cut Value	Use	Cut Value	Use	Cut Value	Use
1	Porosity	0.08	✓	0.08	✓	0.1		0.1		0.1	
2	Water Saturation	0.55	✓	0.55	✓	0.5		0.5		0.5	
3	Clay Volume	0.4	✓	0.4	✓	0.5		0.5		0.5	
4		0.		0.		0.		0.		0.	
5		0.		0.		0.		0.		0.	
6		0.		0.		0.		0.		0.	
7		0.		0.		0.		0.		0.	
8		0.		0.		0.		0.		0.	
9		0.		0.		0.		0.		0.	
10		0.		0.		0.		0.		0.	

Figure 3.16. Cut-off values chosen in this study

3.6. Neutron-Density crossplot

The N-D crossplot is a crossplot that assists with the estimation of the lithology of the formation containing the fluids in defined depths according to the values of Neutron (N) and density (D) which are represented respectively by the axis X and Y while a third-dimension Z represents the Gamma-Ray values and is actually represented in the crossplot by the variety of the colours of the points. N-D crossplot includes three main lines that indicate the common types of the reservoir matrixes: sandstone, limestone, and dolomite. These lines indicate the pure lithology of the mentioned matrixes. The analysis and interpretation of this crossplot can be more complicated and may require detailed information about the mineralogical composition, if the reservoir formation is a combination of different minerals (Glover, 2000; Jurgen, 2015; AAPG WIKI, 2016).

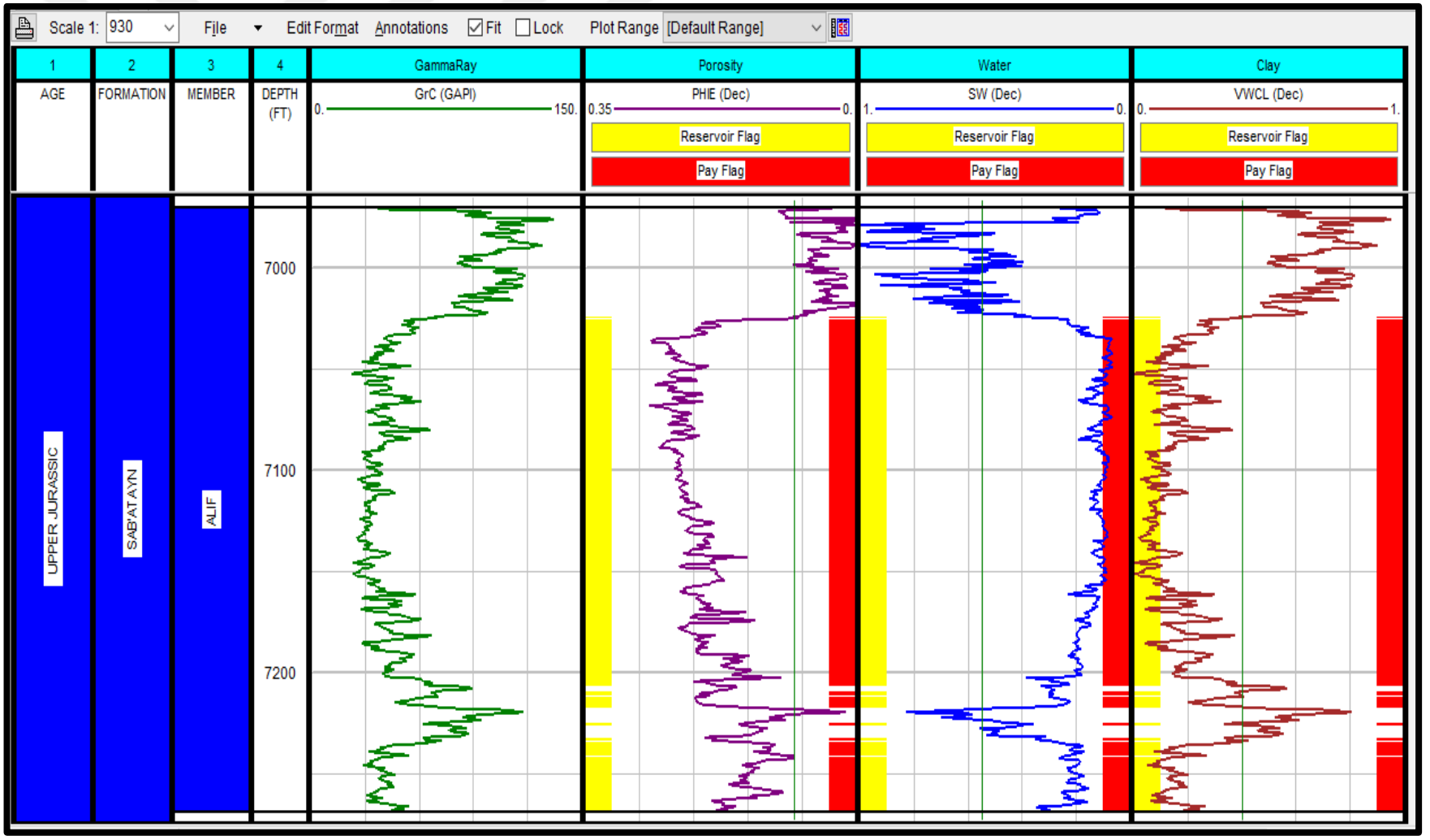

Figure 3.17. Shows the effective porosity, water saturation, and clay volume curves and the reservoir and pay flag of Alif Member (6970.5 – 7268.5 ft) through Al-Raja #36 well by Schlumberger IP (Interactive Petrophysics) software

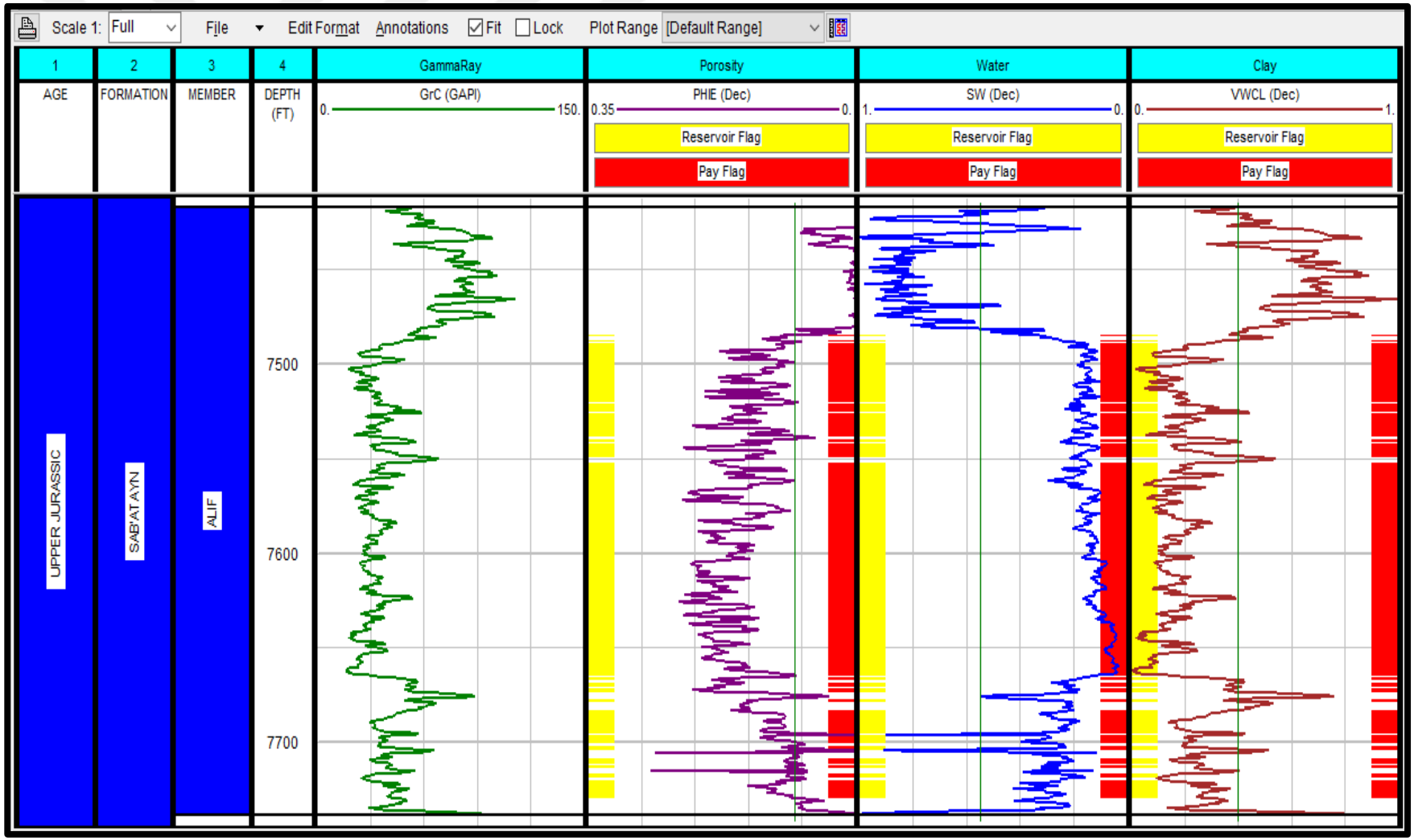

Figure 3.18. Shows the effective porosity, water saturation, and clay volume curves and the reservoir and pay flag of Alif Member (7417 - 7738 ft) through Al-Raja #37 well by IP (Interactive Petrophysics) software

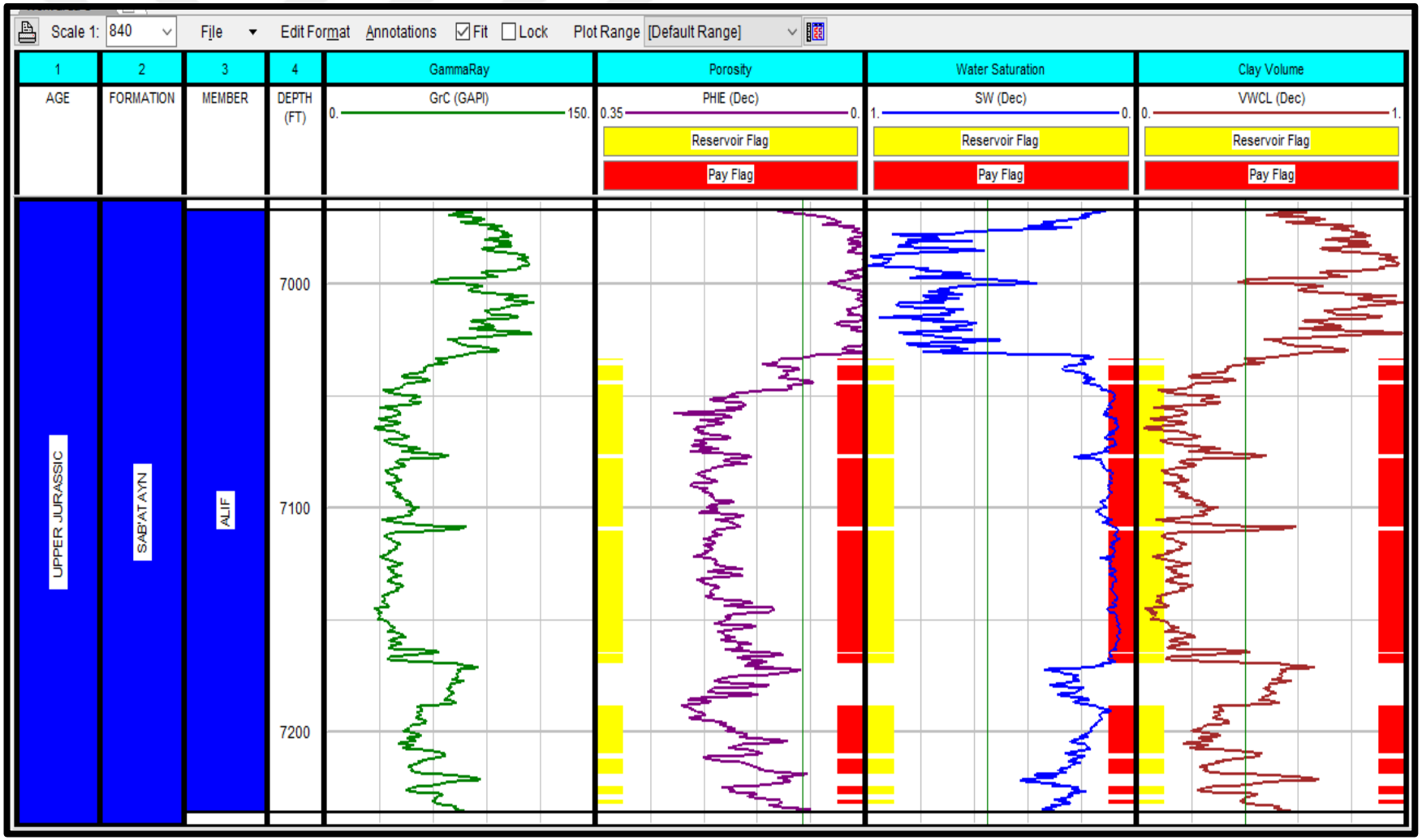

Figure 3.19. Shows the effective porosity, water saturation, and clay volume curves and the reservoir and pay flag of Alif Member (6967 - 7236.5 ft) through Al-Raja #38 well by Schlumberger IP (Interactive Petrophysics) software

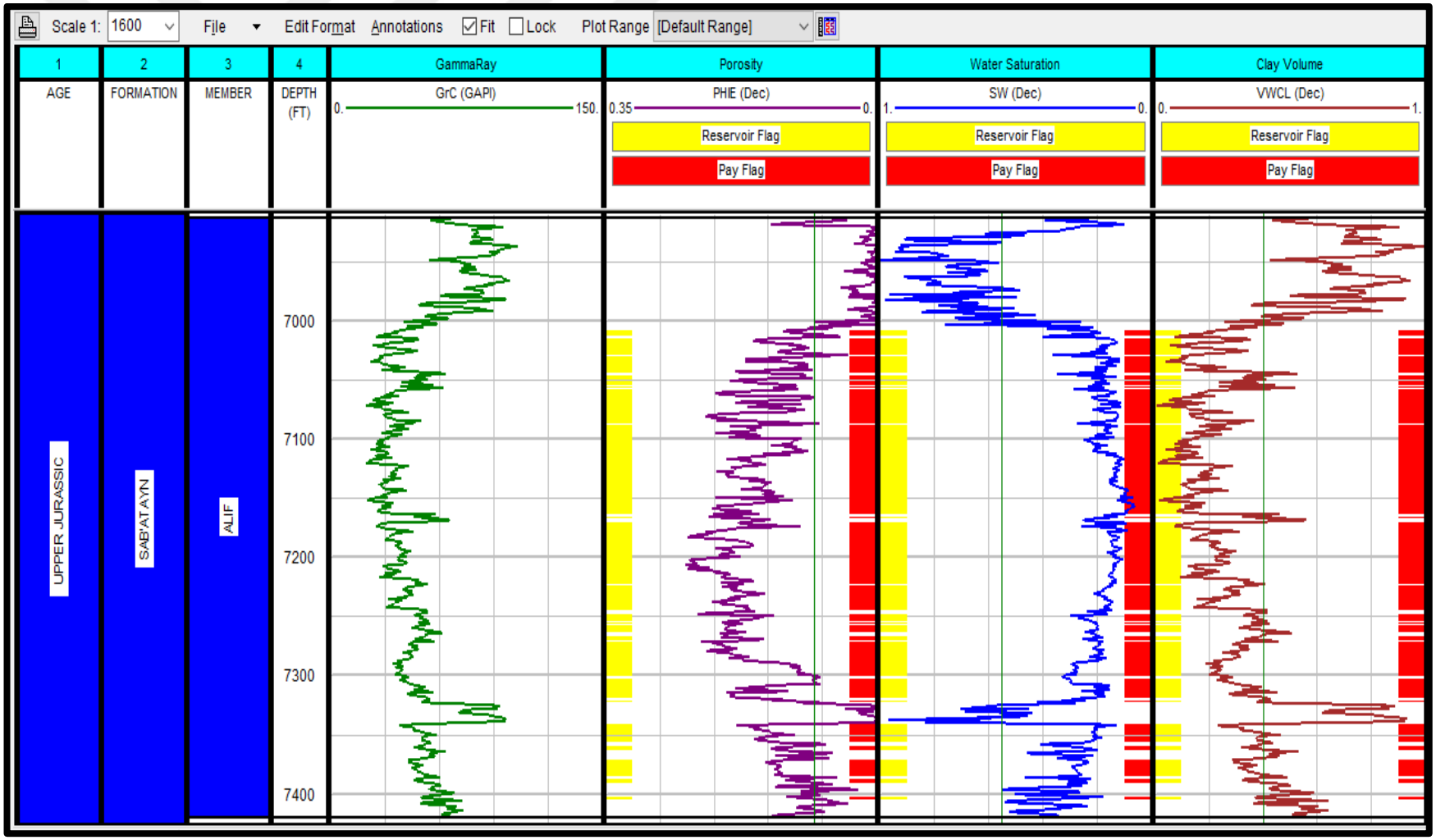

Figure 3.20. Shows the effective porosity, water saturation, and clay volume curves and the reservoir and pay flag of Alif Member (6912 - 7420 ft) through Al-Raja #39 well by Schlumberger IP (Interactive Petrophysics) software

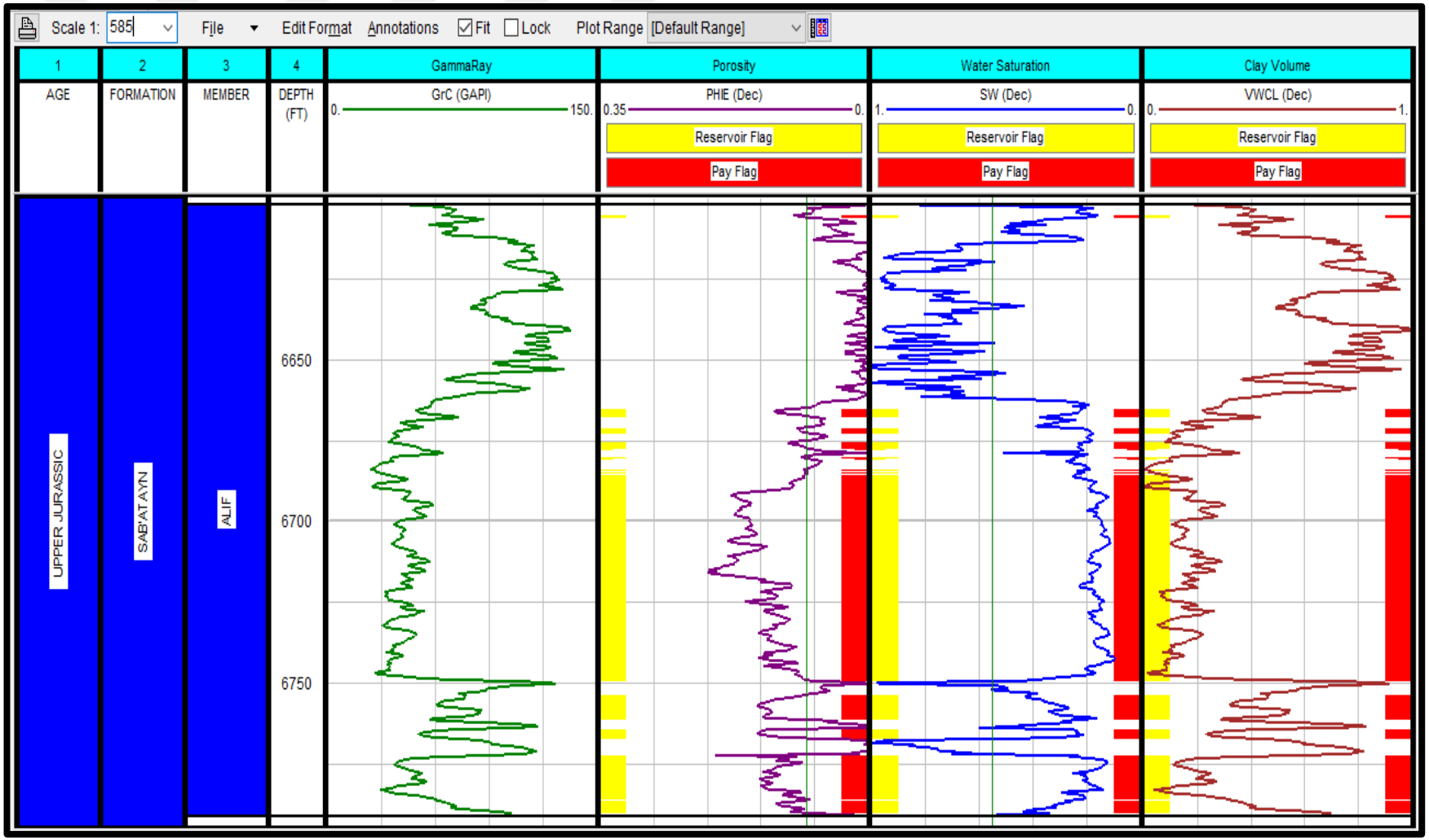

Figure 3.21. Shows the effective porosity, water saturation, and clay volume curves and the reservoir and pay flag of Alif Member (6602 - 6791 ft) through Al-Raja #40 well by IP (Interactive Petrophysics) software

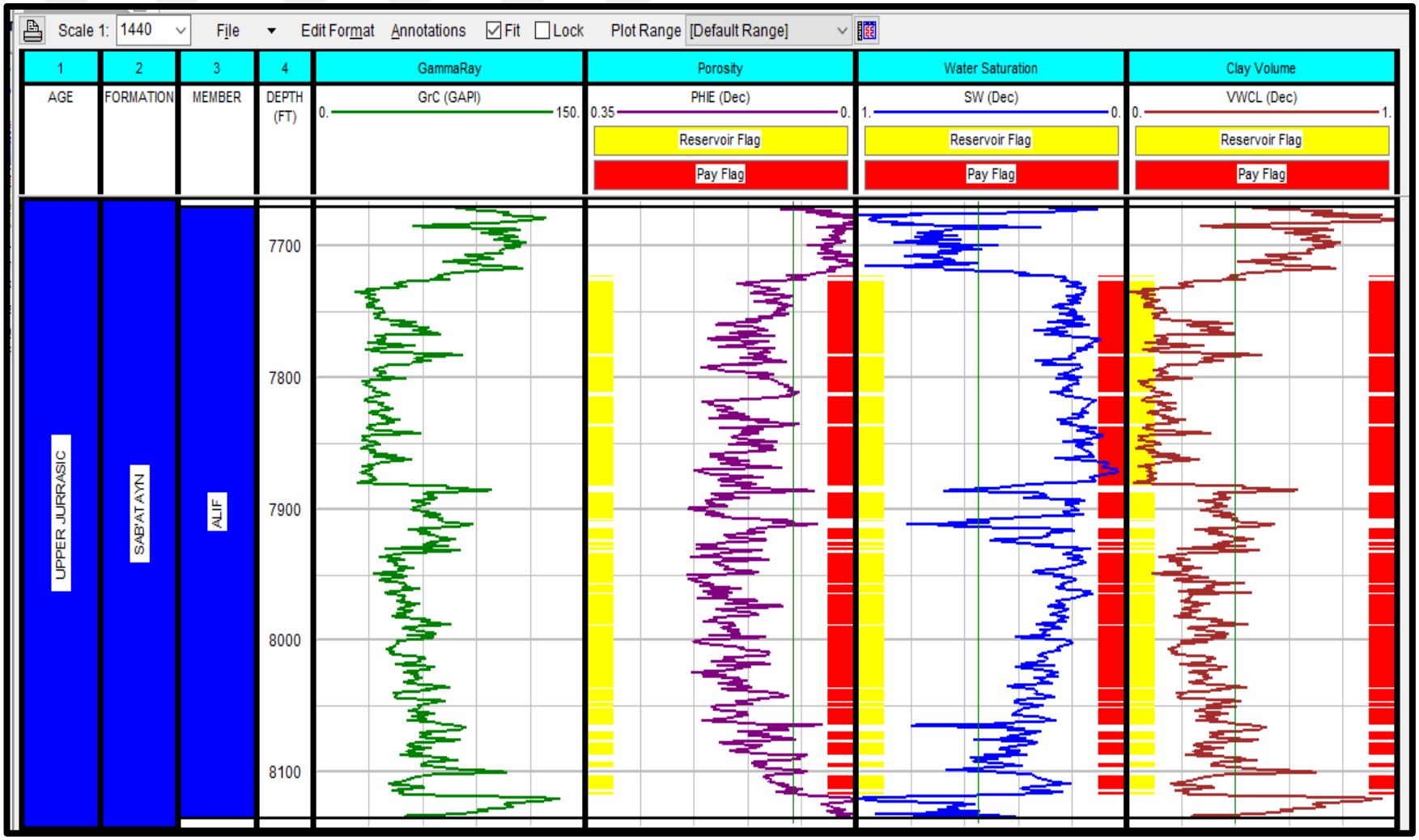

Figure 3.22. Shows the effective porosity, water saturation, and clay volume curves and the reservoir and pay flag of Alif Member (7670 - 8136 ft) through Al-Raja #41 well by IP (Interactive Petrophysics) software

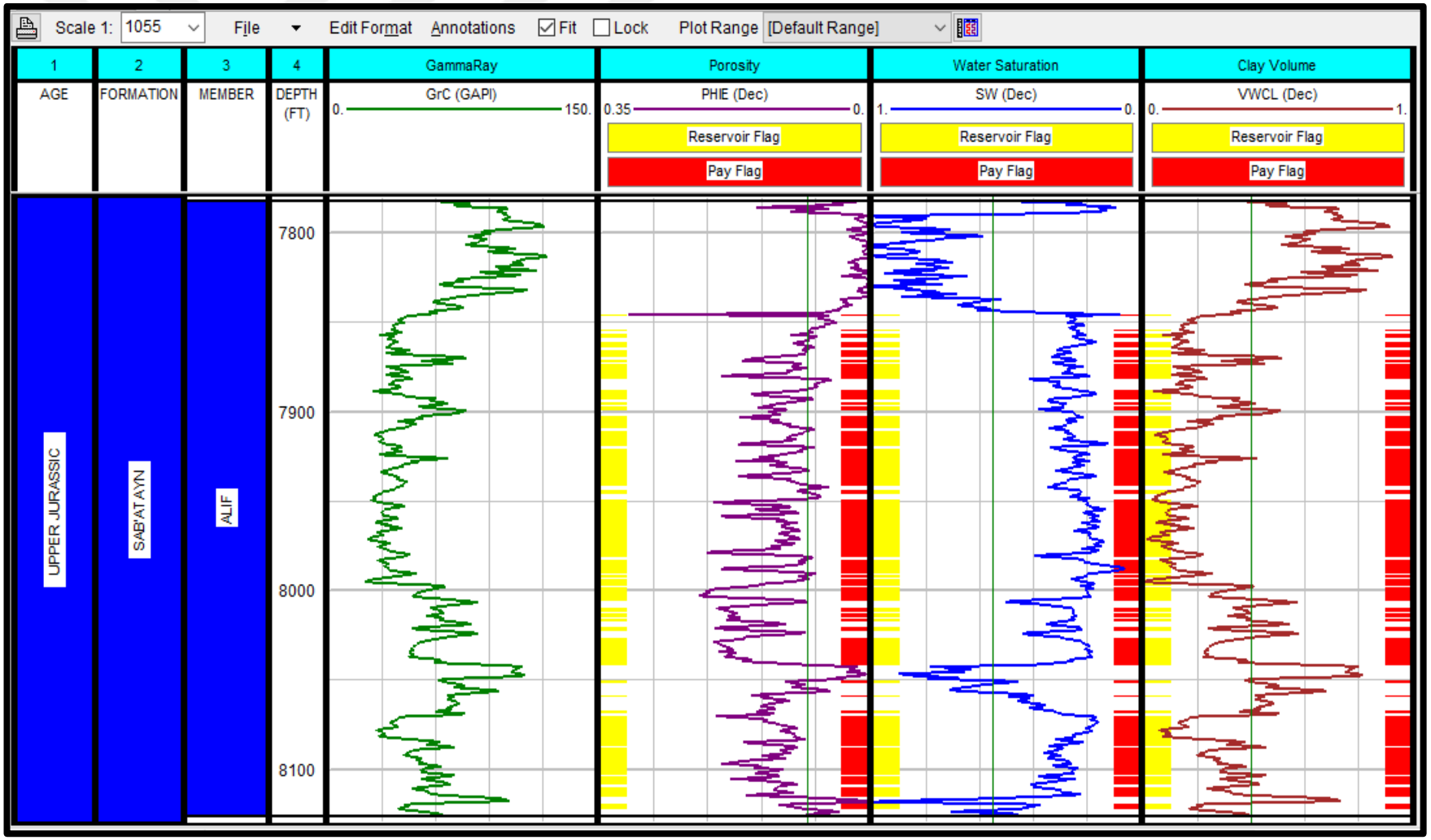

Figure 3.23. Shows the effective porosity, water saturation, and clay volume curves and the reservoir and pay flag of Alif Member (7782 - 8126 ft) through Al-Raja #42 well by IP (Interactive Petrophysics) software

The distribution of the plotted points can be largely influenced by the shale contents. The shale points exist normally in the right lower part of the crossplot and shale content pulls the points down towards the reference point of the shale in the same part. In contrast, when the formation contains gas, the points are shifted to the left upper part of the crossplot. The geometry of the pores and the cementing materials and minerals might also be some extra factors that have impact to some extent on the distribution of the points in this crossplot (Schlumberger, 1989b; Glover, 2000; Jurgen, 2015; AAPG WIKI, 2016).

For example, a point representing a sandstone containing gas is pulled up to the left upper part of crossplot and if it contains shale too it will be shifted towards the right lower part again which locates it on the clean sandstone line again. Similarly, a dolomite may be represented on the limestone line or around it due to the presence of gas. In these cases, we need to have information about the stratigraphy to be able to decide whether the formation contains gas (AAPG WIKI, 2016).

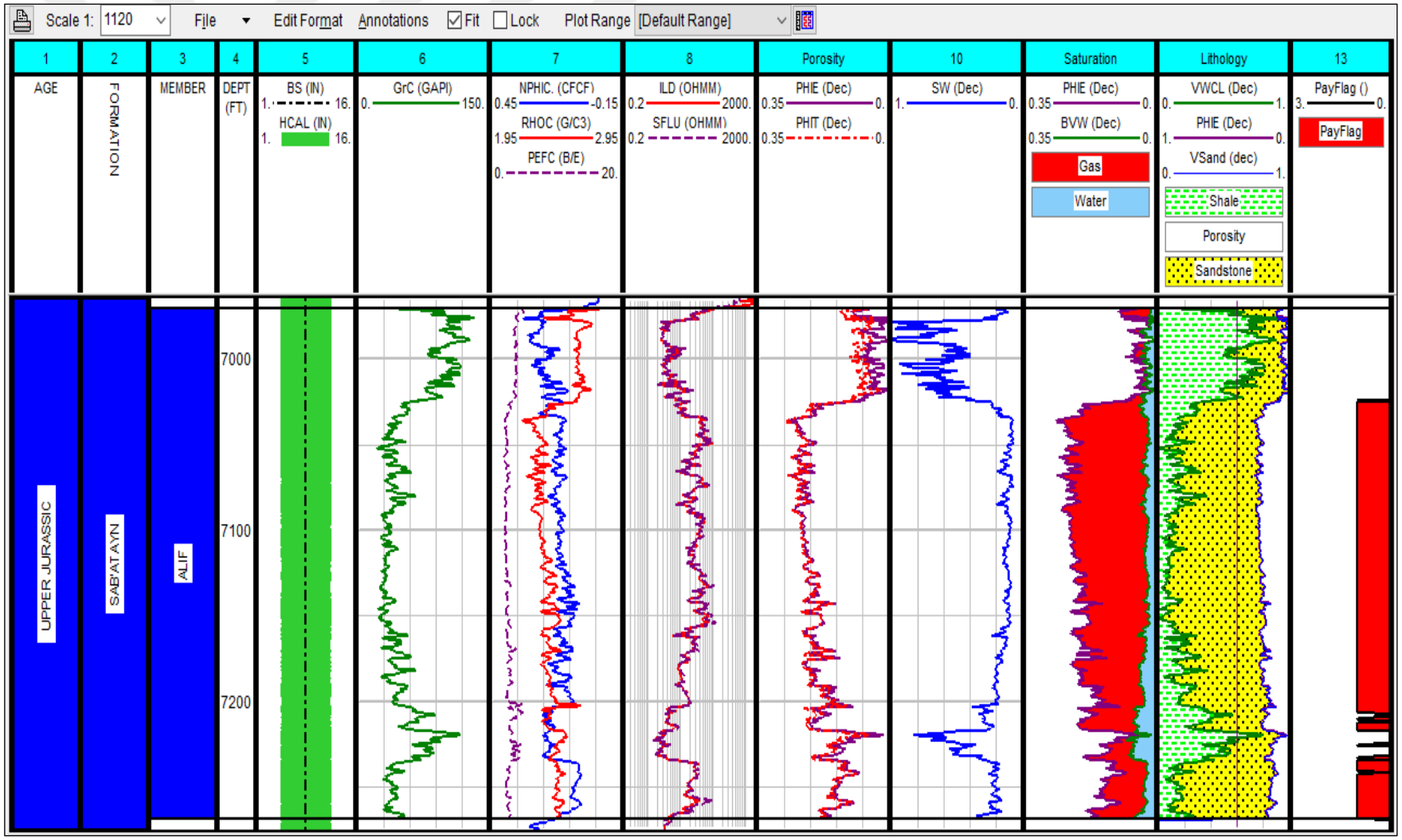

Figure 3.24. Shows the obtained litho-saturation and the corrected log dataset of Alif Member (6970.5 – 7268.5 ft) through Al-Raja #36 well by IP (Interactive Petrophysics) software

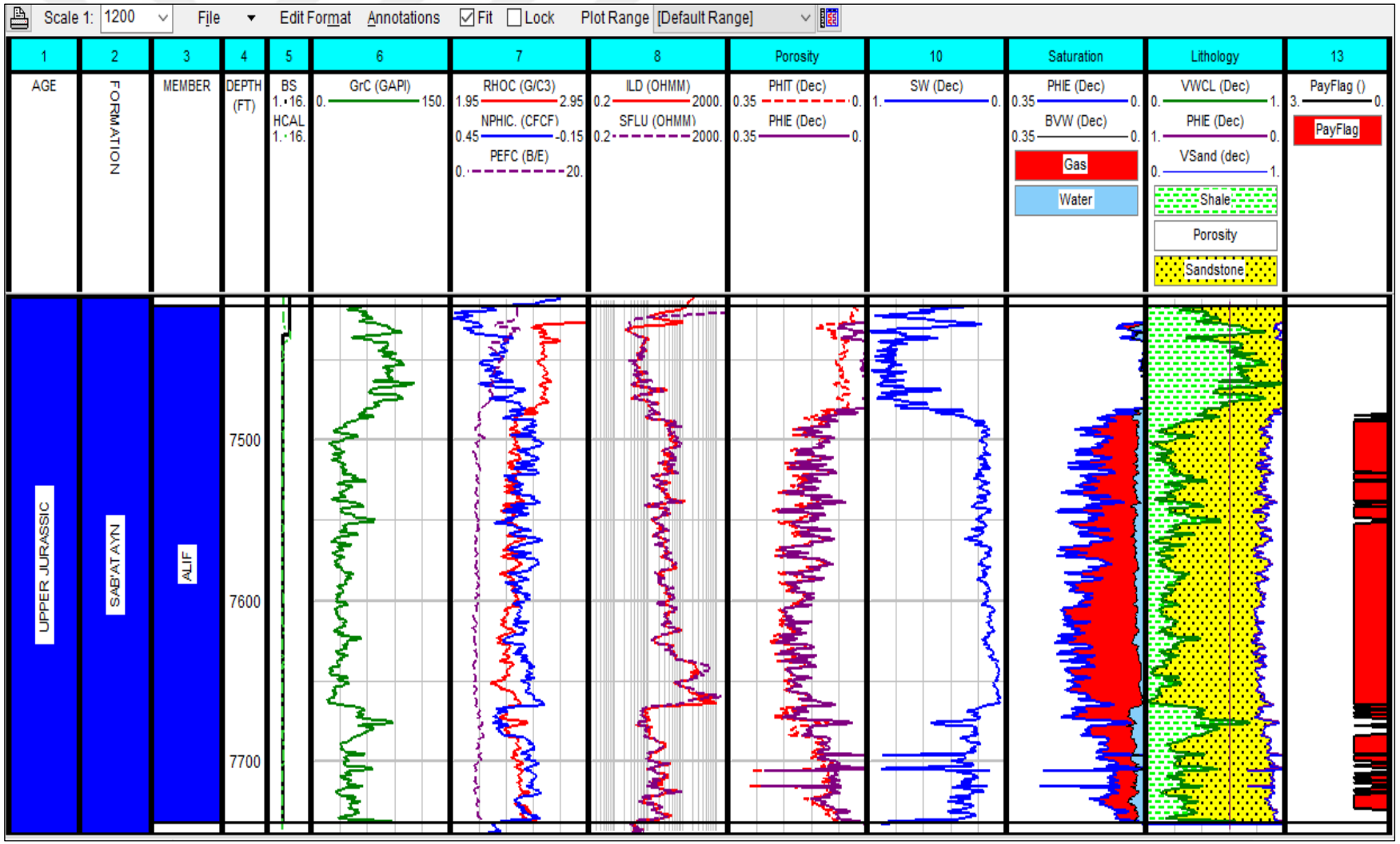

Figure 3.25. Shows the obtained litho-saturation and the corrected log dataset of Alif Member (7417 - 7738 ft) through Al-Raja #37 well by IP (Interactive Petrophysics) software

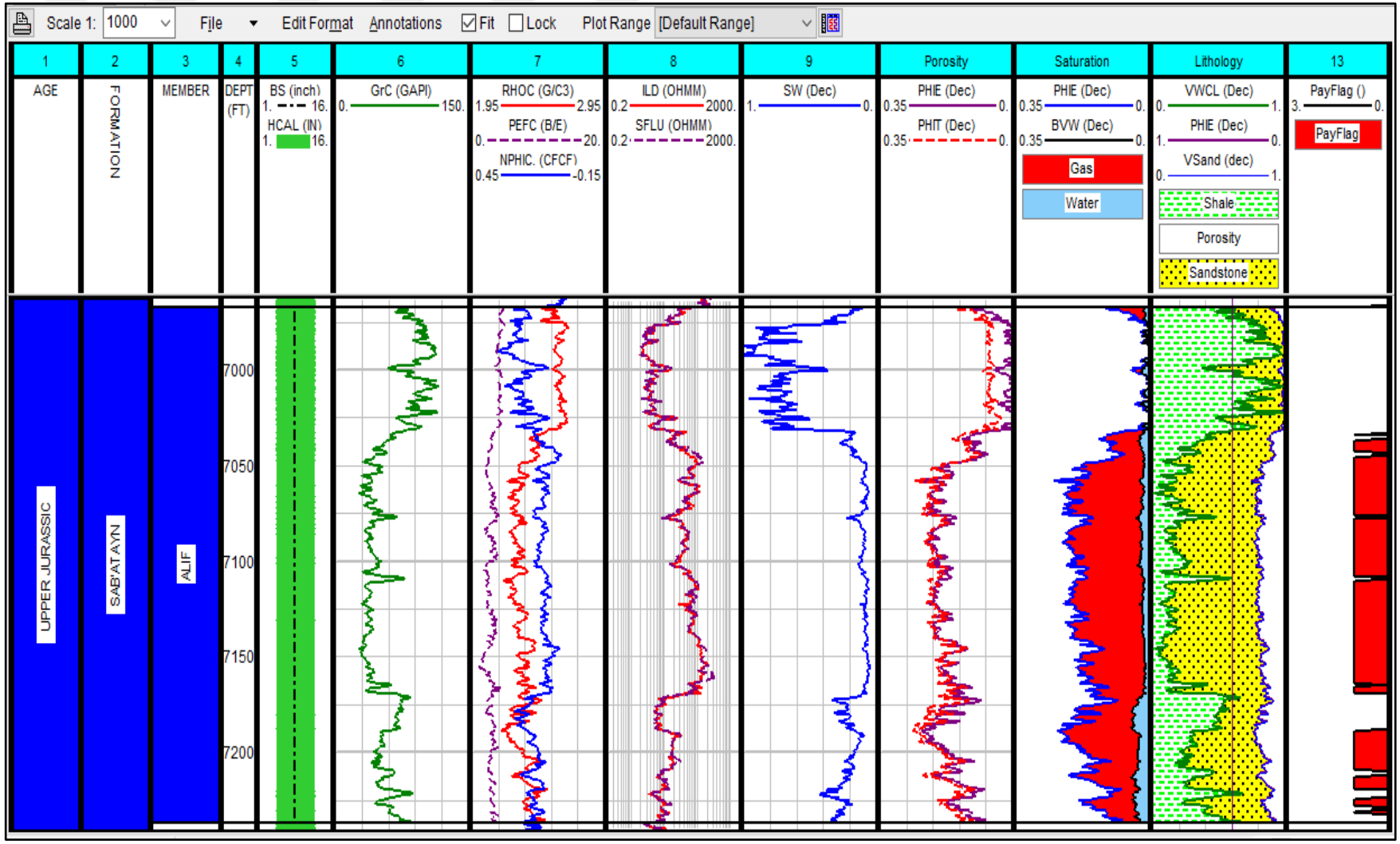

Figure 3.26. Shows the obtained litho-saturation and the corrected log dataset of Alif Member (6967 - 7236.5 ft) through Al-Raja #38 well by IP (Interactive Petrophysics) software

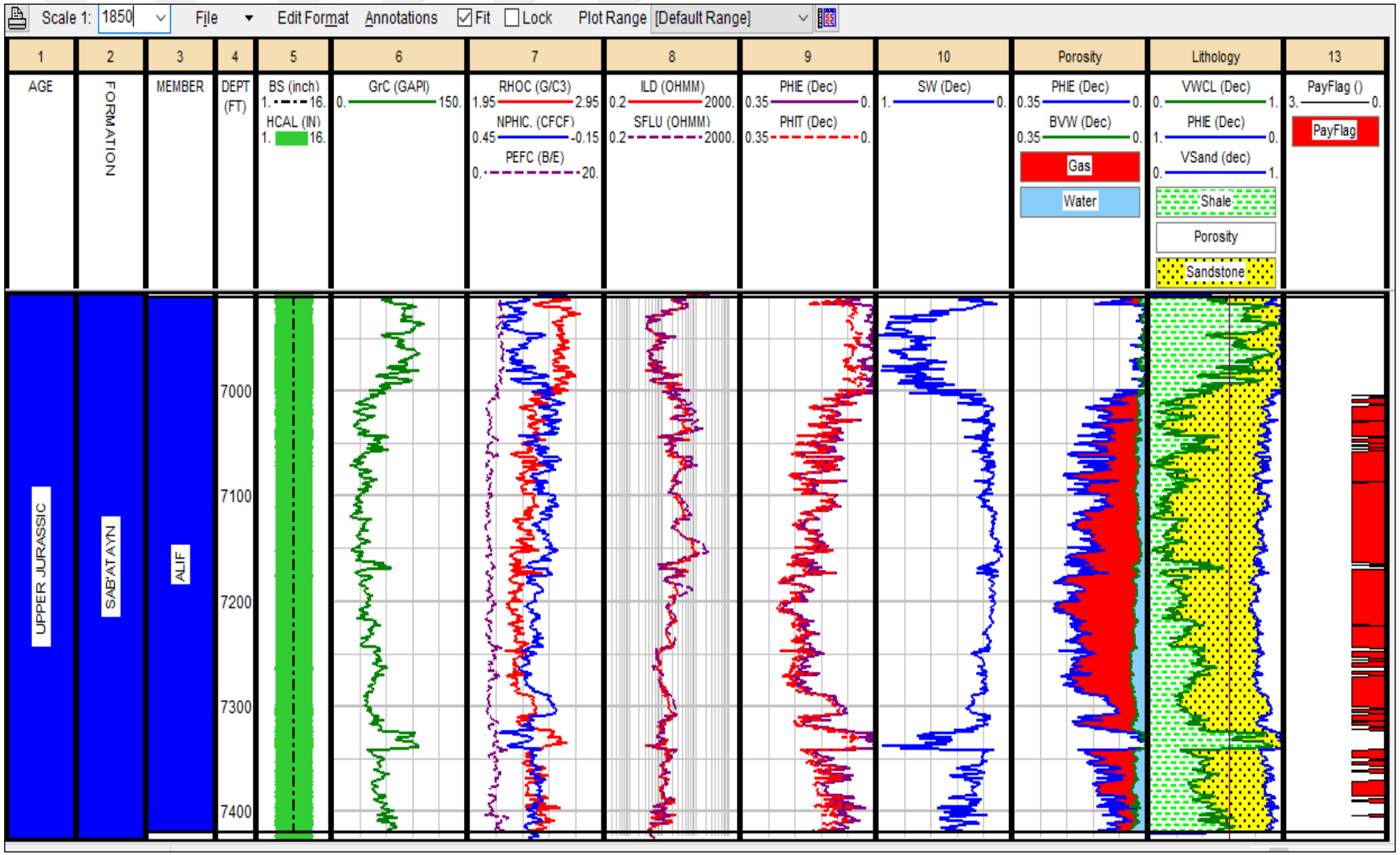

Figure 3.27. Shows the obtained litho-saturation and the corrected log dataset of Alif Member (6912 - 7420 ft) through Al-Raja #39 well by IP (Interactive Petrophysics) software

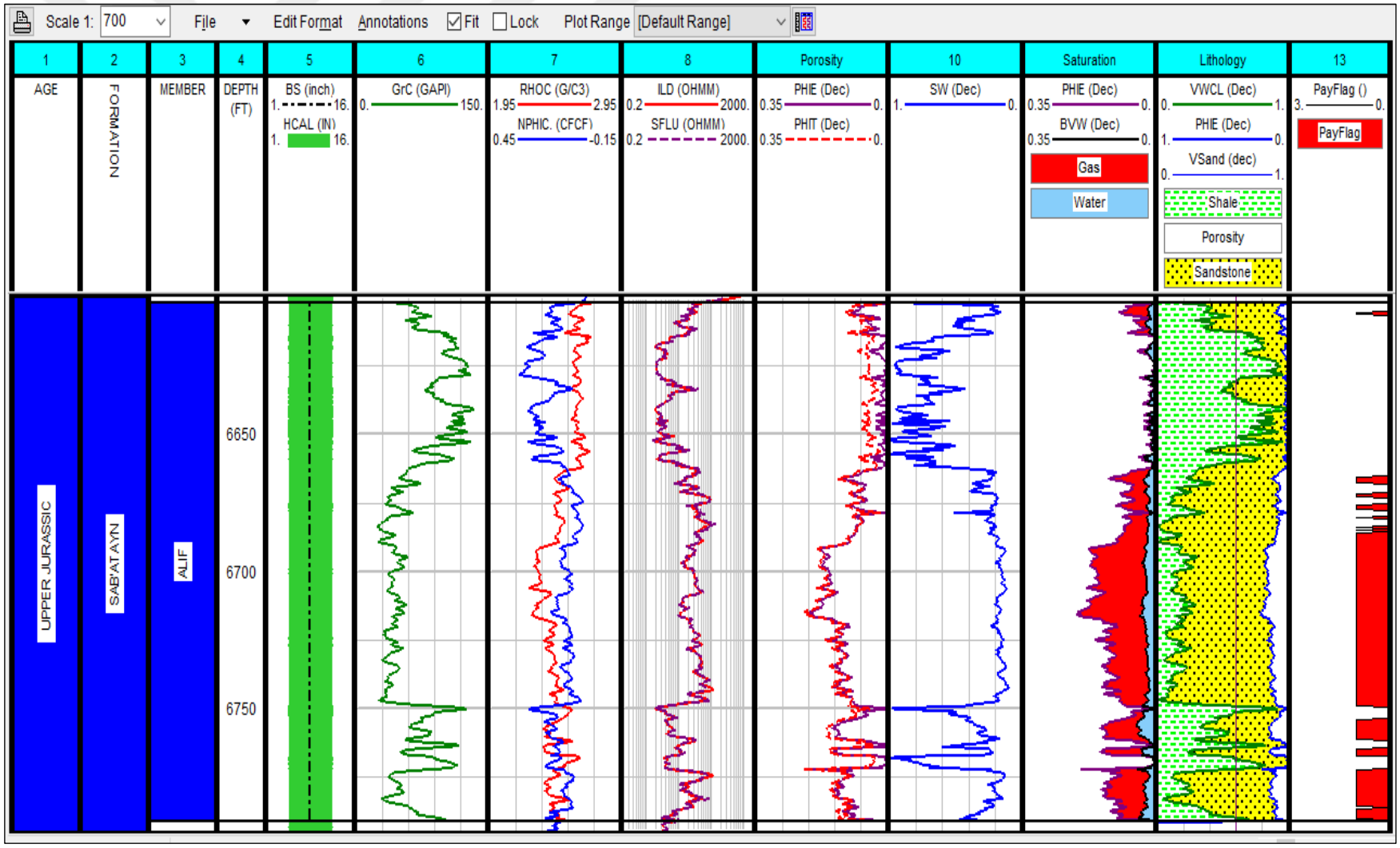

Figure 3.28. Shows the obtained litho-saturation and the corrected log dataset of Alif Member (6602 - 6791 ft) through Al-Raja #40 well by IP (Interactive Petrophysics) software

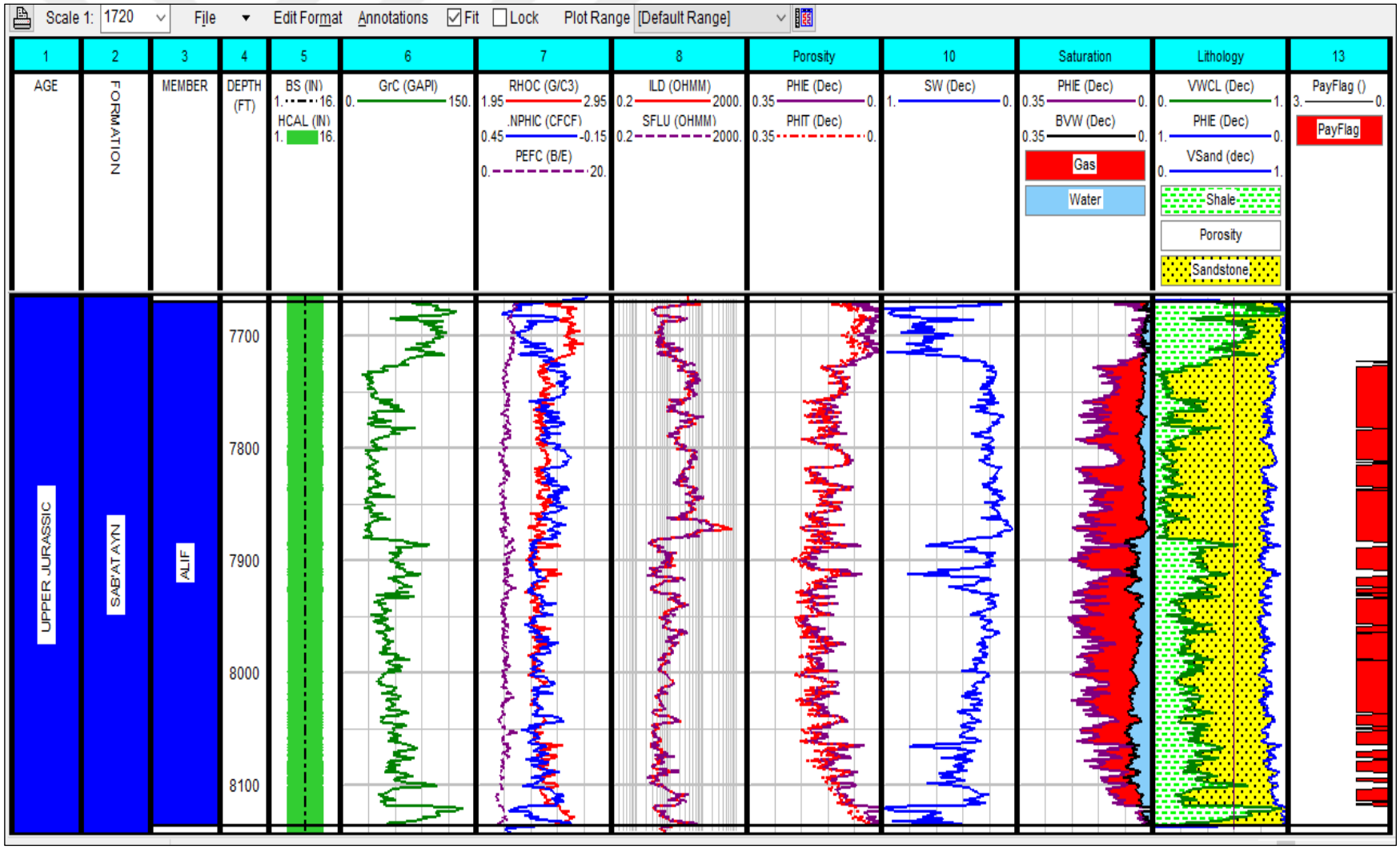

Figure 3.29. Shows the obtained litho-saturation and the corrected log dataset flag of Alif Member (7670 - 8136 ft) through Al-Raja #41 well by IP (Interactive Petrophysics) software

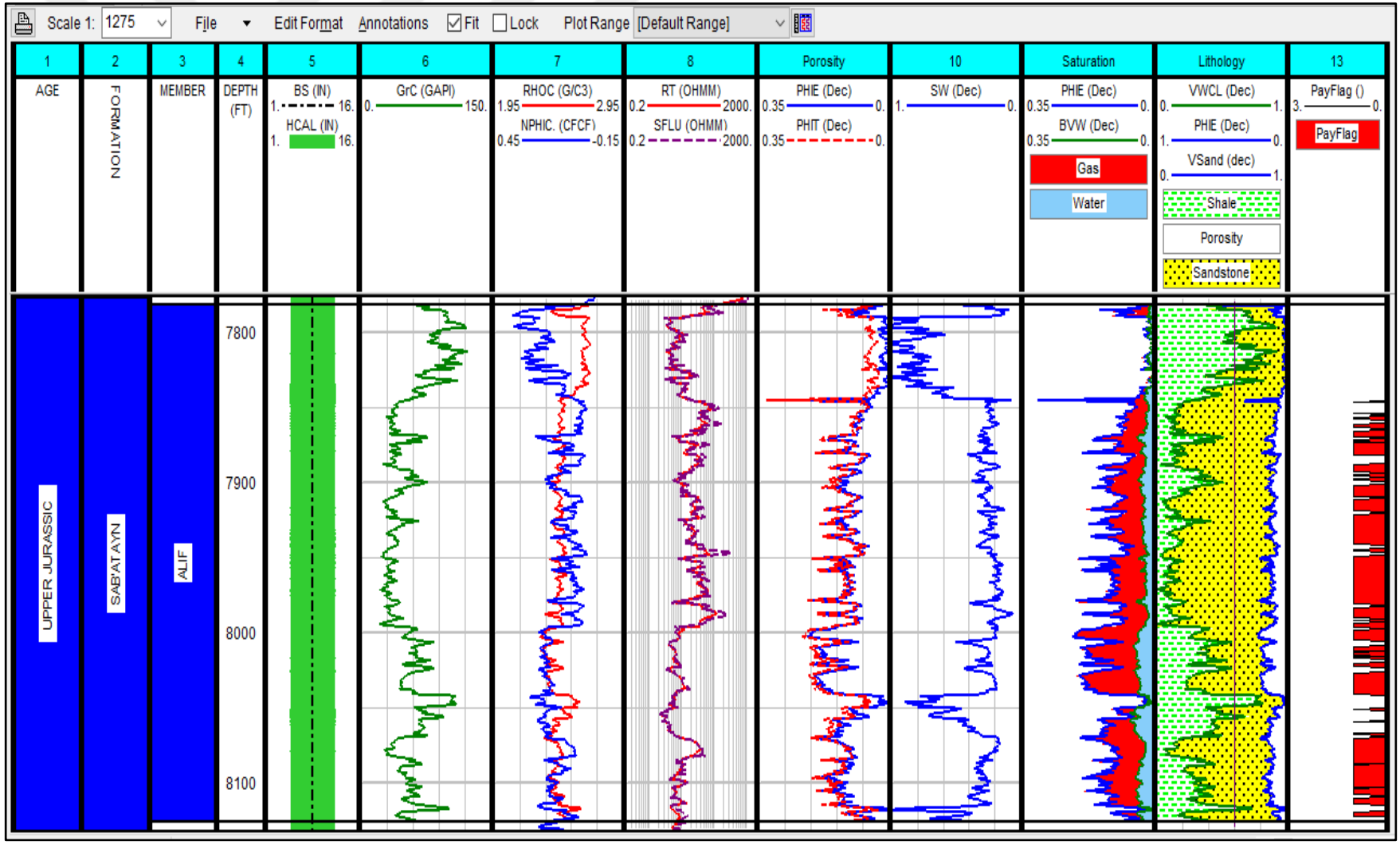

Figure 3.30. Shows the obtained litho-saturation and the corrected log dataset of Alif Member (7782 - 8126 ft) through Al-Raja #42 well by IP (Interactive Petrophysics) software

CHAPTER 4. RESERVOIR EVALUATION

As mentioned before, the main goal of this study is the evaluation of the hydrocarbon reservoir of the Al-Raja Field. In this chapter, the results of both the vertical and horizontal studies for the studied field will be used. The results of the vertical studies have been obtained by Schlumberger Interactive Petrophysics (IP) software where each well have been studied individually. On the other hand, the field has been evaluated horizontally by Surfer software based on the previously obtained results. Taking advantage of Surfer software and the previous results, the required maps of the study area such as thickness distribution maps, shale distribution map, and water distribution map can be prepared. These maps will be seen later in this chapter.

4.1. Vertical Evaluation

As a result of this work, some dataset plots of the boreholes were created to evaluate the saturation of hydrocarbons quantitively in the Al-Raja Field through petrophysical parameters and based on the well logging data. Each dataset plot represents a specific borehole as seen in Figures 4.3., 4.4., 4.7., 4.8., 4.11., 4.12., and 4.13. Each plot consists of a certain number of tracks. The first, second, third, and fourth tracks display the age, the formation, the member, and the zonation of the targeted formation (Alif Member) respectively vs. the depth which is represented in the fifth track. The sixth track displays the corrected Gamma-ray log. The seventh track represents the corrected logs of the density (RHOC), neutron (NPHIC), and Formation Photoelectric Factor (PEFC) logs while the eighth track represents the values of resistivity logs for both deep or invaded zone (ILD) and flushed zone (SFLU). The next track shows the values of total porosity (PHIT) and effective porosity (PHIE) curves. Then, the tenth and eleventh are the fluids saturation curves (water and hydrocarbon). The next track displays the lithology of the Alif Member while the last track displays the pay flag in

Table 4.1. Petrophysical parameters of the Alif Reservoir through Al-Raja including the Top and Bottom of Alif Member, Gross (G), and Net thickness (N), Net/ Gross (N/G) and the average percentage of shale Volume (Ave V_{sh}%), Effective Porosity (Ave PHIE%), Water Saturation (Ave S_w%), and Gas Saturation (Ave SH%)

Well	Member	Top (ft)	Bottom (ft)	G (ft)	N (ft)	N/G	V_{sh}	Av. PHIE %	Av. S_W%	Av. S_{hyd} (Gas) %
RJ- 36	Alif	6970.5	7268.5	298	225.94	0.758	15.3	19.7	14.5	85.5
RJ- 37	Alif	7417	7738	321	212.5	0.662	18.3	14.6	14.6	85.4
RJ- 38	Alif	6967	7236.5	269.5	161.25	0.598	18.9	17.8	11.1	88.9
RJ- 39	Alif	6912	7420	508	316.5	0.623	22.7	15.7	16.7	83.3
RJ- 40	Alif	6602	6791	189	100.5	0.532	19.9	12.9	18.7	81.3
RJ- 41	Alif	7670	8136	466	340.5	0.731	21.5	14.7	23.5	76.5
RJ- 42	Alif	7782	8126	344	190.88	0.555	20.1	13.1	23	77

the Alif Member. All the previous tracks are continuous curves along the Alif Member penetrated by the selected boreholes.

This study allows the estimation of the important petrophysical parameters (shale volume, effective porosity, water saturation) for all the studied wells individually as seen in Table 4.1. In addition, we could estimate the productive zones through all studied wells as seen in Table 4.1.

Based on the previous results, it has become possible to deduce the hydrocarbon saturations through each well. These values are given in Table 4.1. We are able to identify the main lithology of the Alif reservoir, as well.

In conclusion, the reservoir has been evaluated by determining the following:

- Shale Volume (V_{sh}): The obtained average values of the shale volume through the seven studied boreholes of the Al-Raja field range from 15.3 % (minimum value) to 22.7 % (maximum value).
- Effective Porosity (PHIE %): The average values of the effective porosity of each of the seven wells examined in this study vary between 12.9 % (minimum value) and 19.7 % (maximum value).
- Water Saturation (S_W %): The average values of the water saturation of the seven wells studied in this work have a minimum value of 11.1 % and a maximum value of 23.5 %.
- Hydrocarbon Saturation (S_{hyd}): It has been determined through this study that the hydrocarbon present in the reservoir is gas. The average value of its saturation varies from a borehole to another between the limits 76.5 % (minimum) and 88.9 % (maximum).
- Net thickness (N): It refers directly to the estimated total thickness of the productive zones of the reservoir in Alif Member. It takes values greater or equal to 100.5 ft (minimum value) and smaller of equal to 340.5 ft (maximum value). Note that the minimum and maximum values of the average total

thickness of the Alif Member through the study wells are 189 and 508 ft, respectively.

4.1.1. Lithology and zonation

The lithologic composition of the Alif Reservoir of the Al-Raja Field is estimated to be dominant sandstone rock with amounts of shale within it. According to the results obtained in this study, Alif Member will be divided through all the study wells vertically into three zones:

- Alif Formation Top zone: dominated by shale and minor amounts of sandstone.
- Alif Sandstone A zone: dominated by sequences of sandstone beds with minor amounts of shale within.
- Alif Sandstone B zone: dominated by sequences of sandstone beds with minor amounts of shale within.

It is worth noting that the petrophysical criteria of the distinction of the productive zones from non-productive ones in the reservoir were set by the operating company (SEPOC) in the study area as follows: PHI ≥ 8 %, $V_{sh} \leq 40$ % and $S_W \leq 55$ %, as seen in Figure 3.16.

However, the shale volume present in the B zone is relatively more than its volume in the A zone. Generally, Alif Sandstone A and Alif Sandstone B zones are productive zones, but the Alif Formation Top zone is not.

The Density-Neutron crossplot is used, among others, to confirm the evaluation of the reservoir rocks through each borehole study individually. The density (RHOC)-neutron (NPHIC) crossplots (Figures 4.1., 4.2., 4.5., 4.6., 4.9., 4.9., and 4.14.) of the Alif Member in the study boreholes show the plotted points that represent the lithology of the Alif member. The reciprocal influence of gas and shale resulted in some change in the distribution of the plotted points. Some data points are pulled down to the right lower part of the plot due to shale effects. Similarly, some data points were pulled up

towards the plot's upper left part because of gas effects, which explains the presence of some points near the Limestone and Dolomite lines. The Alif Member consists of intercalated layers of different rocks. So, the existence of Calcite and Dolomite is inevitable, but their amounts are much less and may only be present as cement. That's why we only mention the sandstone and shale which make the main lithology, which is also corroborated by the Yemeni operating company SEPOC (SEPOC, 2010) as seen in the first chapter.

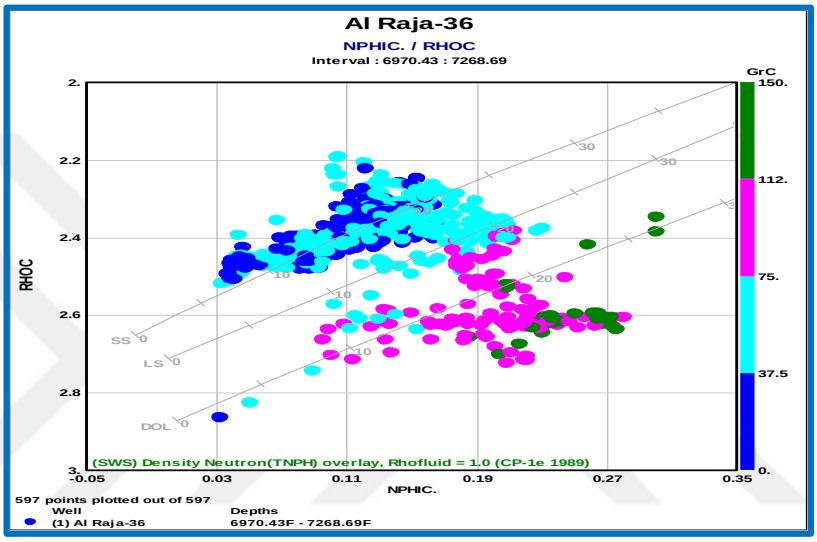

Figure 4.1. NPHIC-RHOC (Neutron-Density) crossplot of RJ#36 borehole by Schlumberger IP software

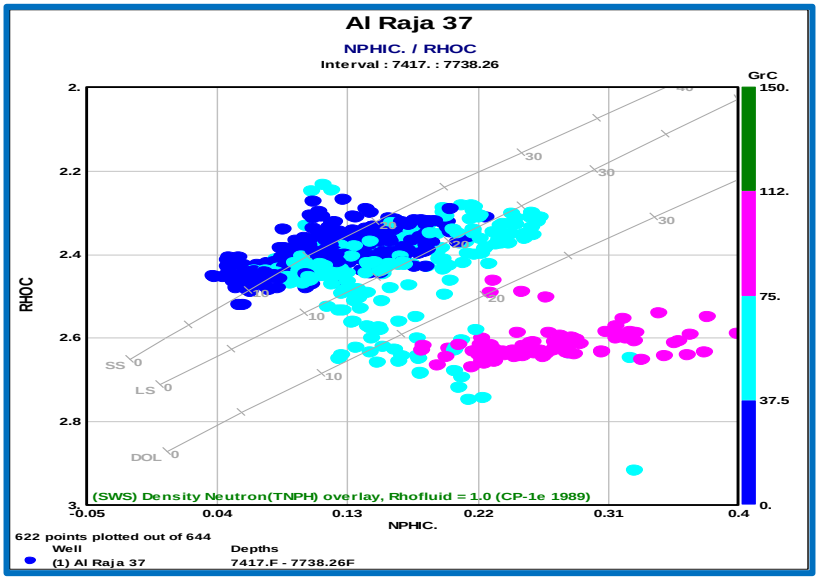

Figure 4.2. NPHIC-RHOC (Neutron-Density) crossplot of RJ#37 borehole by Schlumberger IP software

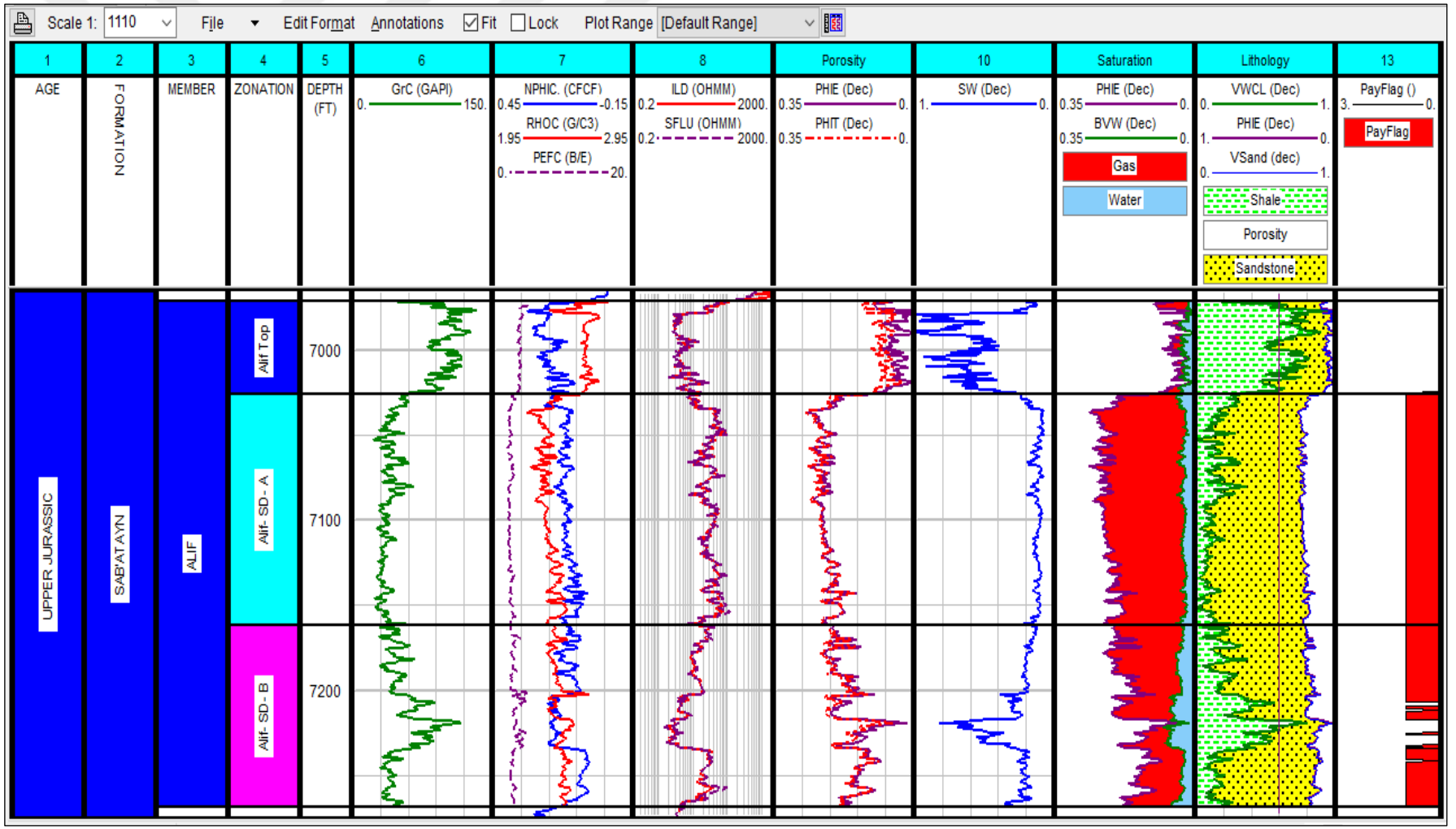

Figure 4.3. Finally obtained dataset plot including the zonation of Alif Member through RJ#36 by IP software

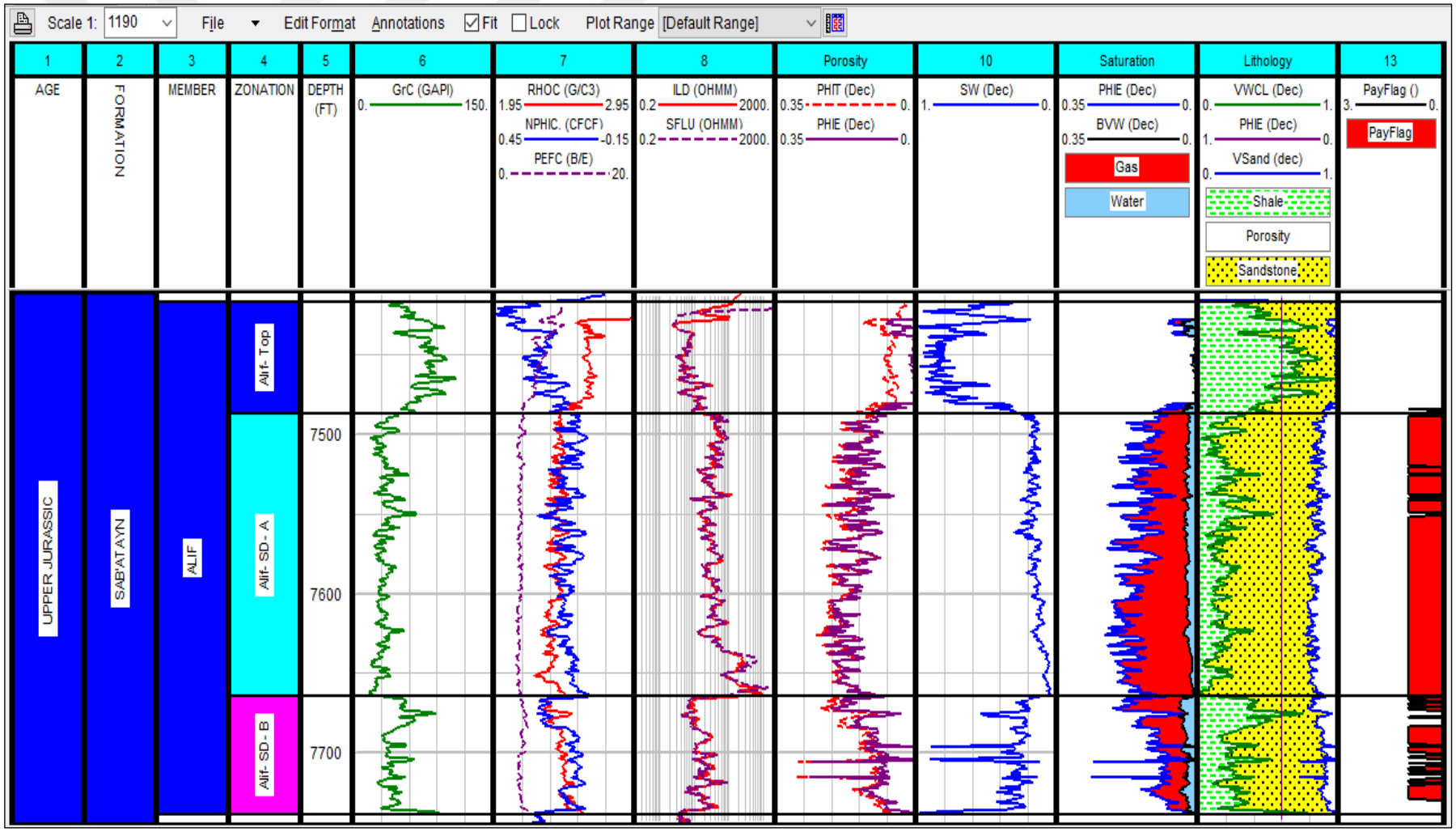

Figure 4.4. Finally obtained dataset plot including the zonation of Alif Member through RJ#37 by IP software

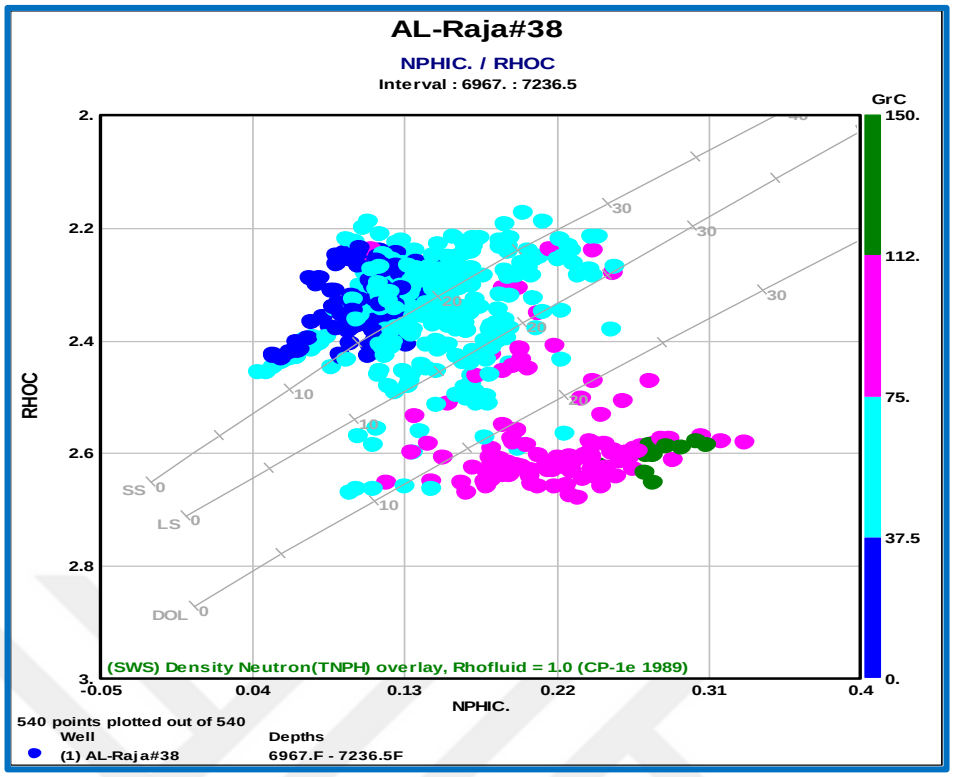

Figure 4.5. NPHIC-RHOC (Neutron-Density) crossplot of RJ#38 borehole by Schlumberger IP software

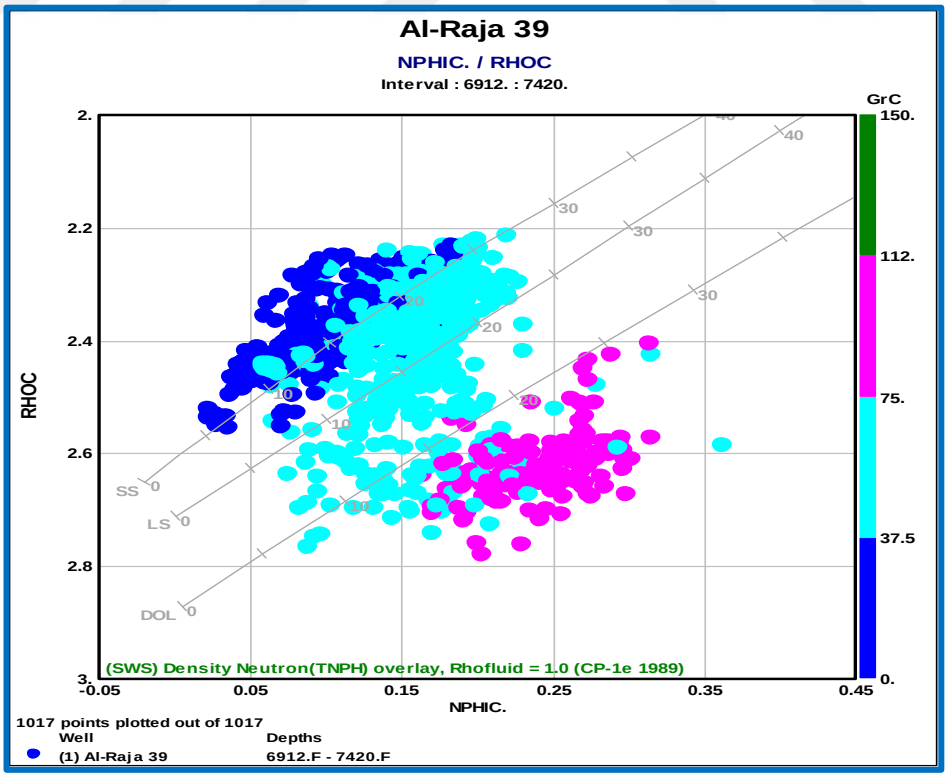

Figure 4.6. NPHIC-RHOC (Neutron-Density) crossplot of RJ#39 borehole by Schlumberger IP software

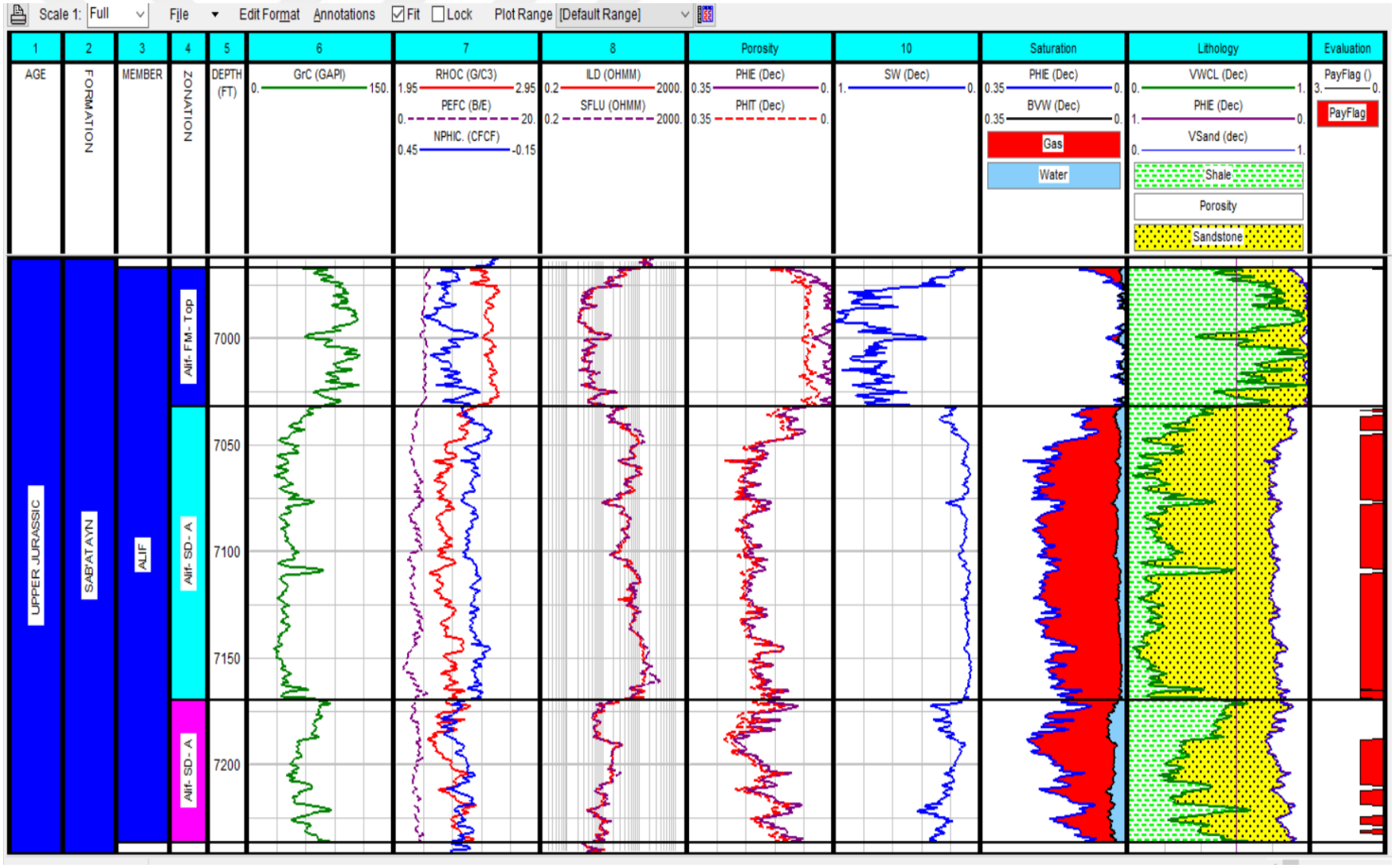

Figure 4.7. Finally obtained dataset plot including the zonation of Alif Member through RJ#38 by IP software

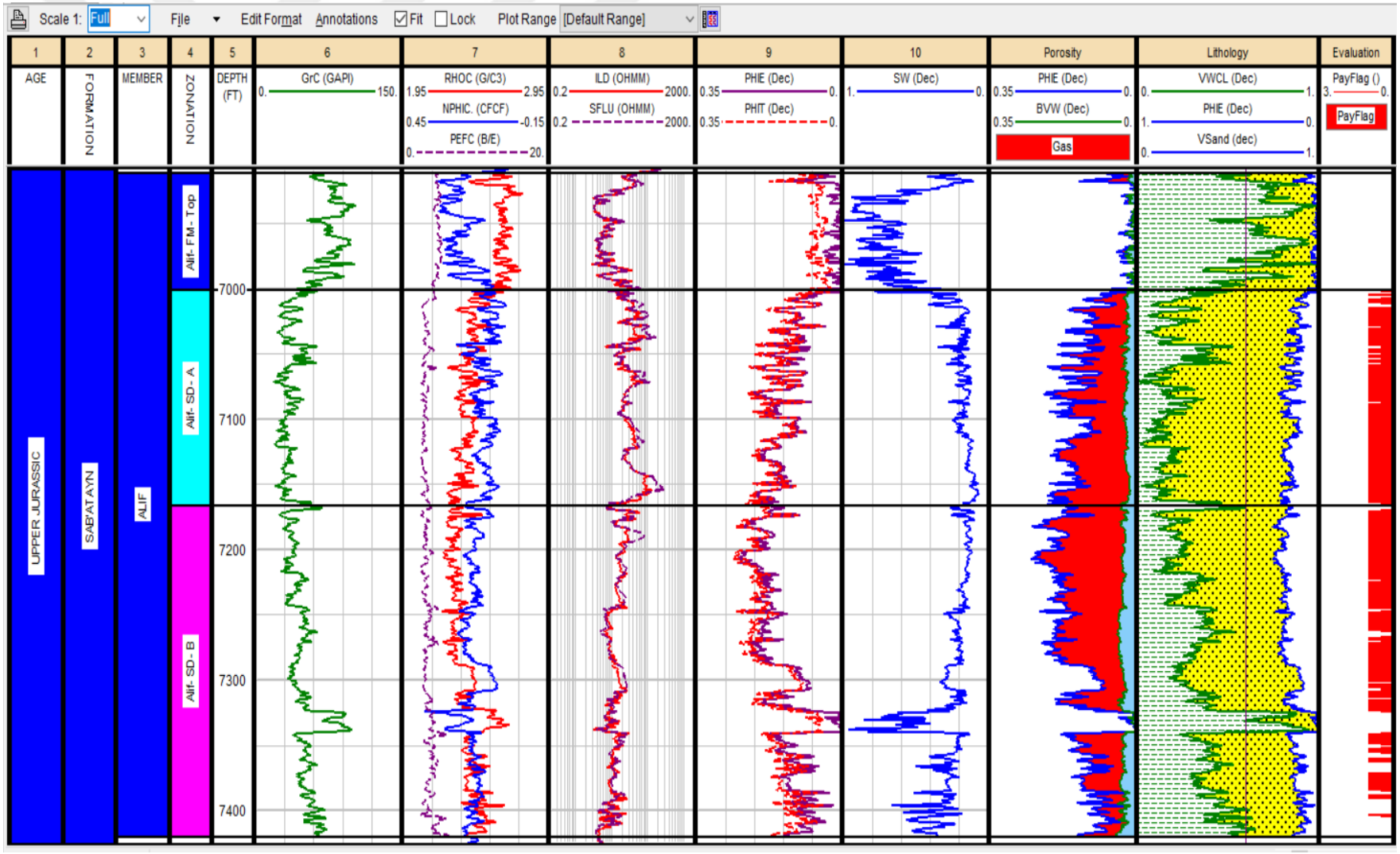

Figure 4.8. Finally obtained dataset plot including the zonation of Alif Member through RJ#39 by IP software

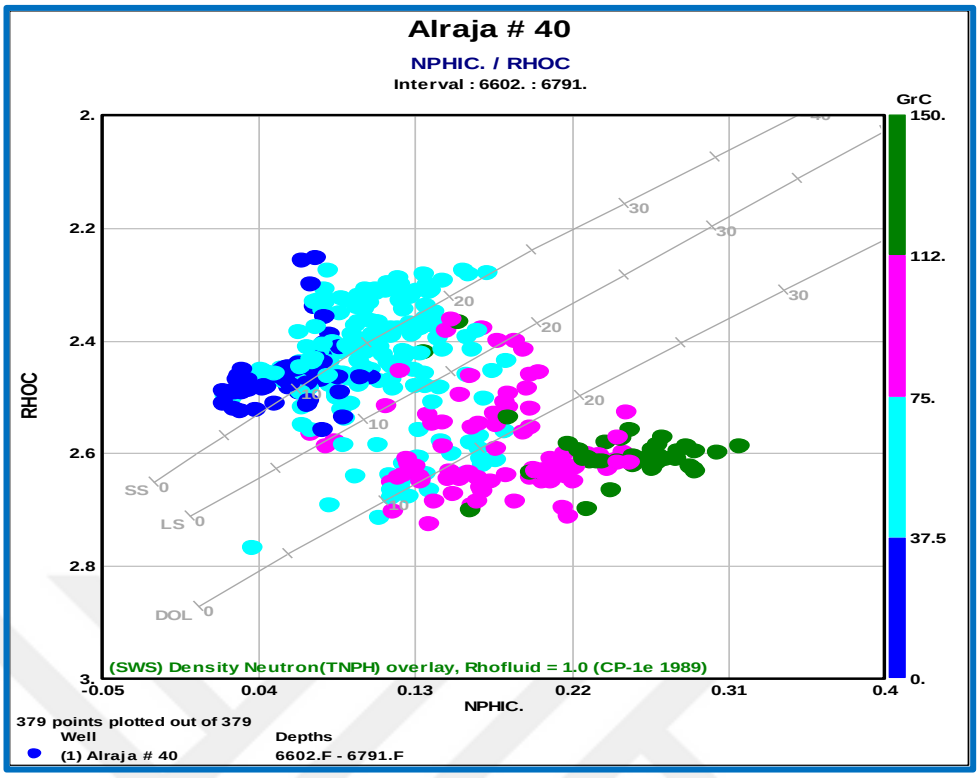

Figure 4.9. NPHIC-RHOC (Neutron-Density) crossplot of RJ#40 borehole by Schlumberger IP software

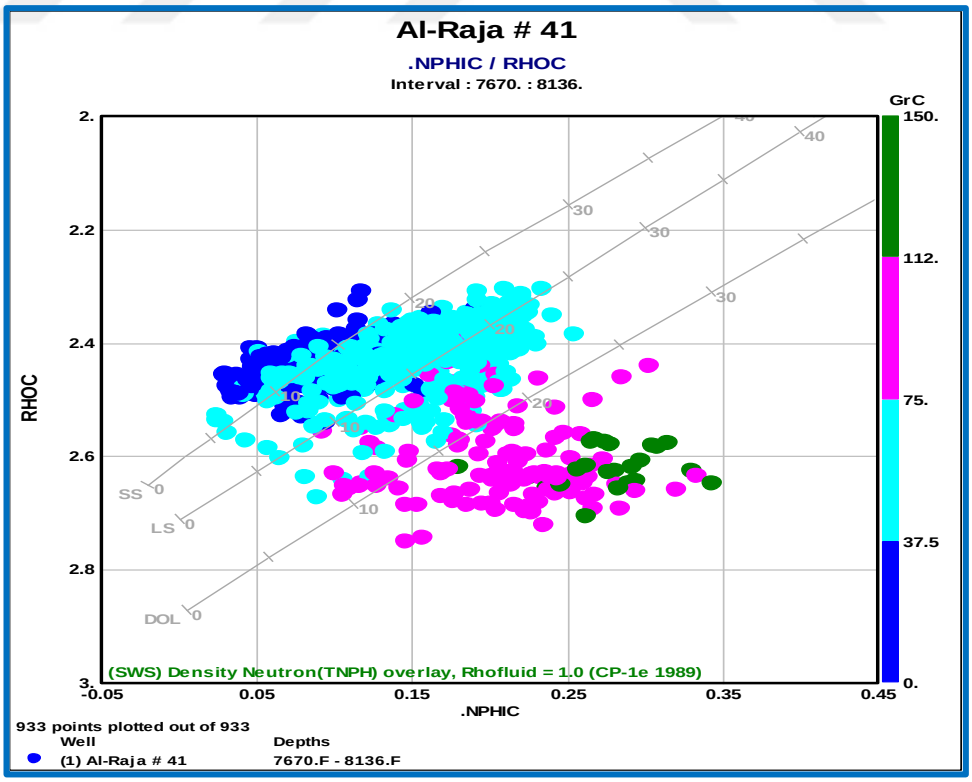

Figure 4.10. NPHIC-RHOC (Neutron-Density) crossplot of RJ#41 borehole by Schlumberger IP software

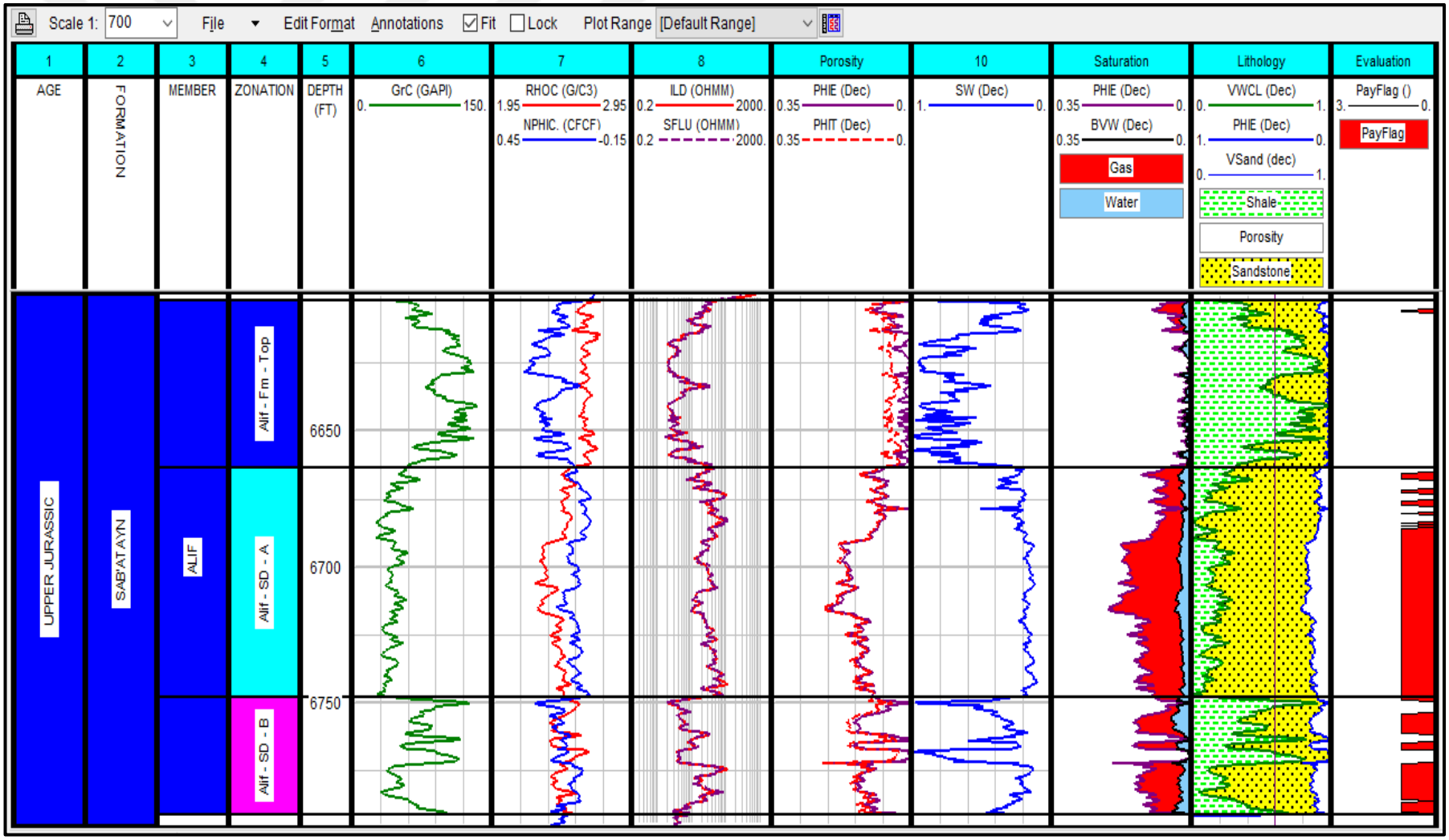

Figure 4.11. Finally obtained dataset plot including the zonation of Alif Member through RJ#40 by IP software

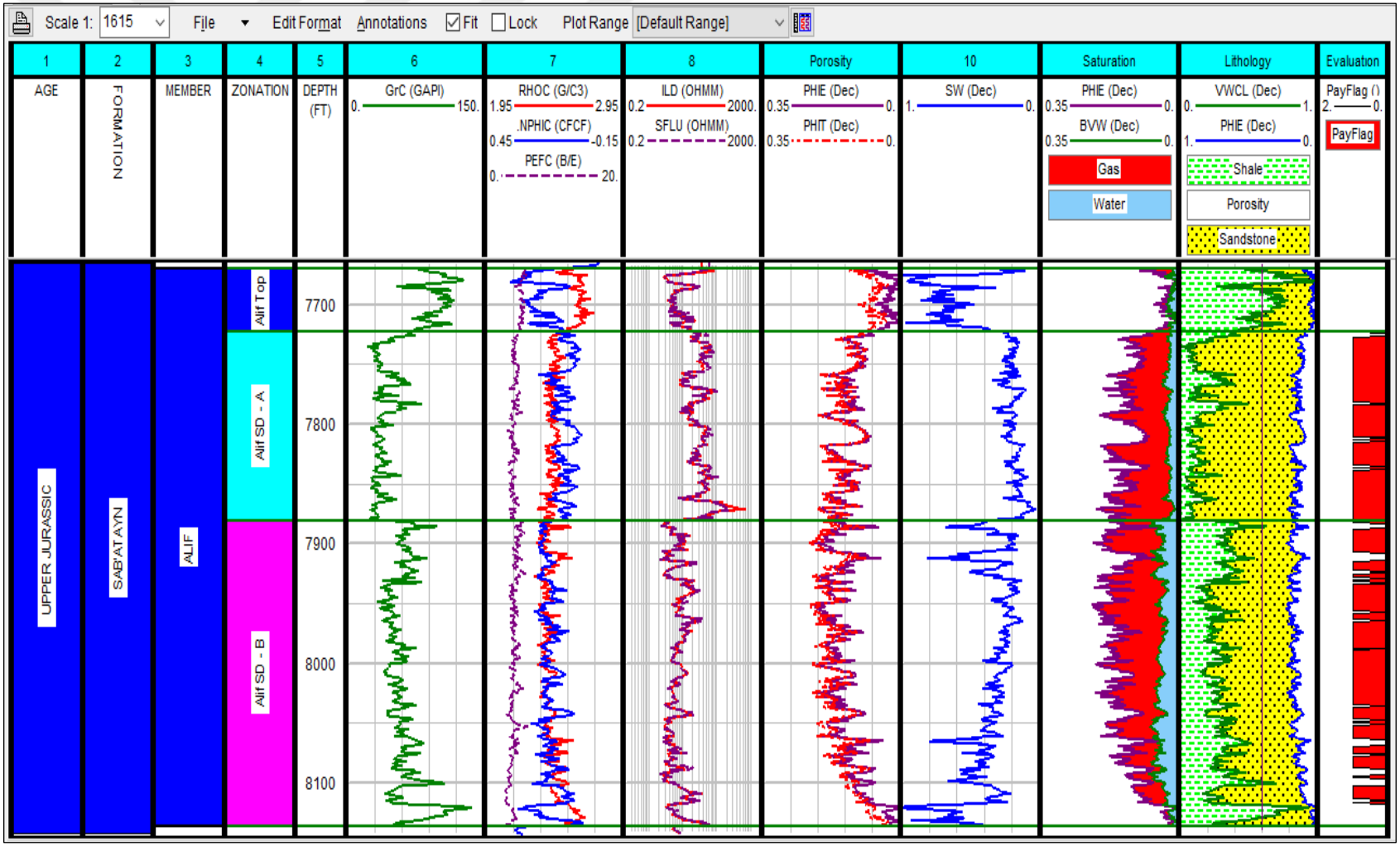

Figure 4.12. Finally obtained dataset plot including the zonation of Alif Member through RJ#41 by IP software

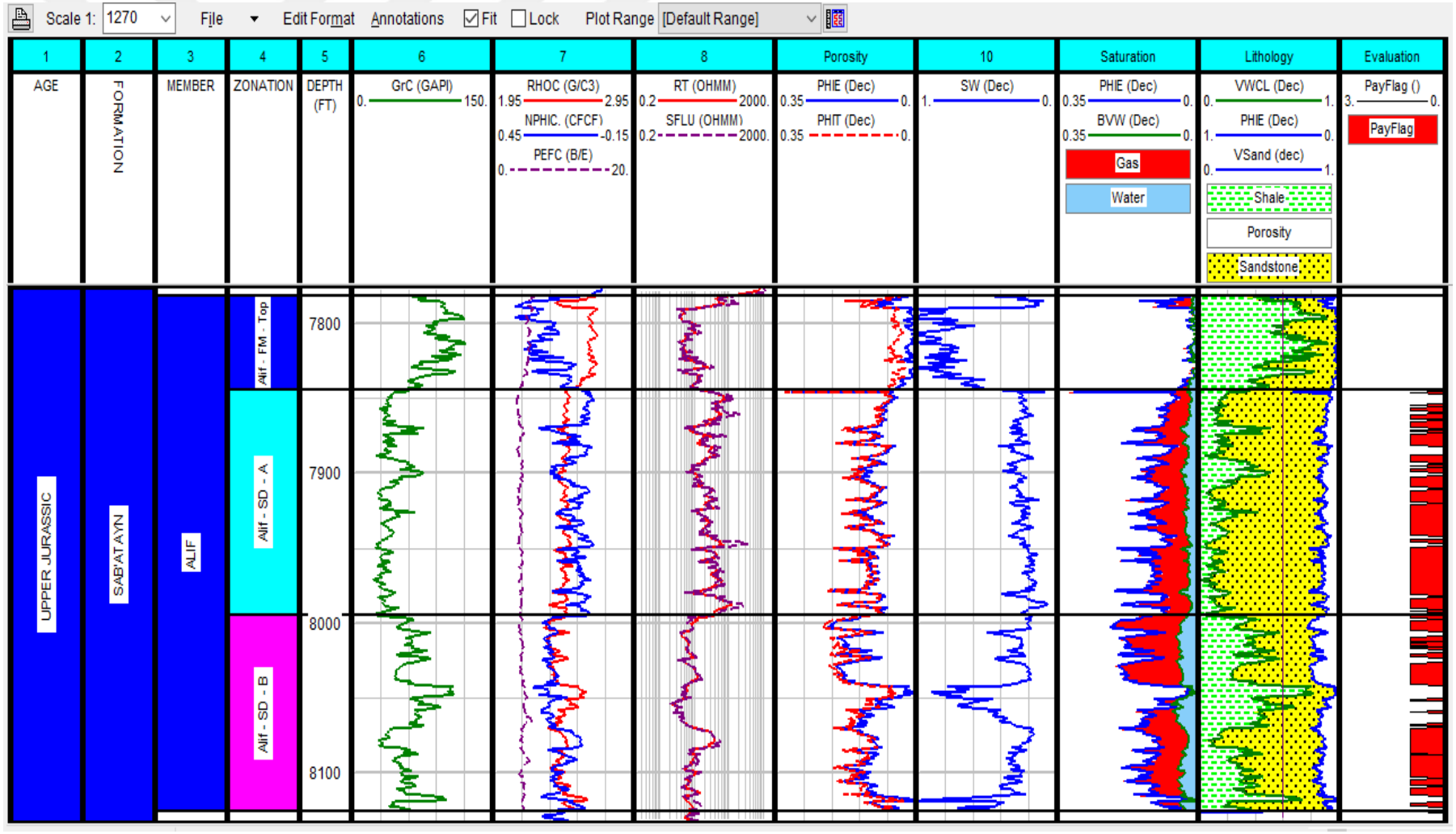

Figure 4.13. Finally obtained dataset plot including the zonation of Alif Member through RJ#42 by IP software

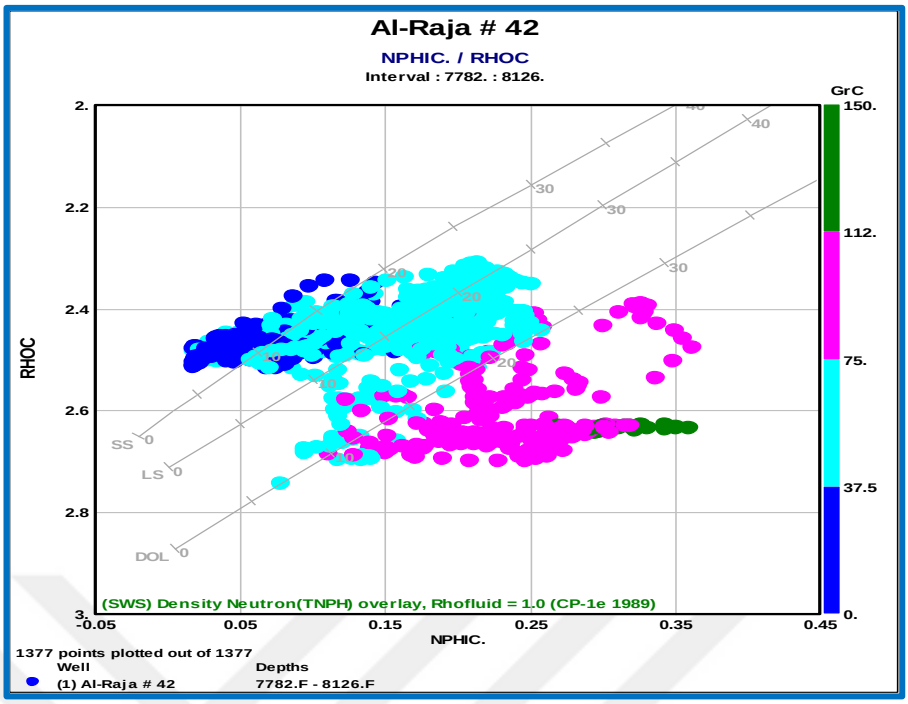

Figure 4.14. NPHIC-RHOC (Neutron-Density) crossplot of RJ#42 borehole by Schlumberger IP software

4.2. Reservoir Characterization

4.2.1. Distribution map of shale volume in Alif member

According to Figure 4.15, which is the distribution map of shale volume in the Alif Member of the study area, we notice that the shale volume varies from a well to another with a minimum value of 15.3 % in RJ-36 and a maximum value of 22.7 % in RJ-39. This map indicates the diminution of the shale content towards the northwest inside the study area.

4.2.2. Distribution map of effective porosity in Alif member

The distribution map of effective porosity of the Alif Member in the study area (Figure 4.16.) shows ups and downs in the average values of effective porosity in the different study wells. The minimum value is detected in RJ-40 as 12.9 %, while the maximum value is detected as 19.7 % in RJ 36. Figure 4.16. shows that the effective porosity increases when moving north-westwards in the study field.

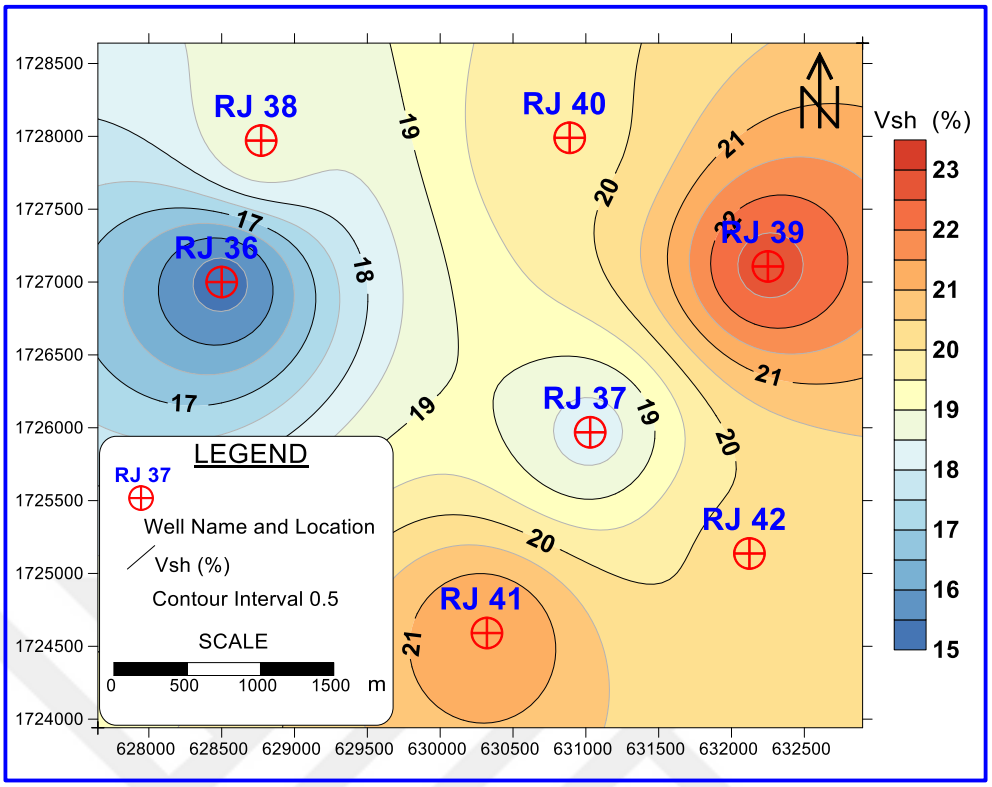

Figure 4.15. Distribution map of shale volume in Alif member within the study area obtained by surfer 17

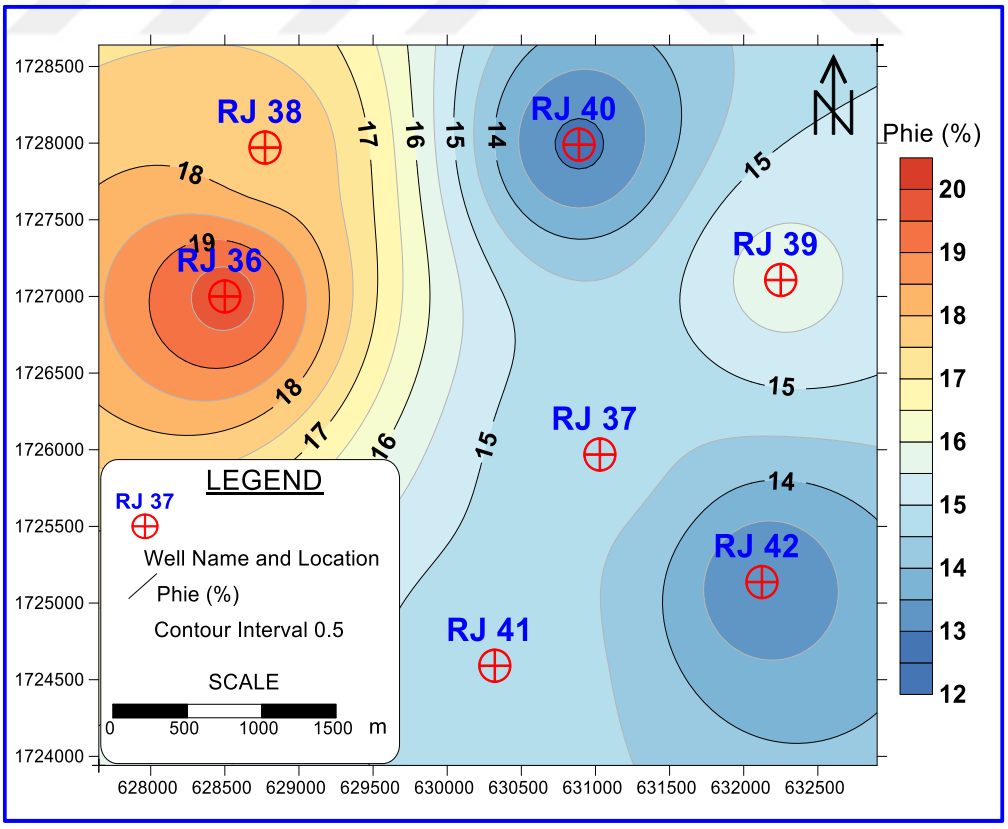

Figure 4.16. Distribution map of effective porosity in Alif member within the study area obtained by surfer 17

4.2.3. Distribution map of water saturation in Alif member

The map of Figure 4.17. displays the distribution of water saturation of the Alif Member in the area containing the wells of this study. The values of this petrophysical parameter vary from 11.1 % (minimum value) in RJ-38 to 23.5 % (maximum value) in RJ-41. This map shows that water saturation takes lower values toward the north-western sides and considerably higher values towards the south and the south-east of the study area.

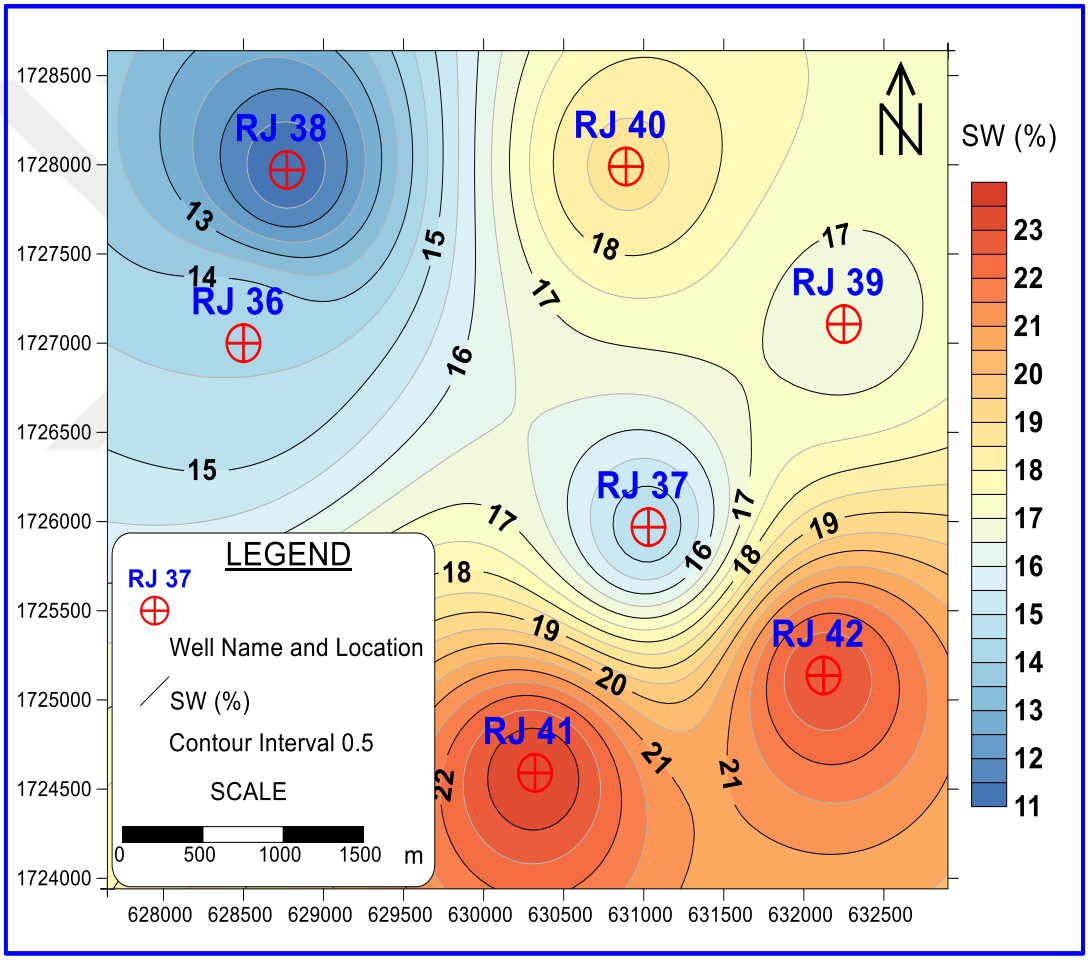

Figure 4.17. Distribution map of water saturation in Alif Member within the study area obtained by Surfer 17

4.2.4. Distribution map of hydrocarbon saturation in Alif member

Figure 4.18. shows the variation of hydrocarbon saturation distribution of the Alif Member in the study area. The values of this parameter start from a minimum value of

76.5% in RJ-41 and reach a maximum value of 88.9% in RJ-38. The map of Figure 4.18. indicates that the values of hydrocarbon saturation go bigger as we go towards the north-western areas and go smaller towards the southern and the south-eastern areas of the study field.

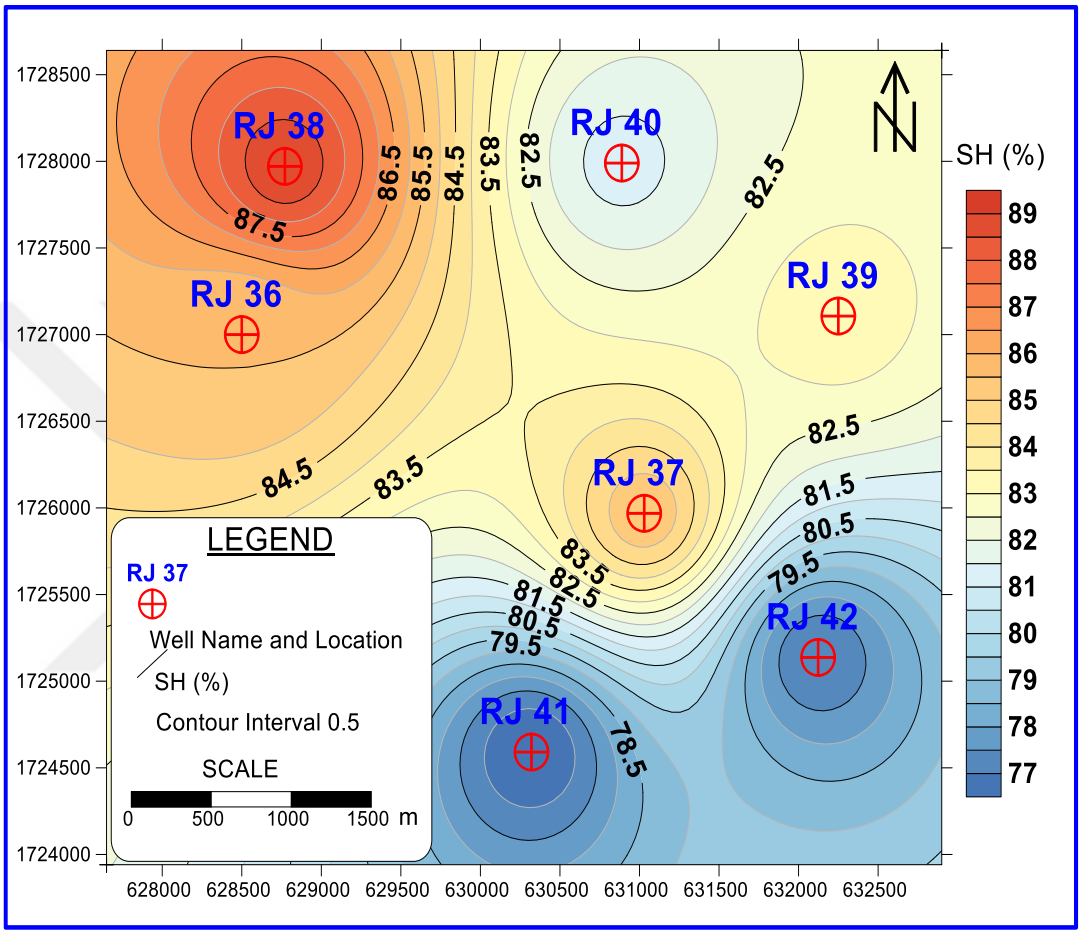

Figure 4.18. Distribution map of Hydrocarbon Saturation in Alif Member in the study area obtained by Surfer 17

4.2.5. Distribution map of net thickness of Alif member

The values of the net thickness of the Alif Member, whose distribution map in the study area is displayed in Figure 4.19. show ups and downs between the different wells. The maximum net thickness is detected in the RJ-41 well (340.5 ft), while the minimum net thickness is 100.5 ft and detected in the RJ-40 well. The distribution map of Figure 4.19. indicates that the net thickness values go higher from the north towards the southern, and the north-eastern areas of the study field.

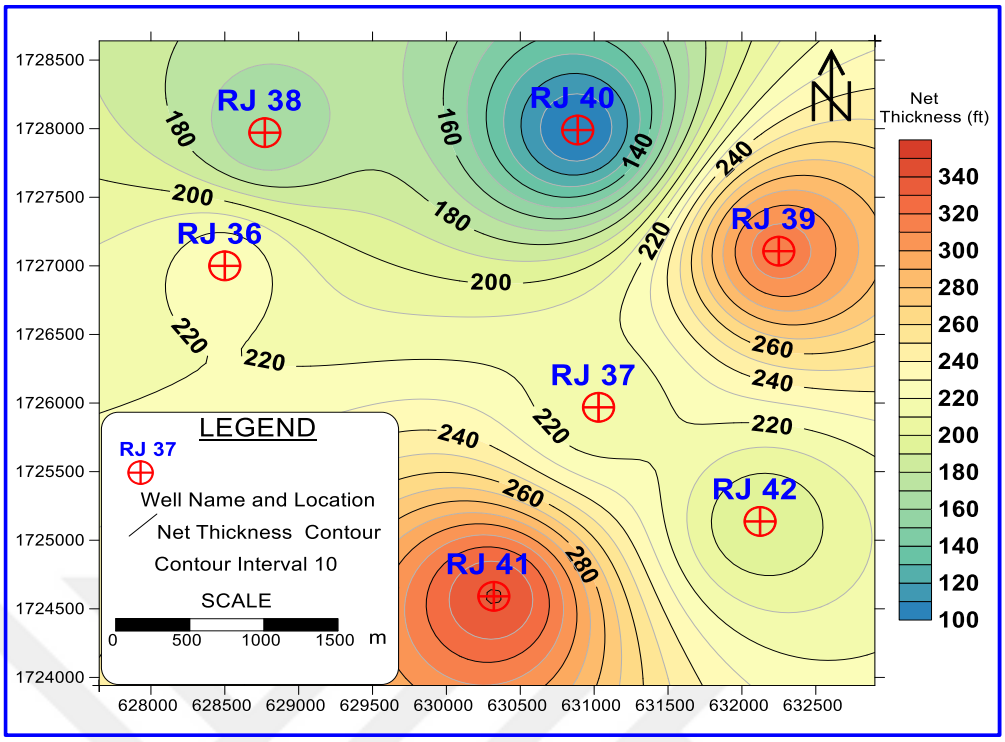

Figure 4.19. Distribution map of net thickness of Alif Member within the study area obtained by Surfer 17

4.2.6. Distribution map of Net to Gross Thickness ratio in Alif Member

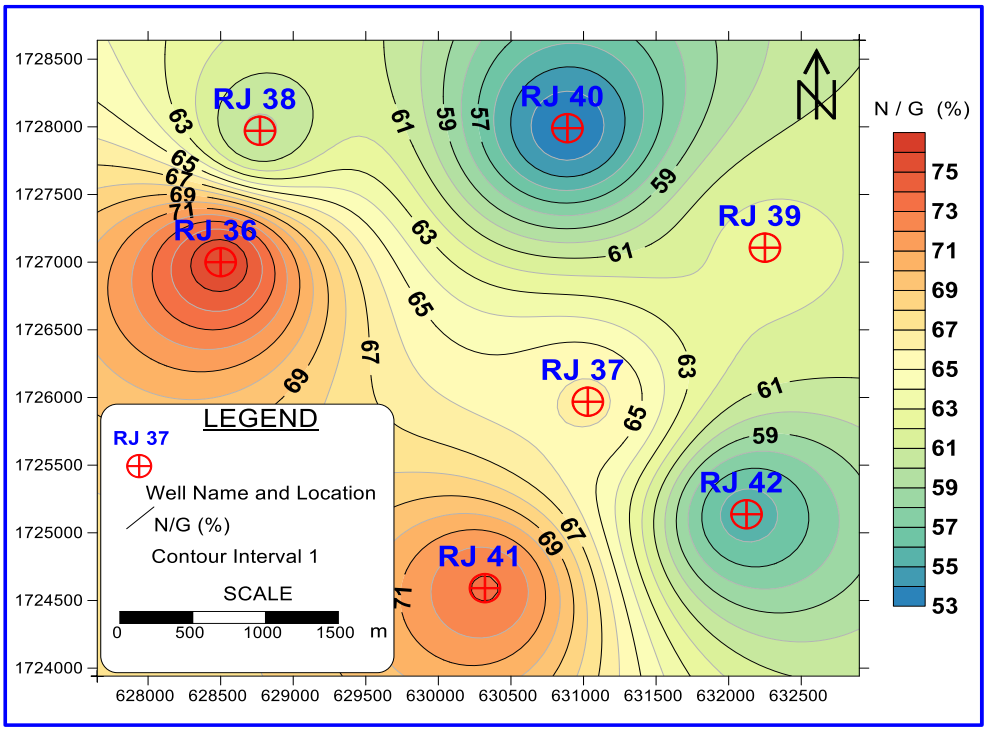

Figure 4.20. Distribution map of Net to Gross thickness ratio of Alif Member through the study area obtained by Surfer 17

Similarly, the Net thickness to Gross thickness ratio values also vary from a well to another between a minimum value of 53.2 % detected in RJ-40 and a maximum value of 75.8 % recorded in the borehole RJ-36. This distribution is displayed in Figure 4.20. The distribution map also shows that the ratio of net thickness to gross thickness increases westwards and southwards and decreases northwards and southeastwards inside the study area.

4.3. Hydrocarbon Potentialities of the Study Area

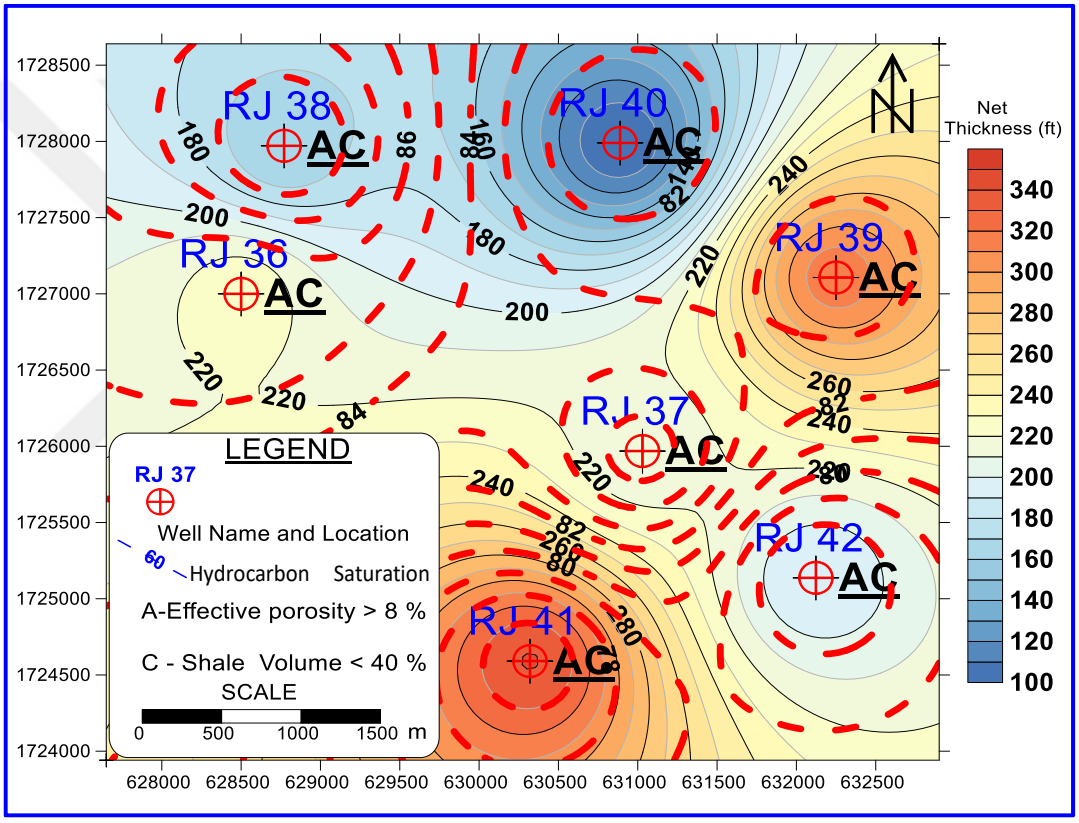

Figure 4.21. Lease map of the Alif Member through the study area obtained by Surfer 17

A lease map of the Alif Member was created as a means of discussing the study area hydrocarbon potentialities (Figure 4.21.). This map was constructed according to the shale content and effective porosity average values, and the pay thickness of the Alif Member. It indicates that the study area has good hydrocarbon potential taking into account its petrophysical parameters whose value range is mentioned in the previous sections. In fact, the study area has hydrocarbon saturation of high values ranging

between 76.5 % and 88.9 % and effective porosity also of high values ranging from 12.9 % to 19.7 %. In addition, shale volume ranges between 15.3 % and 22.7 % which is considered a low amount. Finally, the pay thickness values range from 100.5 to 340.5 ft. As a deduction, the study area is promising, and it should be considered in future exploration works.

This study leads to the following recommendations:

- More interest should be paid to the studied Alif Member of the Sab'atayn formation and the other members of the same formation in the Al-Raja Field using high-quality methods such as the seismic method to obtain more information about the characteristics of the reservoir rocks and minimize the risks of drilling non-productive wells.

- Drilling new wells in the study area, especially its north-western parts, should be planned since it has good petrophysical characteristics.

REFERENCES

AAPG WIKI (2016) *Density-Neutron Log Porosity*, *AAPG WIKI*. Available at: https://wiki.aapg.org/Density-neutron_log_porosity (Accessed: 1 February 2021).

Ahlbrandt, T. S. (2002) 'Madbi Amran / Qishn Total Petroleum System of the Ma′Rib–Al Jawf / Shabwah, and Masila-Jeza Basins, Yemen', *USGS bulletin*.

Al-Areeq, N. (2004) *Sedimentary and Reservoir Study of Clastic Members From Sabatyn Formation in Alif Oil Field (Marib- Shabwa Basin) Republic of Yemen*. Baghdad University.

Al-Ariki, M., Al-Azazi, N. and Gülen, L. (2021) 'Reservoir Evaluation by Well-Logging of the Al-Raja Field, Alif Member, Marib Shabwah (Sab'atayn) Basin, Republic of Yemen', in *International Journal of Scientific & Engineering Research*. IJSER, p. 8. Available at: ijser.org/onlineResearchPaperViewer.aspx?Reservoir-Evaluation-by-Well-Logging-of-the-Al-Raja-Field-Alif-Member-Marib-Shabwah-Sab-atayn-Basin-Republic-of-Yemen.pdf.

Al-Azazi, N. A. S. A. (2010) *Reservoir Petrophysics and Hydrocarbon Potentialities of the Sab'Atayn Formation (Upper Jurassic) in Alif Oil Field, Marib Shabwa Basin, Republic of Yemen*, *Sci. J. Fac. Sci. Minufya Univ*. Menoufiya Univ.Egypt.

Al-Azazi, N. A. S. A. (2016) *Hydrocarbon Evaluation and Geostatical Modeling of The Sab'atayn Formation (Upper Jurassic) in Wadi Bana Oil Field, Marib Shabwa Basin, Republic of Yemen.* Ain Shams University, Faculty of Science, Department of Geophysics, Unpublished Doctoral Dissertation. Egypt.

Al-hasani, A. *et al.* (2018) 'Reservoir characteristics of the Kuhlan sandstones from Habban oilfield in the Sabatayn Basin, Yemen and their relevance to reservoir rock quality and petroleum accumulation', *Journal of African Earth Sciences*, 145(March), pp. 131–147. doi: 10.1016/j.jafrearsci.2018.05.013.

Alaug, A. S. *et al.* (2011) 'Source rock evaluation, modelling, maturation, and reservoir characterization of the block 18 oilfields, Sab'atayn Basin, Yemen', *Iranian Journal of Earth Sciences*, 3(2), pp. 134–152.

Alaug, A. S. *et al.* (2014) 'Palynofacies, organic geochemical analyses and hydrocarbon potential of some Upper Jurassic-Lower Cretaceous rocks, the Sabatayn-1 well, Central Yemen', *Arabian Journal of Geosciences*, 7(6), pp. 2515–2530.

Albaroot, M., Ahmad A.H.M., Nabil Al-Areeq, H. A. (2017) 'HYDROCARBON RESERVOIR CHARACTERIZATION USING WELL LOG IN HALEWAH OILFIELD, MARIB-SHABWA BASIN, YEMEN', *Asian Journal of Science and Technology*, 08(30 th April), pp. 4649–4659. Available at: https://www.researchgate.net/publication/317040926_HYDROCARBON_RESERVOIR_CHARACTERIZATION_USING_WELL_LOG_IN_HALEWAH_OILFIELD_MARIB-SHABWA_BASIN.

Albaroot, M. *et al.* (2016) 'Tectonostratigraphy of Yemen And Geological Evolution: A New Prospective', *International Journal of New Technology and Research*, 2(2), pp. 1–467.

As-Saruri, M. (2004) 'Geological map of Yemen', *General Department of Studies and Research, Petroleum Exploration Authority*.

As-Saruri, M. (no date) 'LITHOSTRATIGRAPHIC CHART OF YEMEN'. Salt Lake City, USA: Petroleum Exploration and Production Authority (PEPA), p. 1.

As-Saruri, M. A., Sorkhabi, R. and Baraba, R. (2010) 'Sedimentary basins of Yemen: their tectonic development and lithostratigraphic cover', *Arabian Journal of Geosciences*, 3(4), pp. 515–527. doi: 10.1007/s12517-010-0189-z.

As-Saruri, M. and Sorkhabi, R. (2014) 'Petroleum systems and basins of Yemen', *AAPG Memoir*, pp. 757–780. doi: 10.1036/13431871M1063617.

Asquith, G. B. and Gibson, C. R. (1982) *Basic well log analysis for geologists*. Tulsa, Oklahoma, USA: American Association of Petroleum Geologists. doi: https://doi.org/10.1306/Mth3425.

Avedissian, A. M. (1988) *Well Logging Analysis*. Baghdad.

Bassiouni, Z. (1994) *Theory, measurement, and interpretation of well logs*. 1st printi. Louisiana, USA: Henry L. Doherty Memorial Fund of AIME, Society of Petroleum Engineers. Available at: https://scholar.google.com/scholar?hl=ar&as_sdt=0%2C5&q=Bassiouni%2C+Z.%2C+%281994%29%3A+Theory%2C+measurements+and+interpretation+of+well+logs%2C+The+Society+of+Petroleum+Engineering&btnG=.

Beydoun, Z. R. *et al.* (1998) 'International lexicon of stratigraphy, Volume III, Republic of Yemen: International Union of Geological Sciences and Ministry of Oil and Mineral Resources', *Republic of Yemen Publication*, 34, p. 245.

Bosence, D. W. J. (1997) 'Mesozoic rift basins of Yemen', *Marine and Petroleum Geology*, 14(6), pp. 611-IN6.

Brannan, J. *et al.* (1999) 'Geological evolution of the central Marib-Shabwa Basin, Yemen', *GeoArabia*, 4(1), pp. 9–34.

Brown, G. F., Schmidt, D. L. and Huffman Jr, A. C. (1989) *Geology of the Arabian Peninsula; shield area of western Saudi Arabia*. US Geological Survey.

Csato, I. (2005) 'Extensional tectonics and salt structures, Marib-Shabwa basin, Yemen', in *AAPG Annual Convention, Dallas*. Sioux Center, pp. 1–6.

Darling, T. (2005) *Well Logging and Formation Evaluation*, *Well Logging and Formation Evaluation*. Elsevier. doi: 10.1016/B978-0-7506-7883-4.X5000-1.

Dewan, J. T. (1983) *Essentials of modern open-hole log interpretation*. Tulsa, Oklahoma, USA: PennWell Books.

Epuh, E. E. and Joshua, E. O. (2020) 'Modeling of porosity and permeability for hydrocarbon Exploration: A case study of Gongola arm of the Upper Benue Trough', *Journal of African Earth Sciences*, 162(April 2017), p. 103646. doi: 10.1016/j.jafrearsci.2019.103646.

Gad, S. and Kusky, T. (2007) 'ASTER spectral ratioing for lithological mapping in the Arabian–Nubian shield, the Neoproterozoic Wadi Kid area, Sinai, Egypt', *Gondwana Research*, 11(3), pp. 326–335. doi: 10.1016/j.gr.2006.02.010.

Geert, K. *et al.* (2001) 'Paleozoic Stratigraphy and Hydrocarbon Habitat of the Arabian Plate', *GeoArabia*, 6(3), pp. 407–442.

Glover, P. W. J. (2000) 'Petrophysics', *University of Aberdeen, UK*.

Google Earth 7.3.3, (2020). Available at: https://earth.google.com/web/@0,0,0a,22251752.77375655d,35y,0h,0t,0r?utm_source=earth7&utm_campaign=vine&hl=en (Accessed: 17 March 2021).

Van der Gun, J. A. M. and Ahmed, A. A. (1995) 'The water resources of Yemen: a summary and digest of available information'.

Gunawan, I. and Al-abbasi, O. A. (2011) 'Challenges of Recovering by-Passed Condensate in Al-Raja Field', in *SPE Asia Pacific Oil and Gas Conference and Exhibition*. Society of Petroleum Engineers, pp. 1–20. doi: 10.2118/145928-MS.

Hakimi, M. H. and Abdullah, W. H. (2015) 'Thermal maturity history and petroleum generation modelling for the Upper Jurassic Madbi source rocks in the Marib-Shabowah Basin, western Yemen', *Marine and Petroleum Geology*, 59, pp. 202–216. Available at: http://dx.doi.org/10.1016/j.marpetgeo.2014.08.002.

Hakimi, M. H., Al-Matary, A. M. and Salad Hersi, O. (2018) 'Late Jurassic bituminous shales from Marib oilfields in the Sabatayn Basin (NW Yemen): Geochemical and petrological analyses reveal oil-shale resource', *Fuel*, 232(May), pp. 530–542. doi: 10.1016/j.fuel.2018.05.138.

Hessami, K., Nilforoushan, F. and Talbot, C. J. (2006) 'Active deformation within the Zagros Mountains deduced from GPS measurements', *Journal of the Geological Society*, 163(1), pp. 143–148. doi: 10.1144/0016-764905-031.

Johnson, P. R. (1998) 'Tectonic map of Saudi Arabia and adjacent areas', *Deputy Ministry for Mineral Resources Technical Report USGS-TR-98-3 (IR 948)*.

Jurgen, S. (2015) *Basic Well Logging and Formation Evaluation*. 1st editio. bookboon.com.

Kamel, M. H. and Mabrouk, W. M. (2003) 'Estimation of shale volume using a combination of the three porosity logs', *Journal of Petroleum Science and Engineering*, 40(3–4), pp. 145–157. doi: 10.1016/S0920-4105(03)00120-7.

Lawver, L. A. *et al.* (2007) 'Plates 2006—atlas of plate reconstructions (750 Ma to present day). University of Texas', *Institute for Geophysics, Austin*.

McQuarrie, N. *et al.* (2003) 'Cenozoic evolution of Neotethys and implications for the causes of plate motions', *Geophysical research letters*, 30(20).

Ministry of Oil and Minerals (no date a) *Gas*. Available at: https://mom-ye.com/site-en/قطاع-الغاز/ (Accessed: 7 February 2020).

Ministry of Oil and Minerals (no date b) *القطاعات الإنتاجية*. Available at: https://mom-ye.com/site-ar/القطاعات-الإنتاجية/ (Accessed: 10 February 2020).

Ministry of Oil and Minerals (no date c) *غاز*. Available at: http://www.mom.gov.ye/index.php?option=com_content&view=article&id=50:2011-01-08-18-47-59&catid=42:gas&Itemid=2 (Accessed: 5 February 2020).

Ministry of Oil and Minerals (2010) 'Concession Map of Yemen'. Sana'a: Ministry of Oil and Minerals, p. 1.

Nabawy, B. S. and Al-Azazi, N. A. S. A. (2015) 'Reservoir zonation and discrimination using the routine core analyses data: the Upper Jurassic Sab'atayn sandstones as a case study, Sab'atayn basin, Yemen', *Arabian Journal of Geosciences*, 8(8), pp. 5511–5530. doi: 10.1007/s12517-014-1632-3.

PEPA (no date a) *Geological & Stratigraphic Settings of Yemen*. Available at: http://www.pepa.com.ye/Geological framework/Geological & Stratigraphic Settings of Yemen.htm (Accessed: 29 September 2019).

PEPA (no date b) *Marib - Blocks (18)*. Available at: http://www.pepa.com.ye/Production Activities/blocks/block 18.htm (Accessed: 9 November 2019).

PEPA (no date c) *Producing Blocks*. Available at: http://www.pepa.com.ye/Production Activities/producing blocks.htm (Accessed: 23 November 2019).

PEPA (no date d) *Production History*. Available at: http://www.pepa.com.ye/Production Activities/production activities.htm (Accessed: 6 February 2020).

Pirson, S. J. (1963) *Handbook of well log analysis for oil and gas formation evaluation*. United States: Prentice-Hall, Inc., Englewood Cliffs, NJ. Available at: https://scholar.google.com/scholar?q=Handbook of well log analysis for oil and gas formation evaluation.

Ramadan, M. A. M. *et al.* (2019) 'Relation between hydrocarbon saturation and pore pressure evaluation for the Amal Field area, Gulf of Suez, Egypt', *Egyptian Journal of Petroleum*, 28(1), pp. 1–9.

Redfern, P. and Jones, J. A. (1995) 'The interior rifts of the Yemen - analysis of basin structure and stratigraphy in a regional plate tectonic context', *Basin Research*, 7(4), pp. 337–356. doi: 10.1111/j.1365-2117.1995.tb00121.x.

Sachsenhofer, R. F. *et al.* (2012) 'Upper Jurassic source rocks in the Sab'atayn Basin, Yemen: Depositional environment, source potential and hydrocarbon generation', *GeoArabia*, 17(4), pp. 161–186.

Schlumberger (1989a) *Cased Hole Log Interpretation Principles/Applications - Introduction*. 4th printi, *Cased Hole Log Interpretation Principles/Applications*. 4th printi. Houston, Texas. USA: Schlumberger Wireline & Testing. Available at: http://www.slb.com/resources/publications/books/ch_lipa.aspx.

Schlumberger (1989b) *Log interpretation principles/applications*. 7th edn. Sugar Land, Texas. USA: Schlumberger Wireline & Testing, Sugarland.

Schlumberger (1997) *Schlumberger Log Interpretation Charts*. Houston, Texas. USA: Schlumberger.

Schlumberger (2008) *Intractive Petrophysics software, Users Manual, Version 3.5.* Aberdeenshire, Scotland: Schlumberger.

Schlumberger (2009) *Log Interpretation Charts*, *Schlumberger*. Sugar Land, Texas. USA: Schlumberger.

SEPOC (2008) *ALRAJA-36_TLD-CNL-AIT-HCAL-GR_MAIN PASS_27OCT08*. Sana'a, Yemen.

SEPOC (2010) *Al-Raja Field Report*. Sana'a, Yemen.

SEPOC (2012) *BLOCK 18 OIL AND GAS RESERVS*. Sana'a, Yemen.

SEPOC (no date) *Yemen's Oil and gas History*. Available at: http://www.sepocye.com/?ID=YOH&fbclid=IwAR2RKjtHnzNtWG-iW56BQ6rRDfpdVFFXiKdWGww1fQg7f-q5TPIjPYd_jqU (Accessed: 3 February 2020).

SPT (1994) *The Petroleum Geology of the Sedimentary Basins of the Republic of Yemen*. LGwynedd, UK.

Stern, R. J. (1985) 'The Najd fault system, Saudi Arabia and Egypt: A late Precambrian rift-related transform system?', *Tectonics*, 4(5), pp. 497–511.

Stern, R. J. and Johnson, P. (2010) 'Continental lithosphere of the Arabian Plate: A geologic, petrologic, and geophysical synthesis', *Earth-Science Reviews*, 101(1–2), pp. 29–67. doi: 10.1016/j.earscirev.2010.01.002.

Taheri, A. *et al.* (1992) 'LOOKING FOR YEMEN'S HIDDEN TREASURE', *Middle East Well Eval Rev Schlumberger*, 12, pp. 12–29.

Tari, G. *et al.* (2016) 'Styles of salt tectonics in the Sab'atayn basin, onshore Yemen', *Arabian Journal of Geosciences*, 9(10), p. 570. doi: 10.1007/s12517-016-2581-9.

Tavakoli-Shirazi, S. *et al.* (2013) 'Pre-Permian uplift and diffuse extensional deformation in the High Zagros Belt (Iran): integration in the geodynamic evolution of the Arabian plate', *Arabian Journal of Geosciences*, 6(7), pp. 2329–2342. doi: 10.1007/s12517-012-0542-5.

Veeningen, R. *et al.* (2015) 'Thermochronology and geochemistry of the Pan-African basement below the Sab'atayn Basin, Yemen', *Journal of African Earth Sciences*, 102, pp. 131–148.

Vita-Finzi, C. (2001) 'Neotectonics at the Arabian plate margins', *Journal of Structural Geology*, 23(2–3), pp. 521–530.

Wagner, W. (2011) *Groundwater in the Arab Middle East*. Berlin, Heidelberg: Springer Berlin Heidelberg. doi: 10.1007/978-3-642-19351-4.

Whitehouse, M. J. *et al.* (2001) 'Precambrian basement character of Yemen and correlations with Saudi Arabia and Somalia', *Precambrian Research*, 105(2–4), pp. 357–369.

Woodmakenize (2019) *Marib-Jawf Contract Area (Block 18)*. Available at: https://www.woodmac.com/reports/upstream-oil-and-gas-marib-jawf-contract-area-block-18-1304029.

Yemen LNG Company (no date) *Project Components*. Available at: http://www.yemenlng.com/ws/en/go.aspx?c=proj_upstream (Accessed: 10 February 2020).

YGSMR (no date) *Introduction to Yemen Geology*. Available at: http://ygsmrb.org.ye/geology/?fbclid=IwAR0aTMRnR6YA1CNxWLi5FFUBrTqtrg2Unjyre63miiHN8dBZTF46RRgJYmk (Accessed: 23 September 2019).

Zhao, P. *et al.* (2016) 'Methods for estimating petrophysical parameters from well logs in tight oil reservoirs: A case study', *Journal of Geophysics and Engineering*, 13(1), pp. 78–85. doi: 10.1088/1742-2132/13/1/78.

RESUME

Name Surname **:** Mustafa ABDULWAHED AL-ARIKI

EDUCATION

Degree	School	Graduation Year
Master	Sakarya University / School of Science and Technology / Geophysical Engineering	Continue
Bachelor	Aden University / Faculty of Oil and Minerals / Oil and Gas Engineering	2014
High School	Taiz High School	2009

JOB EXPERIENCE

Year	Place	Position
2015-2016	The Light Coming from the East Organization	Supervisor of relief operations
2014	OMV	Petroleum Engineer Trainee
2013	Petroleum Exploration & Production Authority (PEPA)	Petroleum Engineer Trainee

FOREIGN LANGUAGE

Arabic, English

PRODUCTS (article, paper, project, ets.)

1- Al-Ariki, M., Al-Azazi, N. and Gülen, L. (2021) 'Reservoir Evaluation by Well-Logging of the Al-Raja Field, Alif Member, Marib Shabwah (Sab'atayn) Basin, Republic of Yemen', in International Journal of Scientific & Engineering Research. IJSER, p. 8.

2- Bachelor's degree final work: Basic Oil & Gas Wells Drilling Engineering, Department of Oil Well Drilling: including Mud, Casing design, cementing, directional drilling, hole problem, from the surface until the bottom of Habban-09 borehole in Shabwah Province, Yemen.

HOBBIES

Reading, Surfing the net, Sports, and body building